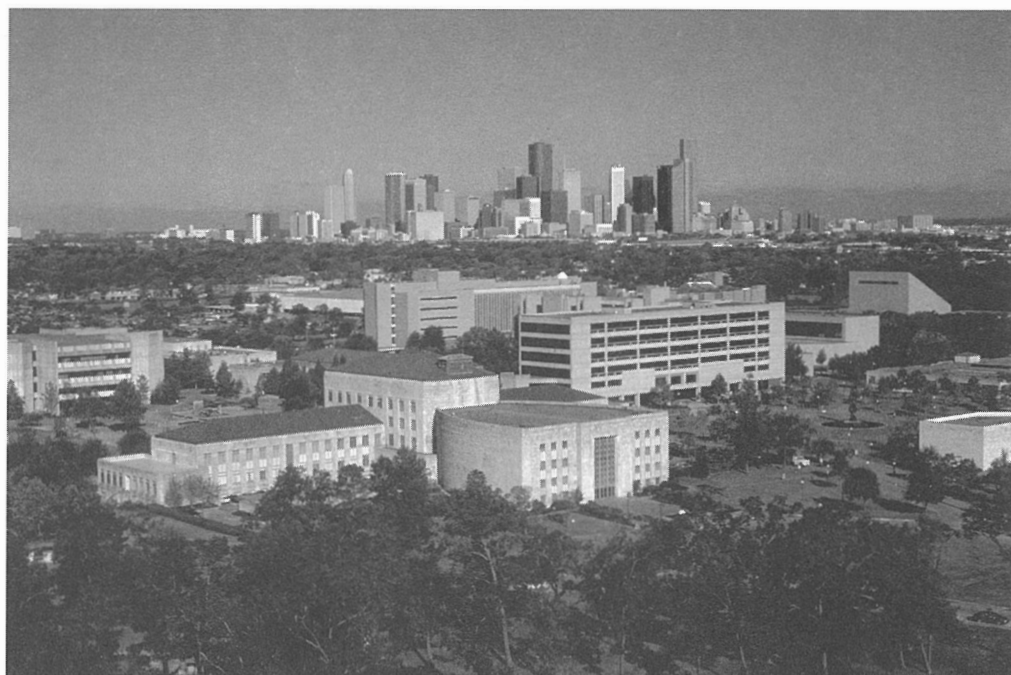


# BULLETIN

OF THE AMERICAN PHYSICAL SOCIETY

PROGRAM OF THE 53rd ANNUAL  
GASEOUS ELECTRONICS CONFERENCE



**October 24–27, 2000**  
**Houston, Texas**

**October 2000**  
**Volume 45, No. 6**

# BULLETIN

OF THE AMERICAN PHYSICAL SOCIETY

Coden BAPSA6

Series II, Vol. 45, No. 6

ISSN: 0003-0503

October 2000

## APS COUNCIL 2000

### President

James S. Langer,\* *University of California, Santa Barbara*

### President-Elect

George H. Trilling,\* *Lawrence Berkeley National Laboratory*

### Vice President

William F. Brinkman,\* *Bell Labs-Lucent Technologies*

### Executive Officer

Judy R. Franz,\* *University of Alabama, Huntsville (on leave)*

### Treasurer

Thomas McIlrath,\* *University of Maryland (emeritus)*

### Editor-in-Chief

Martin Blume,\* *Brookhaven National Laboratory*

### Past-President

Jerome Friedman,\* *Massachusetts Institute of Technology*

### General Councillors

Beverly Berger, Philip Bucksbaum, L. Craig Davis, Stuart Freedman, S. James Gates,\* Leon Lederman, Cynthia McIntyre, Margaret Murnane, Roberto Peccei, Paul Percy,\* Philip Phillips, Helen Quinn,\* Jin-Joo Song, James Trefil, Virginia Trimble,\* Sau Lan Wu

### Chair, Nominating Committee

Michael Turner

### Chair, Panel on Public Affairs

Roberta Saxon

### Division and Forum Councillors

Steven Holt\* (*Astrophysics*), Eric Heller, Harold Metcalf (*Atomic, Molecular, and Optical*), Robert Callender (*Biological*), Stephen Leone (*Chemical*), E. Dan Dahlberg, Allen Goldman, Arthur Hebard,\* Zachary Fisk\* (*Condensed Matter*), Steven White (*Computational*), Jerry Golub (*Fluid Dynamics*), James Wynne (*Forum on Education*), Gloria Lubkin\* (*Forum on History of Physics*), Stuart Wolf (*Forum on Industrial and Applied Physics*), Myriam Sarachik (*Forum on International Physics*), Ed Gerjuoy (*Forum on Physics and Society*), Andrew Lovinger (*Polymer*), Carl Lineberger (*Laser Science*), Howard Birnbaum (*Materials*), John D. Walecka (*Nuclear*), Sally Dawson, Peter Meyers (*Particles and Fields*), Robert Siemann (*Physics of Beams*), Richard Hazeltine (*Plasma*)

\**Members of APS Executive Board*

## ADVISORS

### Sectional Representatives

Kannan Jagannathan, *New England*; Carolyn MacDonald, *New York*; Perry P. Yaney, *Ohio*; Joseph Hamilton, *South-eastern*; Stephen Baker, *Texas*

### Representatives from Other Societies

Ruth Howes, *AAPT*; Marc Brodsky, *AIP*

Editor: Donna M. Baudrau, CMP

Meetings Publications Coordinator:

Vinaya K. Sathyasheelappa

## APS MEETINGS DEPARTMENT

### One Physics Ellipse

College Park, MD 20740-3844

Telephone: (301) 209-3286

FAX: (301) 209-0866

Donna Baudrau, *Director of Meetings and Conventions*

Terri Adorjan, *Senior Meeting Planner*

Karen MacFarland, *Meeting Planner*

Don Wise, *Registrar*

## Staff Representatives

Alan Chodos, *Associate Executive Officer*; Irving Lerch, *Director of International Affairs*; Fredrick Stein, *Director of Education and Outreach*; Robert L. Park, *Director, Public Information*; Michael Lubell, *Director, Public Affairs*; Stanley Brown, *Editorial Director*; Charles Muller, *Director, Journal Operations*; Michael Stephens, *Controller and Assistant Treasurer*

The *Bulletin of The American Physical Society* is published 10X in 2000—March, April, June, July, October (3X), November (2X), and December—by The American Physical Society through the American Institute of Physics. It contains information about meetings of the Society, including abstracts of papers to be presented, as well as transactions of past meetings. Reprints of papers can be obtained only by writing directly to the authors.

The *Bulletin* is delivered, on subscription, by Periodicals mail. Complete volumes are also available on microfilm. **APS Members** may subscribe to individual issues, or for the entire year. **Nonmembers** may subscribe to the *Bulletin* at the following rates: Domestic \$500; Foreign Surface \$520; Air Freight \$545. Information on prices, as well as subscription orders, renewals, and address changes, should be addressed as follows: **For APS Members**—Membership Department, The American Physical Society, One Physics Ellipse, College Park, MD 20740-3844. **For Nonmembers**—Circulation and Fulfillment Division, The American Institute of Physics, Suite 1NO1, 2 Huntington Quadrangle, Melville, NY 11747-4502. Allow at least 6 weeks advance notice. For address changes, please send both the old and new addresses, and, if possible, include a mailing label from a recent issue. Requests from subscribers for missing issues will be honored without charge only if received within 6 months of the issue's actual date of publication.

The *Bulletin of The American Physical Society* (ISSN: 0003-0503) is published ten times a year for The American Physical Society by the American Institute of Physics. 2000 subscription rate is \$500 for domestic nonmembers. Postmaster: Send address changes to *Bulletin of The American Physical Society*, AIP, Suite 1NO1, 2 Huntington Quadrangle, Melville, NY 11747-4502. Periodicals postage paid at Huntington Station, NY, and additional mailing offices.

**On the Cover:** Photo courtesy University of Houston.

# BULLETIN

OF THE AMERICAN PHYSICAL SOCIETY

Vol. 45, No. 6, October 2000

GEC Meeting

## TABLE OF CONTENTS

General Information.....	3
Arranged Oral and Poster Sessions.....	3
Oral Presentations.....	3
Lab Tours.....	4
GEC Student Award for Excellence.....	4
Registration.....	4
Opening Reception.....	4
Conference Banquet.....	4
E-mail and Other Business Services.....	4
Audio-Visual Equipment.....	4
Dining Options.....	4
Guest Program.....	4
Call for Nominations for GEC General and Executive Committees.....	5
GEC Executive Committee.....	5
Conference Secretary.....	6
Please Note.....	6
Epitome.....	7
Main Text.....	9
<i>Tuesday</i> .....	9

<i>Wednesday</i> .....	35
<i>Thursday</i> .....	55
<i>Friday</i> .....	67
<b>Author Index</b> .....	73
<b>Maps</b> .....	At End of Issue
<b>Condensed Epitome</b> .....	Back Cover

---



---

# 53rd Annual Gaseous Electronics Conference

## October 24–27, 2000

### *Houston, Texas*

---



---

## GENERAL INFORMATION

Welcome to the 53rd Annual Gaseous Electronics Conference (GEC), a topical conference of the American Physical Society. The GEC00 program will include a GEC Foundation Talk and the annual GEC Student Award for Excellence. Oral sessions of both invited and contributed papers and two poster sessions will address a broad range of topics. The Red Lion Hotel near the Houston Galleria will serve as headquarters for the conference. All oral sessions will be held at the Red Lion. The Crowne Plaza Hotel, only a minutes walk from the Red Lion, will host the poster sessions.

The GEC Foundation Talk, *Evolution of Computational Studies of Electron Swarm Experiments and Their Application to Discharge Simulations*, will be given by *Hiroaki Tagashira*.

## ARRANGED ORAL AND POSTER SESSIONS ARE:

- Rydberg Atom Phenomena (*Session AT1*)
- Plasma-Surface Interactions (*Session AT2*)
- Chlorine Plasmas (*Session BT1*)
- Sheaths and Boundary Layers (*Session BT2*)
- Electron-Molecule/Molecular Ion Interactions (*Session CT1*)
- Glow Discharges (*Session CT2*)
- High Pressure Arcs (*Session DT1*)
- Inductively Coupled Plasmas I (*Session DT2*)
- Interactions with Excited Species (*Session GW1*)
- Electron-Atom/Molecule Collisions I (*Session IW1*)
- GEC Cell 10-Year Perspective (*Session IW2*)
- Electron-Atom/Molecule Collisions II (*Session KR1*)
- Inductively Coupled Plasmas II (*Session KR2*)
- Atmospheric Discharges/Environmental Applications (*Session LR1*)
- Diagnostics I (*Session LR2*)
- Low Pressure Lamps and Discharges (*Session MR1*)
- Etching/Deposition (*Session MR2*)
- New Materials/Dusty Plasmas (*Session NR2*)
- Discharge Kinetics (*Session PF1*)
- Diagnostics II (*Session PF2*)
- Microdischarges for Displays and Lamps (*Session QF1*)
- Diagnostics III (*Session QF2*)
- RF Glows (*Session ETP1*)
- DC Glows (*Session ETP13*)
- Microwave Glows (*Session ETP18*)
- Glows (*Session ETP20*)
- Plasma-Surface Interactions (*Session ETP27*)
- Electron and Photon Collisions (*Session ETP34*)
- Heavy Particle Collisions (*Session ETP41*)
- Diagnostics: Electrical Methods (*Session ETP47*)
- Diagnostics: Optical Methods (*Session ETP54*)
- Pulsed Plasmas (*Sessions JWP1*)
- Inductively Coupled Plasmas (*Session JWP7*)
- Magnetically Enhanced Plasmas (*Session JWP25*)
- Gas-Phase Chemistry (*Session JWP32*)
- Transport Effects (*Session JWP43*)
- Light Sources/UV Sources (*Session JWP54*)
- Materials Processing/Dusty Plasmas (*Session JWP64*)
- *Postdeadline Posters (JWP77)*

There will also be an open discussion, "Plasma Modeling: Needs and Opportunities," pertaining to the present status and future of plasma modeling. Issues to be addressed include integration of equipment and feature-scale models, fundamental data needs, technology transfer (from model developers to users), and modeling roadmap.

## ORAL PRESENTATIONS

Papers that have been accepted for presentation are listed in the technical program. Invited papers are allotted 25 minutes, with 5 additional minutes for questions and discussion. Oral contributed presentations are allot-

ted 12 minutes, with an additional 3 minutes for discussion. Please check <http://www.chee.uh.edu/GEC00> for poster board dimensions.

## LAB TOURS

A tour of selected physics/chemistry/engineering laboratories and the Texas Center for Superconductivity at the University of Houston (main campus) will take place Thursday, October 26, from 4:00 pm to 6:30 pm. The University is a 20-minute drive from the Red Lion. Transportation to and from campus will be provided. Shuttle busses will begin leaving the Red Lion at approximately 4:00 pm.

## GEC STUDENT AWARD FOR EXCELLENCE

In order to recognize the outstanding contributions students make to the Gaseous Electronics Conference, and encourage further student participation, the GEC will continue to award a prize for the best paper presented by a student. A subcommittee of the GEC executive committee will choose the award winner. Students competing for the \$500 award this year are:

**Leon Bekker**, Eindhoven University of Technology, [LR2.6] - *Thompson Scattering in Fluorescent Lamps*

**Rajesh Dorai**, University of Illinois, [LR1.4] - *Simultaneous Remediation of NO<sub>x</sub> and Oxidation of Soot Using Dielectric Barrier Discharges*

**Sergi Gomez**, Queen's University, [AT2.4] - *Atomic Oxygen Density Measurements in a Low-Pressure Textile Processing Plasma*

**Ahmed Hala**, University of Wisconsin, [BT2.5] - *Presheaths in Two Ion Species Plasma*

**Sivananda Kanakasabharthy**, UT-Dallas, [AT2.3] - *Synchronized Biasing of Ion-Ion Plasma*

## REGISTRATION

The registration desk will be located in the River Oaks room at the Red Lion Hotel. Registration hours will be 6:00 pm to 9:00 pm on Monday, October 23, 2000 and 7:30 am to 3:00 pm on Tuesday through Thursday, October 24–26, 2000. The conference registration fee is \$230 (\$280 if received after September 15, 2000). Students and retirees pay only \$130 for registration. The registration fee includes the opening reception, refreshment breaks, and conference materials. For students and retirees, the banquet is also included in the registration fee.

## OPENING RECEPTION

The University of Houston will sponsor an opening reception for GEC participants and their guests. The reception will start at 7:00 pm and will be held on Monday, October 23, 2000 in the Grand Ballroom at the Red Lion Hotel.

## CONFERENCE BANQUET

A banquet will be held, also at Red Lion, on Thursday, October 26. Conference participants and their guests are encouraged to attend the banquet. The banquet will be preceded by a reception starting at 7:30 pm.

## E-MAIL AND OTHER BUSINESS SERVICES

Free e-mail access will be available to conference participants. Fax, photocopy services, and office supplies will also be available at the Business Center of the Red Lion and Crowne Plaza hotels.

## AUDIO-VISUAL EQUIPMENT

Each conference room will be equipped with an overhead projector and slide projector. If additional equipment is required, please contact the conference secretary.

## DINING OPTIONS

A wide variety of dining options is available for conference participants and their guests. Several restaurants are within a few blocks from the Red Lion or Crowne Plaza hotels. In addition, many fine restaurants, in a variety of price ranges, are located within a mile's range from either hotel. Both the Red Lion and the Crowne Plaza hotels offer **free shuttle** service within a three-mile radius from the hotels.

## GUEST PROGRAM

While it is the capital of the international energy industry, Houston is much more than an oil town. The

city offers a world-renowned Medical Center, the center for American manned space flight, NASA's Johnson Space Center, astonishing performing and visual arts, and the world's largest rodeo! Houston's arts scene thrives on many levels. The city is very proud of its theater district, which boasts nearly 10,000 theater seats for its grand opera, world-class ballet, award-winning theater and superb symphony. Other performance options include a long list of theater companies, dance companies, performance-art groups and classical music performers. The nightlife canvas in the city covers a broad spectrum of entertainment, from indoor/outdoor rock venues to jamming blues joints, intimate jazz haunts and hip downtown music venues. Throughout the year, some of the top names in the music industry headline at the many pavilions, theaters and outdoor spaces. Equally diverse is Houston's visual-arts community. With nearly a dozen major institutions and hundreds of smaller museums and galleries, Houston offers a world of visual inspiration.

Houston is also renowned for the great variety of shopping it provides: the Galleria, the recently opened Uptown Mall, the Highland Village, the River Oaks Shopping Center, the Town and Country Village, antiques in the Upper Kirby District and the Heights neighborhood, colorful stores in the Montrose area and bargains at the Katy Mills and the Conroe Outlet Mall.

Detailed information on Houston may be found at: <http://www.houston-guide.com/>

## **CALL FOR NOMINATIONS FOR GEC GENERAL AND EXECUTIVE COMMITTEES**

The GEC Executive Committee (ExComm) is the governing body of the GEC. It is the responsibility of ExComm to oversee all aspects of the conference. This includes selection of meeting sites, budgetary decisions, selection of special topics and invited speakers, accepting/rejecting abstracts and arranging of the program. The ExComm formally meets 3 times a year: the General Committee and ExComm meetings during the GEC, and the Summer ExComm Meeting where the program of the next GEC is arranged. There are numerous communications between members of the ExComm (usually e-mail) during the year to see to the successful completion of their duties. We have been fortunate over

the years to have a dedicated group of volunteers who have been willing to take on these very necessary roles.

The bylaws of the Gaseous Electronics Conference describe the process whereby members of the ExComm are elected. At the GEC Business Meeting (to be held on Wednesday, October 25, at 11:30 am in the Grand Ballroom at the Red Lion Hotel) nominations are accepted for members of the GEC General Committee (GenComm). The GenComm consists of the ExComm and 6 at-large members elected at the Business Meeting. The eligible voting membership of the GEC (defined as those attending the Business Meeting) elect these 6 at-large members. The GenComm then meets to fulfill its only duty: to elect new members of the ExComm.

The ExComm membership consists of the Chair, Treasurer, Past-Secretary, Secretary, Secretary-elect, past or incoming Chair and 4 at-large members. The Chair is a 4-year term (1-year incoming, 2-years chair, 1-year past-chair), the secretary is a 3-year term (1-year incoming, 1-year secretary, 1-year past-secretary), and all other ExComm members serve 2 years. (The secretary is the person who manages the local arrangements for the meeting and is usually "recruited" and appointed to the ExComm.)

The ExComm welcomes nominations, including self-nominations, for both the GenComm and ExComm. Becoming a GenComm and/or ExComm member provides a unique opportunity to see both how the GEC is run and to influence its future direction by helping to define the programs and choose future sites. Please submit your nominations to the GEC Chair or any member of the ExComm. The ExComm also welcomes inquiries on hosting future GECs.

## **GEC EXECUTIVE COMMITTEE**

Gerry Hays, Chair  
Sandia National Laboratories  
Tim Sommerer, Chair-Elect  
GE Corporate Research  
Demetre Economou, Secretary  
University of Houston  
Leposava Vuskovic  
Past-Secretary  
Old Dominion University  
Robert McGrath

Secretary-Elect  
Pennsylvania State University  
Kristen Steffens, Treasurer  
NIST  
Ara Chutjian  
Jet Propulsion Laboratory  
Bill Graham  
The Queen's University  
Helen Hwang  
NASA Ames Research Center  
Bob Piejak  
Osram Sylvania Inc.  
Tom Rescigno  
Lawrence Livermore National Laboratory  
Peter Ventzek  
Motorola, Inc.  
Yukio Watanabe  
Kyushu University

## CONFERENCE SECRETARY

Professor Demetre Economou  
University of Houston  
Department of Chemical Engineering  
4800 Calhoun Road  
Houston, TX 77204-4792 USA  
713-743-4320 (Voice)  
713-743-4323 (FAX)  
email: [economou@uh.edu](mailto:economou@uh.edu)

## ***PLEASE NOTE***

The APS has made every effort to provide accurate and complete information in this *Bulletin*. Changes or corrections, however, may occasionally be necessary, and may be made without notice after the date of publication. To ensure that you receive the most up-to-date information, please check the meeting *Corrigenda* distributed with this *Bulletin*.



## *Epitome of the 2000 GEC Meeting*

**8:15 TUESDAY MORNING**  
24 OCTOBER 2000

- AT1            **Rydberg Atom Phenomena**  
*MacAdam, Morrison, Dunning*  
Grand Ballroom D, Red Lion Hotel
- AT2            **Plasma-Surface Interactions**  
Grand Ballroom C, Red Lion Hotel

**10:30 TUESDAY MORNING**  
24 OCTOBER 2000

- BT1            **Chlorine Plasmas**  
*Overzet, Donnelly, Nanbu*  
Grand Ballroom D, Red Lion Hotel
- BT2            **Sheaths and Boundary Layers**  
*Rauf*  
Grand Ballroom C, Red Lion Hotel

**13:30 TUESDAY AFTERNOON**  
24 OCTOBER 2000

- CT1            **Electron-Molecule/Molecular Ion Interactions**  
*Larsson, Kimura*  
Grand Ballroom D, Red Lion Hotel
- CT2            **Glow Discharges**  
Grand Ballroom C, Red Lion Hotel

**16:15 TUESDAY AFTERNOON**  
24 OCTOBER 2000

- DT1            **High Pressure Arcs**  
*Coulombe, Gleizes, Murphy*  
Grand Ballroom D, Red Lion Hotel
- DT2            **Inductively Coupled Plasmas I**  
Grand Ballroom C, Red Lion Hotel

**20:00 TUESDAY EVENING**  
24 OCTOBER 2000

- ETP            **Poster Session I**  
Westheimer Ballroom, Crowne Plaza Galleria

**8:00 WEDNESDAY MORNING**  
25 OCTOBER 2000

- FW1            **Foundations of Gaseous Electronics**  
*Tagashira*  
Grand Ballroom, Red Lion Hotel

**9:45 WEDNESDAY MORNING**  
25 OCTOBER 2000

- GW1            **Interactions with Excited Species**  
*Christophorou, Čadež, Pinnaduwege*  
Grand Ballroom, Red Lion Hotel

**11:30 WEDNESDAY MORNING**  
25 OCTOBER 2000

- HW1            **General Business Meeting**  
Grand Ballroom, Red Lion Hotel

**14:00 WEDNESDAY AFTERNOON**  
25 OCTOBER 2000

- IW1            **Electron-Atom/Molecule Collisions I**  
*Crowe, Stelbovics*  
Grand Ballroom D, Red Lion Hotel
- IW2            **GEC Cell—10 Year Perspective**  
*Olthoff, Hebner, Sobolewski*  
Grand Ballroom C, Red Lion Hotel

**16:30 WEDNESDAY AFTERNOON**  
25 OCTOBER 2000

- JWP            **Poster Session II**  
Westheimer Ballroom, Crowne Plaza Galleria

**8:00 THURSDAY MORNING**  
26 OCTOBER 2000

- KR1            **Electron-Atom/Molecule Collisions II**  
*Rescigno, Gay*  
Grand Ballroom D, Red Lion Hotel

KR2 **Inductively Coupled Plasmas II**  
Grand Ballroom C, Red Lion Hotel

19:30 THURSDAY EVENING  
26 OCTOBER 2000

10:30 THURSDAY MORNING  
26 OCTOBER 2000

OR1 **Banquet**  
Grand Ballroom, Red Lion Hotel

LR1 **Atmospheric Discharges/  
Environmental Applications**  
*Inan*  
Grand Ballroom D, Red Lion Hotel

8:00 FRIDAY MORNING  
27 OCTOBER 2000

LR2 **Diagnostics I**  
*Czarnetzki*  
Grand Ballroom C, Red Lion Hotel

PF1 **Discharge Kinetics**  
Grand Ballroom D, Red Lion Hotel

PF2 **Diagnostics II**  
Grand Ballroom C, Red Lion Hotel

13:30 THURSDAY AFTERNOON  
26 OCTOBER 2000

MR1 **Low Pressure Lamps and  
Discharges**  
Grand Ballroom D, Red Lion Hotel

10:15 FRIDAY MORNING  
27 OCTOBER 2000

MR2 **Etching/Deposition**  
*Winstead*  
Grand Ballroom C, Red Lion Hotel

QF1 **Microdischarges for Displays  
and Lamps**  
Grand Ballroom D, Red Lion Hotel

QF2 **Diagnostics III**  
*Anderson*  
Grand Ballroom C, Red Lion Hotel

16:00 THURSDAY AFTERNOON  
26 OCTOBER 2000

NR1 **Lab Tours**  
University of Houston

12:15 FRIDAY AFTERNOON  
27 OCTOBER 2000

NR2 **New Materials/Dusty Plasmas**  
*Meyyappan, Mieno, Morfill*  
Grand Ballroom C, Red Lion Hotel

RF1 **Plasma Modeling: Needs and  
Opportunities**

## MAIN TEXT

## SESSION AT1: RYDBERG ATOM PHENOMENA

Tuesday morning, 24 October 2000; Grand Ballroom D, Red Lion Hotel at 8:15; Ara Chutjian, California Institute of Technology/Jet Propulsion Laboratory, presiding

*Invited Papers*

8:15

**AT1 1 Collisions of Rydberg Atoms with Charged Particles.**

KEITH B. MACADAM, *Department of Physics and Astronomy, University of Kentucky, Lexington KY 40506\**

The long range of Coulomb interactions, together with the large size, long radiative lifetimes and high state densities of highly excited Rydberg atoms, results in inelastic collision cross sections of prodigious size – often large enough to outweigh small number densities in astrophysical and cool laboratory plasmas – and in other unusual features. This talk will provide: (a) a brief survey of the significant features of collisions between electron or positive ions and state-selected Rydberg atoms and of recent experiments<sup>1</sup> to investigate them; (b) an introduction to some of the special techniques that have been developed<sup>2</sup> for preparation, manipulation and detection of Rydberg atoms; and (c) a glimpse at new directions in Rydberg atom collision research.

\*Work supported in part by NSF under grant PHY-9704544.

<sup>1</sup>O. Makarov and K.B. MacAdam, *Phys. Rev. A* **60**, 2131-8 (1999); and K.B. MacAdam, J.C. Day and D.M. Homan, *Comm. At. Mol. Phys./Comm. Mod. Phys.* **1(2)**, Part D, 57-73 (1999).

<sup>2</sup>J.L. Horn, D.M. Homan, C.S. Hwang, W.L. Fuqua III and K.B. MacAdam, *Rev. Sci. Instrum.* **69**, 4086-93 (1998).

8:45

**AT1 2 Unexpected Alignment Phenomena in Near-resonant Energy-transfer Collisions of Rare-gas Atoms with Rydberg Atoms.\***

MICHAEL A. MORRISON, *Univ. of Oklahoma*

Studies of alignment phenomena provide detailed insight into fundamental mechanisms that influence the dynamics and properties of colliding particles.<sup>1</sup> The initial state of the valence electron in the target is aligned (e.g., via multiple pulsed-laser excitation), and inelastic cross sections are analyzed for a dependence on the angle between the polarization of the exciting laser and the relative velocity of the rare-gas projectile. If present, alignment effects signify that the excited electron “remembers” its initial alignment through the collision. Nearly all previous investigations of alignment in near-resonant energy transfer collisions have considered targets in *low-lying* excited states, not Rydberg states. The qualitative explanations of alignment effects observed in these experiments—arguments predicated on the formation of a transient quasi-molecular electronic state—are not germane to collisions with *Rydberg* atoms, where the electron’s comparatively low speed and extremely diffuse probability density invalidate a molecular (Born-Oppenheimer) description of the dynamics. Hence cross sections for collisions with *Rydberg* atoms were not expected to manifest alignment effects. Nevertheless, recent measurements<sup>2</sup> revealed unambiguous alignment phenomena in the  $17d \rightarrow 18p$  transition in Ca resulting from collisions with ground-state Xe atoms at a single mean relative velocity. Coterminal quantum calculations at the University of Oklahoma<sup>3</sup> confirmed these results and, by exploring a wide range of relative velocities, uncovered hitherto unknown oscillatory structures in the cross sections for this transition. As initially mysterious as the alignment effects themselves, these oscillations depend strikingly on the initial and final magnetic quantum numbers of the electron. Application of semi-classical and classical techniques illuminate the physical mechanisms behind these structures.

\*Funded by NSF grant PHY-9722055.

<sup>1</sup>J. P. J. Driesen and S. R. Leone, *J. Phys. Chem.*, **96**, 6136 (1992) and Refs. therein.

<sup>2</sup>E. M. Spain, M. J. Dalberth, P. D. Kleiber, S. R. Leone, S. S. Op de Beek, and J. P. J. Driesen, *J. Chem. Phys.*, **102**, 9532 (1995)

<sup>3</sup>W. A. Isaacs and M. A. Morrison, *Phys. Rev. A*, **57**, R9 (1999)

9:15

**AT1 3 High Rydberg atoms: a nanoscale electron collisions laboratory.**F. BARRY DUNNING, *Department of Physics & Astronomy, Rice University, 6100 Main St., Houston, TX 77005*

Atoms in which one electron is excited to a state of large principal quantum number  $n$ , termed Rydberg atoms, are physically very large. The average separation between the excited electron and core ion is such that, in collisions with neutral targets, they behave not as an atom but rather as a pair of independent particles. Studies of collision processes that are dominated by the electron/target interaction can provide information on electron/molecule scattering at energies that extend down to a few microelectronvolts. Collisions with attaching targets can lead to ion formation through electron capture in a binary interaction between the excited electron and target molecule. Capture leads to creation of transient, excited parent negative ions that may subsequently dissociate, undergo autodetachment, or be "stabilized" by intramolecular vibrational relaxation. New insights into each of these processes, and into the lifetime of the intermediate (on a ps timescale), can be obtained by measuring the angular and velocity distributions of the positive and/or negative ions produced in Rydberg atom collisions. Collisions with Rydberg atoms also provide a novel source of dipole-bound negative ions, and have demonstrated the importance of dipole-supported real and virtual states in superelastic electron scattering from polar targets. These applications of Rydberg atoms will be discussed together with some recent results. Research supported by the National Science Foundation and the Robert A. Welch Foundation.

**SESSION AT2: PLASMA-SURFACE INTERACTIONS**

Tuesday morning, 24 October 2000

Grand Ballroom C, Red Lion Hotel at 8:15

S. Rauf, Motorola, Inc., presiding

*Contributed Papers*

8:15

**AT2 1 Ion Energy Distributions Inside Silicon Structures at the RF-Biased Electrode in an Inductively-Driven Discharge**

ION ABRAHAM, *Sandia National Labs* JOSEPH WOODWORTH, MERLE RILEY, PAUL MILLER, *Sandia National Labs* We report the energy distributions of ions striking an rf-biased electrode in discharges in an inductively-driven Gaseous Electronics Conference Reference cell. Using a mass-and-energy sensitive ion analyzer we examined the ion energy spectra for ions of several masses in discharges containing mixtures of the noble gases Ar, Ne, and Xe. The ions were sampled thru a pinhole in the rf-biased lower electrode. Silicon structures were also bonded to the pinhole plate, and the influence of pinhole position with respect to the silicon structure was examined. Oscillations of the plasma potential and the rf-bias waveforms on the driven electrode were directly measured to compare to the ion energy spectra. The ion energy distributions, which had a single peak and a width of 3.5 eV (FWHM) when the electrode was not biased, split into double peaked distributions as rf-bias was applied to the electrode. The influence of ICP coil power, rf-bias power, and pressure was investigated. Measurements of plasma densities and temperatures as well as comparisons to model ion energy distributions will be presented. Sandia is a multiprogram laboratory operated by Sandia Corporation, a Lockheed Martin Company, for the United States Department of Energy under Contract DE-ACO4-94AL85000.

8:30

**AT2 2 Energy and Angular Distribution of Ions Effusing from a Hole in Contact with a Plasma**

DOOSIK KIM, CHANG-KOO KIM, DEMETRE ECONOMOU, *Department of Chemical Engineering, University of Houston, Houston, TX 77204-4792\** The energy and angular distribution of ions extracted from a hole in contact with a low-temperature plasma have been investigated both computationally and experimentally. A single hole is thought to be a well-defined system for understanding the interaction of a plasma with a biased grid. Such plasma-grid interaction finds ap-

plications in neutral beam etching, ion sources, satellite thrusters, etc. The plasma parameters (Debye length), hole diameter and thickness determine the characteristics of the ions (and fast neutrals) extracted through the hole. We have developed a Monte Carlo simulation to follow the trajectories of ions and fast neutrals from the bulk plasma through the sheath and out the hole. Collisions with gas phase species and the walls of the hole are taken into account. We have also measured the energy and angular distribution of ions effusing from a hole on a wall in contact with a high density plasma. A hemispherical sectioned electrode is used as the detector. The hole diameter is varied from 25 to 1000 microns and the hole aspect ratio (depth to diameter) is varied from 0.25 to 10. The energy and angular distributions in both experimental data and simulations reflect the strong disturbance of the sheath when the hole size exceeds the local Debye length.

\*Work supported by Sandia National Labs and the NSF

8:45

**AT2 3 Synchronized Biasing of Ion-ion plasma**

SIVANANDA KANAKASABAPATHY, *University of Texas at Dallas* MARWAN KHATER, *University of Texas at Dallas* LAWRENCE OVERZET, *University of Texas at Dallas* Ion-ion plasmas are relatively electron-free, positive and negative ion only plasmas formed in the afterglow of Pulsed-power high electron affinity gas (e.g.:  $\text{Cl}_2$ ) discharges. They hold the potential to provide ambipolar fluxes of positive and negative ions that could reduce differential charging of high anisotropy structures which cause etch non-idealities. Time-resolved Langmuir probe and Microwave Interferometry measurements in a pulsed ICP discharge show that electrons are quickly lost to dissociative attachment (10's of  $\mu\text{secs}$ ) after turning power off. Time-resolved mass spectrometry has correlated the vanishing of electrons and consequently the confining plasma potential to the incipience of a negative ion ( $\text{Cl}^-$ ) surface flux. Parametric characterization of Pulsed  $\text{Cl}_2$  discharges has indicated that low pressures (1 mTorr), high powers (300 W peak), mid duty ratios (50%) and low pulse frequency (500 Hz), maximize this negative ion flux. Langmuir probe ion density decay rate measurements have shown ion-ion recombination to be the dominant loss process. We observe reproducible alternating irradiations of positive ( $\text{Cl}_2^+$ ) and negative ( $\text{Cl}^-$ ) ions corresponding to the negative and positive half-cycles respectively of a low frequency (20 kHz) bias applied to the mass spectrometer pinhole. This bias is applied as a phase-locked burst that is synchronized with the formation of ion-ion plasmas. Parametric char-

acterization of this novel extraction technique reveals a bi-modal frequency response of the  $\text{Cl}^-$  surface flux. This presentation is based upon work supported by the NSF under Grant No. CTS-9713262.

9:00

**AT2 4 Atomic Oxygen Density Measurements in a Low Pressure Textile Processing Plasma** SERGI GOMEZ, PHILIP G. STEEN, WILLIAM G. GRAHAM, *Dept. of Pure and Applied Physics, The Queen's University of Belfast, Northern Ireland* There is increasing interest in plasma processing of textile materials. Here the effect of textile materials on atomic oxygen densities in a low pressure oxygen plasma has been investigated. Polypropylene and polyester samples were placed on the lower electrode of an inductively coupled Gaseous Electronic Conference (GEC) reactor, operated at low power. Operation with and without sample material is contrasted by comparing spatially resolved laser induced fluorescence (LIF) measurements of atomic oxygen at pressures from a few Pa to 133 Pa, and input powers from 10 to 300 W. The decrease of atomic oxygen density close to the exposed samples may be characterised by the net sticking coefficient,  $\alpha$ , which can be estimated from the concentration profile. We have obtained values for  $\alpha$  of  $0.3 \pm 0.1$  for stainless steel and  $0.28 \pm 0.08$  for polypropylene. Atomic oxygen dissociation fractions from a simple kinetic model agree to within a factor of 1.7 with those measured with LIF. \*Work supported by the EU BRITE programme.

9:15

**AT2 5 Molecular Dynamics Simulations of Fluorocarbon Film Etching and Deposition** J. TANAKA, *Mechanical Engineering Research Laboratory, Hitachi, Ltd.* The fluorocarbon surface layer formed during fluorocarbon plasma processing plays important roles; namely, the film prevents its underlayer from being etched by energetic ions, it provides etchants to the underlayer, and it also provides various radicals to plasma. To understand the mechanism of fluorocarbon-film formation, we have already formulated a C-F interatomic force potential<sup>1</sup>. Molecular dynamics simulations using this potential illustrates how fluorocarbon films are formed and etched by  $\text{CF}^+$ ,  $\text{CF}_2^+$ , and  $\text{CF}_3^+$ . The ratio of the number of carbon to fluorine atoms in the incoming ions determines fluorine concentration in the very near surface layer. And this concentration governs the etching of the fluorocarbon layer. In our previous study, the simulations were terminated too shortly (i.e., only 700 repetitions). In the current study, however, ion bombardments were repeated up to 4000 times. As a result, it was found that etch rate of the film fluctuates significantly. The transient properties of radical desorption after ion impacts are also presented.

<sup>1</sup>J. Tanaka et al., *J. Vac. Sci. Technol. A* **18**, 938 (2000).

9:30

**AT2 6 SiO<sub>2</sub> etching with ion energy distribution control** YASMIN ANDREW, *Center for Plasma Aided Manufacturing, University of Wisconsin-Madison* EUNSUK KO, JASMINE MACHIMA, RARCHAWDEE SILAPUNT, ANA I. TEIXEIRA, SHIANG-BAU WANG, AMY E. WENDT, *Center for Plasma Aided Manufacturing, University of Wisconsin-Madison* Ion energy distribution function (IEDF) control has been proposed by Wang and Wendt<sup>1</sup> as a method to improve fine feature profile control and SiO<sub>2</sub>/photoresist etch selectivity. An IEDF control technique could preserve the etched profile by shaping the IEDF to reduce the number of deflected ions or to modify the potential distribution along the etching profile. Improvement of etch selectivity reduces the demand for thick photoresist and the lithography technology challenge. The IEDF of a C<sub>4</sub>F<sub>8</sub>/Ar plasma used to sequentially etch blanket films of photoresist and SiO<sub>2</sub>, has been controlled using Wang and Wendt's tailored wafer bias waveform technique. The helicon etching tool uses a 3 kW, 13.56 MHz pulsed power supply. The power supply to the substrate stage provides arbitrary bias voltage waveforms, which have been carefully tailored to control the IEDF. Ion energy flux measurements have been made from the compensating slope of the tailored bias waveform. Comparison of these measurements with a conventional RF sinusoidal bias waveform is described. Finally, in situ laser interferometry measurements of SiO<sub>2</sub>/photoresist etch selectivity are presented.

<sup>1</sup>S. B. Wang and A.E. Wendt, "Control of ion-energy distribution at substrates during plasma processing" submitted to *J. Appl. Phys.* 1999.

9:45

**AT2 7 Carbon particle deposition by pulsed laser deposition coupled with RF plasma in rare gas environment\*** YOSHIYUKI SUDA, TOMOYUKI ONO, MASAMICHI AKAZAWA, YOSUKE SAKAI, *Hokkaido University, Sapporo, 060-8628, Japan* Carbon nano-particle production by pulsed laser deposition (PLD) has been intensively investigated because the particles are expected to be used as a high effective electron source.<sup>1</sup> In this report we will present the result of carbon particle generation by rare gas RF plasma aided PLD and the possibility to control the size and the structure of the particles by varying plasma condition (e.g. ambient gas, pressure). An ArF excimer laser (fluence: 5 J/cm<sup>2</sup>; wavelength: 193 nm; repetition rate: 10 Hz; typical deposition time: 30 min) is used as a light source, and the target material is sintered graphite. The RF plasma is generated in a helical coil installed between the substrate and target. The pressure of Ar and He is varied from 1.3 to 53 Pa. The surface morphology and structure of the particles are measured by a scanning electron microscope (SEM), an atomic force microscope (AFM), and an X-ray photoelectron spectroscope (XPS). The dependence of the size and property of the particles on the plasma condition are discussed.

\*Work in part supported by Grant-in-Aid 11750245 by the Ministry of Education, Science, Sports and Culture, Japan.

<sup>1</sup>Y. Suda, *Thin Solid Films*, in press

**SESSION BT1: CHLORINE PLASMAS**

Tuesday morning, 24 October 2000; Grand Ballroom D, Red Lion Hotel at 10:30; Helen Hwang, Eloret Corporation, presiding

*Invited Papers***10:30****BT1 1 Experimental Measurements of Ion-Ion Plasma Formation.\***

LAWRENCE J. OVERZET, *University of Texas at Dallas, Plasma Applications Laboratories, P.O. Box 830688, EC33, Richardson, TX 75083-0688*<sup>†</sup>

Ion-ion plasmas are also known as "nearly electron free" plasmas. Since the electron density is negligible, the positive ions and negative ions can dominate the flow of charge and both could potentially be used to process surfaces. Given appropriate biasing conditions, both positive and negative ions can be accelerated into a processing surface. Indeed, we will show mass spectrometric measurements of alternating irradiations of  $\text{Cl}^-$  and  $\text{Cl}_2^+$  ions in the afterglow of chlorine discharges. In addition, the ion flux to a processing surface decreases by about a factor of 2 from the active discharge to the initial ion-ion plasma. Using alternate irradiations from ion-ion plasma is an exciting possibility that several researchers have begun investigating since it could lower charge build-up on the surface and consequent device damage. We too have been examining ion-ion plasmas from a variety of perspectives. We have focused on better understanding how one might efficiently form ion-ion plasmas and on their spatial and temporal attributes. We have found that the transition to ion-ion plasma can occur quickly after the RF excitation is extinguished and that the subsequent decay of the ion-ion plasma is often dominated by ion-ion neutralization. These reactions can cause the plasma ion density to become more uniform in the early afterglow. We are also still learning to better probe ion-ion plasma and interpret the results. note

\*This material is based upon work supported by the National Science Foundation under grant number CTS-9713262 and by the UTD program in Electrical Engineering.

<sup>†</sup>Graduate students S. Kanakasabapathy, M. Khater and J. Kleber largely carried out the work. The author would like to thank his collaborator on ion-ion plasma research, D. Economou, along with M. Goeckner.

**11:00****BT1 2 Dynamics of Pulsed Chlorine Plasmas with and without Substrate RF-Bias.**

VINCENT M. DONNELLY,\* *Bell Laboratories, Lucent Technologies*

Pulsed plasmas can significantly decrease plasma-process-induced damage and reduce unwanted etch profile anomalies. In electronegative plasmas (e.g. chlorine), these benefits are often attributed to the build-up of negative ions (e.g.  $\text{Cl}^-$ ) in the OFF time, and the charge reduction that occurs when these negative ions reach the wafer. A reduction of the period-averaged electron temperature ( $T_e$ ) and impingement of low-energy positive ions are also thought to be important in reducing charge build-up and damage. We report results of a study of a chlorine, inductively-coupled pulsed plasma operated with and without a continuous radio frequency (rf) bias applied to the wafer stage. Without stage bias,  $T_e$  decays rapidly in the OFF period, as does electron density ( $n_e$ ) on a somewhat longer time scale. The decay in  $n_e$  is accompanied by a buildup in  $\text{Cl}^-$ . The plasma dynamics in the presence of rf bias power are nearly the same as with no bias in the first 20  $\mu\text{s}$  of the OFF period. Then, however, after reaching a minimum of 0.5 eV,  $T_e$  starts to increase rapidly and reaches values even higher than the steady state ON time values. Since  $n_e$  is still quite high when  $T_e$  goes through the minimum, the sheath near the wafer does not collapse and negative ions do not reach the wafer. In a previous study in a similar reactor, damage to thin gate oxide layers during aluminum etching was reduced while operating with a pulsed source and a continuous bias. This implies that the decreased damage cannot be attributed to a reduction of charging of the wafer by negative ions. We further show that increasing the duration of the OFF time or increasing the bias power leads to the transition of the plasma into a reactive ion etching (RIE) mode, when the decaying positive ion density reaches the level sustained by the stage power.

\*co-author: Mikhail V. Malyshev

**11:30****BT1 3 Comparison of Measured and Simulated Etch Rates in an Inductively-Coupled Plasma Reactor.**

K. NANBU, M. SHIOZAWA, H. SASAKI, *Institute of Fluid Science, Tohoku University*\*

Much work has been published on inductively coupled plasmas (ICP) for materials processing. However, one cannot predict yet the etch rate distribution on wafer only from computer simulation. Here we consider the etching of a rf biased silicon wafer using chlorine ICP. Our goal will be to construct a full simulation method the use of which makes it possible to predict measured etch rates. However, even for a simple chlorine plasma, surface chemistry on the wafer is complicated and we have only few data usable in simulations. Therefore, at present it is practical to introduce a simple reaction model including one or two free parameters and determine the parameters by comparing the simulated and

measured etch rates. In our apparatus eight-turn coils are wound on the quartz cylinder with diameter of 200 mm and height of 400 mm. The quartz cylinder is connected to the diffusion chamber with diameter of 347.6 mm and height of 400 mm. The electromagnetic field is calculated using Ventzek, Hoekstra and Kushner's method. The production rate of Cl radicals in this field is obtained using the Monte Carlo method for electron collisions. The transport, recombination, and surface reaction of radicals are calculated using the DSMC method. The effect of ion assist on silicon etching is simply represented by the reaction probability on the wafer. That is, all effects of electrostatic field and wafer biasing on the acceleration of ions are pushed into the reaction probability that is determined with the help of measured data. Comparison of simulations and measurements will be presented at the Conference.

\*Special thanks to Mr. M. Takahashi's effort in measurements

#### SESSION BT2: SHEATHS AND BOUNDARY LAYERS

Tuesday morning, 24 October 2000; Grand Ballroom C, Red Lion Hotel at 10:30; M. Goeckner, University of Texas at Dallas, presiding

#### Invited Paper

10:30

#### BT2 1 Nonlinear Plasma-Circuit Interaction in RF Plasma Processing Reactors.

SHAHID RAUF, *DigitalDNA™ Laboratories, Motorola Inc., 3501 Ed Bluestein Blvd., MD K-20, Austin, TX 78721*

Non-equilibrium plasmas interact with external radio-frequency (RF) circuitry through the sheaths. The sheaths at different reactor surfaces are generally coupled to each other and their current-voltage relationship is highly nonlinear. Consequently, one can observe a number of nonlinear phenomena in RF discharges including harmonic generation and interaction of different RF sources. This paper describes our work on the fundamental characteristics of plasma-circuit interaction in capacitively and inductively coupled discharges. Several applications that have resulted from this work are also discussed. This investigation utilizes a sheath-circuit model that has been coupled to the Hybrid Plasma Equipment Model.<sup>1</sup> The model has been characterized using electrical measurements on the GEC reference cell. Results show that nonlinear sheaths lead to currents and voltages that have significant amplitude at higher harmonics. As a consequence, external circuits that may appear similar to the plasma at the fundamental frequency can yield different plasma characteristics. Another consequence of the sheath's nonlinear behavior is that RF sources at different frequencies can interact with each other. The resulting plasma and electrical characteristics are therefore different from those due to the sum of individual sources.<sup>2</sup> The plasma-circuit interaction can be utilized in a number of ways to control or probe into the behavior of RF discharges. It is, for example, demonstrated that electrical measurements coupled with a sheath model can be used to measure plasma properties.<sup>3</sup> One can also fine tune the ion energy distribution at the electrodes by adjusting the RF bias voltage waveform.<sup>4</sup> Plasma-circuit interaction will be discussed in the context of both electronegative and electropositive plasmas.

<sup>1</sup>S. Rauf and M. J. Kushner, *J. Appl. Phys.* 83, 5087 (1998).

<sup>2</sup>S. Rauf and M. J. Kushner, *IEEE Trans. Plasma Sci.* 27, 1329 (1999).

<sup>3</sup>S. Rauf and M. J. Kushner, *Appl. Phys. Lett.* 73, 2730 (1998).

<sup>4</sup>S. Rauf, *J. Appl. Phys.* 87, 7647 (2000).

#### Contributed Papers

11:00

**BT2 2 Boundary effects on electron and ion transport\*** ALEX VASENKOV, *Department of Chemistry, University of British Columbia, 2036 Main Mall, Vancouver, British Columbia, V6T 1Z1, Canada* BERNIE SHIZGAL, *Department of Chemistry, University of British Columbia, 2036 Main Mall, Vancouver, British Columbia, V6T 1Z1, Canada* The non-hydrodynamic behavior of electrons and/or ions near an electrode is studied. A system of electrons or ions in argon and helium is considered in the positive one-dimensional spatial half-space with an absorbing boundary at the origin which represents an electrode. A flux of electrons or

ions is assumed to originate at infinite distance from the boundary. Elastic collisions for electrons and charge-exchange collisions for ions with the background moderator are taken into account. We solve the kinetic Boltzmann equation for electron and ion distribution functions in space and velocity with two direct numerical methods and a Monte Carlo simulation. The density and temperature profiles are determined and the departure from hydrodynamic behavior near the boundary is studied. The objective of the present work is to construct a self-consistent model of a discharge which couples the Poisson equation for the electric field with the electron/ion Boltzmann equation.

\*Acknowledgment is made to the Donors of the Petroleum Research Fund, administered by the American Chemical Society for support of this research (PRF 34689-AC6)

11:15

**BT2 3 Semianalytical ion dynamics model for non-collisional sheaths** DEEPAK BOSE, *Eloret Corp.* T. R. GOVINDAN, *NASA Ames Research Center* M. MEYYAPPAN, *NASA Ames Research Center* It is a formidable task to resolve a sub millimeter scale collisionless sheath in a multidimensional reactor scale model. Besides, the drift-diffusion formulation for ion transport becomes invalid in the sheath region. This makes it important that we have an analytical sheath model that can be used at plasma boundaries. When the rf bias frequency and the ion plasma frequency are of the same order, the ion inertia allows it to only partially follow the sheath field oscillations, thus making an exact analytical solution difficult. Miller and Riley [J. Appl. Phys. 82, 3689 (1997)] modeled the ion inertia by using the assumption of a damped potential. However, they did not include the effect of ion current oscillations inside the sheath. In this work we extend their model by including the effect of ion current modulation. We find marked improvements in the predictions of electric field, displacement current, and ion energy when compared with a full numerical solution of ion transport equations.

11:30

**BT2 4 Improving boundary conditions for the Child-Langmuir sheath model** M. S. BENILOV, *Departamento de Física, Universidade da Madeira, Largo do Município, 9000 Funchal, Portugal* A collision-free space-charge sheath formed by cold ions at a negative surface is considered. The method of matched asymptotic expansions is applied, small parameter being the ratio of the electron temperature to the sheath voltage. Two expansions are considered, one describing bulk of the sheath where the electron density is exponentially small as compared to the ion density, and another describing the outer section of the sheath in which the electron and ion densities are comparable. Boundary conditions for equations describing the bulk are obtained by matching with a solution describing the outer section. A choice is found of the boundary conditions such that the model have exponential accuracy. A physical meaning of these conditions is that the ions are accelerated in the outer section from the

Bohm velocity to twice the Bohm velocity and that the voltage drop in the outer section equals  $\frac{3}{2}kT_e/e$ . The model predicts the electric fields and ion velocity at the surface and the thickness of the ion layer to the accuracy of several per cent for sheath voltages exceeding  $3kT_e/e$ . The validity of the derived boundary conditions is not restricted to the case of a collisionless sheath: they are applicable also in cases when collisions play a role in the bulk of the sheath, provided that the Debye length in the quasineutral plasma is much smaller than the mean free path for collisions of ions and neutral particles.

11:45

**BT2 5 Presheaths in two ion species plasma** AHMED HALA, *University of Wisconsin-Madison* A new technique that uses ion acoustic wave velocity was developed to measure the ion flow-velocity in plasma presheaths. The plasma potential was measured simultaneously in the presheath using an emissive probe in Argon plasma at 1, 1.5 and 2 mTorr pressures. The presheath was found to be mobility limited. The potential drop relative to electron temperature in the presheath increased as the pressure increased to allow ions falling in the presheath to reach Bohm velocity. The technique also provided a way of measuring the total collision cross section for ion velocities that range between thermal to sound velocities. A different new technique was developed to measure the concentration of two ion species in two-ion plasma. By measuring the ion acoustic wave group velocity and electron temperature in the bulk region, the concentration of the two ion species can be determined. A new phenomenon was discovered as result of the interaction of the two ions in the presheath of Ar-He plasma. Due to the streaming of the two ion species in the electric field of the presheath, a two-ion stream instability was found to exist. The technique of measuring the ion drift velocity was extended to the two species plasma. The measured ion velocities and ion concentration show that Argon ions are moving faster than their sound velocity near the boundary while He ions are moving in a weak electric field. At the sheath edge the two ions are moving with one velocity that validates the Bohm criterion for two ion species.

#### SESSION CT1: ELECTRON-MOLECULE/MOLECULAR ION INTERACTIONS

Tuesday afternoon, 24 October 2000; Grand Ballroom D, Red Lion Hotel at 13:30; Kevin Martus, William Paterson University, presiding

##### Invited Paper

13:30

#### CT1 1 Electron-molecular ion interaction studied in storage rings.

MATS LARSSON, *Department of Physics, Stockholm University, Box 6730, S-113 85 Stockholm, Sweden E*

Ion storage rings have emerged as an excellent tool for the study of electron-molecular ion interaction. Molecular ions are stored at MeV energies in the ring for tens of seconds, which effectively removes vibrational excitations. They are allowed to interact with a cold electron beam in one section of the ring. Neutral or charged particles arising from the interaction of the stored ions with the electrons are detected. The collision energy is controlled by the cathode voltage of the electron gun. In Stockholm, the heavy-ion storage ring CRYRING is used to study molecular ions. Dissociative electron-molecular ion recombination will be described, and studies of molecular oxygen and water ions will be used as examples.



## Contributed Paper

14:00

**CT1 2 Preliminary observations of the dissociative recombination reaction of  $\text{He}_2^+$  from the  $v=4$  vibrational level.** KENNETH HARDY, I. BONICHE, L. COMAN, M. FAXAS, L. SIMONS, *Physics Department, Florida International University, Miami, FL 33199\** Measurements of the velocities of the final product state atoms from the dissociative recombination (DR) reaction of the  $\text{He}_2^+$  molecular ion in the  $v=4$  vibrational state have been made. The reaction populated the  $1s3s$  and  $1s3p$  atomic levels at  $184864.9 \text{ cm}^{-1}$  and  $185564.6 \text{ cm}^{-1}$ . We observed DR of  $\text{He}_2^+$  from different rotational states of the  $v=4$  vibrational level.

## Invited Paper

14:15

**CT1 3 Electron Scattering Processes from Plasma Processing Gases: CF<sub>3</sub>I, C<sub>3</sub>F<sub>8</sub> and C<sub>4</sub>F<sub>8</sub>.** MINEO KIMURA, *Graduate School of Science and Engineering, Yamaguchi University\**

Brief review of the current level of understanding of electron scattering processes from plasma processing gases such as CF<sub>3</sub>I, C<sub>3</sub>F<sub>8</sub> and C<sub>4</sub>F<sub>8</sub> will be presented. Experimental as well as theoretical studies for these gases have been carried out last a few years by several groups, and although the amount of cross-section data is still far from sufficient, we are able to establish the data set for some processes in these gases. I will briefly discuss possible next-generation processing gases.

\*The work was supported in part by the Ministry of Education, Science, Culture and Sport in Japan

## Contributed Papers

14:45

**CT1 4 Dissociative Electron Attachment in Chlorofluoromethanes\*** PAUL BURROW, *University of Nebraska-Lincoln* K. AFLATOONI, *University of Nebraska-Lincoln* The total dissociative electron attachment (DEA) cross sections of the chlorofluoromethanes are determined in an electron beam experiment and correlated with the vertical attachment energies (VAE) for formation of the lowest temporary negative ion states of these compounds. The latter are determined independently by electron transmission spectroscopy (ETS) and correspond to the energies of the anions at the equilibrium geometries of the neutral molecules. As we observed previously in the chloroalkanes<sup>1</sup>, the peak DEA cross sections are well correlated with VAE. For values of VAE between 0.9 to 3.0 eV, the peak DEA cross sections vary by more than four orders of magnitude. The correlation is attributable to the remarkably monotonic variation of the temporary anion widths, arising from their finite lifetimes, over this range of VAE.

\*Supported by NSF.

<sup>1</sup>K. Afatooni and P.D. Burrow, *J. Chem. Phys.* in press, July 2000.

15:00

**CT1 5 Dissociative electron attachment process to CF<sub>3</sub> radicals** D. HAYASHI, G.M.W. KROESEN, *Eindhoven University of Technology* To elucidate the electron attachment process to CF<sub>3</sub> radicals, electronic and geometrical structures of CF<sub>3</sub><sup>-</sup> and its parent CF<sub>3</sub> radicals were calculated by GAUSSIAN 98 package. All computations were carried out by Hartree-Fock method with the standard 6-311++G\*\* basis. The geometrical structures were optimised by the second-order Moller-Plesset perturbation theory. When a low-energy electron (< 5 eV) is captured by the ground-

Using TOF techniques we determined the velocities of the final product atoms and from this directly measured the kinetic energy released in the DR reaction from which the rotational energies can be determined. Using the energies of the rotational states  $F_v(J)$  and the expression,  $F_v(J) = B_v J(J+1) + D_v J^2(J+1)^2$ , the rotational constants  $B_v$  and  $D_v$  of the  $v=4$  level of the molecular ion were determined. Here, new experimental results from studies of the DR reaction in helium are presented and the preliminary results for the rotational constants are  $B_v = 6.11 \pm 0.2 \text{ cm}^{-1}$  and  $D_v = 9.5 \times 10^{-5} \pm 0.0004 \text{ cm}^{-1}$  for the  $v=4$  vibrational level.

\*I.B. thanks NSF REU;M.C.,M.F.,L.S.,and K.H. thank LLNL HBC/MU and NASA

state CF<sub>3</sub>(C<sub>3v</sub>), it is plausible that they first form a negative ion state (denoted as CF<sub>3</sub><sup>-\*</sup>) with the same geometry (bond length of C-F ( $r_{CF}$ ) and angle FCF and symmetry as those of CF<sub>3</sub>, and then CF<sub>3</sub><sup>-\*</sup> changes its geometry. The potential energy of CF<sub>3</sub>, CF<sub>3</sub><sup>-\*</sup> and the ground-state negative ion CF<sub>3</sub>(C<sub>3v</sub>) were examined by scanning  $r_{CF}$ . The potential energy of CF<sub>3</sub><sup>-\*</sup> at the equilibrium  $r_{CF}$  of CF<sub>3</sub> is the same as that of CF<sub>3</sub>, while that of CF<sub>3</sub><sup>-</sup> is 0.5 eV lower than that of CF<sub>3</sub>. The potential energy surface of dissociation channel CF<sub>3</sub><sup>-</sup> → F<sup>-</sup>(<sup>1</sup>S) + CF<sub>2</sub>(<sup>1</sup>A<sub>1</sub>) was calculated as a function of C-F<sup>-</sup>( $r_{CF}$ ). The dissociation state F<sup>-</sup> + CF<sub>2</sub> locates a few tens meV higher to the equilibrium state of CF<sub>3</sub>. These results imply that the attachment of low-energy electrons (~ 1 eV) results in the formation of CF<sub>3</sub><sup>-\*</sup>. Since the total energy of the CF<sub>3</sub><sup>-\*</sup> is slightly exothermic against the dissociation, it automatically dissociates into F<sup>-</sup> + CF<sub>2</sub>.

15:15

**CT1 6 Electron Interactions with CF<sub>3</sub>I** LOUCAS CHRISTOPHOROU, *NIST* JAMES OLTHOFF, *NIST* CF<sub>3</sub>I is a potential plasma processing gas that has a short environmental lifetime and that produces copious quantities of CF<sub>3</sub><sup>+</sup> and CF<sub>3</sub> in low temperature plasmas. Low-energy electron collision data for CF<sub>3</sub>I are sparse. Limited cross section data are available only for total and differential elastic electron scattering, electron-impact ionization, and electron attachment. These data have been synthesized and assessed and will be presented and discussed. There is a need for further scrutiny of these data and for measurements of the cross sections of all other main electron-collision processes. There is a need also for measurements of the electron transport, ionization, and attachment coefficients of this molecule.

## SESSION CT2: GLOW DISCHARGES

Tuesday afternoon, 24 October 2000

Grand Ballroom C, Red Lion Hotel at 13:30

Vikas Midha, GE Research and Development, presiding

## Contributed Papers

13:30

**CT2 1 Kinetic modeling of a collisionlessly heated planar surface-wave plasma in terms of non-local electron energy distribution function** I. GHANASHEV, L. TSENDIN,\*H. SUGAI, Nagoya University, Japan Recent measurements in low pressure surface-wave plasma (SWP) showed well pronounced non-Maxwellian electron energy distribution functions (EEDFs) with  $f(\epsilon)$  decreasing significantly slower than a Maxwellian EEDF at high electron energies  $\epsilon > 10$  eV. This combination of many high-energy electrons with low electron temperature of the bulk, low-energy electrons can partially explain the reported superior dry etching performance of SWPs. In this contribution we present a kinetic model of low pressure ( $\sim 10$  mTorr) argon SWP in slab geometry at conditions for which the electron diffuses in real space much faster than in energy space, so that the non-local approximation can be applied and the EEDF can be considered a function of the total energy  $f(\mathbf{v}, \mathbf{r}) = f(m_e v^2/2 + e\Phi(\mathbf{r}))$ . The electrons are heated by diffusing in energy space from lower to higher energies. A non-Maxwellian EEDF with slowly decaying tail similar to the experimentally observed one is obtained if the electrons' diffusion coefficient (in energy space) increases with their energy. This is indeed the case for low-pressure SWPs, where only high energy electrons not confined by the plasma potential can reach the high potential energy zone near the plasma boundary in order to be scattered to other energies by the microwave field localized there.

\*St. Petersburg State Technical University, Russia

13:45

**CT2 2 Modeling of Large Diameter Microwave Discharges Excited by a Coaxial Structure** L.L. ALVES, CFP, IST (Portugal) C. BOISSE-LAPORTE, G. GOUSSET, LPGP, Univ. Paris-Sud (France) This paper deals with the modeling of low pressure, large diameter 2.45 GHz surface wave discharge excited by a coaxial structure. A  $m = 0$  propagation mode develops between an inner antenna (metal rod), surrounded by dielectric of radius  $R_A$ , and an outer conductor of radius  $R_B \gg R_A$ . A stationary one-dimensional fluid model is used to calculate the radial profiles of densities and fluxes of positive ions and electrons, the space-charge field  $E_r$ , and the electron mean energy. In cold ion approximation, the structure of the ion transport equations is responsible for the introduction of a *critical point*  $r = r_c$  where the ion drift velocity vanishes<sup>1</sup>. This radial position is a priori unknown, its calculation being made using the condition  $E_r(r_c) = 0$ . The system formed by the fluid equations and boundary conditions can be solved given  $pR_B$  ( $p$  is the gas pressure), the electron density  $n_e(r_c)$ , and the hf electric field profile  $E_{hf}(r)$ , yielding the two *eigenvalues*  $r_c$  and the reduced field at  $r = R_A$ ,  $E_{hf}(R_A)/p$ . The model is applied to discharges in helium and argon, at  $R_A \approx 1 - 2$  cm,  $R_B \approx 25 - 50$  cm,  $p \approx 10 - 50$  mTorr and  $n_e(r_c) \approx 10^{11} - 10^{12}$  cm<sup>-3</sup>. The paper discusses in detail non-local

effects associated with electron mean energy transport, and compares the results obtained with typical solutions for a non-coaxial structure.

<sup>1</sup>H.B. Valentini *et al.*, Plasma Sources Sci. Technol. 4, 353 (1995)

14:00

**CT2 3 Antenna Effects on Excitation of Surface-Wave Modes in 915MHz UHF Plasmas** MASA AKI NAGATSU, AKIRA ITO, HIDEO SUGAI, Department of Electrical Engineering, Nagoya University NAOKI TOYODA, Nissin Inc. In comparison with 2.45 GHz, the 915 MHz surface-wave (SW) discharge enables one to produce larger and more uniform plasmas without density jump. The discharge power efficiency strongly depends on the SW modes excited by antenna. In this paper, we compare four types of slot antenna, that is, a crossed, two transverse, two longitudinal and four combined slots in 915 MHz SW plasma of 40 cm in diameter. The transverse magnetic (TM) modes having mode numbers of  $m=3, n=2$  and  $m=1, n=4$ , i.e.,  $TM_{32}$  and  $TM_{14}$  modes, were observed just below the square quartz window in both the cases of two-longitudinal slots and crossed slot antennas. Theoretical analysis of TM modes in the present geometry agrees with the results of spatial distribution measurements of electric fields. Depending on the antenna structure, the plasma production efficiency strongly changed. To understand such behaviours, we introduce a simple analytical model simulating a waveguide-resonator system. This work was supported by a Grant-in-Aid for Science Research from the Ministry of Education, Science, Sports and Culture in Japan.

14:15

**CT2 4 Kinetic Study of the Afterglow of a Nitrogen Microwave Discharge** V. GUERRA, IST, Lisboa, Portugal P.A. SÁ, FEUP, Porto, Portugal J. LOUREIRO, IST In the afterglow of  $N_2$  discharges it is usually considered that the electrons have not sufficient energy to affect the relaxation of heavy-species. However, since the characteristic times for electron loss by ambipolar diffusion are of the same order as those for the relaxation of heavy-species, the principle of small perturbation caused by electron collisions in the early afterglow must be carefully investigated. In this work we solve the time-dependent Boltzmann equation for the electron energy distribution function, with a term for electron losses by diffusion taking into account the transition from ambipolar to free diffusion regimes. We show that non-negligible processes by electron impact survive in a discharge at  $p=2-10$  Torr up to times of  $\sim 10^{-4}-10^{-3}$ s. Another important part of our study concerns the kinetics of heavy-particles. It was experimentally observed the appearing of the emission bands of the  $1^+$  system  $N_2(B \rightarrow A)$  in a separated zone, localized downstream from the discharge after a dark space, showing that  $N_2(B)$  must be created in the afterglow. We developed a kinetic model for a nitrogen microwave discharge at 433 MHz and  $p=2.56$  Torr. Once the concentrations of the various species are calculated, the time-evolution of the concentrations is analysed in the post-discharge by considering a set of coupled time-varying kinetic master equations. The results lead us to conclude that the mechanisms responsible for the enhancement of  $N_2(B)$  concentrations in the post-discharge have their origin in collisions of long-lived  $N_2(X, v)$  molecules with  $N(^4S)$  atoms.

14:30

**CT2 5 Effect of the wall temperature on N atoms concentration in a wave driven  $N_2$  discharge** V. GUERRA, E. TARTAROVA, F.M. DIAS, C.M. FERREIRA, *IST, Lisboa, Portugal* In this work we present an investigation on the different N atom creation and loss channels in a surface wave sustained discharge operating at 500 MHz. The theoretical study is based on a discharge model which couples in a self-consistent way particle kinetics, energy exchange pathways and plasma-wall interactions. Non-linear wave power absorption along the plasma column induces an axial variation of all discharge quantities and of wall conditions. The decrease of the electron density  $n_e$  towards the plasma column end results in a decrease of the atom density [N] because ground state  $N(^4S)$  atoms are created mainly by electron impact dissociation processes. Electronic excitation of  $N(^4S)$  atoms and quenching of  $N_2(A)$  metastable particles in collisions with  $N(^4S)$  atoms are the dominant loss channels along the main part of the discharge length. However, close to the plasma column end, due to decrease of the wall temperature  $T_w$  and  $n_e$ , the contribution of wall reassociation strongly increases and dominates as a loss channel. A validation of the theoretical prediction has been performed by measurements of the 7442.3 Å (transition  $3p\ ^4S_0 \rightarrow 3s\ ^4P$ ) line intensity along the discharge length and by externally induced changes in  $T_w$ . "Local" heating/cooling of the wall, near to the plasma column end results in an increase/decrease of the line intensity. Since  $n_e$  and the gas temperature remain approximately constant as  $T_w$  changes, the variation of the line intensity can be correlated to changes in the  $N(^4S)$  density as the results demonstrate.

14:45

**CT2 6 Electron Heating in Pulsed Atmospheric Pressure Glow Discharges** ROBERT H. STARK, FRANK LEIPOLD, CHUNQI JIANG, HISHAM MERHI, KARL H. SCHOENBACH, *Old Dominion University, Norfolk, Virginia 23529* Atmospheric pressure glow discharges in air and noble gases have been operated by using microhollow cathode discharges as plasma cathodes [1]. In these discharges the electron energy distribution is determined by the value of the reduced electric field (E/N). Pulsing the discharges causes the electron energy distribution to shift into an energy range where the ionization rate increases strongly. In order to study this effect, a 10 ns high voltage pulse was applied to a dc glow discharge in atmospheric air. Electrical measurements of the temporal development of current and voltage and optical measurements of the integral emission intensity during the pulse and in the afterglow of the discharge have shown an increase in electron life time from 200 ns at 10 kV/cm to approximately 1.6  $\mu$  at 30 kV/cm. The measured effect can be used to reduce the power consumption of glow discharges and to induce and enhance certain plasma processes. [1] Robert H. Stark and Karl H. Schoenbach, *Appl. Phys. Lett.*, 74, 3770 (1999) This work was funded by the Air Force Office of Scientific Research (AFOSR).

15:00

**CT2 7 Simulation of Transients in Plasma Processing Reactors Using Moderate Parallelism\*** PRAMOD SUBRAMONIUM, MARK J. KUSHNER, *University of Illinois/Urbana-Champaign* Quantifying transient phenomena in plasma processing, such as startup, shutdown, recipe changes or pulsed operation, are important to optimizing plasma and materials properties. These long

term phenomena are difficult to resolve in multi-dimensional plasma equipment models due to the large computational burden. Hybrid models, which sequentially execute modules, may not be adequate to resolve the physics of transients. In this paper, we describe a new numerical technique in which a moderately parallel implementation of a hybrid plasma equipment model is used to address long term transients. In this implementation, the Electromagnetics Module (EMM), Electron Energy Transport Module (EETM) and the Fluid Kinetics Module (FKM) of the Hybrid Plasma Equipment Model are executed in parallel. Rate coefficients are continuously updated in EETM and are immediately available in shared memory for FKM. Electric fields from the EMM and FKM are, likewise, continuously updated and are immediately available for the EETM. Results will be discussed for 2-dimensional plasma properties during transients and pulses in low pressure inductively coupled plasmas for etching.

\*Work supported by NSF (CTS99-74962), SRC and AFOSR/DARPA.

15:15

**CT2 8 Electron Trapping by the Electric Field Inversion Mechanism in a dc Glow Discharge** MARIO J. PINHEIRO, *IST, Lisbon, Portugal* We investigate the existence of the electric field reversal in the negative glow of a dc discharge, its location, the width of the well trapping the electrons, the slow electrons scattering time as well the fraction of ions build up in the glow and returning to cathode. A simple analytical model is presented which includes a Boltzmann transport equations for electrons submitted to an external electric field E along x, the ions conservation equation in a diffusion-dominated plasma and the Poisson equation. The position of the field reversal is found to be at  $x = d\beta - R/2\alpha$ , where  $d$  is the distance between electrodes,  $\beta \equiv \sqrt{2D/K}\sqrt{E_0/E_c}$  with  $D = (d/r_D)^2$  ( $r_D$  is the Debye radius),  $K = l/d$  ( $l = 1/\sqrt{2n_0\sigma_{ion}^*}$  is the electrons effective mean free path) is the Knudsen number and  $E_0$  and  $E_c$  are, resp., the non-dimensional electric field (defined by  $eE/mv_0^2$ ) at the cathode ( $v_0$  represents the initial velocity of electrons emitted from the cathode) and the "critical electric field" equal to  $1/K\sqrt{2}\sigma_{ela}/\pi$ , holding where the field reversal is settled down ( $\sigma_{ela}$  is the non-dimensional elastic cross section at thermal energies,  $\sigma_{ela}/\sigma_{ion}^*$ ),  $R \equiv \sqrt{\beta^2 - 4\alpha\gamma}$ ,  $\alpha \equiv D/K^2E_c$  and  $\gamma \equiv E_0$ . The condition for occurrence of field reversal is  $D > 2$ . The slow electrons scattering time trapped in the well is given by  $\tau \approx 2dE_c^2K^4v_0D_e$ , with  $D_e = D_e/v_0d$  and  $D_e$  is the electron diffusion coefficient at thermal energies. Those expressions have possible utility in fluid-Monte Carlo hybrid models.

15:30

**CT2 9 Nonlocal electron kinetics and excited atoms in S- and P-striations** CHRISTIAN WILKE, *Institut für Physik, E.-M.-Arndt-Universität, 17489 Greifswald, Germany* JURI B. GOLUBOVSKI, *SPbU, Saint Petersburg, Russia* VSEVOLOD A. MAIOROV, *SPbU, Saint Petersburg, Russia* IRINA A. POROKHOVA, *SPbU, Saint Petersburg, Russia* JRGEN BEHNKE, *Institut für Physik, E.-M.-Arndt-Universität, 17489 Greifswald, Germany* JRGEN F. BEHNKE, *Institut für Physik, E.-M.-Arndt-Universität, 17489 Greifswald, Germany* The numerical solution of Boltzmann kinetic equation involving the spatial gradients, elastic, and inelastic collisions, is obtained for the experimentally measured fields in S- and P-striations in neon. The peculiarities of the electron distribution function formation are analysed, in particular, the presence of the electron bunching effect. The important

consequence of the nonlocal formation of a distribution function is the imposition of the maximum of the ionization rate upon a phase of electron density increase, which can be a reason of ionization wave propagation. On the basis of nonlocal electron kinetics the detailed model of excitation and ionization in neon, including four metastable and resonance states  $2p^53s$ , and ten radiating states  $2p^53p$ , is constructed, which allows to study the role of various processes in the population and destruction of the excited states in different phases of a striation. The excited atom densities were

measured in different phases of striation by the method of emission and absorption with sufficiently high temporal and spatial resolution, taking the radial inhomogeneity of a discharge into account. These densities can give an information about the distribution of fast electrons. The comparison of experimental and calculated profiles of excited atom densities has been performed. The good quantitative correspondence of experimental and theoretical profiles is observed for metastable, resonance, and radiating states.

#### SESSION DT1: HIGH PRESSURE ARCS

Tuesday afternoon, 24 October 2000; Grand Ballroom D, Red Lion Hotel at 16:15; Darryl Michael, GE Research and Development, presiding

#### Invited Paper

16:15

##### DT1 1 Arc-Cathode Attachment Modes in High-Pressure Arcs.

SYLVAIN COULOMBE, *GE Corporate Research and Development Center, Niskayuna, NY 12309, USA*

Three different modes of attachment at the cathode are observed with high-pressure arcs: i) diffuse, ii) constricted (so-called hot spot), and iii) cathode spot-like. The exact form taken by the arc attachment depends mainly on the refractory character and electron emission properties of the cathode material, the geometry of the cathode, the arc current and gas fill composition and pressure. In this paper, the recent theoretical developments made in the field are discussed. First, the physical model self-consistently treating the near-cathode arc equations and the two-dimensional cathode thermal problem is described. Then, the existence of the two modes of arc attachment on a refractory cathode (diffuse and hot spot) is explained through the non-uniqueness of the thermal solution in the cathode when exposed to a nonlinear heat source (arc).<sup>1</sup> The predictions obtained with a pure Ar arc (3.75 atm) on a long cylindrical W cathode (1.5 mm-diameter) reveal that a diffuse mode solution typically exists for arc currents larger than  $\sim 3.5$  A giving rise to a minimum cathode temperature of 3050 K, increasing monotonically with the arc current (roughly 60 K/A). For arc currents below  $\sim 3.5$  A, only constricted solutions exist. For a 200  $\mu\text{m}$ -diameter attachment, the cathode surface temperatures range from 3600 to 3750 K for arc currents ranging respectively from 2 to 3 A. The theoretical analysis is then further extended to the arc attachment on non-refractory cathodes. A notable observation made from this analysis is that the strong erosion rates observed on such cathodes can no longer be seen only as a consequence of their non-refractory nature, but more importantly, as a necessarily condition for the self-sustaining attachment of the arc.<sup>2,3</sup> Indeed, high local metallic vapor pressures built up by the strong local thermal vaporization of the cathode are required for the maintenance of a high density of ions in the cathode sheath, which in turns, is responsible for maintaining high cathode surface temperatures and high surface electric fields. Both effects combined give rise to a copious thermo-field emission of electrons and a self-sustaining operation of the arc attachment. For a Cu cathode, the local metallic vapor pressure at the attachment point (cathode spot) is expected to fall in the 25–65 atm range. This pressure becomes lower as the cathode material becomes more refractory. The analysis of these different arc attachment modes allowed the introduction of a simple set of conditions needed to achieve a self-sustaining attachment. The principal ones are: i) The fraction of the incoming heat flux from the arc available for conduction in the cathode needs to be larger than zero. ii) The slope of the dependence of this conduction flux to the cathode surface temperature needs to be negative. iii) The ratio of the ion to electron emission currents at the cathode surface needs to be no larger than unity. <sup>1</sup>M. S. Benilov, *Phys. Rev. E*, **58**, 6480 (1998). <sup>2</sup>J. -L. Meunier and S. Coulombe, *Pure & Appl. Chem.*, **70** 1175 (1998). <sup>3</sup>S. Coulombe and J. -L. Meunier, *Plasma Sources Sci. Technol.*, **6** 508 (1997).

#### Contributed Papers

16:45

**DT1 2 Self-consistent modelling of arc-cathode interaction in HID lamps** M.S. BENILOV, M.D. CUNHA, *Departamento de Física, Universidade da Madeira, Largo do Município, 9000 Funchal, Portugal* A numerical model of the interaction of the arc plasma with a hot thermionic cathode is presented. The model includes two modules, one calculating the near-cathode plasma layer and another calculating temperature distribution in the cath-

ode body. The model of the near-cathode plasma layer is based on the conventional concept that the current transfer through the layer is one-dimensional and a dominating contribution to the energy flux from the plasma to the cathode surface is given by ion bombardment, while the dominating cooling mechanisms is cooling due to thermionic emission. The temperature distribution in the cathode body is governed by the heat conduction equation, the boundary condition at the cathode surface being equation of the heat balance (the density of the energy flux from the plasma equals sum of the density of the heat flux removed by thermal conduction

into the cathode body and of radiation losses). The resulting 2D non-linear boundary-value problem is solved by iterations with the use of a finite-difference method with direct solving of finite-difference equations. Input parameters of the model are plasma-producing gas and its pressure, cathode material, and near-cathode voltage (or arc current); all other parameters are found, including temperature distribution in the cathode body and on the surface. Results of calculations for conditions of a model arc lamp are presented and found to agree with the experimental data.

17:00

**DT1 3 A Numerical Bifurcation Study of Energy Balance Equation for High Pressure Arc** YAN-MING LI, OSRAM SYLVANIA, INC. The one dimensional energy balance (Elenbaas-Heller) equation for a cylindrical radiating, wall-stabilized high pressure arc, combining with discharge current continuity and ohmic heating was formulated as a parametrized non-linear two point boundary value problem. The branching parameter could be

expressed in terms of discharge current, wall temperature, transport parameters that described the thermal, electrical and radiating properties of the plasma, and the computed temperature profile. Numerical continuation technique was used to study such problem. Parameter regions with single solution, multiple solutions, no solution, were identified and two turning points were found numerically. The first turning point was found to be the point connecting both the low and high temperature branch of the solutions. The existence of such turning point was due to the exponential behavior of the ohmic heating term and was quite analogous to the Bratu problem [1]. The existence of second turning point was due to the radiation loss term. Without the radiation loss, the second turning point could not be found. Detailed calculations were performed for high pressure mercury arcs [2]. The relationship between the second turning point and computed current-electric field characteristics will be elaborated. [1] Uri M. Ascher et al., "Numerical Solution of Boundary value Problems for Ordinary Differential Equations," P.89, (1081) Prentice Hall [2] R. J. Zollweg, J. Appl. Phys., Vol. 49, P. 1077 (1978)

#### Invited Papers

17:15

**DT1 4 Recombination Kinetics in the Afterglow of a High-Pressure Arc**

ALAIN GLEIZES, *Centre de Physique des Plasmas et de leurs Applications de Toulouse, UMR CNRS 5002, Universiti Paul Sabatier, 118 route de Narbonne, F31062 Toulouse cedex 4, France*

Modern high-voltage circuit-breakers are filled up with SF<sub>6</sub> gas at a pressure of several atmospheres. AC current interruption occurs after current zero during a short phase of a few microseconds characterized by a fast cooling of the arc plasma due to convection and turbulence produced by overpressure effects. During this quenching phase the electrical conductance of the plasma and thus the electron number density must decrease rapidly in order to create a dielectric medium between the contacts capable to withstand the recovery voltage. We present first a kinetics study based on thermal equilibrium and on the previous knowledge of the temperature evolution, showing that the electrons disappear mainly by three mechanisms: three-body recombination at high temperature; dissociative recombination and dissociative attachment at intermediate and low temperature. A second study, coupling chemical kinetics and a two-dimension hydrodynamic modeling, has been performed in two conditions: thermal equilibrium and two-temperature plasma. The results show that departures from equilibrium remain weak, because in particular of the recombination of the electrons with S<sub>2</sub><sup>+</sup> ions. Finally, we will present the study of an SF<sub>6</sub> and SF<sub>6</sub>-N<sub>2</sub> arc plasma recombination in the presence of impurities. The theoretical prediction of the by-product formation has been compared with some experimental results obtained by gas chromatography, demonstrating the role of oxygen and carbon in the recombining plasma.

17:45

**DT1 5 Demixing in Atmospheric-Pressure Arcs.**

A. B. MURPHY, *CSIRO Telecommunications and Industrial Physics, Sydney, Australia*

Most atmospheric-pressure arcs of industrial interest contain mixtures of gases. In arc welding, for example, mixtures of argon with helium, hydrogen, carbon dioxide or oxygen are used. Demixing is a diffusion-driven phenomenon that leads to the partial separation of the different chemical elements present in such arcs. Typically the chemical elements with lower mass and higher ionization energies are concentrated in the high-temperature regions of the arc. A two-dimensional numerical model of demixing in atmospheric-pressure free burning arcs has been developed.<sup>1</sup> The model incorporates the combined-diffusion-coefficient treatment of diffusion,<sup>2</sup> which allows all species derived from a particular chemical element to be grouped together. Arcs in mixtures of argon with helium, hydrogen, oxygen and nitrogen have been investigated. It is predicted that demixing causes large changes in composition, up to a factor of four compared to a fully-mixed plasma. The predictions have been compared to spectroscopic measurements of argon-nitrogen, argon-

helium and argon-hydrogen arcs, with generally good agreement being observed.<sup>3</sup> The model has been used to obtain significant physical insights into the importance of the different demixing mechanisms, which include demixing due to partial pressure gradients, demixing due to collisional forces, demixing due to thermal diffusion, and cataphoresis. The model also allows the investigation of the effect of demixing on parameters such as arc temperature and flow, and heat flow to the electrodes. It is found that demixing can significantly alter the latter parameter, which is critical in welding applications.

<sup>1</sup>A. B. Murphy, Phys. Rev. E, **55** (1997) 7473-94; J. Phys. D, **31** (1998) 3383-90.

<sup>2</sup>A. B. Murphy, Phys. Rev. E, **48** (1993) 3594-604.

<sup>3</sup>A. B. Murphy and K. Hiraoka, J. Phys. D, submitted.

**SESSION DT2: INDUCTIVELY COUPLED PLASMAS I**  
 Tuesday afternoon, 24 October 2000  
 Grand Ballroom C, Red Lion Hotel at 16:15  
 John Trow, Applied Materials, presiding

### Contributed Papers

16:15

**DT2 1 A self-consistent plasma-sheath model for the ICP reactor** DEEPAK BOSE, *Eloret Corp.* T. R. GOVINDAN, *NASA Ames Research Center* M. MEYYAPPAN, *NASA Ames Research Center* Accurate determination of ion flux on a wafer requires a self-consistent, multidimensional modeling of plasma reactor that adequately resolves the sheath region adjoining the wafer. This level of modeling is difficult to achieve since non-collisional sheath lengths are usually 3-4 orders of magnitude smaller than the reactor scale. Also, the drift-diffusion equations used for ion transport becomes invalid in the sheath since the ion frictional force is no longer in equilibrium with drift and diffusion forces. The alternative is to use a full momentum equation for each ionic species. In this work we will present results from a self-consistent reactor scale-sheath scale model for 2D inductively coupled plasmas. The goal of this study is to improve the modeling capabilities and assess the importance of additional physics in determining important reactor performance features, such as the ion flux uniformity, coil frequency and configuration effects, etc. Effect of numerical dissipation on the solution quality will also be discussed.

16:30

**DT2 2 Experimental Characterization of Instabilities in Low Pressure Inductive Discharges with Attaching Gases\*** A.M. MARAKHTANOV, M.A. LIEBERMAN, A.J. LICHTENBERG, P. CHABERT, *University of California, Berkeley* R.W. BOSWELL, *The Australian National University* M. TUSZEWSKI, *Los Alamos National Laboratory* Plasma instabilities have been observed in low-pressure inductive processing discharges with O<sub>2</sub> and Ar/SF<sub>6</sub> mixtures. Instabilities consist of charged particle density, electron temperature and plasma potential oscillations observed both with electrostatic probe and optical emission measurements. A planar probe has been used to measure the positive ion density oscillations. Electron density oscillations have been measured with a small cylindrical Langmuir probe and with microwave interferometry. For SF<sub>6</sub>, instability windows in pressure and driving power have been explored for gas pressures between 2.5 and 100 mTorr and absorbed powers between 150 and 900 W. For most pressures, increasing power is required to obtain the instability with increasing pressure, with the frequency of the instability increasing with pressure, mainly lying between 1 and 100 kHz. For Ar/SF<sub>6</sub> mixtures, we observe similar qualitative

behavior although the window of instability decreases when the argon partial pressure increases. For all cases, we observe a strong influence of the matching network.

\*Work supported by National Science Foundation Grant ECS-9820836 and the State of California UC-SMART Program under Contract 97.01

16:45

**DT2 3 Modeling Instabilities in Low Pressure Inductive Discharges with Attaching Gases\*** P. CHABERT, M.A. LIEBERMAN, A.J. LICHTENBERG, A.M. MARAKHTANOV, *University of California, Berkeley* We develop a volume-averaged (global) model to describe instabilities observed in low-pressure inductive discharges with attaching gases. We consider a cylindrical discharge containing electrons, positive ions and negative ions. Negative ions are created by attachment and are either lost at the walls or destroyed in the plasma volume by recombination with positive ions and by detachment due to impact on metastable excited neutrals. The driving power is applied to the discharge through a conventional L-type matching network containing variable series and shunt capacitors. We consider idealized inductive and capacitive electron energy deposition. The particle and energy balance equations are solved considering quasi-neutrality in the plasma volume and at the walls to produce the dynamical behavior. As pressure or power are varied to cross a threshold, the instability is born at a Hopf bifurcation, with relaxation oscillations between inductive and capacitive modes causing modulations of charged particle densities, electron temperature and plasma potential. The model qualitatively agrees with experimental observations, and it shows a strong influence of the matching network.

\*Work supported by National Science Foundation Grant ECS-9820836 and the State of California UC-SMART Program under Contract 97.01

17:00

**DT2 4 Ionization instabilities of inductive discharges** M M TURNER, *Dublin City University, Ireland* B CROWLEY, *Dublin City University, Ireland* D VENDER, *Dublin City University, Ireland* G CUNGE, *Dublin City University, Ireland* At last year's meeting we reported an inductive discharge instability and attributed it to ponderomotive force effects. This explanation seems to us now to be improbable. In this paper we will present PIC-MCC computer simulations and other evidence tending to show that the main effect is produced by multi-step ionization. We will also refer to a surprisingly voluminous older literature on radio-frequency discharge instabilities. Such instabilities have been reported most frequently but not exclusively in rare gases, and the first reports apparently appeared as long ago as 1927.

17:15

**DT2 5 Plasma Production and Confinement by an Immersed Antenna** MAHMOOD NASSER, HIROHARU FUJITA, *Department of Electrical and Electronic Engineering, Saga University, Honjo 1, Saga 840-8502, Japan* FUJITA LAB. TEAM In the ICPs, the inductive coupling element has been physically outside the discharge region except for few applications, where the coupler was placed inside the discharge region. This design has a distinct advantage in metal sputtering applications. Metal deposition on the dielectric plasma-vessel walls of non-immersed ICPs eventually suppresses plasma generation by acting as a single-turn, short-circuited secondary winding. Here, we are representing an immersed type antenna where a confinement was developed by generating magnetic field lines around the antenna. These magnetic field lines were established by superposing a DC current on the RF current of the antenna. The space potential and the electron temperature were found to decline upon increasing the DC current, while the plasma density showed an increase in its value.

17:30

**DT2 6 A New Remote Plasma Source for HDP-CVD Process Chamber Dry-Cleaning** MICHAEL COX, *Applied Materials* KEN LAI, NAREN DUBEY, DAVID TRAN, PADDY KRISHNARAJ, MANUS WONG, PETER LOEWENHARDT, CHRIS LANE, ALAN COLLINS, *Applied Materials* LEN MAHONEY, JJ GONZALEZ, *Advanced Energy* A new class of remote plasma sources has been developed for use in the semiconductor industry for process chamber cleaning. These sources employ no capacitive coupling in their plasma generation and are appropriate for use with fluorine-based chamber dry cleaning recipes. This property, combined with low cost make them superior to microwave sources currently in use in the industry. Fundamental principles of the design of one such source jointly developed by Applied Materials and Advanced Energy, as well as process results in an Applied Materials HDP-CVD reactor will be discussed. Performance of the unit will be shown, including reduction in the use of NF<sub>3</sub> for chamber cleaning purposes.

17:45

**DT2 7 Etch of Non-Volatile Materials for System on a Chip Integration of Memory and Passive RF components.** ROBERT STEIMLE, *Motorola Semiconductor Product Sector* ARTURO MARTINEZ, *Motorola Semiconductor Product Sector* SHERRY STRAUB, *Motorola Semiconductor Product Sector* MICHAEL HARTIG, *Motorola Semiconductor Product Sector* Advanced System on a Chip integration of memory and RF devices require etching of materials traditionally considered to be non-volatile. Many of these materials have been traditionally removed by ion milling or in a sputtering chamber. In this paper we discuss the process development required to etch non-volatile materials in an inductively coupled plasma (ICP) etch chamber. Of particular importance, for the development of an etch in a ICP chamber, is the generation of etch byproducts which are non-conductive. A variety of techniques (Conductivity Measurements, Optical Emission Spectroscopy, Residual Gas Analysis, RF Impedance Measurements) used to guide process development of will be presented. Properties of the etched films including smoothness, corrosion susceptibility, and magnetic properties, will also be discussed.

## SESSION ETP: POSTER SESSION I

Tuesday evening, 24 October 2000

Westheimer Ballroom, Crowne Plaza Galleria at 20:00

## ETP 1 RF GLOWS

**ETP 2 2D-t modeling of a pulsed ICP with biased wafer in CF<sub>4</sub>/Ar\*** T. SHIRAKI, T. MAKABE, *Department of Electronics and Electrical Engineering, Keio University at Yokohama, Japan* Study of oxide etching by the aid of high density inductively coupled plasma (ICP) is still important to the development of the etcher with flux uniformity of active species on the exposed-wafer under high voltage application, and to the control of the charging damage to the processing wafer. Charging free plasma etching of oxide film may be realized by a pulsed-operation of ICP with cw bias voltage on the wafer. In this study, we developed the RCT modeling of cw ICP into a pulsed ICP, and we investigate space and time characteristics of the active species in front of the biased-wafer surface. A plasma in a cylindrical quartz chamber of 10 cm in diameter, wound around the wall by one turn current coil driven at 13.56 MHz, is maintained by a pulsed-mode at 50 mTorr in CF<sub>4</sub>/Ar. Then, the wafer of 4 cm in diameter, set at the position of 5 cm from the coil surface, is highly biased to reactively etch the oxide film at low frequency, 678 kHz. We discuss the influence of the on/off-time in the pulsed operation of the ICP and the bias voltage amplitude on the fluxes of electrons, positive and negative ions to the wafer. Also, the functional separation between the plasma source and the bias voltage is discussed.

\*Work is partly supported by STARC in Japan

**ETP 3 2D-t modeling of pulsed-2f-CCP in CF<sub>4</sub>(5%)/Ar for oxide etching\*** G. WASHIO, K. MAESHIGE, N. NAKANO, T. MAKABE, *Department of Electronics and Electrical Engineering, Keio University at Yokohama, Japan* Capacitively coupled plasma (CCP) source with different frequency source at each of parallel plate electrodes is a powerful tool for doing etching. A time modulation of CCP by a pulsed-power operation may be one of the practical solution of the development of the charging free plasma process for etching. Then, (very) high frequency (VHF) power source is operated in a pulse mode, although the opposite bias electrode with patterned wafer is in cw operation at low frequency (LF). In this study, modeling has been performed in order to investigate the fluxed of positive and negative ions, and electrons to the wafer surface as a function of frequency (13.56 MHz, 100 MHz), amplitude and on/off period of the (V)HF source, as well as the amplitude of the LF (678 kHz) bias voltage at 50 mTorr in CF<sub>4</sub>(5%)/Ar. We employed the RCT model, and also a hybrid model<sup>1</sup> consisting of Monte Carlo particle model of fast electrons and the RCT model. In particular, we discuss the rule of negative ions on the wafer surface during off-period in CF<sub>4</sub>/Ar system with dissociative electron attachment at finite electron energy without thermal attachment.

\*Work is partly supported by STARC in Japan

<sup>1</sup>E. Shidoji, N. Nakano, T. Makabe, *Thin Solid Films* 351 (1999) 37-41

**ETP 4 Two-dimensional modeling of RF capacitively coupled discharges** A. SALABAS, *CFP, IST (Portugal)* G. GOUSSET, *LPGP, Univ. Paris-Sud (France)* L.L. ALVES, *CFP, IST (Portugal)* This paper reviews the formulation and updates some numerical procedures usually adopted in 2D, time-dependent fluid models to study the transport of charged particles in RF capacitively coupled discharges<sup>1,2</sup>. The description of charged particle transport is made by solving the continuity and momentum transfer equations, coupled with Poisson's equation and the electron mean energy transport equations. Non-local effects are taken into account by computing the electron transport parameters as a function of the electron mean energy via a homogeneous, two-term Boltzmann equation solver. More appropriate boundary conditions for the electron and ion fluxes are used successfully. Inertia terms in the ion momentum transfer equations are considered by generalizing the concept of effective electric field<sup>2</sup>. The 2D fluid model is solved for a GEC Cell reactor type (6.4 cm radius and 3.2 cm interelectrode distance) operating at frequency 13.56 MHz and pressures between 68 mTorr-1 Torr in electropositive (He) and electronegative (SiH<sub>4</sub>+H<sub>2</sub>) gases. The simulations reproduce better experimental DC self-bias voltages reported earlier<sup>3</sup>, and give coupled electrical powers that agree with previous works.

<sup>1</sup>J.P. Boeuf and L.C. Pitchford, *Phys. Rev. E* **51**, 1376 (1995)

<sup>2</sup>G.J. Nienhuis *et al.*, *J. Appl. Phys.* **82** 2060 (1997)

<sup>3</sup>O. Leroy *et al.* *Plasma Source Sci. Technol.* **7** 348 (1998)

**ETP 5 CF<sub>2</sub> detection in radio-frequency discharges containing c-C<sub>4</sub>F<sub>8</sub>** A. N. GOYETTE, *National Institute of Standards and Technology* YICHENG WANG, *National Institute of Standards and Technology* Octafluorocyclobutane (c-C<sub>4</sub>F<sub>8</sub>) has been reported to serve as a highly selective plasma etching gas. CF<sub>x</sub> radicals, particularly CF<sub>2</sub>, are play important roles in the anisotropic etching of SiO<sub>2</sub>. As such, we have conducted a series of quantitative measurements of CF<sub>2</sub> radical densities in rf discharges generated in c-C<sub>4</sub>F<sub>8</sub>. Discharges were sustained in a GEC rf reference cell and column densities determined using ultraviolet broadband absorption spectroscopy. With this technique, absolute line-integrated densities can be determined. The influence of plasma operating conditions such as discharge pressure, power, and gas flow rate on the CF<sub>2</sub> density are investigated.

**ETP 6 Increase in Plasma Density using Plasma-Sheath Resonance in a Capacitively Coupled Plasma** N. GOTO,\*T. MAKABE, *Keio University* An increase in plasma density was observed under the condition that plasma-sheath resonance occurs in a capacitively coupled plasma. Plasma-sheath resonance is expected to be a new source for low pressure plasma processing, because it is found from XPDP1 that the resonance can induce a strong electric field even in the bulk plasma, and the plasma density is dependent on a strong electric field in a capacitively coupled plasma. Parameters for generating the plasma-sheath resonance at a constant applied frequency, such as 13.56MHz, are plasma density, magnetic flux density and direction, and the ratio of sheath thickness to gap distance between two electrodes. In this study, the angle of magnetic field was varied >from 6 to 16 degrees with respect to the electrode surface. The slight increase in plasma density was measured using a double probe in Ar at 13.56MHz. The angle of the magnetic field at the peak of the plasma density decreased from 14 to 10 degrees, as the plasma density and magnetic flux density increase, >from 8 × 10<sup>8</sup> cm<sup>-3</sup> to 1.7 × 10<sup>10</sup> cm<sup>-3</sup> and from 1.8mT to 3.2mT, respectively. The experimental results were com-

pared to the theoretical relation between the direction of the magnetic field and plasma density at different magnetic flux densities in the plasma-sheath resonance.

\*Also at Central Research Institute of Electric Power Industry

**ETP 7 Decomposition Rate of CO<sub>2</sub> in a CCRF Discharge** T. DINH, S. POPOVIC, L. VUSKOVIC, *Department of Physics, Old Dominion U., Norfolk, VA 23529* Variation of gas mixture during decomposition of CO<sub>2</sub> affects substantially the electron energy distribution function (EEDF) and the rate coefficient for dissociative excitation, which is controlling the process. Decomposition of CO<sub>2</sub> was studied in a CCRF discharge in a Martian Simulant Gas mixture that has 95% CO<sub>2</sub>, in the pressure range 4-8 Torr. The discharge cell had the discharge volume 2-4 cm<sup>3</sup>, and power density into the discharge was 0.5-5 W/cm<sup>3</sup>. Small gas flow was kept constant during the discharge. Mean electron temperature and density were measured via a double floating cylindrical Langmuir probe. Their values were in the range 2-6 eV, and 5 × 10<sup>8</sup>-5 × 10<sup>9</sup> cm<sup>-3</sup>, respectively. The distribution of electron temperature and density along the longitudinal and transversal discharge axis showed that they had maxima near the center of the discharge gap. Gas temperature in the discharge was measured using the rotational spectra of a CO bands and with the thermocouple probe. For present discharge conditions it had the value between 300-450 K. Under the same discharge conditions, experimental values of CO<sub>2</sub> decomposition was measured with a quadrupole mass spectrometer. Results are compared with the model, developed on the basis of the composition-dependent calculation of the EEDF.

**ETP 8 Radio Frequency Biasing of an Ion-Ion Plasma** VIKAS MIDHA, BADRI RAMAMURTHI, DEMETRE ECONOMOU, *Department of Chemical Engineering, University of Houston, Houston, TX 77204-4792* A one-dimensional fluid model for simulating the effects of RF bias applied to an ion-ion plasma was developed. The full ion momentum and continuity equations were coupled to the Poisson equation for the electrostatic field. Special emphasis was placed on the effect of applied bias frequency. Due to the lower temperature and greater mass of negative-ions compared to electrons, the sheath structure in ion-ion plasmas changes significantly as the bias frequency is varied. For low bias frequencies (100 kHz), the charge distribution in the sheath is monotonic (switching from positive to negative) during each half cycle. For intermediate frequencies (10 MHz), when the bias period approaches the ion transit time through the sheath, double layers form with both positive and negative charges coexisting in the sheath. For high frequencies, beyond the plasma frequency (60 MHz), plasma waves are launched from the bulk plasma and the sheath consists of multiple peaks of positive and negative charge (multiple double layers). For a relatively large range of bias frequencies (up to the plasma frequency), each electrode is bombarded alternately by high energy positive and negative ions during an RF bias cycle. For bias frequencies greater than the plasma frequency, however, the electrode is bombarded simultaneously by low energy positive and negative ions with ion energies approaching the ion temperature. It was also found that the ion energy increases with the applied bias potential. At relatively high pressures (greater than 20 mTorr), the ion energy at low frequencies (100 kHz) is limited by collisions and the peak ion energy may be increased by using a higher bias frequency (10 MHz). At lower pressures, however, the effect of collisions is mitigated while the effect of ion transit time becomes significant as the bias frequency increases. In this case, a low bias frequency is favorable for extracting high energy ions from the plasma.



**ETP 9 Development of compact RF plasma source using electron sheath resonance technique** YASUNORI OHTSU, YOUSUKE INOUE, HIROHARU FUJITA, *Department of Electrical and Electronic Engineering, Saga University, 1 Honjomachi, Saga 840-8502, Japan* FUJITA LAB. TEAM, Developments of plasma processing techniques have been proposed many plasma production methods such as electron cyclotron resonance (ECR) microwave discharge, dc or radio frequency (RF) magnetron discharge, helicon discharge and so on. However, capacitively coupled RF discharge has been used widely for a long time with keeping non-improvement. Low-pressure radio frequency (RF) plasma has been produced using a new method of electron sheath resonance (ESR). The technique employs the electron resonance between the cyclotron motion and sheath reflection caused by the wave riding effect in a capacitively coupled RF discharge in a magnetic field. It was confirmed that the increase in plasma density for resonant magnetic flux density was based on this electron acceleration mechanism from a viewpoint of electron energy distribution. We now are trying to develop compact plasma source using ESR technique.

**ETP 10 Decoupling characteristics of different frequency power supply for dual frequency capacitive coupling plasma reactor** NOBUHIKO NAKANO, *Keio University* TOSHIAKI MAKABE, *Keio University* Decoupling characteristics of different frequency power supply for dual frequency capacitive coupling plasma reactor The improvement of the dual frequency capacitive coupling plasma (2f-CCP) reactor performance is required for the future fine processes. HF or VHF applied to the upper electrode for the plasma production, and LF is applied to the wafer for the bias. These functional separation of plasma density and ion energy control is the important point of this reactor. In this work, the decoupling characteristics of 2f-CCP is examined by the relaxation continuum model. The conventional combination of 14MHz and 1MHz has strong coupling that increase the plasma density twice under the density is the order of  $10^{10}\text{cm}^{-3}$ . On the other hand, the combination of 100MHz(VHF) and 1MHz shows the nice decoupling under the low pressure ( $< 50\text{Torr}$ ) and high density  $10^{11}\text{cm}^{-3}$  condition. Also, we found the plasma density decreasing that is affected by the strong bias voltage near the minimum sustaining condition. Finally, we propose that VHF plasma source and HF bias for 2f-CCP is the nice combination for a high performance plasma etching tool to control the plasma density and ion energy separately.

**ETP 11 Effect of Metastable Atoms in an RF Argon Discharge** MARISA ROBERTO,\* *ITA HELEN SMITH, UC Berkeley* A planar one-dimensional particle-in-cell simulation with Monte Carlo Collisions (XPDP1) has been used to study 13.56 MHz argon discharge including metastable species. Reactions such as metastable creation, ionization from the metastable state, metastable quenching to resonant level and metastable-metastable collisions were taken into account. The effect of pressure and applied voltage on the metastable density was examined. At low pressure the metastable density profile is peaked in the center, typical of diffusion-type profiles, while at high pressure and high voltage the profile is strongly peaked at the sheath edges. The shape of the profile is determined by mean free path for electrons and metastables in the discharge. A comparison between discharges with and without metastables is presented.

\*M. Roberto thanks FAPESP for financial support.

**ETP 12 A Monte Carlo Collision Model to Study RF Discharges with a Mixture of Argon and Oxygen** MARISA ROBERTO,\* *ITA HELEN SMITH, UC Berkeley* A planar one-dimensional particle-in-cell simulation with Monte Carlo Collisions (XPDP1) has been used to study a 13.56 MHz argon/oxygen discharge with 1 Torr of argon and 0.05 Torr of oxygen. Reactions such as metastable quenching by  $\text{O}_2$ , charge transfer between  $\text{Ar}^+$  and  $\text{O}_2$  and Penning ionization are taken into account. It was found that quenching of argon metastables by molecular oxygen and charge transfer between  $\text{Ar}^+$  and  $\text{O}_2$  are important in determining the metastable and ion profiles for this gas mixture. A comparison with a pure argon plasma and a pure oxygen plasma was also made. The effect of applied voltage is investigated.

\*M. Roberto thanks FAPESP for financial support.

### ETP 13 DC GLOWS

**ETP 14 Electron and Excited Particle Kinetics in Axially Symmetric Hollow Cathodes** F. SIGENEGER, S. GORTCHAKOV, R. WINKLER, *Institut für Niedertemperatur-Plasmaphysik, Greifswald, Germany* S. PFAU, *Institut für Physik, Greifswald, Germany* For a cylindrical helium discharge, consisting of a central hollow cathode and two, on both sides symmetrically arranged anodes, the radial variations of the electron properties and the excited atom densities have been theoretically studied. These investigations refer to the axial center region of the open cathode cylinder where the axial plasma inhomogeneity is of less importance. For gas pressures of some Torr and discharge currents of some mA, measured radial courses of the electric field have been used as input data. The radial variations of the electron properties and the excited atom densities have been determined by self-consistently solving the radial-dependent electron Boltzmann equation and the particle balance equations of the excited atoms. A strongly nonlocal radial evolution of the electron kinetic quantities has been found. This evolution is enforced by the transition from the dominant field action in the cathode fall to the strong collisional dissipation in the negative glow, where still a large population of the electron energy distribution at higher energies is found. The profiles of the excited atoms markedly differ from each other and significantly change with the gas pressure. A comparison of some results with measured ones shows satisfactory agreement.

**ETP 15 Formation of Negative Hydrogen Ions in a Ne-H<sub>2</sub> Hollow Cathode Discharge** TSVETELINA PETROVA, *University of Sofia* GEORGE PETROV, *Berkeley Research Associates, Inc.* The negative hydrogen ion sources operate in pure hydrogen and essentially depend on the discharge configuration. Negative hydrogen ions can also be generated in a mixture of noble gases and hydrogen. If hydrogen is diluted with neon or other noble gas, the vibrational states, the main factor for efficient H<sup>-</sup> formation, become more populated compared to pure hydrogen, which leads to more efficient formation of H<sup>-</sup>. The properties of the Hollow Cathode Discharge (HCD) are unique (e-beam character, high electron density, low electron temperature etc.) and these properties may further enhance the formation of H<sup>-</sup>. For this purpose a mixture of neon and hydrogen is used for optimization of H<sup>-</sup> ion source. A model has been developed which describes Ne-H<sub>2</sub> mixture in a conventional HCD. The calculations are spatially averaged and emphasize on both electron and ion kinetics. The Electron Energy Distribution Function (EEDF), H<sub>2</sub> Vibrational

Distribution Function (VDF) and a comprehensive collisional-radiative model are selfconsistently solved to describe in details both the electron and ion kinetics. Some conclusions can readily be drawn: (i) A mixture of Ne and H<sub>2</sub> is more efficient for generation of H- than pure hydrogen. (ii) The optimum mixture of H<sub>2</sub> and Ne is 1-5% hydrogen and 95-99% neon. (iii) H- is formed from highly excited vibrational states of H<sub>2</sub>:  $v=6$  to  $v=10$ . (iv) Even small admixture of hydrogen greatly affects the discharge properties: EEDF, VDF, electron and ion densities and degree of dissociation of hydrogen.

#### ETP 16 Interaction Between Acoustic Shock Wave and Glow Discharge

S. POPOVIC, L. VUŠKOVIC, *Department of Physics, Old Dominion U., Norfolk, VA 23529* We are studying the interaction between propagating acoustic planar shock wave and weakly ionized gas in a high-pressure dc glow discharge. This interaction appears to be polarity-dependent and substantially different in the positive column than in the cathode region<sup>1,2</sup>. Several agents emerging from the acoustic shock wave modify its precursor zone with respect to free stream conditions. These are fluxes of charged particles accelerated or reflected from the potential barrier in double electric layer, radiation from relaxation zone, and ion-acoustic waves. Our study attempts to provide a detailed insight into the processes initiated by these agents and to give the character and the extent of the modification. We will present a quantitative discussion of ion flux penetration in the free stream region, changes in ion composition, the ionization-recombination process, and transfer of radiation from shock layer and relaxation zone to precursor zone. The conditions in precursor region thus prepared become the initial conditions for the processes in the relaxation region. Using this approach we analyze interaction of shock wave with the negative glow, and with the positive column in the co-directional geometry.

<sup>1</sup>P. Bletzinger and B. N. Ganguly, *Phys. Lett. A* **258** 342 (1999).

<sup>2</sup>S. Popović and L. Vušković, *Physics of Plasmas* **6** 1448 (1999).

#### ETP 17 Experimental and Theoretical Study of Electrons and Excited Atoms in a Neon DC Column Plasma

DIRK UHR-LANDT, MARTIN SCHMIDT, *Institut für Niedertemperatur Plasmaphysik, 17489 Greifswald, Germany* ANDREAS DINKLAGE, STEFFEN FRANKE, MATTHIAS OTTE, SAMIR SOLYMAN, CHRISTIAN WILKE, *Institut für Physik, E.-M.-Arndt-Universität, 17487 Greifswald, Germany* The positive column of inert gas glow discharges is an outstanding model to verify methods for the description of spatial inhomogeneous low temperature plasmas. Therefore, a steady and comprehensive base of experimental data is required. A report on extensive probe measurements and laser spectroscopic studies of a cylindrical neon glow discharge at a pressure of 90 Pa and low discharge currents (current  $i=(0.25 \dots 30)$  mA, tube radius  $r=1.5$  cm) is given. The results are compared with those of a self-consistent column plasma model. In addition to the axial electric field in the column, the radial space-charge and floating potential and the radial variation of the isotropic part of the electron velocity distribution have been determined by probe diagnostics. Absolute number densities of neon atoms in the four lowest excited states as functions of the radial position have been measured by laser absorption spectroscopy. The self-consistent model of the positive column comprises an appropriate treatment of the radially inhomogeneous kinetics of electrons, ions and excited atoms in the plasma and the self-consistent determination of the radial and axial electric field.

#### ETP 18 MICROWAVE GLOWS

##### ETP 19 Single Surface Multipactor Experiment on a Dielectric Surface

R. B. ANDERSON, *University of Michigan* W. GETTY, *University of Michigan* M. L. BRAKE, *University of Michigan* Y. Y. LAU, *University of Michigan* R. M. GILGENBACH, *University of Michigan* A. VALFELLS, *University of Michigan* S. A. ANDERSON, *University of Michigan* A novel experiment for single surface multipactor on a dielectric surface is underway at the University of Michigan. The experiment consists of a small brass microwave cavity in a high vacuum system. The cavity is 15 cm in length with an outer diameter of 10 cm. A pulsed, variable frequency microwave source at 2.5 GHz, 5kW peak excites the TE<sub>111</sub> mode with a strong electric field parallel to the dielectric surface. The microwave pulses are monitored by microwave diodes. An electron probe measures electron current and provides qualitative temporal behavior of the multipactor electron current with respect to the microwave pulses. Phosphor is used to detect multipactor electrons by photoemission and is proposed as a diagnostic that could possibly detect the location of multipactor on a dielectric and detect areas of stronger or weaker breakdown. The microwave fields will be monitored along the length of the cavity. Detailed modeling of the cavity's fields with HFSS is being developed and the results will be used to analyze the experiment. This work was supported by DOE: DE-FG02-98ER54475 A002

#### ETP 20 GLOWS

##### ETP 21 Generation of High-Pressure, High-Density, Non-Equilibrium Plasma Using Microwave-Excited Microgap Discharge

A. KONO, T. SUGIYAMA, T. GOTO, *Nagoya University, Nagoya 464-8603, Japan* H. FURUHASHI, Y. UCHIDA, *Aichi Institute of Technology, Toyota 470-0392, Japan* A new plasma source using a microgap electrode system (100- $\mu$ m wide, 10-mm long, two electrodes separated by 100  $\mu$ m) is being studied to produce a high-pressure ( $> \sim 1$  atm), high-density, non-equilibrium plasma in the cw basis. Dc and rf (13.56 MHz) powers produced a stable glow discharge in the atmosphere, but the current was constricted and the glow did not extend along the microgap; the glow was also confined within a thin layer near the electrodes and the most of the gap space was dark. In the microwave (2.45 GHz) excitation, on the other hand, the glow filled the entire gap length (10 mm) and was nearly uniform across the gap. To characterize the plasma in the microgap, light scattering measurement was carried out using a frequency-doubled Nd:YAG laser as the light source. For an atmospheric discharge at a nominal microwave power of 100 W, no Thomson-scattering signal was observed, indicating that the electron density was  $< \sim 5 \times 10^{14}$  cm<sup>-3</sup>. The N<sub>2</sub> rotational Raman spectrum was observed when the discharge was off but it almost disappeared when the discharge was turned on, indicating that the gas temperature in the microgap rose above 1000°C. The effect of gas flow and the discharges with Ar and other gases are under investigation.

##### ETP 22 Modelling of excitation and ionization processes in homogenous APDG in nitrogen.

Y.B. GOLUBOVSKII, V. MAIOROV, *Institute of Physics, State University of St. Petersburg, Russia* J. BEHNKE, J.F. BEHNKE, *Institute of Physics, 17487 Greifswald, Germany* Atmospheric pressure is presented as well as modelling results of the dielectric controlled APGD between two flat electrodes. Very important for APGD description are various

excitation and ionization processes. These rates were described in terms of the EEDF, found from the Boltzmann equation with regard for elastic and quasielastic impacts, excitation of electron-excited states of  $N_2$  molecules, and collisions with vibration-excited  $N_2$  molecules. Calculated EEDF was used to obtain the rate coefficients of direct and stepwise excitation and ionization by electron impact in dependence on electric field and vibration temperature. The study of associative excitation and ionization in collisions of vibration-excited and metastable nitrogen molecules showed their essential role in formation of APGD parameters. The distribution of vibration-excited molecules was obtained for a given electric field with regard for excitation in electron impacts, VT- and non-resonant VV- processes.

**ETP 23 Spectroscopic characterization of an atmospheric pressure glow discharge (APGD)\*** S. GOMEZ, P.G. STEEN, T. MORROW, W.G. GRAHAM, *Dept. of Pure and Applied Physics, The Queen's University, Belfast BT7 INN, Northern Ireland* P.A.F. HERBERT, *Plasma Ireland Ltd., Cork, Ireland* Recently there has been considerable interest in atmospheric discharges operating in a glow discharge mode i.e. with a spatial and sheath structure similar to that of low pressure glow discharges [1,2,3]. Here spectroscopy has been used to characterise an atmospheric pressure glow discharge (APGD), operating in air but with various other gases flowing through the inter-electrode space and with textile samples ranging from polyester to wool also present in that space. The emission spectra from 250nm to 800nm were dominated by emission from  $N_2$  but when textile samples were present OH emission at around 310nm was also observed. Electron temperatures of  $0.5 \pm 0.1$  eV were determined from the relative intensities of Ar emission lines. When nitrogen was the flowing gas the vibrational states exhibited a Maxwellian distribution with a temperature of 2000K. 1. S. Kanazana et al. *J.Phys.D.*, 21, 836 (1988) 2. J.R.Roth, *Industrial Plasma Engineering*. (IOPP, London) 1995 3. F. Massine et al. *J. Appl. Phys.* 83, 3411-3420 (1998).

\*Supported by the EU-Brite programme as part of the Plasmatex project.

**ETP 24 Modeling of Uniform and Filamentary Dielectric Barrier Discharges in Helium at Atmospheric Pressure** VITALY A. SCHWEIGERT; UWE KORTSHAGEN, *University of Minnesota, Mechanical Engineering* The dominant tendency of atmospheric pressure plasmas operated as dielectric barrier discharges is to appear in filamentary form. However, it has recently been demonstrated that under certain conditions uniform glow discharges can be operated at atmospheric pressures. We have studied this effect numerically using a two-dimensional fluid model for electrons and ions in helium. Electron and ion transport are described in the drift-diffusion approximation. The electron and ion continuity equation are solved along with the Poisson equation. Our model indicates that the filamentation of the discharge is favored by nonuniform charging of the dielectric. High driving frequencies and high levels of preionization favor uniform glow discharges. The results of our model are qualitatively consistent with experimental results. This work is supported by the US Department of Energy under grant DE-FG02-00ER54583.

**ETP 25 Dielectric Barrier Discharge in Nitrogen: Transition from the Filamentary to the Glow Mode** HANS-ERICH WAGNER, *Affiliation RONNY BRANDENBURG, Affiliation PETER MICHEL, Institute of Physics, Ernst-Moritz-Armdt University of Greifswald, 17489 Greifswald, Domstr. 10a, GERMANY* FRANCOISE MASSINES, *Laboratoire de Genie Electrique de Toulouse, Universite Paul Sabatier 118, route de Narbonne, 31062 Toulouse Cedex, FRANCE* KIRILL V. KOZLOV, *Moscow State University, Department of Chemistry, 119899 Moscow, RUSSIA* The electrical and optical characteristics of the dielectric barrier discharge (DBD) in nitrogen with a trace admixtures of oxygen ( $< 100ppm$ ) at atmospheric pressure have been investigated by means of cross-correlation spectroscopy (second positive and first negative systems of nitrogen, time resolution within a sub-nanosecond range), current measurements and emission spectroscopy (general spectra of the discharge, synchronized with the current). A symmetrical electrode arrangement with both electrodes covered by the dielectrics (glass or alumina, discharge gap width of 1mm) was used. The electrical power supply provided voltage frequencies within the 1 - 6kHz range. Depending on the purity of the working gas as well as on the feeding voltage amplitude, several essentially different steady-state discharge modes have been observed, including the glow (diffuse) mode for pure nitrogen, and the filamentary mode with a profound cathode-directed streamer (similar to that one observed in air) for nitrogen with an admixture of oxygen. The transient (intermediate) mode of the discharge has been found to be an asymmetrical one as regards the electrode polarity, despite of the symmetrical discharge cell arrangement. In the latter case, for the first half-wave of the feeding voltage the filament development mechanism is shown to consist of the two consequent ionizing waves (respectively: cathode- and anode-directed), while for the second half-wave, only a cathode-directed streamer has been observed. Finally, the possible physical models for the described above discharge modes are briefly discussed.

**ETP 26 Kinetic properties and convergence of particle simulation of discharges** M M TURNER, *Dublin City University, Ireland* One of the attractions of particle simulation over other kinetic simulation procedures is that it has a well-developed theoretical basis, and its limitations are fairly well characterized. This work has not been revisited for the case of collisional particle in cell simulations, i.e. PIC-MCC. We show in this paper that adding Monte Carlo collisions does affect the kinetic properties of the simulation. In most cases, this is fortunately of no importance, but examples can be produced where there is serious difficulty. These include applications of implicit algorithms to high density discharges, and cases such as negative glows where coulomb collisions are important and the electron energy distribution function is highly sensitive to noise in the simulation. However, we will show that in the majority of cases, PIC-MCC is robust with respect to statistical noise, and convergence with respect to the number of computational particles is readily achieved.

#### ETP 27 PLASMA-SURFACE INTERACTIONS

**ETP 28 2D profiles of a pulsed-two-frequency CCP by emission selected** CT T. FUJITA, T. MANO, T. MAKABE, *Keio University at Yokohama, Japan* Capacitively coupled plasma (CCP) with the powered electrode, driven by very high frequency (VHF), and with the other electrode, biased by low frequency (LF)

voltage, is the conventional tool for oxide etching. Deep sub-micron etching of contact hole or trench with high aspect ratio is limited by an anomalous etching and gate oxide damage caused by a charging on the microscopic structure. A pulsed-operation of the 2f-CCP may reduce the charge build-up inside the trench or contact hole with high aspect ratio. In the previous study,<sup>1</sup> we have observed 2D-space profiles of the pulsed-2f-CCP in a time-averaged fashion by using emission selected computerized tomography (CT). In this study, we have carried out CT measurements of the spatiotemporal profile in great detail in the off period of the plasma power under cw bias application in CF<sub>4</sub>/Ar at 25 mTorr, in order to investigate the influence of the high bias-voltage at LF (700 kHzB/A(B2.8 MHz) in the oxide etching on the plasma. Discussion is given for the functional separation between VHF and LF sources, and the ion transport to the wafer.

<sup>1</sup>T. Kitajima, Y. Takeo, Z. Lj. Petrović, and T. Makabe, Appl. Phys. Lett. (accepted for publication)

**ETP 29 A modified Gaseous Electronics Conference Reference Cell for the study of plasma-surface-gas interactions.** M.J. GOECKNER, *Electrical Engineering, University of Texas at Dallas* J.M. MARQUIS, B.J. MARKHAM, A.K. JINDAL, *Electrical Engineering, University of Texas at Dallas*\* The Inductively Coupled Plasma (ICP) Gaseous Electronics Conference (GEC) Reference Cell provides a standard system for the study of plasma sciences. In this paper, we present a version of the ICP GEC cell that has been designed to allow studies of the interactions between a plasma, gas-phase chemistry, and surface-phase chemistry. Specifically, this modified GEC reference cell has specially designed interior walls that can be heated/cooled (10 to 200 °C) and moved. In addition, these walls can be coated with various materials (Al<sub>2</sub>O<sub>3</sub>, SiO<sub>2</sub>, etc). Design specifications and initial results will be presented.

\*Thanks to M.J. Kushner and L.J. Overzet for helpful discussions. This project is supported by NSF, DOE and The University of Texas at Dallas.

**ETP 30 A Flexible Plasma System for the study of plasma-surface-gas interactions.** A.K. JINDAL, *Electrical Engineering, University of Texas at Dallas* J.M. MARQUIS, B.J. MARKHAM, M.J. GOECKNER, *Electrical Engineering, University of Texas at Dallas*\* A novel flexible plasma system (FPS) has been developed to study the interactions between a plasma, gas-phase chemistry, and surface-phase chemistry. While various plasma sources can be used, initially this system is configured with a hollow cathode source. Like the modified GEC reference cell, also presented at this conference, this system has specially designed interior walls that can be heated/cooled (10 to 200 °C) and coated with various materials (Al<sub>2</sub>O<sub>3</sub>, SiO<sub>2</sub>, etc). Here however, the interior walls also serve as electrodes and can not be moved. Design specifications and initial results will be presented.

\*Thanks to M.J. Kushner and L.J. Overzet for helpful discussions. This project is supported by The University of Texas at Dallas.

**ETP 31 Electron-Stimulated Desorption from the Products of Chemisorption of C<sub>2</sub>F<sub>3</sub>Cl and C<sub>2</sub>Cl<sub>4</sub> on Si(100)\*** JASON E. SANABIA, *Chemical Physics Program* GREGORY D. COOPER, *Department of Physics* JON ORLOFF, *Department of Electrical and Computer Engineering* JOHN H. MOORE, *Department of Chemistry and Biochemistry, University of Maryland, College*

*Park, MD 20742.* Temperature-programmed desorption (TPD), electron-stimulated desorption (ESD), and temperature-programmed electron-stimulated desorption (TP-ESD) have been used to probe the chemical nature of chemisorbed C<sub>2</sub>F<sub>3</sub>Cl and C<sub>2</sub>Cl<sub>4</sub> on Si(100). In the TPD experiments, silicon-containing etching products desorbed at high temperatures. Essentially none of the precursor desorbed molecularly. In the ESD experiments, only positive and negative halogen ions desorbed as a result of an incident low-energy (0-100 eV) electron beam. The electron-stimulated desorption of neutral species was not detected. The halogen ion signals were measured as a function of incident electron energy (for various substrate temperatures). The threshold is above 12 eV for positive ions and above 5 eV for negative ions. Finally, in the TP-ESD experiments, halogen ion signals as a function of substrate temperature (for 100 eV incident electrons) were measured. The shapes of the positive and negative halogen ion intensities versus temperature are strikingly similar. We conclude that the halogen ions originate from the same chemical species, and that the variation of the ion intensity with temperature reflects the changing concentration and orientation of that species on the surface.

\*Supported by NSF grant CHE-99-04843.

**ETP 32 Experimental Measurements of Plasma-Grid Interaction\*** CHANG-KOO KIM, DEMETRE ECONOMOU, *University of Houston, Department of Chemical Engineering, Houston, TX 77204-4792* Understanding plasma-grid interaction finds applications in neutron generators, ion beam assisted growth and etching of thin films, neutral beam etching, ion thrusters, etc. The flux, energy and angular distributions of ions and/or fast neutrals incident on the target are of primary importance in these applications. These quantities depend critically on the shape of the meniscus (plasma-sheath boundary) formed over the grid holes. In this paper experimental results for Ar plasmas in contact with a hole have been obtained in terms of the flux, energy and angular distributions of ions. The energy distribution of ions showed different behavior according to the ratio of the hole diameter to the sheath thickness. For the case of 10 micron-diameter hole (smaller than the sheath thickness), the ion energy distribution had double peaks, while single peaks occurred for the case of 1270 micron-diameter hole (larger than the sheath thickness) due to plasma leakage. In all cases, the peak, mean and maximum ion energy decreased as pressure was increased but were independent of power. The angular distributions of ions depended both on the ratio of the hole diameter to the sheath thickness and the aspect ratio of the hole. For the case of 10 micron-diameter hole, the ion angular distributions had Gaussian shapes. For the case of holes through which plasma leaked (508 micron- and 1270 micron-diameter holes), the ion angular distributions peaked off-axis, showing loss of anisotropy due to plasma leakage. The ion angular distributions through higher aspect ratio holes (thickness to diameter ratio 2:1) were narrower compared to lower aspect ratio holes (1:5) because of more sidewall collisions in the case of the higher aspect ratio holes.

\*Supported by Sandia National Laboratories

**ETP 33 Structures of energy dissipation of plasma in a thin discharge cell** NARIAKI IMAMURA, *Kagoshima University* JYUN SAKAGUCHI, *Kagoshima University* SYU-ICHIRO ASATANI, *Kagoshima University* KOZO OBARA, *Kagoshima University* We present effects of interaction between condensable gas atoms and walls in plasma derived from spectroscopic investigation. Intensities of emission spectra from Hg atoms exponen-

tially increased as temperature increased. Below 310 K, the activation energies of group A (370, 579 nm) and group B (404, 435 and 546 nm) were 0.45 eV and 0.67 eV, respectively. The activation energy of group B coincided with that of evaporation from mercury surface. Above 310 K, the activation energy of group B decreased to 0.34 eV, which is a half of the energy of evaporation from liquid mercury. This result suggests a structural change of adsorbed mercury atoms from multi-layer to monolayer. Time dependence of emission spectra induced by temperature perturbation with amplitude 1 K and period 800 s was investigated. Below 310 K, characteristics of Xe, Ar and Hg were correlated. However above 310 K, the correlation between them was changed; high harmonic modes were remarkably excited in both cases but second harmonic mode of Xenon spectrum disappeared. Spatial distribution of emission intensity from Hg showed 2x3 structure.

#### ETP 34 ELECTRON AND PHOTON COLLISIONS

**ETP 35 Benchmark Calculations for Electron Collisions with Noble Gases** KLAUS BARTSCHAT, *Drake University*\* Previous Breit-Pauli R-matrix work [1-3] has been extended to model electron-impact-induced transitions between the lowest 31 states in neon, argon, krypton, and xenon. Sample results for total cross sections, as well as selected angle-differential benchmark parameters, will be presented for incident electron energies between threshold and 30 eV. The results will be compared with available experimental data and predictions from other theoretical approaches. 1. V. Zeman *et al.*, *Phys. Rev. Lett.* **79**, 1825 (1997) 2. K. Bartschat and V. Zeman, *Phys. Rev. A* **59**, R2552 (1998) 3. K. Bartschat and A.N. Grum-Grzhimailo, *J. Phys. B* (2000), in press

\*This work is supported by the National Science Foundation under grant PHY-0088917.

**ETP 36 Electron Impact Excitation Collision Strengths for Fe X\*** SWARAJ TAYAL, *Clark Atlanta University* Electron collision excitation strength for transitions between the fine-structure levels of the  $3s^23p^5$ ,  $3s3p^6$ ,  $3s^23p^43d$ ,  $3s3p^53d$ , and  $3s^23p^44s$  configurations in Fe X are calculated using a semirelativistic R-matrix approach which takes into account parts of the Breit-Pauli Hamiltonian. We included 49 fine-structure levels in our scattering calculation. These levels are represented by configuration-interaction wave functions. Rydberg series of resonances converging to the excited state thresholds are explicitly included in the calculation. Our results show some differences with the available other calculations. Effective collision strengths are evaluated by averaging the electron collision strengths over a Maxwellian distribution of electron energies over a wide temperature range.

\*This research work is supported by NASA

**ETP 37 Formation of Ground-State Si Atoms Following Electron Impact Dissociation of SiH<sub>4</sub> and SiF<sub>4</sub>\*** NINA ABRAMZON, *Stevens Institute of Technology, Hoboken, NJ* THOMAS RAYNOR, *Stevens Institute of Technology, Hoboken, NJ* KURT BECKER, *Stevens Institute of Technology, Hoboken, NJ* KEVIN MARTUS, *William Paterson University, Wayne, NJ* A combination of electron scattering and laser-induced fluorescence (LIF) techniques was used to measure absolute cross sections for the

formation of ground - state Si atoms following electron impact dissociation of SiH<sub>4</sub>, and SiF<sub>4</sub>. The Si atoms resulting from the electron impact dissociation of these molecules are probed by LIF of the Si 389 nm transition followed by the emission of the Si 288 nm line. The reversed detection scheme of probing by LIF the Si 288 nm transition followed by the emission of Si 389 nm is also possible. This detection schemes allow a detection of the Si atoms which is final-state specific. Results have been obtained so far for the formation of Si(1S) atoms. The neutral dissociation cross section for the formation of Si(1S) atoms from SiH<sub>4</sub> peaks at 60 eV with a maximum value of about  $4 \times (10^{-17})$  cm<sup>2</sup>. Preliminary results for SiF<sub>4</sub> indicate that the corresponding cross section is comparable.

\*Work Supported by DOE and NASA

**ETP 38 Electron Impact Ionization of TiCl<sub>x</sub>(x=1-3)\*** R BASNER, *INP Greifswald, Germany* M SCHMIDT, *INP Greifswald, Germany* H DEUTSCH, *Univ. Greifswald, Germany* V TARNOVSKY, *Stevens Institute of Technology, Hoboken, NJ* KURT BECKER, *Stevens Institute of Technology, Hoboken, NJ* Titanium tetrachloride (TiCl<sub>4</sub>) is the precursor of choice for the plasma-assisted chemical vapor deposition of TiN. Any effort to understand and model the key plasma-chemical reactions in the deposition plasma requires a knowledge of the ionization properties of TiCl<sub>4</sub> parent molecules and of the TiCl<sub>x</sub> (x=1-3) free radicals that are produced in the plasma. We report the results of absolute ionization cross sections measurements for the TiCl<sub>x</sub> (x=1-3) free radicals using the fast-beam technique. Dissociative ionization channels are the dominant ionization path ways for all TiCl<sub>x</sub> free radicals. A complete account of the measured cross sections and appearance energies will be presented at the Conference together with a comparison of the measured cross sections with predictions from semi-classical and semi-empirical calculations.

\*Work supported by the VW Stiftung, Germany and the U.S. DOE.

**ETP 39 Electron-Impact Total Ionization Cross Section for TiCl<sub>4</sub>\*** M. A. ALI, *Howard Univ.* K. K. IRIKURA, Y.-K. KIM, *NIST* We have applied the binary-encounter-Bethe (BEB) theory<sup>1</sup> to calculate the electron-impact total ionization cross section for TiCl<sub>4</sub>. We find that the BEB cross section is lower by almost 40% than the experimental cross section measured by Basner *et al.*<sup>2</sup> A semiempirical cross section calculated by Basner *et al.* is also lower than their experimental cross section. They suggested that autoionization resulting from the excitation of inner valence orbitals with binding energies between 25 eV and 50 eV might be responsible for the difference. Although it is common to find distinct autoionization thresholds in atoms, they do not stand out in most molecules, perhaps due to the proximity of successive molecular orbital thresholds close in binding energies.<sup>3</sup> This molecule may provide an interesting case to study the role of autoionization in polyatomic molecules. The BEB ionization cross sections for TiCl<sub>x</sub>, x = 1-3, will also be reported at the meeting.

\*Work supported in part by DOE's Office of Fusion Energy Sciences and NIST's Advanced Technology Program.

<sup>1</sup>Y.-K. Kim and M. E. Rudd, *Phys. Rev. A* **50**, 3954 (1994).

<sup>2</sup>R. Basner *et al.*, *Thin Solid Films*, in print.

<sup>3</sup>H. Nakatsuji *et al.*, *J. Chem. Phys.* **97**, 2561 (1992).

**ETP 40 Low Energy Positron Scattering from Atoms and Molecules\*** J.P. SULLIVAN, S.J. GILBERT, C.M. SURKO, *University of California, San Diego* A new positron accumulation and storage apparatus has made available for the first time a source of positrons with a thermal energy spread ( $\Delta E \leq 25$  meV).<sup>1</sup> This source can be used as a reservoir for the formation of a high resolution positron beam, tunable from 0.05 to greater than 10 eV. Using this beam, positron scattering measurements have been made with high resolution ( $\approx 20$  meV FWHM) in a region of energies ( $< 1$  eV) that has not previously been accessible for positron experiments. Cross sections are measured by making use of the properties of the positrons in the confining magnetic field which is used for trapping and beam collimation.<sup>2</sup> Cross sections for the vibrational excitation of several molecules (e.g., CO, CH<sub>4</sub>, CO<sub>2</sub> and H<sub>2</sub>) by positron impact will be presented, along with differential cross sections for Ar and Kr at various energies. Plans for the future include performing total cross section measurements down to very low energies. The technical difficulties in performing these experiments at low values of positron energy ( $\leq 0.5$  eV) will also be discussed.

\*Supported by the National Science Foundation

<sup>1</sup>Gilbert et al., *Appl. Phys. Lett.* 70, 1944 (1997)

<sup>2</sup>Gilbert et al., *Phys. Rev. Lett.* 82, 5032 (1999)

#### ETP 41 HEAVY PARTICLE COLLISIONS

**ETP 42 Alignment and Orientation dependence of inelastic cross sections in slow Li+He collisions.\*** BIDHAN SAHA, *Florida A&M University* The dependence of the collision dynamics on the shape and spatial alignment of the excited Rydberg atom has drawn considerable attention recently [1]. We report theoretical results for the influence of the target excitation prior to the collision on the quenching of low-lying Li atoms by He atoms at thermal velocities. The semi-classical, impact parameter, close-coupling method based on a molecular expansion augmented with plane-wave translation factor has been employed to evaluate the inelastic cross sections. Details will be presented at the meeting. [1] B. C. Saha and A. Kumar, *Ind. J. Phys.* 73B, 687 (1999); *Phys. Rev. A* 61,032709 (2000).

\*Work supported by Research Corporation and NSF-CREST

**ETP 43 Electron Transfer To Spatially Oriented Molecules** JIPING ZHAN, *Rice University* BEIKE JIA, *Rice University* PHILIP R. BROOKS, *Rice University* Fast atoms collide with molecules spatially oriented by hexapole state selection techniques. Collisions of the neutral species at energies of about 4 eV produce positive and negative ions which are detected by time of flight mass spectrometry. Electron transfer from the atom produces negative ions, and frequently these ions are different from those formed by bombardment with free electrons. Orientation normally has a large effect on electron transfer and in cases where several negative ions are formed, different ions may be preferentially formed at different ends of the molecule.

**ETP 44 Cross Sections for Elastic Collisions between Rare Gas Atoms from 0.01 eV to 10 keV.** A.V. PHELPS, *JILA, U. of Colorado and NIST* We calculate sets of differential and integral cross sections for elastic collisions of He-He, Ne-Ne, Kr-Kr, Xe-Xe, and Ne-Xe for use in gas discharge modeling. The techniques are those used in recent studies of Ar-Ar collisions.<sup>1</sup> Interaction

potentials based on theory and experiment are used with quantum mechanical scattering theory in the WKB approximation. The available viscosity, diffusion, and thermal conductivity measurements, differential scattering measurements, and beam attenuation measurements agree well with the theoretical results. At all energies the theoretical differential scattering cross sections are sharply peaked in the forward direction. In the cases of He-He and Ar-Ar, the very limited differential scattering data for inelastic scattering at high energies are correlated with the elastic scattering results. We hope that the glaring uncertainties in the elastic and inelastic differential cross sections introduced by inelastic collisions at energies above about 500 eV will encourage theoretical and/or experimental work on this topic.

<sup>1</sup>A. V. Phelps, C. H. Greene, and J. P. Burke Jr., *J. Phys. B* (submitted) (2000)

#### ETP 45 Studies of Charge Exchange Interactions between Protons and Gas Targets.

DAVID BIXLER, *Angelo State University* We are studying the absolute cross sections for the emission of Balmer-alpha and Balmer-beta radiation from collisions of protons with various gases. When a proton interacts with a neutral gas molecule, there is a probability that an electron from the gas molecule will transfer to the proton, forming a neutral hydrogen atom and an ionized molecule. Occasionally the electron is captured into an excited energy state; and the product excited hydrogen atom will undergo a decay process, and emit a photon of light. The Balmer radiation is produced when the electron transfers from a high energy state to the n=2 energy level of hydrogen. Studies of the radiation produced by a particular interaction reveal the cross section for electron capture into these excited states of hydrogen. The Physics research laboratory at Angelo State University houses a linear particle accelerator capable of producing an intense, monoenergetic beam of protons in the energy range of 4-20 keV. The beam interacts with a known pressure of target gas, and a photomultiplier tube monitors the emission of Balmer radiation. The intensity of the emission is related mathematically to the cross section for electron capture into a particular excited state. I will present the current state of this research at Angelo State University.

#### ETP 46 Doubly differential cross sections and longitudinal momentum distributions in the single ionization of Ne by fast ion impact

D.M. McSHERRY, S.F.C. O'ROURKE, D.S.F. CROTHERS, *DAMTP, The Queen's University of Belfast, N.Ireland, BT7 INN* There are very few experimental data sets for doubly differential cross sections (DDCS) for targets heavier than helium due to the difficulties in collecting data with conventional spectrometers. However with the recent developments in efficient spectrometers combined with recoil momentum spectroscopy, experimental results for the single ionization of Ne by 3.6MeV/u Au<sup>53+</sup> impact were obtained[1]. At the conference we consider these results in the context of our theoretical results achieved using continuum-distorted-wave quantum mechanical models, in particular the CDW-EIS approximation, which has had much success in the non-perturbative regime[2]. Doubly differential cross sections for helium shall also be considered in comparison to Ne and longitudinal electron and recoil ion momentum distributions will be examined. [1]. R. Moshhammer, P.D. Fainstein, M.Schulz, W.Schmitt, H.Kollmus, R.Mann, S.Hagmann and J.Ullrich, *Phys. Rev. Lett.* 83 (1999) 4721. [2]. S.F.C. O'Rourke, I.Shimamura and D.S.F. Crothers, *Proc. R. Soc. Lond. A* 452 (1996) 175.

## ETP 47 DIAGNOSTICS: ELECTRICAL METHODS

**ETP 48 Langmuir Probe Measurements in Inductively Coupled  $\text{CHF}_3/\text{Ar}$  and  $\text{CHF}_3/\text{O}_2/\text{Ar}$  plasmas\*** S.P. SHARMA, M.V.V.S. RAO\*, M. MEYYAPPAN, *NASA-Ames Research Center* Plasma parameters, such as, electron number density ( $n_e$ ), electron temperature ( $T_e$ ), electron energy distribution function (EEDF), mean electron energy ( $E_e$ ), ion number density ( $n_i$ ), and plasma potential ( $V_p$ ), have been measured by using Langmuir probe in low-pressure (10-50 mTorr) inductively coupled  $\text{CHF}_3/\text{Ar}$  and  $\text{CHF}_3/\text{O}_2/\text{Ar}$  plasmas generated in the GEC cell. The measurements were made at the center of the plasma, keeping the lower electrode grounded, for various  $\text{CHF}_3/\text{Ar}$  and  $\text{CHF}_3/\text{O}_2/\text{Ar}$  mixtures operating at 10-50 mTorr pressures and two input RF power levels, 200 and 300 W. EEDF data show a strong Druyvesteyn distribution with relatively lower number of low energy electrons as compared to a Maxwell distribution and a large electron population with energies higher than the plasma potential. The results further show that at low  $\text{CHF}_3$  concentrations ( $< 50\%$ ) the electron number density remains nearly constant with increase in pressure. At higher  $\text{CHF}_3$  concentrations, however, it decreases with increase in pressure. Plasma potential and electron temperature increase with decrease in pressure and with increase in  $\text{CHF}_3$  concentration. An analysis of the above observations and mechanisms will be presented.

\*\*ELORET

**ETP 49 Diagnostics for Electron-Beam Produced Process Plasmas** DAVID D. BLACKWELL,\*SCOTT G. WALTON,<sup>†</sup>DARIN LEONHARDT, DONALD P. MURPHY, RICHARD F. FERNSLER, WILLIAM E. AMATUCCI, ROBERT A. MEGER, *Plasma Physics Division, U.S. Naval Research Laboratory, DC 20375-5346* EDBERTHO LEAL-QUIROS,<sup>‡</sup> *Polytechnic University of Puerto Rico, Hato Rey, PR 00918* NRL has developed a Large Area Plasma Processing System based on electron beam ionization of gases<sup>1</sup>. The LAPPS plasma source, having low electron temperature and low pressure, make it ideal for probe diagnostics. However, such measurements can become difficult due to the presence of large magnetic fields, RF biases on the processing surface, high energy electrons, and multiple ion species. We have developed probe diagnostics with to overcome these difficulties. RF compensation methods for Langmuir probes and resolution of distribution functions on RF timescales with specially designed energy analyzers allow measurement of instantaneous and time averaged plasma properties, while increased digital resolution allows for more realistic representation of non-Maxwellian distribution functions. Magnetic based diagnostics give us instantaneous readings of fluxes to process surfaces and relation to RF biases applied. Two test chambers were used. One was an inductively coupled source (75 cm diameter x 25 cm high) with a spiral RF antenna coupled to the plasma through a glass window. The other was a mini-version of LAPPS (40 cm diameter x 55 cm high) where the sheet of plasma is produced by a hollow cathode. We will be presenting measurements of the ion and electron energy distribution functions acquired with energy analyzers and Langmuir probes. This will include a variety of experimental conditions (gas type, plasma type), particularly in the vicinity of RF biased

substrates. Impedance characteristics of RF biased substrates under various geometries. Comparisons between the effectiveness of different probe diagnostics and correlations to other in situ diagnostics such as mass spectrometry, microwave transmission, and optical spectroscopy methods.

\*NRL-NRC Postdoctoral Research Associate

<sup>†</sup>NRL-NRC Postdoctoral Research Associate

<sup>‡</sup>NRL-NRC Faculty Research Associate

<sup>1</sup>See presentations by co-authors at this conference

**ETP 50 External RF Filtering for Langmuir Probes** AMY WENDT, *University of Wisconsin - Madison* RF plasma potential fluctuations are known to be an important influence on the current-voltage characteristics of Langmuir probes. Suppression of these effects is often desirable in order to use conventional Langmuir probe analysis to determine plasma properties. One approach is to use a "filter" with a large RF impedance between the probe tip and ground, so that the probe tip tracks the plasma potential fluctuations. Generally, these filters must be introduced as close to the probe tip as possible to avoid the effects of the stray capacitance of the probe shaft. This can involve installing components inside of a long tube, making in situ tuning of the filter impossible. In this study, we introduce a 3-stage tunable external filter made of passive circuit elements. The circuit design incorporates the stray capacitance of the probe, and includes inductive elements to cancel its associated admittance, resulting in a high impedance between the probe tip and ground. This method has been implemented to suppress the effects of  $\sim 20$  V plasma potential fluctuations at 13.56 MHz and its second and third harmonics. Measurements have been made and will be reported for an inductively coupled plasma operated in argon at pressures in the range 5-30 mTorr.

**ETP 51 Electrical Structure and Charged Particle Fluxes in  $\text{SF}_6/\text{Ar}$  Plasmas** P.B. VERDONCK, A. GOODYEAR, P.R.J. BARROY, N.ST.J. BRAITHWAITE, *The Open University*\*  $\text{SF}_6$  plasmas are routinely used for the etching of silicon in a wide range of applications including Micro Electro-Mechanical Systems (MEMS) where etch geometry is of prime importance. Etch geometries are influenced by not only the gas phase chemistry of the plasma but also its electrical potential structure. A range of diagnostics has been deployed to examine the composition of  $\text{SF}_6/\text{Ar}$  plasmas in a Reactive Ion Etching (RIE) system. Measurements of positive ion flux have been made using a capacitively coupled, radio frequency biased, planar probe technique<sup>1</sup>. The probe was mounted into the surface of the earthed electrode. Identification of the ion species and their distribution of energy at the same surface was conducted using a quadrupole mass and energy spectrometer. Use of the planar probe in parallel with the spectrometer provides a useful normalisation of the species-integrated ion flux to the surface. At pressures in excess of about 25 Pa when electronegativity is high the ion flux from  $\text{SF}_6/\text{Ar}$  mixtures is lower than from pure Ar. At lower pressures the addition of  $\text{SF}_6$  to Ar has the opposite effect on total ion flux owing to  $\text{SF}_5^+$  and  $\text{SF}_3^+$  being readily produced.

\*Work supported by the EPSRC, Grant Nos. GR/L82380, GR/L83387 and FAPESP, Brazil

<sup>1</sup>J P Booth, N St J Braithwaite, A Goodyear, and P Barroy, *Rev. Sci. Instrum.*, in press (July 2000)

**ETP 52 Time resolved electron and temperature measurements in a pulsed planar microwave discharge** A. ROUSSEAU, E. TEBOUL, *LPGP, Universit Paris-Sud / CNRS, France* N. LANG, J. ROEPCKE, *INP Greifswald, Germany* Spatially and time resolved Langmuir probe measurements are performed in a pulsed hydrogen microwave discharge. The plasma reactor is made of a slotted wave guide which radiates through a quartz window and creates a plasma. Pulse duration is 1 ms long with a duty cycle ratio equal to 0.1, pressure and power are equal to 33 Pa and 600 W respectively. Measurements are performed close to the quartz window, where electron density and electro magnetic field are maximum. A special shielded Langmuir probe is used in order to avoid electromagnetic perturbation. Under our experimental conditions, the sheath is slightly collisional so that Chen probe current is corrected in order to take into account ion current depletion due to collisions. Both electron densities and temperature exhibit strong spatial modulations from 2 to 15 E10 cm<sup>-3</sup> and from 2 to 7 eV respectively. Time evolution of the plasma density shows that a steady state is reached within 0.3 ms.

**ETP 53 Measurement of Electron Densities in a Pulsed Atmospheric Pressure Air Discharge** FRANK LEIPOLD, ROBERT H. STARK, KARL H. SCHOENBACH, *Old Dominion University, Physical Electronics Research Institute, Norfolk, VA 23529* Microhollow cathode discharges have been shown to serve as plasma cathodes for atmospheric pressure air discharges [1]. The high pressure discharges are operated dc at currents from 10 mA up to 30 mA and at average electric fields of 1.25 kV/cm. The electron density in the dc discharge was measured by an interferometric technique [2]. For a dc filamentary air discharge with a current of 10 mA, the radial electron density distribution was found to be parabolic with a total width of 660  $\mu\text{m}$  and an electron density of  $n_e = 10^{13} \text{ cm}^{-3}$  in the center of the discharge. The diagnostic technique has now also been applied to pulsed discharges. It was found that the method provides electron densities measurements for discharges with durations as low as 5  $\mu\text{s}$ . The spatial distribution of the index of refraction in the pulsed discharge was obtained by shifting the discharge volume through the laser beam and by using an inversion method to obtain the radial index profile. For the electron density with a assumed parabolic profile, the maximum value was measured as  $1.17 \cdot 10^{14} \text{ cm}^{-3}$ . (10 mA atmospheric pressure air discharge. The temperature profile was found to be gaussian with a half width of 1.3 mm. Acknowledgement This work was funded by the Air Force Office of Scientific Research in Cooperation with the DDR&E Air Plasma Ramparts MURI Program. References [1] Robert H. Stark and Karl H. Schoenbach, *Appl. Phys. Lett.* 74, 3770 (1999) [2] Frank Leipold, Robert H. Stark, and Karl H. Schoenbach, to appear in *J. Phys. D.*, *Appl. Phys.*

#### ETP 54 DIAGNOSTICS: OPTICAL METHODS

**ETP 55 CF, CF<sub>2</sub> and SiF densities in inductively driven discharges** GREG HEBNER, *Sandia National Laboratories, Albuquerque NM* Laser induced fluorescence was used to measure the spatially resolved CF, CF<sub>2</sub> and SiF radical density in inductively driven discharges containing fluorocarbon gases. Measurements of the spatially resolved CF density were performed in C<sub>2</sub>F<sub>6</sub> and CHF<sub>3</sub> containing discharges as functions of inductive power, pressure and bias condition on a silicon substrate. In addition, CF rotational temperatures were calculated, assuming saturated spectra. Measurements of the spatially resolved CF<sub>2</sub> and SiF density

were performed in C<sub>4</sub>F<sub>8</sub>, C<sub>2</sub>F<sub>6</sub> and CHF<sub>3</sub> containing discharges as functions of inductive power, pressure and bias condition. SiF rotational temperatures were also estimated. As the inductive coil power was increased, the SiF density in the center ( $r = 0 \text{ cm}$ ) increased while the CF<sub>2</sub> density decreased and the CF density slightly decreased. In all cases, the radical density in the center of the glow increased with pressure changes from 5 to 30 mTorr while changes in the bias power had little influence on any of the measured radical densities. The spatial distribution of the CF and SiF density peaked in the center of the discharge. The CF<sub>2</sub> density had a local maximum in the center of the plasma with a decreasing density at the edge of the glow. However, the CF<sub>2</sub> density outside the glow region was a factor of 2 - 6 higher than the density inside the glow region, depending on the gas. CF and SiF rotational temperatures were between 450 and 750 K. This work was performed at Sandia National Laboratories and supported by SEMATECH and the United States Department of Energy (DE-AC04-94AL85000). Sandia is a multiprogram laboratory operated by Sandia Corporation, a Lockheed Martin Company, for the U. S. Department of Energy.

**ETP 56 An Electric Field Measurement Method based on Spectroscopy of Argon Atoms** V.P. GAVRILENKO, H.J. KIM, J.B. KIM, M.D. BOWDEN, K. MURAOKA, *Kyushu University, Japan* In recent years, we have developed a method for measurement of the magnitude of electric fields in discharge plasmas based on laser spectroscopic measurements of argon atoms. In this paper, we report significant improvements in the detection limit for electric field and the detection accuracy. Measurements of Stark spectra were made in the sheath region of a glow discharge using laser optogalvanic spectroscopy. The wavelength of the laser radiation was tuned to the transitions  $4s - nf$  ( $n = 7, 8, \dots, 14$ ) of the argon atom. For  $n = 11$ , the lower limit for electric field measurements was estimated to be 14 V/mm. The improvement in detection limit was achieved mainly by calculating the dependence of energy levels of argon atoms on the strength of the electric field, by solving the Schrodinger equation for the argon atom, and using these calculated results to determine the electric field from experimental spectra. In addition, a method to determine the direction of the electric field, based on measuring Stark spectra with different laser polarizations, will be described.

**ETP 57 Correlation between Gas Phase and Substrate Surface on Fabrication of Low-k Films in ECR Plasma with C<sub>4</sub>F<sub>8</sub> and Perfluorocarbon-Replacement Gases** MASAYUKI NAKAMURA, KUNGEN TEI, SEIGO TAKASHIMA, MASARU HORI, TOSHIO GOTO, *Dept. of Quantum Eng., Nagoya Univ., JAPAN* NOBUO ISHII, *Tokyo Elec. Ltd., JAPAN* Recently, fluorocarbon films are expected to be new materials for the intermetal dielectrics with a low dielectric constant in multilevel interconnections of future high speed ULSIs. Since these fluorocarbon films are formed by plasma CVD, the composition and distribution of gas phase species are very important to improve the film characteristics. In this study, we have formed fluorocarbon films on the substrate and measured spatial distribution of absolute CF and CF<sub>2</sub> radical densities using infrared diode laser absorption spectroscopy (IRLAS) combined with laser-induced fluorescence (LIF) in ECR fluorocarbon plasmas. In C<sub>4</sub>F<sub>6</sub> and C<sub>3</sub>F<sub>6</sub> plasmas, where these gases have C=C bond and fluorocarbon film depositions of dielectric constant 3.0 were observed but in C<sub>4</sub>F<sub>8</sub>, etching was observed. In C<sub>4</sub>F<sub>8</sub> plasma, CF radical densities were higher and CF<sub>2</sub> were lower than those in others, CF<sub>2</sub> radical densities in the



vicinity of the chamber wall were higher than those in plasma region at every plasma. On the other hand, the deposition rate of fluorocarbon films on 8 inch Si wafer indicated hill type distribution in  $C_4F_6$  and  $C_3F_6$  plasmas. These results suggest fluorocarbon films are not mainly formed by CF and  $CF_2$  radicals. The behaviors of C atom and higher radicals in ECR plasma are also discussed.

**ETP 58 Determination of quenching coefficients of rare-gases in a hydrogen RF discharge by time resolved emission spectroscopy\*** T. GANS, V. SCHULZ-VON DER GATHEN, H.F. DÖBELE, *Institut für Laser- und Plasmaphysik, Universität Essen, Germany* Small amounts of rare-gases admixed to hydrogen plasmas can be used to reveal by their emission details on the excitation mechanisms. At pressures exceeding 50 Pa collisional quenching influences some emission lines. A novel ICCD camera operating at 13.56 MHz allows us to measure even faint lines with time resolution. CCRF hydrogen plasmas exhibit a field reversal during which an intense electron current provides collisional excitation for 10-15 ns in the sheath region. After this excitation there are no longer electrons inside the sheath for the rest of the RF-cycle. It is therefore possible to determine quenching coefficients from the lifetime of the fluorescence at various pressures (30-400 Pa). The result for the Ar 2p1 line agrees very well with the result reported in connection with laser excitation of the corresponding level. All other observed Ar-lines are influenced by cascade contributions from higher states. The influence of cascades and results for emission lines of various rare-gases are presented.

\*Supported by the DFG in the frame of the SFB 191

**ETP 59 Emission and Electrical Measurements to Assess Actinometry in SF<sub>6</sub>/Ar/O<sub>2</sub> SiC Etching Discharges** MICHAEL BROWN, *Innovative Scientific Solutions, Inc., Dayton, OH* JAMES SCOFIELD, *Air Force Research Laboratory, Wright-Patterson AFB, OH* BISWA GANGULY, *Air Force Research Laboratory, Wright-Patterson AFB, OH* In SiC etching plasma devices, we have recorded plasma emission from Ar, F and O atoms in SF<sub>6</sub>/Ar/O<sub>2</sub> RF discharges as a function of pressure, input power and mixture fraction. At fixed power, the emission intensities rise nearly linearly with increasing pressure between 100 and 300 mTorr; with pressure increases to 600 mTorr, the emission intensity rolls off due to the increase in collisional de-excitation and the decrease in E/n. The Ar emission from excited states with differing radiative lifetimes indicates a lower limit on the temperature rise of 130 K with a pressure increase to 600 mTorr at 40 W. At fixed pressure, Ar and O emission shows a similar functional dependence on input power with a roll off at the higher powers. In contrast, the F emission increase with increasing power is nearly linear. This may reflect the fact that F atoms are produced by dissociative attachment of SF<sub>6</sub> (for lower E/n conditions) in addition to direct electron impact dissociation. Electrical measurements, with a variable inter electrode gap, indicate that the E/p ratio does drop with increasing input power. The SiC etch rate also increases nearly linearly with input power up until the polymer build up becomes the rate limiting process. Spatially resolved emission measurements show that Ar and F emission profiles follow each other while the O atom emission profile falls off faster near the ground electrode.

**ETP 60 VUV and Optical Emission Characterization of Fluorocarbon SiO<sub>2</sub> Etch Processes and Correlation to Etch Feature Quality\*** H. HSUEH, E. DANDAPANI, R. MCGRATH, R. MESSIER, *Penn State University* B. JI, E. KARWACKI, *Air Products and Chemicals, Inc.* Fluorocarbon discharges used for SiO<sub>2</sub> etch were characterized using optical (OES) and VUV emission spectroscopy. Actinometry was used to monitor atomic fluorine concentration ( $N_F$ ) as power, pressure and gas mix were varied. Thermal oxide films were photolithographically patterned to define 0.5-2.0  $\mu m$  trench features, and then etched in an AMAT Mark II reactor. Etch rate, selectivity and feature critical dimension were measured using SEM and other techniques. DC self-bias was also recorded for each set of process conditions. Good etch features, etch rates of 1175  $\text{\AA}/min$ , and selectivity of 7.9 were obtained for reactor operation at 750 W, 80 mTorr, and with a gas mixture of  $CF_4/CHF_3/Ar$  at 85/10/5 sccm. Etch rate, selectivity and feature critical dimensions observed have been correlated to actinometric estimates of  $N_F$ , to self-bias voltage and to OES and VUV emissions. While varying process conditions around the reference values defined above,  $N_F$  was found to increase monotonically between 0.75 and  $1.2 \times 10^{13}/cm^3$  as pressure was increased from 70 to 100 mTorr, as power was increased from 650 to 850 W, and as  $CF_4$  gas fraction was increased from 5th reference gas mixture, etch rate was found to increase (1150 to 1550  $\text{\AA}/min$ ) with increasing power, and to decrease (1550 to 550  $\text{\AA}/min$ ) with increasing pressure. In these cases, etch rate trend tracked the self-bias voltage established. However, when  $CF_4$  gas fraction was increased from 5  $\text{\AA}/min$ , while  $N_F$  concentration increased by only 15 self-bias varied by only 8 feature profiles, and associated reaction processes will be presented.

\*Work supported by Air Products and Chemicals, Inc.

**ETP 61 Laser absorption spectroscopy of a pulsed inductively coupled plasma in Ar and CF<sub>4</sub>/Ar** N. ITAZU, Y. MIYOSHI, T. MAKABE, *Department of Electronics and Electrical Engineering, Keio University at Yokohama, Japan* Inductively coupled plasma (ICP) has been used as metal and Poly-Si etching for ULSI circuits fabrications. Oxide etching process by high density ICP is still under development. Then, a pulsed-ICP operation may be attractive and effective for charging free plasma processes of the oxide film etching. In this work, the authors have investigated the structure of a pulsed-ICP with wafer in the processing room in Ar and the mixture  $CF_4(5\%)/Ar$  from the probed metastable atom,  $Ar(^3P_2)$  observed by using Laser absorption spectroscopy. The absorption line of the long lived metastable  $Ar(^3P_2)B''(BAr(2p_7))$  at 772.376 nm has been selected to estimate the transport process of the active neutral species from the plasma source close to the external current coil to the wafer surface. The pulsed-ICP as a function of modulation period and duty ratio are compared with those in a CW-ICP by the aid of the metastable density distribution and also the emission spectroscopy. We discuss the function of the pulsed-ICP, and in particular, the effect of the wafer on the plasma.

**ETP 62 Atomic nitrogen and oxygen density measurements in low-pressure dc discharge** M. A. BRĂTESCU, Y. SAKAI, T. KAMADA, *Hokkaido University, Sapporo 060-8628 Japan* In the last years, in the field of plasma processing technology, atomic nitrogen and oxygen play an important role in chemical processes. Using laser absorption spectroscopy, with tunable laser diodes, we have measured the density of  $O(3^5S_2)$  and  $N(3s^4P_{3/2})$  in a dc

discharge in different experimental conditions: gas mixtures ( $O_2$  + noble gas,  $N_2$  + noble gas,  $N_2O$  + noble gas, air,  $N_2O$  in air), concentrations of the molecular gas in the noble gas (0.01%–90%), total pressures (0.1–3 Torr), discharge current 3 mA. The used noble gases were argon and helium. The detection sensitivity of the laser absorption method was  $10^6$  atoms/cm<sup>-3</sup>. The density of  $N(3s^4P_{5/2})$  in  $N_2$  + noble gas mixtures was  $8 \times 10^6$  cm<sup>-3</sup>, which was smaller than the density of  $O(3^5S_2^o)$  in the similar  $O_2$  + noble gas mixture discharges, i.e.  $10^{10}$  cm<sup>-3</sup>. Higher density of  $N(3s^4P_{5/2})$   $1.2 \times 10^7$  cm<sup>-3</sup> was measured in  $N_2O$  + noble gas discharge. The density of  $N(3s^4P_{5/2})$  in  $N_2O$  + air is two orders of magnitude higher than the density of  $O(3^5S_2^o)$ . The dependences of the atomic oxygen and nitrogen densities on  $N_2O$  concentration in air showed that oxygen was mainly produced by  $O_2$  dissociation and nitrogen was mainly produced by  $N_2O$  dissociation. Difference of dissociation processes between O and N production was discussed.

#### ETP 63 Spatial distribution of excited C and Ar concentration in laser ablation carbon plume in Ar filling gas

M. A. BRATESCU, Y. SAKAI, Y. SUDA, M. MIZUNO, *Hokkaido University, Sapporo 060-8628 Japan* Pulsed laser ablation of graphite is a reliable method for preparation of newly found materials, like fullerenes, diamond like carbon fine particles and thin films. Using laser absorption spectroscopy, the densities of C and Ar excited species in the plume are measured. They are also compared with emission spectroscopy. An ArF excimer laser (193 nm, 20 ns pulse duration, 2 Hz repetition rate, 5 J/cm<sup>2</sup> fluence) was focused on a graphite target in argon as buffer gas (0.1–20 Torr pressure). The density of  $Ar(4s'[1/2]_1^o)$  was measured using a laser diode (LD) tuned to the resonant transition ( $4s'[1/2]_1^o - 4p'[1/2]_1$ ) at 826.680 nm, with an output power 3 W/cm<sup>2</sup>. Changing the LD position (0.5 mm resolution) in the laser ablation plasma, we obtained the density distributions of  $Ar(4s'[1/2]_1^o)$ . We calculate the  $Ar(4s'[1/2]_1^o)$  expansion velocity of about  $10^5$  cm/s and the lifetime of  $Ar(4s'[1/2]_1^o)$  in the plume. The  $Ar(4s'[1/2]_1^o)$  density increased with pressure, having a maximum at  $p = 5$  Torr, due to frequent excitation collisions by electrons,  $C^+$ ,  $C_2^+$ , etc. and decreased with pressure for  $p > 5$  Torr, due to collisional quenching. The maximum  $Ar(4s'[1/2]_1^o)$  density was  $2.5 \times 10^{12}$  cm<sup>-3</sup> and the time integration of  $Ar(4s'[1/2]_1^o)$  produced by a laser pulse was  $5 \times 10^{13}$  cm<sup>-3</sup>  $\mu s$ .

#### ETP 64 Application of Laser Thomson Scattering Diagnostics to a Micro-Discharge for a Plasma Display Panel

Y. NOGUCHI, A. MATSUOKA, M. D. BOWDEN, K. UCHINO, K. MURAOKA, *Kyushu University, Japan* As one part of a study to improve the light emission efficiency of the plasma display panel (PDP), the applicability of Thomson scattering to the measurement of electron temperature and density in a PDP discharge was investigated. Two main difficulties for the application were assessed. (i) The size of the plasma in a single PDP cell is about 0.2 mm, and so the scattering volume size should be below 0.1 mm. This means that the Thomson scattering signal may be very small. (ii) The pressure of the discharge gas is about 500 Torr, and so Rayleigh scattering may be a problem for the Thomson scattering measurements. Also, the stray light may be very strong because the wall of the discharge cell is very close to the scattering volume. For item (i), we estimated the expected signal intensity. It

was found that the signal could be detected by optimizing the system and using photon-counting methods. For item (ii), a triple-grating polychromator was fabricated, and then, the stray light rejection on the order of  $10^{-8}$  at 1 nm from the laser wavelength was achieved. This rejection level sets the required stray light level to be equivalent to the Rayleigh scattering intensity from argon gas at a pressure of 10,000 Torr. We demonstrated that this stray light level could be achieved experimentally even when the scattering volume was set to be a distance of 0.1 mm from the electrodes in a PDP cell.

#### ETP 65 Challenges of Thomson scattering in molecular gas plasmas

C.E. THOMPSON, P.G. STEEN, T. MORROW, W.G. GRAHAM, *Dept. of Pure and Applied Physics, The Queen's University of Belfast, Northern Ireland.* Thomson scattering (TS), an established diagnostic in high density fusion plasmas, has recently been used in lower density laboratory plasmas. Here a TS system using the second harmonic of a Nd:YAG laser and an ICCD as detector has been set up and successfully used to investigate low density Ar plasmas in an inductively coupled GEC cell. To extract the TS signal from other scatter and noise each TS spectrum was produced from five data sets taken under different conditions, allowing removal of background signal, stray light, Rayleigh scatter and plasma emission. A comparison factor was introduced to account for neutral density depletion by plasma heating. This methodology proved successful in argon, a monatomic gas, but extending investigation to nitrogen plasmas has shown that molecular gases require different data handling; in particular, the Raman scattering contribution must be considered. Here we review the successful demonstration of TS in argon and the methodology employed, and discuss the challenges to be overcome for successful use in molecular gas plasmas.

#### ETP 66 Laser Scattering Diagnostics of a Microwave Discharge Plasma

S. NARISHIGE, S. SUZUKI, K. UCHINO, K. MURAOKA, *Kyushu University, Japan* T. SAKODA, *Kitakyushu Nat. Coll. Tech.* In order to understand reaction processes in a microwave discharge plasma that is used for diamond thin film fabrication, we are planning to use various laser scattering diagnostic techniques. Until now, Raman scattering has been applied successfully to measurements of molecular densities and temperatures in the plasma under the diamond deposition condition. Recently, much effort was made to establish laser Thomson scattering because it was thought to be a unique method that could measure directly electron densities and temperatures of microwave plasma produced in moderate pressure gases. The first trial was performed for the microwave plasma produced in a pure hydrogen gas at a pressure of 20 Torr. Although the degree of ionization of the plasma was very low ( $< 10^{-6}$ ), Thomson scattering signals could be detected clearly by using a double-monochromator that has stray light rejection of  $10^{-6}$ , at the differential wavelength of 1 nm from the laser wavelength. In order to confirm the validity of present Thomson scattering measurements, linearity of Thomson scattering signal was checked against laser energy experimentally. Also, numerical estimations of possible one-photon ionization of excited hydrogen atoms/molecules and multi-photon ionization of

the ground state hydrogen atoms showed that their contributions were many order of magnitudes less than the measured electron density. From these results, we concluded that influence of laser perturbation in the present measurements was negligible.

**ETP 67 He Metastable Density in a Double Layer Formed by a Diameter Discontinuity in a Positive Column** J. M. WILLIAMSON, *Innovative Scientific Solutions, Inc., Dayton, OH* B. N. GANGULY, *Air Force Research Laboratory, Wright-Patterson Air Force Base, OH* E The population density profile of triplet helium metastable was measured in the double or multiple space charge<sup>1</sup> layer formed at an abrupt transition of the tube diameter in a positive column discharge by diode laser absorption. The double layer was formed at the transition of a 2.6 cm diameter to 0.6 cm diameter tube in a static pressure discharge. The line-integrated He 2<sup>3</sup>S<sub>1</sub> population density profile in the double layer region was determined from the absorption of a diode laser operating at 1083 nm. The triplet metastable density profiles were measured for discharge currents of 1, 2, and 5 mA at 1 Torr pressure. Spatially resolved He 3<sup>3</sup>D to 2<sup>3</sup>P emission profiles were also measured. The diode laser absorption and plasma induced emission profiles both show enhanced production of 2<sup>3</sup>S and 3<sup>3</sup>D states in the double layer region compared to the unperturbed positive column with higher current density (0.6 cm diameter) and the magnitude is strongly dependent on the discharge polarity.<sup>1</sup> H. S. Maciel and J. E. Allen, *J. Plasma Physics* **42**, 321 (1989).

**ETP 68 Diagnostics of H<sup>-</sup> and D<sup>-</sup> in High-Density H<sub>2</sub> and D<sub>2</sub> Plasmas by Laser Photodetachment and Optical Emission Spectroscopy** H. YAMAGUCHI, K. SASAKI, K. KADOTA, *Department of Electronics, Nagoya University, Japan* M. GOTO, S. MORITA, K. KAWAHATA, *National Institute for Fusion Science, Japan* In the present work, we propose a simple method for diagnostics of negative ions in hydrogen plasmas. Since the present method employs optical emission spectroscopy, it has good accessibility to fusion and processing plasmas which have a limited number of observation ports. The principle of the method is based on mutual neutralization reaction between positive and negative ions (H<sup>+</sup> + H<sup>-</sup> → H + H\*). Excited hydrogen atoms are produced by this reaction, and the excited state decays with optical emissions. If we detect the optical emission from H\* produced by this reaction, we can monitor negative ions in plasmas. This method has been demonstrated in an oxygen plasma successfully (T. Ishikawa, D. Hayashi, K. Sasaki, and K. Kadota, *Appl. Phys. Lett.* **72**, 2391 (1998)). Experiments were carried out in pulse-modulated high-density H<sub>2</sub> and D<sub>2</sub> plasmas. Optical emission at the H<sub>α</sub> line was observed in the afterglow. The H<sup>-</sup> density was measured by probe-assisted laser photodetachment. Temporal variation of the emission intensity due to H<sup>+</sup> + H<sup>-</sup> → H + H\* was compared with that of the product between H<sup>+</sup> and H<sup>-</sup> densities.

**ETP 69 Modeling of relaxation phenomena after photodetachment in RF SiH<sub>4</sub> discharges** MIN YAN, ANNEMIE BOGAERS, RENAAT GIJBELS, *Department of Chemistry, University of Antwerp, Belgium* WIM GOEDHEER, *FOM-Institute for Plasma Physics, The Netherlands* PLASMA SIMULATION TEAM, MODELING OF LOW TEMPERATURE PLASMA COLLABORATION, The complete relaxation mechanism after instantaneous laser-induced photodetachment in an electronegative discharge has been studied by a kinetic 1-D PIC/MC model.

The results show that the different diffusion speeds of extra electrons and anions lead to a significant change in the electric field, and hence in the EEDF, the reaction rates of the electron impact collisions, and finally in the whole discharge. The EEDF recovers synchronously with the electron density profile. The recovery time of ion densities is about one order of magnitude longer than that of electrons due to different recovery mechanisms. The recovery time is closely related to the pressure of the gas and the efficiency of the photodetachment. The modeled behavior of the recovery of all the charged particles as well as the electric field qualitatively agrees very well with experimental results from the literature [1,2]. [1] M. Bacal, P. Berlemont, A. M. Bruneteau, R. Leroy, and R. A. Stern, *J. Appl. Phys.*, **70**, 1991, 1212. [2] P. Devynck, et al., *Rev. Sci. Instrum.* **60**, 1989, 2873

**ETP 70 Investigations on Electric Field Distributions in a Microwave Discharge in Hydrogen** D. LUGGENHÖLSCHER, U. CZARNETZKI, H.F. DÖBELE, *Institut für Laser- und Plasmaphysik, Universität GH Essen, D-45117, Germany* Microwave discharges play an important role as plasma sources for industrial applications like surface modification and thin film deposition. The electric field distribution in the plasma determines the electron density and energy distribution and the homogeneity of the discharge. The typical amplitude of the electric field is of the order of 100 V/cm. Up to now, this low field strength was not within the reach of laser spectroscopic techniques for electric field measurements. Recently, we have developed a novel technique in atomic hydrogen that allows the measurement of low electric fields down to 5 V/cm. The electric field is determined from the Stark splitting of high Rydberg states (typically n=14-20). Here this technique is applied to a pulsed microwave discharge at 2.45 GHz in hydrogen. The spatial and temporal field distribution is investigated in a commercial plasma source (SLAN). The cylindrical discharge chamber has a diameter of 160 mm and a length of 500 mm; typical power is of the order of 1 kW at pressures of a few 10 Pa. The measurements show that both microwave and plasma microfields contribute to the electric field in the steady state case. In the pulsed mode the microwave field is dominant during the transient switch-on phase while in the off phase the micro field can be measured.

**ETP 71 Measurements of molecular radical densities in a CF<sub>4</sub> capacitively coupled RF-discharge** P. FENDEL, A. FRANCIS, U. CZARNETZKI, H.F. DÖBELE, *Institut für Laser- und Plasmaphysik, Universität GH Essen, D-45117, Germany* An asymmetric capacitively coupled RF-discharge is operated in CF<sub>4</sub> at pressures between 20 Pa and 100 Pa and RF-power of the order of several 10 Watts. The stainless steel electrodes have a diameter of 8 cm with a 2.5 cm separation. The discharge can be operated either cw or pulsed with a switch-off time of about 10 s. CF and CF<sub>2</sub> radical densities are measured by laser induced fluorescence spectroscopy. Excitation and observation wavelengths are at λ=233 nm/λ=255 nm (CF) and λ=262 nm/λ=271 nm (CF<sub>2</sub>), respectively. The spatial and temporal (after switching off the RF-power) profiles of the radical densities are investigated. From these data the sticking coefficients at the electrode surfaces and the effective source strength distributions in the plasma volume are inferred. Under our experimental conditions the effective sources for both CF and CF<sub>2</sub> are within the plasma volume while the electrodes are sinks even when the discharge is powered. The effective CF sources are located mainly within the sheath close to

the powered electrode while the effective  $CF_2$  sources are closer to the grounded electrode. Decay time measurements as a function of pressure give an indication for an additional volume loss process for CF, while the  $CF_2$  densities decay by diffusion to the walls only.

**ETP 72 Time resolved diagnostics in  $CF_4 / H_2$  plasmas by electron attachment mass spectrometry and optical emission spectroscopy.** HANS-ERICH WAGNER, JUERGEN MEICH-SNER, VALJA KROUTILINA, RENE LERCH, *Institut für Physik, 17487 Greifswald*, LOW TEMPERATURE PLASMA PHYSICS AND CHEMISTRY TEAM, *Institute of Physics, University of Greifswald* In the case of a parallel plate symmetrical 50kHz low pressure discharge in  $CF_4 - H_2$  mixtures (discharge current 10 – 40mA, total pressure 10 – 30Pa, hydrogen admixture 0 – 80%, closed system) the main stable products (e.g.  $F_2$ ,  $CF_4$ ,  $C_2F_6$ ,  $C_3F_8$ ) of plasma chemical reactions have been time resolved investigated by the electron attachment mass spectrometry (EAMS), investigating them according their resonant electron attachment cross sections. The EAMS was realised by means of a HAL EQP 300 Hiden Analytical system, extended by the (-) RGA mode. The plasma chemical reaction kinetics is characterised by the time dependent consumption of molecular hydrogen and the production of higher molecular fluorocarbons. These measurements were completed by optical emission spectroscopy of electronic excited species (e.g. atomic fluorine, molecular hydrogen).

**ETP 73 Diagnostics of the Single Filament Barrier Discharge in Air by Cross-Correlation Spectroscopy** HANS-ERICH WAGNER, *Affiliation RONNY BRANDENBURG, Affiliation PETER MICHEL, Institute of Physics, Ernst-Moritz-Arndt University of Greifswald, 17489 Greifswald, Domstr. 10a, Germany* KIRILL V. KOZLOV, *Moscow State University, Department of Chemistry, 119899 Moscow, Russia* LOW TEMPERATURE PLASMA PHYSICS AND CHEMISTRY COLLABORATION; The temporal and spatial development of a single filament barrier discharge was investigated at atmospheric pressure. The used technique allows spectral and phase resolved measurements in the time scale 1...200ns at a spatial resolution of 0.1mm. The single filament is produced with the frequency of about 6kHz. A symmetrical electrode arrangement with both electrodes covered by the dielectrics (glass or alumina, discharge gap width of 1mm) was used. The time resolution in the sub ns scale was realized by a correlation technique in single photon counting mode [1]. The spectral investigations are focussed on the second positive system (wavelength 337nm) and the first negative system (wavelength 391nm) of nitrogen. The measurements allow a detailed visualization and interpretation of the streamer development. In combination with a kinetic model of the dominant excitation as well quenching processes there is the possibility to get informations on the temporal and spatial development of the reduced field strength  $E/n$ , too. [1] K. V. Kozlov et al, Proc. XIth Conf. on Gas Discharges and their Applications (1995) II-42

**SESSION FW1: FOUNDATIONS OF GASEOUS ELECTRONICS**

Wednesday morning, 25 October 2000; Grand Ballroom, Red Lion Hotel at 8:00; Peter Ventzek, Motorola, Inc., presiding

*Invited Paper***8:00****FW1 1 Evolution of Computational Studies of Electron Swarm Experiments and Their Application to Discharge Simulations..**HIROAKI TAGASHIRA, *Muroran Institute of Technology*

Electron swarm experiments are important since they provide a unique link between gas discharge studies and atomic and molecular collision physics. In the talk, I shall aim to give an account for essential differences between the electron swarm properties when electron gain (ionization) and/or loss (electron attachment) processes, i.e. "reaction processes," are present and not. Importance of the modes of observation of electron swarms, such as the steady-state Townsend, pulsed Townsend, and time-of-flight experiments in determining electron swarm parameters is stressed. Development of computational studies is described with accentuation in clarifying the above mentioned aspect of electron swarms, and their possible application to gas discharge simulations will be given.

**SESSION GW1: INTERACTIONS WITH EXCITED SPECIES**

Wednesday morning, 25 October 2000; Grand Ballroom, Red Lion Hotel at 9:45; Bill Graham, The Queen's University of Belfast, presiding

*Invited Papers***9:45****GW1 1 Electron Interactions with Excited Atoms and Molecules.**LOUCAS CHRISTOPHOROU, *NIST*

This talk is based on a comprehensive recent review of electron interactions with excited atoms and molecules.<sup>1</sup> A comparison will first be made of the cross sections for electron scattering from - and ionization of - ground and excited atoms. As a rule, the cross sections for the latter far exceed the cross sections for the former. The larger polarizabilities of the atomic excited states compared with the respective ground states largely account for the higher electron scattering cross sections from excited atoms and also for other significant differences between the scattering cross sections of ground-state and excited atoms such as the absence of the Ramsauer-Townsend minimum in the electron scattering cross sections of the excited heavier-rare gases. With the exception of a few limited measurements on electron scattering from singlet oxygen and electron-impact ionization of metastable N<sub>2</sub>, the field of electron scattering from excited molecules remains wide open. There has been however substantial work on dissociative and nondissociative electron attachment to ro-vibrationally excited molecules that demonstrates the role of the total internal energy of the excited molecule on the dissociation cross section in the case of dissociative attachment and autodetachment in the case of nondissociative attachment. Recent experiments have shown that the cross sections for dissociative electron attachment to electronically excited molecules can be very much larger than for the ground state molecules, although quantitative measurements are still lacking. The field of electron interactions with excited molecules is full of basic challenges and potential for applications. <sup>1</sup>L. G. Christophorou and J. K. Olthoff, *Advances in Atomic, Molecular, and Optical Physics*, B. Bederson and H. Walther (Eds.), Academic Press, Boston, Vol. 44, Chap. 7.

**10:15****GW1 2 Low-Energy Dissociative Electron Attachment to Vibrationally-Excited H<sub>2</sub> Molecules.\***IZTOK CADEŽ, *J. Stefan Institute, Ljubljana, Slovenia*<sup>†</sup>

Vibrationally excited hydrogen molecules (VEH) are present in distant interstellar clouds as well as in different laboratory and technological hydrogen plasmas. They are formed by de-excitation of higher electronic states, by molecular gas reactions, or by hydrogen atom recombination on solid surfaces. Because of the fundamental role of the hydrogen molecule, and the need for understanding plasma processes and media, the study of VEH is important and interesting. The current status of experimental and theoretical knowledge on dissociative electron attachment to VEH will be presented.

Strong enhancement of the dissociative attachment cross section in 4 eV incident-energy region ( $e + H_2(X^1\Sigma_g^+, v) \rightarrow H_2^-(^2\Sigma_u^+) \rightarrow H^- + H(1s)$ ) with  $v^1$  is the most striking feature of this resonant process. We used this effect to develop a method for  $H_2(v)$  diagnostics<sup>2</sup>. Some characteristic vibrational distributions of  $H_2$  molecules formed by recombination on metal surfaces<sup>3</sup> will also be presented. Possible future experimental studies of dissociative attachment to VEH will be discussed.

\*Work performed mostly at D.I.A.M., Université Pierre et Marie Curie, Paris, France. Financial support from the University and CNRS is gratefully acknowledged.

<sup>†</sup>Present address: Jet Propulsion Laboratory, California Institute of Technology, Pasadena, CA.

<sup>1</sup>Allan and Wong, Phys. Rev. Lett. 41 (1978) 1791.

<sup>2</sup>Popović et al., Meas. Sci. Technol. 1 (1990) 1041.

<sup>3</sup>Schermann et al., J. Chem. Phys. 101 (1994) 8152, Čadež et al., J. Chem. Phys. 106 (1997) 4745.

#### 10:45

#### GW1 3 Electron Attachment to Rydberg States and Its Implications for Low-Temperature Plasmas\*

LAL PINNADUWAGE, *Oak Ridge National Laboratory and the University of Tennessee, Knoxville*

The presence of negative ions in low-temperature plasmas can have important implications: In many instances, the presence negative ions may affect the discharge characteristics, lead to dust formation, and may influence deposition and etching characteristics of material processing plasmas. Efficient negative ion formation has been observed in many low-temperature plasmas, where the component molecular gases are only weakly electronegative. For example, studies on silane and methane plasmas have shown them to contain relatively high negative ion densities. Another example is hydrogen volume discharges that are being developed for the generation of  $H^-$  ions for neutral beam generation. For many years,  $H^-$  formation in these discharges has been attributed to electron attachment to high-vibrational states of the  $H_2$  molecule. However, several researchers have recently pointed out that the observed  $H^-$  densities are too large to be explained via electron attachment to vibrationally-excited states. Our studies on laser- and discharge-excited molecules indicate that negative ion formation via electron attachment high-Rydberg states is an extremely efficient process. When a molecule is excited to an energy above and close to the ionization threshold, a multitude of Rydberg states converging to various vibrational/rotational ionization thresholds of the molecule can be populated. Our own studies, as well as several ZEKE (ZEro Kinteic Energy) spectroscopic studies, have shown that such core-excited Rydberg states have characteristically long lifetimes of the order of microseconds. Our mass spectroscopic studies show that the mass spectra arising from electron attachment to Rydberg states of complex molecules can be quite different from those due to electron attachment to their ground state counterparts. The cross sections that we estimate for electron attachment to Rydberg states are orders of magnitude larger compared to typical cross sections associated with ground state counterparts, but are consistent with cross sections that have been measured for Rydberg states for other electron-induced collision processes, such as  $s$ - and  $m$ -mixing collisions. The main result of collisions of Rydberg states with neutral species is also to lead to  $s$ - and  $m$ -mixing (except for collisions with polar molecules, which could lead to the ionization of the Rydberg molecule), which would further lengthen their lifetimes. The above measurements and their implications will be summarized and discussed. \* This research was supported by the DOE EMSP program and the ORNL Seed Money Program. Oak Ridge National Laboratory is managed by UT-Battelle, LLC, for the U.S. Dept. of Energy under contract DE-AC05-00OR22725.

#### Contributed Paper

#### 11:15

**GW1 4 From Laser-Cooled Atoms to an Ultracold Neutral Plasma** T. KILLIAN, S. KULIN, M. LIM, S. ROLSTON, *National Institute of Standards and Technology, Gaithersburg, MD 20899-8424* By photoionizing laser-cooled xenon atoms just above the ionization threshold, we create an ultracold neutral

plasma with initial electron and ion energies as low as 100 millikelvin and 10 microkelvin respectively. We observe plasma oscillations of the electron density and observe effects of strong Coulomb coupling of the electrons. At high density and low temperature, a large fraction of the charged particles collisionally recombine to form Rydberg atoms. This recombination appears to deviate from the normal behavior expected for three-body recombination.

**SESSION HW1: GENERAL BUSINESS MEETING**

Wednesday morning, 25 October 2000; Grand Ballroom, Red Lion Hotel at 11:30; Gerald Hays, Sandia National Laboratories, presiding

**SESSION IW1: ELECTRON-ATOM/MOLECULE COLLISIONS I**

Wednesday afternoon, 25 October 2000; Grand Ballroom D, Red Lion Hotel at 14:00; Klaus Bartschat, Drake University, presiding

*Invited Papers***14:00****IW1 1 Correlation studies of excitation and ionization of simple atoms by electron impact.**

ALBERT CROWE, *University of Newcastle, Newcastle upon Tyne NE1 7RU, United Kingdom*

Experimental correlation studies of electron impact excitation and ionization provide the most sensitive tests of theoretical predictions of these processes. In the simpler cases the magnitudes and phases of the excitation amplitudes can be extracted from the experimental data. Hence they lead to a better fundamental understanding of the processes and to a better estimate of integrated cross sections with a diverse range of applications. The scattered electron-polarized photon correlation method used to study excitation and the (e,2e) method to study ionization will be outlined, together with examples. Emphasis will be placed on recent advances in both excitation and ionization studies using three-particle coincidences. These are often used to study collisions involving two active atomic electrons. While there have been major theoretical advances in describing single atomic electron processes, it will be shown that theory generally gives poor agreement with experimental data for collisions involving two atomic electrons.

**14:30****IW1 2 The Coulomb Three-Body Problem.**

ANDRIS T STELBOVICS, *Center for Atomic, Molecular and Surface Physics, Division of Science and Engineering, Murdoch University, Perth, 6150 Western Australia*

Significant theoretical progress has been achieved in the most fundamental of three-body Coulomb problems, namely the electron-Hydrogen system, in the past decade. A considerable amount of experimental data is available for this system making it an ideal testing ground for theoretical modeling. We will discuss important milestones in the theoretical development and computational methods, particularly above the ionization threshold for this archetypical three-Coulomb-particle system. One of the most interesting problems remains that of describing the ionization boundary condition completely and implementing it in a computational framework. Direct coordinate-space methods for solving the Schrödinger differential equation numerically are showing considerable promise and some of our current work (with S. Jones) and matching procedures for ionization will be reported.

WEDNESDAY AFTERNOON \ IW1

*Contributed Papers***15:00****IW1 3 Electron Impact Excitation of the Ne 2p<sup>5</sup>3s configuration**

M. LARSEN, X GUO, G KLEIBAN, J WRKICH, M. A. KHAKOO, *Physics Department, California State University, Fullerton* PHYSICS DEPARTMENT, CALIFORNIA STATE UNIVERSITY, FULLERTON TEAM, E Accurate experimental differential cross sections and cross section ratios for the electron impact excitation of the Ne 2p<sup>5</sup>3s configuration at 20, 25, 30 40, 50 and 100eV incident energies will be presented. The data were taken using the method of mixtures with atomic H<sup>1</sup> and are normalized to the H(n=2) convergent close-coupling cross sections<sup>2</sup>. Comparison with other experimental data and current theoretical

models will be made. <sup>1</sup> M. A. Khakoo et al., Phys. Rev. A v61, 12701 (1999) <sup>2</sup> I. Bray and A. Stelbovics, Phys. Rev. A v46, 6995 (1992)

**15:15****IW1 4 Electron-Impact Excitation of Krypton and Comparison with Other Rare-Gas Atoms\***

J. ETHAN CHILTON, M. D. STEWART, CHUN C. LIN, *University of Wisconsin-Madison* Electron-impact optical cross sections for the 2p → 1s (Paschen's notation) emissions of Kr have been measured over a range of electron energies from onset to 250 eV and at different gas pressures between 0.04 and 3 mTorr. By measuring cascade transitions into the 2p levels from higher-lying levels and subtracting

this component from the observed transitions out of the  $2p$  levels, we have determined the cross sections for direct electron excitation of the  $2p$  levels. The general trends of the variation of these cross sections are studied and compared with the other rare-gas atoms. The results of Ne/Ar and of Xe represent two extremes, with Kr being an intermediate case, and their relation to the atomic structure is discussed.

\*Supported by the U.S. Air Force Office of Scientific Research.

15:30

**IW1 5 ELECTRON-WATER COLLISIONS PROBED BY DIRECT AND LASER INDUCED FLUORESCENCE\*** T. HARB, W. KEDZIERSKI, J.W. McCONKEY, *University of Windsor, Ontario, Canada, N9B 3P4*. A crossed electron- supersonic gas beam system, coupled with photon detection in the 300 nm region, has been used to study production of OH in dissociating collisions. Use of LIF techniques enables the X state to be studied with rotational resolution. Analysis of the rotational distribution together with detailed measurements of the near-threshold excitation function of OH(X) reveals the presence of a number of dissociative excitation processes. These include direct and cascade excitation and dissociative attachment. Both dipole allowed and spin exchange transitions in the parent molecule are significant.

\*Research supported by the Natural Sciences and Engineering Research Council of Canada.

15:45

**IW1 6 The Total Elastic Cross Section for Electron Scattering from SF<sub>6</sub>** R J GULLEY, H CHO, S J BUCKMAN, *Australian National University* Absolute differential cross sections for vibrationally elastic scattering of electrons from SF<sub>6</sub> have been measured at 11 energies between 2.7 and 75 eV for scattering angles between 10° and 180°. The differential measurements use the magnetic angle-changing technique of Read and Channing in combination with the relative flow technique to obtain absolute elastic scattering cross sections at backward angles (135°-180°). These cross sections have been extrapolated in the forward direction to enable the integral elastic cross section to be calculated. The cross section derived from this process is in excellent agreement with that proposed recently at the previous GEC meeting<sup>1</sup> and supports the hypothesis that several of the earlier measurements underestimate the integral elastic cross section between 5 and 75 eV. <sup>1</sup>L. Christophorou, J Olthoff, R Siegel, M Hayashi and Y Nakamura *Bull. Am. Phys. Soc.* **44** 20 (1999).

#### SESSION IW2: GEC CELL - 10 YEAR PERSPECTIVE

Wednesday afternoon, 25 October 2000; Grand Ballroom C, Red Lion Hotel at 14:00; Mark Kushner, University of Illinois at Urbana-Champaign, presiding

#### Invited Papers

14:00

**IW2 1 The GEC Cell: An "Historical" Overview.**  
JAMES OLTHOFF, *NIST*

It has been 10 years since the presentation at the 1980 Gaseous Electronics Conference of the first comparison of data obtained using GEC RF Reference Cells. Those initial measurements showed that measurements made on ostensibly identical plasma reactors produced similar results, although not without some difficulty. Since then, the number of GEC Cells in operation has grown substantially, as has the number and sophistication of the applied diagnostics. This talk will briefly summarize the history of the development of the GEC Cell (including comments on its continuing evolution), and then will present an overview of the plasma diagnostics that have been applied to the GEC Cell, with an emphasis on results obtained from electrical and mass spectrometric investigations. Finally, the talk will conclude with some remarks on the impact that the GEC Cell concept has made in the areas of plasma diagnostics development and use, modeling, and reactor performance.

14:30

**IW2 2 A whirlwind tour of 10 years of progress in optical and microwave diagnostics in the GEC rf reference cell.**

GREG HEBNER, *Sandia National Laboratories, Albuquerque NM*

When the GEC rf reference cell concept was initiated 10 years ago, one of the key considerations was to design a flexible discharge chamber that was amiable to modeling while retaining excellent access for diagnostic measurements. Since its adoption by research groups around the world, there has been a myriad of excellent, novel and innovative measurements of fundamental discharge physics and chemistry mechanisms that have greatly advanced our understanding of rf excited plasmas. This talk will touch upon the highlights of a decade of work by numerous groups and then look towards potential future directions. The author is supported by Sandia National Laboratories, a multiprogram laboratory operated by Sandia Corporation, a Lockheed Martin Company, for the U. S. Department of Energy (DE-AC04-94AL85000).



*Contributed Papers*

15:00

**IW2 3 Characterization of GEC reference reactors.\*** W.G. GRAHAM, E. COSTA I BRICHA, C.S. CORR, S. GOMEZ, J. MCFARLAND, P.G. STEEN, C.E. THOMPSON, *Dept. of Pure and Applied Physics, The Queen's University, Belfast BT7 INN, Northern Ireland* C.M.O. MAHONY, *University of Ulster, Northern Ireland* The low temperature plasma physics group at Queen's University Belfast, has two GEC reference cells, one in capacitive and the other in inductive configuration. A range of experimental techniques have been used in their characterisation. These include measurement of electrical properties, Langmuir probes for electron energy distribution function (eedf) measurements, spatially and temporally resolved emission spectroscopy, laser induced fluorescence and Thomson Scattering. In addition a 2D+1 computer simulation, based on the Berkeley-developed XOOPIE code, has been developed for the GEC geometry. The systems have been operated in Ar, He, H<sub>2</sub>, D<sub>2</sub> and O<sub>2</sub>. Ongoing work including the study of the capacitive to inductive transition and instabilities, eedf and atom density measurements in molecular gases and the measurement of temporally resolved eedfs will be discussed and compared with simulations.

\*Supported largely by the UK EPSRC and also by the EU-Brite programme as part of the Plasmatex project.

*Invited Paper*

15:30

**IW2 5 Using Radio-Frequency Electrical Measurements as a Plasma Diagnostic.**  
MARK SOBOLEWSKI, *NIST, Gaithersburg, MD 20899, USA*

Radio frequency (rf) current and voltage measurements are an important and convenient tool for monitoring rf discharges. These measurements are compatible with commercial reactors and with the manufacturing environment. Recently, many methods have been proposed for using rf electrical measurements to monitor process-relevant plasma properties. These methods rely on models that relate measured electrical parameters to physical properties such as the densities, fluxes, and energies of electrons and ions. Unfortunately, the models that are used often rely on untested assumptions. In particular, the sheath regions of the plasma are difficult to model without the aid of simplifying assumptions. To test these assumptions and to provide a firmer foundation for rf-based diagnostics, electrical studies were performed in high-density discharges in an inductively coupled GEC Reference Cell, at pressures of 0.67-4.0 Pa, inductive source powers up to 370 W, rf bias powers up to 150 W, and rf bias frequencies of 0.1-13.56 MHz. External measurements of current and voltage waveforms were combined with capacitive probe measurements of the rf plasma potential and independent measurements of ion current and ion energy. Together, these measurements provide enough information to test electrical diagnostic techniques and the models that these techniques are based on. Here, a comprehensive test and comparison of methods for determining the ion flux in argon discharges will be presented. Methods which use high-frequency or low-frequency approximations to ion motion were found to be less accurate than methods based on a new, complete model of the time-dependent ion dynamics in the plasma sheath. Ion flux results from SF<sub>6</sub> and fluorocarbon plasmas and methods for obtaining ion bombardment energies from rf measurements will also be presented.

15:15

**IW2 4 2D+1 PIC-MCC Modelling of a RF driven, capacitively coupled GEC reference cell.** E. COSTA I BRICHA, P.G. STEEN, W.G. GRAHAM, *Dept. of Pure and Applied Physics, The Queen's University of Belfast, Northern Ireland.* C.M.O. MAHONY, *N.I.B.E.C., University of Ulster at Jordanstown, Northern Ireland.* C A two-dimensional Particle In Cell (PIC) PC-based code is used to describe a RF driven, capacitively coupled GEC reference cell. The main objective is to model the response to particular diagnostic tools. A two dimensional, cylindrically symmetric model is required to adequately describe charged particle losses. The present code is based on XOOPIE(1), which was developed by the UC Berkeley group. The GEC reference cell configuration includes a blocking capacitor to simulate the GEC external circuit and so allow ab initio development of the DC bias. The GEC geometry has required the use of non-linear cell volumes to reduce calculating time without compromising accuracy, as well as the use of reduced ion mass. A new diagnostic has been introduced into the code. Spatially and temporally resolved collision maps can be plotted, allowing prediction of the plasma emission. Results are compared with experimental data. (1) <http://www.ptsg.eecs.berkeley.edu/xoopic/xoopic.html> Supported by EU BRITE.

SESSION JWP: POSTER SESSION II  
 Wednesday afternoon, 25 October 2000  
 Westheimer Ballroom, Crowne Plaza Galleria at 16:30

## JWP 1 PULSED PLASMAS

**JWP 2 Two-Dimensional Simulation of Pulsed-Power Electronegative Plasmas** BADRI RAMAMURTHI, DEMETRE ECONOMOU, *Department of Chemical Engineering, University of Houston, Houston, TX 77204-4792* Low pressure electronegative plasmas are widely used for the fabrication of sub-micron semiconductor devices. Recently, pulsed power operation has emerged as a promising technique for reducing charge induced damage and etch profile distortion (e.g., notching) associated with conventional continuous wave discharges. This paper will report results of a 2-D fluid simulation of a pulsed-power inductively-coupled chlorine plasma. Simulation results show spontaneous separation of the plasma into an ion-ion core and an electron-ion periphery, depending on the negative ion to electron density ratio. The transition from an electron-dominated plasma to an ion-ion plasma in the afterglow was captured. The spatiotemporal evolution of the plasma for varying pressure, power, pulsing frequency and duty ratio has been studied. The evolution of negative ion density profiles is especially complex due to the formation of self-sharpening fronts during plasma "on" and subsequent back-propagation of the fronts during the plasma "off" stage of the pulse. Reactor geometry has a strong influence on negative ion evolution.

**JWP 3 Ionization/Recombination Model for the Initial Stage of Pulsed Discharges** S. POPOVIĆ, P. KESSARATI KOON, L. VUSKOVIĆ, *Department of Physics, Old Dominion U., Norfolk, VA 23529* At low gas temperature and low electron density the associative ionization processes generate important population of molecular ions, such as  $\text{Ar}_2^+$  in argon and  $\text{N}_4^+$  in nitrogen. These ions are heavier than atomic ions that normally occur in thermal plasmas at high electron density or at low pressures. Their presence has certain consequences to gas-dynamic properties of gas discharges at high pressures and low degree of ionization. We are studying the effect of molecular ions on the acoustic effects associated with the plasma filament expansion in the initial stage of pulsed dc and microwave-excited discharges. The expansion creates a compression effect that leads to the temporary formation of periodic pockets of cold gas, separated from the hot plasma by a shock structure. Current oscillations and macroscopic instabilities in the developing, filamentary stage of a pulsed d.c. discharge in noble gases are among the effects that typically occur at this stage, but still remain unexplained. In order to treat quantitatively the ionization-recombination process, associative ionization and dissociative recombination of molecular ions were included. Solving a system of non-steady state equations using the available rate coefficients and including the absorption and diffusion of resonant radiation, we derived distribution of atomic, molecular and ionic species across the expanding filament.

**JWP 4 Evolution of spatial density profiles in pulsed plasma of electronegative gases** E.A. BOGDANOV, A.A. KUDRYAVTSEV, *St.Petersburg State University, Russia*. \* The analysis performed had shown, that in the spatial and temporal evolution of the plasma profiles two different physical processes (and the cor-

responding two stages) are to be distinguished. The ion density profiles expand due to the ion-ion ambipolar diffusion and temporal dependence of its boundary spreading is more close to parabolic law than linear one. In the external zone, where the negative ions are practically absent, the usual electron-ion ambipolar diffusion dominates. The electron density decays faster, than exponentially with time during transition to the second stage. The evolution of density profiles proceeds in different ways depending on ratio positive and negative ions mobilities  $g$ . If  $g < 1$ , the electron profile in the inner region is convex. In the  $g > 1$  case, when the selfconsistent electrostatic field accelerates the less mobile negative ions in the plasma volume center, the interesting phenomenon arises, which has not analogies in case of the usual electron-ion plasmas. It is clear that in this case the ambipolar ion-ion field in the inner region has to accelerate also the electrons. To compensate outward directed electron drift flux, their density gradient has to change its sign. It leads to the surprising nonmonotonic electron density profiles.

\*This work is supported RFME grant N 97-0-5.3-33 and RFBR grant N 98-02-17778.

**JWP 5 Experimental investigations of spatio-temporal evolution of charged particle densities in afterglow oxygen plasma** A.A. KUDRYAVTSEV, V.G. MISHAKOV, I.N. SKOBLO, T.L. TKACHENKO, M.O. CHAYKA, *St.Petersburg State University, Russia*. Experimental investigation [1] of spatio-temporal evolution of charged plasma species in afterglow oxygen plasma have been continued. The temporal probe current-voltage characteristics at different distances along the radius of the tube and the time dependence of the saturation currents to a probe in a fixed bias voltage were performed. It was confirmed that the decay of oxygen low-pressure plasma takes place in two distinct stages (the electron-ion stage, and the ion-ion stage). In the first, the negative ions are locked within a discharge volume and plasma in this stage is depleted of electrons and positive ions. The electron density decay is faster, than exponential, and practically all electrons leave plasma volume during finite time. The moment of electron runaway correlates with sharp jump on saturation current of a positive ion for peripheral positions of a probe. Apparently it is connected to a sharp change of plasma potential with transition to the ion-ion plasma. The temporal dependencies saturation current of positive ions with different radiuses are various, i.e. the shape of spatial profiles of positive ion density change in time. As this changing the positive ion density on a periphery slower than in a center, ionic density profiles are expanding in time and its boundary propagates towards the tube walls. This work is supported RFBR grant N 98-02-17778. [1]. S.A.Gutsev, A.A.Kudryavtsev, V.A.Romanenko. *Tech.Phys.* 40 (1995) 1131.

**JWP 6 Sheath relaxation in pulsed discharges** K.-U. RIEMANN, TH. DAUBE, *Theoretische Physik 1, Ruhr-University Bochum, D-44780 Bochum, Germany* The sheath and presheath relaxation in front of an electrode biased to high negative voltage pulse is investigated on the basis of ion fluid equations as well as of a PIC-MC simulation. The electrons are assumed to be Boltzmann distributed and the ions are governed by charge exchange collisions. The electron Debye length is small compared with the ion mean free path. Switching on a high negative voltage, three phases on different time scales may be distinguished: The matrix extraction phase, the sheath expansion phase and the presheath relaxation initiated by a rarefaction wave. In a similar manner the processes caused by switching off a high negative voltage may be

characterized. All these phenomena are mixed up if voltage pulses of finite duration are applied. We present numerical results exhibiting typical relaxation phenomena for single pulses as well as for periodic pulses with various frequencies and pulse forms. Results for the particularly important matrix extraction phase are compared with an efficient step model of the homogeneous matrix sheath [1]. [1mm] [1] K.-U. Riemann and Th. Daube, *J. Appl. Physics* **86**, 1202 (1999).

#### JWP 7 INDUCTIVELY COUPLED PLASMAS

**JWP 8 Electron Temperature control in ICP using grid and its use for control the ion ratio in CF<sub>4</sub> / Ar plasma** K. H. BAI, KAIST J. I. HONG, *Samsung Electronics* H. Y. CHANG, KAIST Electron temperature control using grid with dc bias voltage in ICP was studied. EEDFs were measured to obtain the plasma parameters. Electron temperature was controlled from 2 to 0.5eV when grid bias voltage varied from 20 to -20V. We used this electron temperature control method to CF<sub>4</sub> / Ar plasma. It was possible to control the ion ratio of CF<sub>x</sub><sup>+</sup> / CF<sub>y</sub><sup>+</sup> (x,y = 1,2,3) by this method.

**JWP 9 The electron cyclotron resonance in a weakly magnetized radio frequency inductive discharge** CHINWOOK CHUNG, *Korea Advanced Institute of Science and Technology (KAIST)* HONG-YOUNG CHANG, KAIST The electron energy distribution function (EEDF) is measured by an rf compensated Langmuir probe under a weak DC magnetic field against various applied frequencies  $\omega/2\pi = 9, 13.56$  and 17 MHz. It is found that the EEDF at electron cyclotron resonance (ECR) is clearly transformed from Bi-Maxwellian EEDF into a distinctive Maxwellian EEDF. The electron temperature from the EEDF has a maximum at the ECR condition and the magnetic field with the maximum electron temperature changes according to the ECR condition. The electron density near the ECR greatly increases. The calculated energy diffusion coefficient well explains the effective heating of low energy electrons at the ECR. We present the first direct evidence of the ECR in rf inductive discharge and the effect of the ECR on electron heating by the EEDF.

**JWP 10 Spatial and temporal dependencies of ion energy distributions in an ICP Workstation** J.A. REES, C.L. GREENWOOD, S.J. PHILLIPS, D.L. SEYMOUR, I.D. NEALE, *Hidden Analytical Ltd. 420 Europa Boulevard, Gemini Business Park, Warrington, England, WA5 5UN* Inductively coupled plasmas, in which the exciting RF coil has been wound around a cylindrical reactor, have been used by a number of groups for studying the plasma surface modification of a range of materials, including polymer films. It has been found that beneficial effects are sometimes obtained by using pulsed rather than continuous RF excitation. The observed effects are due in part to the energies of the plasma ions and neutral species impacting on the materials exposed to the plasma. The present paper describes observations, carried out for 13.56 and 50MHz plasmas in argon and carbon dioxide, of the energies of mass-selected ions arriving at a grounded electrode as a function of axial position in the plasma. Time resolved measurements were also made during the 'off' period of a plasma pulsed at a repetition rate of 1.5kHz. The ion energies depend strongly on whether the RF coupling is purely inductive or includes a significant capacitive element.

**JWP 11 Experimental measurements on an inductive ring discharge in oxygen and nitrogen** J. J. GONZALEZ, D. M. SHAW, M. WATANABE, G. J. COLLINS, *Dept. of Electrical Engineering, Colorado State University, Fort Collins, CO 80523* N. TAKAHASHI, *Department of Materials Science, Shizuoka University, 3-5-1 Johoku, Hamamatsu 432-8561, Japan* Inductive ring discharges where the closed plasma loop forms the secondary circuit of a ferrite core radio frequency transformer are promising plasma sources of reactive gas species for materials processing such as etching and plasma assisted CVD. In this work, we present experimental measurements of the induced plasma ring voltage and current taken over a wide pressure range (0.01 to 1 Torr) of nitrogen and oxygen for several plasma ring tube geometries. Scaling rules governing discharge electrical parameter variation with plasma ring geometry and applied rf power (350 kHz) are discussed. Additionally, preliminary results of a crude zero order model relating the measured electrical parameters and the gas pressure of the discharge to the production and loss mechanisms of various reactive plasma species is presented.

**JWP 12 Electrical model of an inductive ring discharge in argon** J. J. GONZALEZ, D. M. SHAW, M. WATANABE, H. UCHIYAMA, G. J. COLLINS, *Dept. of Electrical Engineering, Colorado St. Univ., Fort Collins, CO 80523* Inductive ring discharges with a closed plasma loop forming the secondary circuit of a rf transformer were investigated in the 1960's as plasma sources for gas ion lasers and fusion research because of their efficiency at producing high charge density ( $n_e \approx 10^{13} \text{ cm}^{-3}$ ). More recently, due to improvements in both ferrite core materials and rf power supply technology, ring discharges are finding application as high efficiency lighting devices and radical generators for materials processing. Herein, we analytically model an inductively coupled ring discharge over a wide range of argon pressure (mTorr to 10's of Torr) and applied rf (350 kHz) power ( $50 < P_{rf} < 300 \text{ W}$ ). Only single step ionization is considered as a particle formation mechanism. For our geometry, ion free diffusion to the walls dominates charged particle loss from the ring discharge at low pressures ( $p < 0.1 \text{ Torr}$ ) and ion ambipolar diffusion to the walls dominates in the mid-pressure range ( $0.1 < p < 5 \text{ Torr}$ ). At the highest pressures investigated ( $5 < p < 30 \text{ Torr}$ ), three body electron-ion recombination in the bulk plasma takes over as the primary particle loss mechanism. The plasma electron density and temperature are determined from the model using measured plasma ring voltage and current. Comparisons between the modeled plasma density and Langmuir probe measurements agree to within a factor of 2 - 4 over the entire range of plasma parameters covered.

**JWP 13 Observation of anomalous field penetration in collisional, cylindrical ICP discharges** JOHN D. EVANS, FRANCIS F. CHEN, DONALD ARNUSH, *UCLA* Measurements of the radial penetration of RF-generated B-fields are performed in a large diameter cylindrical ICP. A loop antenna surrounds a dome-shaped Pyrex top that sits on top of a magnetic bucket.  $R_{top} = 15 \text{ cm}$  height of top,  $R_{bucket} = 18 \text{ cm}$ , bucket height 30cm,  $N = 10^{11} \text{ cm}^{-3}$ ,  $T_e = 3 \text{ eV}$ ,  $P_{rf} < 1.4 \text{ kW}$ ,  $f_{rf} = 2-27.12 \text{ MHz}$ ,  $P_0 = 1-100 \text{ mT}$ . Field penetration ("skin") depths  $L_{sd}$  are measured in the outer plasma region ( $r > R/2$ ) that are consistent with collisional skin depth theory. However, in the interior region ( $r < R/2$ ), non-monotonic radial profiles and interference phenomena that resemble standing wave behavior (e.g. nodes) are observed, where no propagating waves are predicted to occur. Similar phenomena have been observed by other groups [1], but for chamber sizes

such that R Lsd. Such observations were explained as manifestations of the anomalous skin effect (ASE), the electromagnetic analog of Debye shielding. However, these phenomena are more apparent as Po (and collisionality) is increased, in apparent contradiction to the predictions of ASE theory. Results of a detailed experimental investigation of interference phenomena under conditions that fall outside of the ASE regime will be presented, as well as a simple physical picture that resolves this apparent paradox. [1]. B. Joye and H. Schneider, *Helv. Phys. Acta* 51, 804 (1978).

**JWP 14 Global Model of Inductively Coupled Ar Plasmas using Two-Temperature Approximation** T. KIMURA, K. OHE,

*Nagoya Institute of Technology* The electron energy distribution function (EEDF) is measured with a Langmuir probe in an inductively-coupled RF (13.56 MHz) Ar discharge in the pressure range from 5 mTorr to 70 mTorr, by changing the power injected into the plasma up to 100 W. The EEDFs measured at pressure of 5 mTorr formed a bi-Maxwellian structure in the low-energy region below the lowest excitation threshold energy, while the EEDF structure in the high-energy region has a large depletion of high energy electrons. The EEDF measured at the pressure higher than 10 mTorr can be approximated using two-temperature distribution, which represent a low-energy region below the lowest excitation threshold energy with higher temperature and a high-energy region with lower temperature. Global model using two-temperature distribution is proposed and compared with the experimental results. The model consists of the rate equations for neutrals and charged particle and an energy-balance equation for electrons together with the balance equation for high-energy electrons. Pressure dependences of the electron density and temperatures predicted in the model agree with the experimental results except in the pressure lower than 10 mTorr.

**JWP 15 Atomic Chlorine and Chlorine Negative Ion Density Measurements in Ar/Cl<sub>2</sub> Inductively Coupled Plasmas\***

C.M.O. MAHONY, P.D. MAGUIRE, O.A. OKPALUGO, *University of Ulster, N. Ireland* C.S. CORR, S. GOMEZ, W.G. GRAHAM, P.G. STEEN, *The Queen's University of Belfast, N. Ireland* Cl<sup>-</sup> and Cl densities were measured in inductively coupled Ar/Cl<sub>2</sub> plasmas driven at 14MHz. Rf input powers of 10 to 80W, Ar/Cl<sub>2</sub> pressures of 0.5 to 12 Pa and Cl<sub>2</sub> fractions up to 10 percent were used. We used a frequency quadrupled NdYAG laser (266 nm) to photo-detach Cl<sup>-</sup> and a simple tungsten probe to collect detached electrons. A compensated Langmuir probe was used to measure plasma electron density. For LIF 233 nm radiation was used for two-photon excitation of atomic chlorine to an excited state. Subsequent fluorescence at 725 nm was measured with an ICCD. At powers < 30W and pressure of 1.3 Pa with 5 percent Cl<sub>2</sub>, the Cl<sup>-</sup> density is > half the total negative charge density. The negative ion fraction decreases markedly to a few percent as pressure is increased to 12 Pa. A similar but less dramatic decrease is observed as power is increased to 80W. Relative atomic chlorine densities increase both with power and pressure. Initial calibration with xenon indicates significant dissociation of Cl<sub>2</sub>.

\*UK EPSRC supported.

**JWP 16 Two-dimensional Particle-In-Cell Monte Carlo Simulations of High Density Plasma Sources** VITALY A. SCHWEIGERT, UWE KORTSHAGEN, *University of Minnesota, Mechanical Engineering*

The direct use of a conventional PIC-MCC technique for modeling of high-density inductive plasmas suffers from problems caused by the statistical noise of the charge and

current density. We have developed a technique which allows to significantly reduce the level of the statistical noise by using the plasma quasineutrality. We consider a two-dimensional, axially symmetric, inductive discharge. We solve the Maxwell equations for different harmonics in the vector potential using a finite-difference scheme and kinetic equations for both electrons and ions using a Monte-Carlo approach. We compare our numerical results with those found using the two-term approximation for the electron distribution function and with experimental results. We also discuss the importance of collisionless heating for the conditions in our experiments. This work is supported by NSF under grant ECS-9713137 and DOE under grant ER54554.

**JWP 17 Current, Voltage and Power Measurements in Ar/Cl<sub>2</sub> Inductively Coupled Plasmas Using Close-Coupled Probes\***

O.A. OKPALUGO, S. LAVERTY, P.D. MAGUIRE, C.M.O. MAHONY, *University of Ulster, N. Ireland* W.G. GRAHAM, *Queen's University Belfast, N. Ireland* The use of derivative probes for electrical measurements in rf process plasmas is relatively well established for capacitive systems compared to inductive (ICP) sources where the measurement and analysis is more challenging. Accuracy of the phase measurements is critical requiring robust and calibrated probe transforms. We have used derivative close coupled I-V sensors and subsequent Fourier analysis and probe transforms to measure coil currents and voltages. From this we determined delivered rf source power, less transmission and matching network losses. Our ICP system was excited at 14 MHz from 5W to 80W input powers for both 100 percent Ar and 95 percent Ar / 5 percent Cl<sub>2</sub> at a pressure of 2.7 Pa. The measured power delivered to the plasma is different for pure argon and the mixtures indicating process dependence. Our work on further development of probe transforms indicate pure argon plasmas have average transmission and match network losses of 15 percent over the above range.

\*UK EPSRC Supported.

**JWP 18 EEDF Measurements in an Ar/CF<sub>4</sub> ICP Discharge** M.

D. BOWDEN, P. SUANPOOT, K. UCHINO, K. MURAOKA, *Kyushu University, Japan* M. NOGUCHI, *Fukuoka Inst. Technology* We report measurements of the EEDF in a low-pressure inductively coupled plasma operated in a mixture of Ar and CF<sub>4</sub> gases. Measurements were made using the technique of laser Thomson scattering. Various checks were made to ensure that possible perturbations induced by the high intensity laser used for the measurement did not affect the measurement. The plasma measurements indicate that the EEDF in a pure Ar discharge was Maxwellian but addition of CF<sub>4</sub> gas to the gas mix resulted in a non-Maxwellian EEDF. Even relatively small amounts of CF<sub>4</sub> gas in the discharge altered the shape of the EEDF. Preliminary analysis of the results indicated that electron-molecule vibrational excitation collisions were a likely cause of the change in EEDF. These results and further analysis will be presented and discussed. In addition, a separate measurement system, designed for use in very low density plasmas, will be described.

**JWP 19 Characteristic of ICP Discharge Produced by a Novel External Antenna** MAHMOOD NASSER, HIROHARU

FUJITA, *Department of Electrical and Electronic Engineering, Saga University, Honjo 1, Saga 840-8502, Japan* FUJITA LAB. TEAM, E Intensive studies on the inductively coupled plasma (ICP) and the helicon discharges have been made because they can meet most of plasma processing requirements. The characteristics

of ICP discharge produced by a novel external antenna are experimentally investigated. This novel antenna was constructed from a combination of helical and spiral antenna. A sudden increase in luminosity and plasma density was observed as RF power was increased, which indicates the mode conversion from capacitively coupled CCP to inductively coupled ICP discharge. The combined antenna produced the highest plasma density for the same amount of power as compared with spiral and helical antennas. The space potential and the oscillating amplitude were suddenly decreased as increasing the power indicating the mode conversion. The measurements of the electron energy distribution functions predicted a difference in the profile as the mode discharge changes from CCP to ICP.

**JWP 20 Study of the E-to-H and H-to-E mode transitions in an ICP using mass spectrometry** CAROLE MAURICE, GERRIT KROESEN, *Eindhoven university of Technology* Radio frequency inductive discharges are currently widely used in the manufacture of integrated circuits. Their ability to control independently the plasma density, by adjusting the power, and the ions energies, with an external bias is one of the major issues of these plasma sources. Studies showed that two clear distinct power modes exist: A dominant capacitive coupling discharge (E-mode) at low power and a dominant inductive coupling discharge (H-mode) at high power. We placed a Plasma Process Monitor perpendicularly to the substrate electrode and recorded ion energy distributions in an Ar plasma for different pressures at the substrate level. The mode transitions E-to-H and H-to-E and the hysteresis linked to them are clearly to be seen. Placing and removing a faraday shield in the system allowed us to distinguish the influence of the different modes on the energy distributions. In the mean time, measurements were performed with a Plasma Impedance Monitor to get information on the dissipated power in the discharge and the impedance of the plasma load.

**JWP 21 Instabilities in fluorocarbon ICP plasmas** JEAN-PAUL BOOTH, *Laboratoire de Spectrometrie Physique, Grenoble University, France* HANA ABADA, *Laboratoire de Spectrometrie Physique, Grenoble University, France* Several recent studies (Lieberman and al<sup>1</sup>, Tuszewski<sup>2</sup>) have shown the presence of instabilities in low pressure inductively coupled discharges with electronegative gases (O<sub>2</sub>, Ar/SF<sub>6</sub>). Lieberman and al<sup>1</sup> have proposed an explanation for this effect in terms of electron attachment processes causing an oscillation between capacitive and inductive coupling modes. We have observed similar instabilities in ICP fluorocarbon plasmas (CF<sub>4</sub>, C<sub>2</sub>F<sub>6</sub>, CHF<sub>3</sub>) by observing the optical emission from the plasma. In CF<sub>4</sub> plasmas, the optical emission is modulated by up to 90% at frequencies 200-1 kHz at 1-20 mtorr with rf powers of 300 W and 500W. We have also observed an interesting phenomenon whereby inductive/capacitive oscillations occur during several hundreds of ms, in between periods of stable capacitive operation lasting several hundreds of ms.

<sup>1</sup>M. A. Lieberman, A. J. Lichtenberg and A. M. Marakhtanov, *App. Phys.* Vol75,3617 (1999).

<sup>2</sup>M. Tuszewski, *J. Appl. Phys.* 79, 8967 (1996).

**JWP 22 Inductively coupled plasma source symmetry in the presence of a current node.** J.M. MARQUIS, *University of Texas at Dallas* M.H. KHATER, L.J. OVERZET, M.J. GOECKNER, *University of Texas at Dallas*\* As industry moves towards processing larger substrates, there is a need for larger uniform plasma sources. Due to transmission line effects, large traditional planar

inductively coupled plasma sources produce non-uniform plasmas, and thus non-uniform processing rates across the substrate. Recently, a three dimensional coil geometry, which can reduce these non-uniformities, was introduced.<sup>1</sup> This previous work examined the uniformity of both the traditional planar source and a three dimensional source without a current node present on the line. It was found that the 3-D source produced more azimuthally symmetric electromagnetic fields and hence more uniform etches. In this paper, we examine standing wave effects on the field intensities and symmetries when a current node is present on both a planar and a 3-D coil. Here, field strength measurements, made with a B-dot probe in the absence of plasma, are compared with the results of a predictive model of the system.

\*Supported by Texas Advanced Technology Program No. 009741-0081-1999.

<sup>1</sup>M.H. Khater and L.J. Overzet, Submitted to *Plasma Sources Sci. Technol.*; US Patent 6,028,285.

**JWP 23 Reduction of deposition ionization fraction in ionized physics vapor deposition due to metal re-sputtering off the substrate** MIRKO VUKOVIC, *Tokyo Electron Arizona, Inc.* In ionized physical vapor deposition the sputtered metal neutral atoms from a target are thermalized by collisions with a working gas (usually argon). A large fraction of them is ionized by an electron-argon plasma generated by an auxiliary plasma source. Accelerated by the sheath at the substrate, the metal ions are deposited at the bottom of large aspect ratio features. RF bias is commonly used to further reduce the angular spread of the metal ion flux. The argon ion flux re-sputters some of the deposited metal off the substrate. Due to collisions with the argon gas, a fraction of the re-sputtered metal flux is back-scattered to the substrate. This results in a reduction of the effective ionization fraction of the metal flux to the substrate. A Monte-Carlo simulation of the re-sputtered metal neutrals, followed by a diffusion equation solution of the thermalized metal neutral transport in presence of ionization is used to model the metal transport in one dimension. The effective ionization fraction of the combined incident and re-sputtered flux is calculated. In particular, argon pressure and bias voltage effects on the effective ionization fraction are considered.

**JWP 24 Calculation of Reticle Temperature during Etching Process in ICP** HAN-MING WU, *Intel Corp* WILMAN TSAI, *Intel Corp* In the present paper, the simulation of heat transport on reticle is carried out with the consideration of ion bombardment heating effect in high-density plasma reactor. Using the collisionless Godyak sheath model, the ion energy distribution function (IEDF) is numerically calculated. Then the ion bombardment energy flux on wafer is obtained by means of integral over all energy spectrums. The radiation of the reticle is considered as a main cooling mechanism. The heat transport equation is solved to get the temperature profile across the reticle. A series calculation is conducted for various ICP power, species and RF bias on the reticle. The results show that the ion bombardment heating can potentially be a critical issue in HDP etching as long as the photoresist temperature is concerned.

#### JWP 25 MAGNETICALLY ENHANCED PLASMAS

**JWP 26 A Compact Nitrogen Radical Source by Helicon-Wave Discharge Employing a Permanent Magnet** H. KOKUBU, K. SASAKI, K. KADOTA, *Department of Electronics, Nagoya University, Japan* D. HAYASHI, *Faculty of Applied Physics, Eindhoven University of Technology, The Netherlands*

We have developed a nitrogen radical source excited by helicon-wave discharge in  $N_2$  gas. Major features of the present radical source are 1) high electron and radical densities, 2) low operational gas pressure below 1 mTorr, and 3) compactness by employing a permanent magnet. The plasma density and the degree of dissociation in the radical source were examined by using an electrostatic double probe and optical emission spectroscopy, respectively. High electron density of  $2 \times 10^{12} \text{ cm}^{-3}$  was obtained at a gas pressure of 1 mTorr and an rf power of 600 W. Bright emissions from N radicals were observed. The degree of dissociation was expected to be several tens of percent according to the results of optical emission spectroscopy. The present radical source has potential applications in production of various nitride films such as GaN and  $\beta\text{-C}_3\text{N}_4$ .

**JWP 27 Direct measurement of the energies of neutral species from magnetron plasmas** P.A. READ, J.A. REES, P.J. HATTON, D.J. MILLS, I.D. NEALE, *Hidden Analytical Ltd. 420 Europa Boulevard, Gemini Business Park, Warrington, England, WA5 5UN* For plasma deposition systems the role of energetic neutral particles in controlling the tribological properties of the deposited films is not well documented. While there have now been many measurements of the energy distributions of positive and negative ions arriving at growing films from a variety of plasmas, the situation is not the same for neutral particles. The relative number densities of the various neutral species are readily determined but their energy distributions are more difficult to observe. A particularly interesting plasma reactor in this context is the unbalanced magnetron reactor for which the number of energetic neutrals reaching the substrate are likely to be considerably higher than for other reactors. The present paper describes measurements carried out for a small magnetron, operated with copper, aluminium and carbon cathodes, of the energies of neutral atoms and positive ions arriving from the magnetron at a grounded substrate.

**JWP 28 Hybrid Particle-Fluid Simulation of Low-Pressure DC Magnetron Discharges** VLADIMIR SERIKOV, *Nippon Sheet Glass Co., Ltd., Japan* HIROHIKO IWASE, *Nippon Sheet Glass Co., Ltd., Japan* SHINJI KAWAMOTO, *Nippon Sheet Glass Co., Ltd., Japan* A hybrid numerical model has been developed for simulation of low-pressure direct current discharges that are widely used in thin film deposition technologies. It incorporates two modules: a Monte Carlo particle solver for fast secondary electrons emitted from the cathode, and a FEM fluid solver (based on the drift-diffusion continuity equations coupled with Poisson's equation) for bulk plasma parameters. The ionization and fast-electron thermalization rates obtained in the particle module are communicated as source terms to the fluid module, whereas the electric field and ion flux to the cathode calculated in the fluid module are fed back to the Monte Carlo module. The whole procedure is repeated until convergence. Applicability of the developed model is demonstrated by simulations of 1D direct current discharge at 50 mTorr and 2D magnetron discharge at 5 mTorr in argon. The spatial distributions of plasma parameters and electric field are presented and discussed. The results of the hybrid model are compared with those obtained by the PIC-MC method, the predicted target erosion profile for the magnetron being in good correspondence with the measured one.

**JWP 29 A study of dc discharge in cylindrical magnetron - comparison of experiment and PIC model** J. F. BEHNKE, C. CSAMBAL, *EMA University, Institute of Physics, 17487 Greifswald, FRG* M. TICHY, P. KUDRNA, J. RUSZ, *Charles University in Prague, Faculty of Mathematics and Physics, V Holesovickach 2, 180 00 Praha 8, Czech Republic* We present experimental and numerical study of the DC discharge in cylindrical magnetron in argon. The grounded discharge chamber-anode has 110 mm in length and 60 mm inner diameter. The co-axially placed cathode has 10 mm in diameter. The magnetic field is created by couple of coils. Experimental results have been obtained by radially movable planar Langmuir probe with its plane perpendicular to the magnetic field lines. The radial profiles of the floating and plasma potential, plasma density, and the electron energy distribution function have been measured. Numerical results were obtained using the modified 1D PIC code (Berkeley). The comparison between experiment and model results computed at similar conditions shows reasonable agreement in plasma density and electron mean energy. The computed electric field is usually higher than the experimental one. This difference we explain by the end effects that are not taken into account in 1D model.

**JWP 30 Kinetic model of entire cylindrical magnetron discharge.** I.A. POROKHOVA, J.F. BEHNKE, J. BEHNKE, *Institute of Physics, E.-M.-Arndt-University, 17487 Greifswald, Germany* Y.B. GOLUBOVSKII, *Institute of Physics, State University of St. Petersburg, Russia* of magnetron configuration in crossed electric and magnetic field is represented. The discharge modelling is based on numerical solution of the spatially inhomogeneous Boltzmann equation, equation of ion motion, current balance and Poisson's equation. Axially applied magnetic field abruptly decreases radial anisotropy of the electron distribution function, and co-direction of the fields responsible for current transport and ambipolar diffusion reduces the problem to one-dimension in real space. The results for electric field profile, distribution function, and macroscopic properties describe formation of the cathode-fall and negative glow regions, extended positive column and anode sheath. The model's self-consistency permits one to find internal parameters in terms of external ones, trace the interdependency of plasma characteristics, and investigate relaxation processes of electrons in near-electrode regions.

**JWP 31 Development of a New Sputter System using Magnetic Neutral Loop Discharge Plasma Technology** YAW OKRAKYI, *Miyazaki University* YOUL-MOON SUNG, *Miyazaki University* MASAHISA OTSUBO, CHIKAHISA HONDA, KIICHIRO UCHINO, *Kyushu University* KATSUNORI MURAOKA,\* A new type plasma system using Neutral Loop Discharge (NLD) plasma technology has been developed for research into electron behavior and also for sputtering application. This technology is characterized by plasma production in the multi null field on the target surface, where the capacitive RF electric field is applied without an antenna. The system consists of a doughnut-shaped target and multi-pole type permanent magnets. Eight pairs of magnets are equally spaced around the circumference of 2 circles such that they sandwich the doughnut-shaped target. Each magnet pole produces a maximum field strength of approximately 650G on the pole surface and makes the L (the distance from the ECR plane to the NL) region of about 20mm on

the target surface with a width of 75mm. From the results of the electron motion modeling in this system, we found that electrons near the null region on the target surface moves in meandering orbits like in NLD plasma. Initial results obtained using this new discharge will be presented.

\*The authors would like to thank M. Itoh, T. Hayashi and T. Uchida of ULVAC Japan Ltd for the technical advice in this work.

## JWP 32 GAS-PHASE CHEMISTRY

### JWP 33 Carbon Nanotube Production in CO Laser Pumped Carbon Monoxide Plasmas

ELKE PLOENJES, PETER PALM, VISH SUBRAMANIAM, IGOR ADAMOVICH, WILLIAM RICH, BABU VISWANATHAN, HAMISH FRASER, *The Ohio State University, 206 W. 18th. Ave, Columbus, Ohio* A novel method for the synthesis of carbon nanotubes will be presented. Carbon monoxide in a CO-Ar gas mixture is optically pumped using a continuous wave CO laser. The CO molecules absorb the laser radiation on the lowest 10 vibrational transitions and transfer energy to high vibrational states by vibration-vibration energy exchange collisions. This leads to a highly nonequilibrium energy distribution in the CO which provides enough energy for the CO disproportionation reaction to occur:  $\text{CO} + \text{CO} \rightarrow \text{C} + \text{CO}_2$ . This experimental technique consequently produces the free carbon necessary for the growth of carbon nanotubes and other carbon clusters while maintaining near room temperature in the plasma. Our technique can produce substantial quantities of nanotubes at low pressure (50 Torr) due to the efficient carbon production and is scalable to higher pressures and therefore, to larger production quantities. We will present the effect of metal catalysts on production rates and nanotube quality for our experimental technique as well as effects of plasma temperature and gas pressures. Single- and multi-walled carbon nanotubes have been observed in the deposited material with concentrations of better than 50%. The plasma conditions are monitored using emission spectroscopy.

### JWP 34 Catalytic effect of noble gases in the reaction of plasma-chemical of hexamethyldisiloxane (HMDSO) in the dielectric discharge (DBD)

AXEL SONNENFELD, JUERGEN F. BEHNKE, *University of Greifswald, Institute of Physics, Domstr. 10a, 17487 Greifswald, FRG* KIRILL V. KOZLOV, *Moscow State University, Department of Chemistry, 119899 Moscow, Russia* REACTIVE SPUTTERING TEAM, PLASMA CHEMISTRY IN DIELECTRIC BARRIER DISCHARGES COLLABORATION, of HMDSO in the DBD (glass-glass electrode set-up, 2 mm gap, 1 kHz voltage) was studied in mixtures of  $\text{N}_2 + \text{He}$  and  $\text{N}_2 + \text{Ar}$  in an open gassystem at 1 atm. Gas mixing ratio was chosen as a main variable parameter. initial HMDSO content was kept constant at 0.2 %. Yields of the main gas-phase products and the decomposition degree of HMDSO were determined by means chromatography. We found that an increase of the noble gas content in a working mixture results in a growth of the product yields. explain this effect, we carried out semi-empirical calculations of the kinetic of electrons in the gas mixtures, considering the experimentally obtained burning voltages depending on the gas mixture. The results calculated show that a rise of the noble gas content increases the mean electron energy.

### JWP 35 Molecular Composition of Polymerized Species in Fluorocarbon Plasmas

KUNIHIDE TACHIBANA, KAZUO TAKAHASHI, *Dept. of Electronic Science and Engineering, Kyoto University* In fluorocarbon ( $\text{C}_4\text{F}_8$  and  $\text{C}_5\text{F}_8$ ) plasmas, formation mechanisms of polymers were investigated by the characterization with X-ray photoelectron spectroscopy (XPS) and gel permeation chromatography (GPC). The molecular compositions of the polymers in the films deposited on the substrate and in the particles formed in the gas phase were elucidated by these chemical analyses. The XPS results showed that the particles were carbon-rich and composed of highly branched molecules in contrast to the film composition. From the GPC measurements, the particles were found to contain ultra-high mass polymers, whose molecular weights were around 100,000. On the contrary, the deposited film contained polymers with molecular weights distributed below 2,000, in which oligomers, monomers and fragmented products were included. Present study suggests that these polymers are involved in the formation of cross-linked networks of the films and the particles via surface reactions, where the cross-linking is enhanced by the ion bombardment. The formation mechanism of the high mass species and the intermediate products is discussed from the experimental results of gas phase diagnostics by FT-IR absorption spectroscopy and electron attachment mass spectrometry.

### JWP 36 Production of Fullerenes from Various Carbon Materials by Means of the JxB Arc Method

TETSU MIENO, *Dept. Physics, Shizuoka Univ.* MOHAMMAD. K. H. BHUIYAN, *Dept. Physics, Shizuoka Univ.* In order to improve production efficiencies of fullerenes, the JxB arc method has been developed and increase of production rates of fullerenes and decrease of carbon deposition on a cathode are obtained. For mass production of higher fullerenes and endohedral metallo-fullerenes, a revolver-type fullerene producer with the JxB arc has been developed, where as much as 50 carbon material rods can be automatically fed to the arc region and automatic production of fullerenes are realized. A chip-material injection type reactor with the JxB arc has been also developed to produce fullerenes from various plant-carbon materials and used carbon-based materials, resulting in successful fullerene production. By these methods, low cost mass production of many kinds of fullerenes are continuously examined. Ref.: T. Mieno FULLERENES Vol. 7 (Electrochem. Soc.) (1999) 453-461. T. Mieno, Fullerene Sci. Technol. Vol. 8, No. 3 (2000) in press.

### JWP 37 Variations of Heat Flux and Emission in Gas Arc by Gravity-Oscillation for Fullerenes Production

TETSU MIENO, *Dept. Physics, Shizuoka Univ.* AKIRA YAMASHIRO, *Dept. Physics, Shizuoka Univ.* Production rates of higher fullerenes, endohedral metallo-fullerenes and carbon nanotubes tremendously increases at gravity-free condition in the gas arc method where a half-atm He gas is introduced and a carbon anode is sublimated by electron heating. In order to understand the gravity effect of arc production of carbon clusters, heat flux and emission intensity in a He gas arc in a oscillating gravity field are measured by means of a 12 m-high vertical-swing-tower, where gravity change from 0 G to 3 G with period of 2.3 s. As a result, the heat flux from the arc region is strongly modified by the gravity change and response time is less than 0.1 s. Quick response of the heat convection modifies the heat flux. The emission intensity varies in hysteresis-like manner and when the gravity changes from high gravity to

low gravity it becomes maximum, otherwise it becomes minimum when the gravity from low to high. The reason is attributable to the modulation of gas temperature by modulation of the heat flux. Ref. T. Mieno, FULLERENES Vol. 7 (Electrochem. Soc.) (1999) 749-755.

**JWP 38 Vibrational frequencies and electron affinities of Si<sub>2</sub>H<sub>5</sub> radicals** D. HAYASHI, M.M. HEMERIK, G.M.W. KROESEN, *Eindhoven University of Technology* Heavy Si<sub>m</sub>H<sub>n</sub> radicals and their anions are considered as precursors for the formation of silicon-particulates and *α*:Si surfaces in silane plasmas. It is of importance to apply diagnostics featuring high-sensitivity for the detection of such large molecules having low-densities. However, no optical and molecular data on Si<sub>m</sub>H<sub>n</sub> required for the diagnostics have ever been reported. We have calculated the harmonic vibrational frequencies and electron affinities of Si<sub>2</sub>H<sub>5</sub> (Si<sub>2</sub>H<sub>5</sub><sup>-</sup>) and Si<sub>2</sub>H<sub>6</sub> by GAUSSIAN 98 package. Computations were carried out by MP2,MP4/HF method and B3LYP/DFT using several basis functions (6-31G(3pd,3fd), DZP, etc.). Si<sub>2</sub>H<sub>5</sub> had strong fundamental vibrational frequencies (873, 2215, 2232 and 2278 cm<sup>-1</sup>) in the wavelength regions, where the IR-CRDS can be applied. The electron affinity of Si<sub>2</sub>H<sub>5</sub> was -0.73 eV at B3LYP/6-31G(3pd,3fd) level. The applicability of electron attachment mass spectroscopy and IR cavity ring down spectroscopy were confirmed.

**JWP 39 Polymerization mechanisms in fluorocarbon ICP discharges** JEAN-PAUL BOOTH, *Laboratoire de Spectrometrie Physique, Grenoble University, France* GILLES CUNGE, *CNRS/LETI, Grenoble, France* HANA ABADA, *Laboratoire de Spectrometrie Physique, Grenoble University, France* GILLES CARRY, *LPGP, Paris, France* Polymerisation mechanisms were investigated in several fluorocarbon gas discharges (CF<sub>4</sub>, C<sub>2</sub>F<sub>6</sub>, CHF<sub>3</sub>) in an inductively coupled plasma by the mean of optical and electrical diagnostics. The absolute axial concentration profiles of CF and CF<sub>2</sub> radicals were determined by LIF combined with UV broad-band absorption for various plasma conditions. The relative F atom concentration was monitored by actinometry, the polymer deposition rate was measured using a quartz crystal microbalance, and the ion flux to the grounded walls was determined using an rf-biased ion flux probe. The polymer film formation mechanism appears to be ion assisted deposition of multi-carbon unsaturated (neutral and ionic) C<sub>x</sub>F<sub>y</sub> species (y ≪ 2x), similar to that recently observed in capacitively coupled discharges. The respective influences of the ion flux, the F atom concentrations and the CF<sub>x</sub> radicals on the polymer deposition rate will be discussed and compared to capacitively-coupled plasmas. We propose several mechanisms to explain the presence of heavy oligomeric species in the gas phase of low pressure, high density plasmas.

**JWP 40 Decomposition of Benzene Using a Low Pressure DC Glow Discharge in Nitrogen\*** K. SATOH, N. KUDOH, H. ITOH, H. TAGASHIRA, *Muroran Institute of Technology, Japan* M. SHIMOZUMA, *Hokkaido University, Japan* Decomposition process of benzene in a low pressure dc glow discharge in nitrogen is investigated. The gas pressure of nitrogen and benzene mixture is set to 0.5, 1.0, 1.5 and 2.0 Torr, and the partial pressure of benzene is varied from 2 to 20%. In order to monitor the decomposition process, the temporal variation of the optical emission of the discharge is measured by Photonic Multi-channel Analyzer

(Hamamatsu PMA-11). The spectra of CN(919.0nm etc), C<sub>2</sub>(810.8nm) and H<sub>α</sub>(656.3nm), which are regarded as the fragments of benzene, are measured with those of nitrogen molecules and ions. The temporal variations of the emission intensity of the fragments and nitrogen are seen simultaneously, so that it is likely that benzene is decomposed while the emission intensity is temporally varying, and that nitrogen excited molecules and ions make a contribution to the decomposition of benzene. It is assumed that the removal of benzene can be judged by monitoring the variation of the emission intensity of CN, since the variation is measured most clearly in this study.

\*This work was supported by Grant-in-Aid (No.11750223) of the Ministry of Education, Science, Sports and Culture, Japan.

**JWP 41 Gas Phase Reaction of Atmospheric Pressure Discharge with Streamer Propagation -Modeling using Boltzmann Equation and Rate Equation-** MASAMICHI KOGURE, FUMIYOSHI TOCHIKUBO, TSUNEO WATANABE, *Tokyo Metropolitan University* High-pressure non-equilibrium plasmas formed by gas discharges are useful tools for harmful gas treatment. Although these discharges are localized with active streamers, using zero-dimensional rate equation is still useful method to investigate the gas phase reaction process. Several works using rate equations were carried out assuming the averaged electric field. However, the electric field in the real streamer has a very strong and sharp peak with a width of a few ns and a height of roughly 1000 Td. The evolution of radical production in the real streamer seems to be different from that in the averaged field model. In this work, the gas phase reaction in the streamer was calculated using zero-dimensional rate equations coupled with electron's Boltzmann equation. We assumed a very sharp pulsed electric field, which was taken from a two-dimensional streamer modeling or a simple calculation of moving streamer head. In the real discharge, the electron avalanche occurs toward the streamer head; the new streamer head with high electric field is successively formed after the multiplied electrons are transported from there. Therefore, the electron flux proportional to drift velocity was taken into account. The V-V collision of N<sub>2</sub>(X) was also considered. The time evolution of radical and electron densities agrees with those of two-dimensional streamer modeling.

**JWP 42 Enhancement of VOC removal using a Dielectric Barrier Discharge into a catalyst** T. MINEA, S. PASQUIERS, A. ROUSSEAU, A. JORAN, N. SIMIAND, *LPGP, Universite Paris-Sud/CNRS, France* F. AUNTIN, J.M. TATIBOUET, J. BARRAULT, *LACCO / CNRS Poitiers, France* We report on the feasibility of a pulsed Dielectric Barrier Discharge (DBD) inside a complex shape monolith structure, in air at atmospheric pressure. The combination of a non-thermal plasma with a catalyst is actually a very promising way for VOC removal and for flue gas treatment. The DBD is produced by a 40 kV voltage pulse through a 4 channels monolith, 5.5 mm thick in cordierite, with a repetition rate ranging from 1 up to 100 Hz. Influence of the repetition rate and of the dielectric thickness, in plexyglass, on the injected power and on the number of current filaments in the discharge volume is reported. Comparison is performed with a DBD without monolith. Moreover discharge electrical parameters have been studied in case of a monolith coated with Pt catalyst. The efficiency for VOC destruction of our plasma/catalyst association is investigated using a test molecule, 2-heptanon. We show that the discharge enhances 2-heptanon removal and permits its destruction at a much lower temperature value than using the catalyst only.



## JWP 43 TRANSPORT EFFECTS

**JWP 44 Afterglow Ambipolar Diffusion of a Mixture of Anions** ALAN GALLAGHER, JILA, NIST and Univ. of Colorado, Boulder, CO 80309 Mass spectrometer measurements of the anions in a silane discharge requires collecting the anions in the afterglow, after the discharge sheath has collapsed A.A.Howling, L. Sansonnens, J.L.Dorier, and Ch.Hollenstein J. Appl. Phys. 75, 1340 (1994). Since the heavier anions diffuse more slowly and are collected later, competing recombination and diffusion to electrodes biases the observations in favor of lighter anions. In an attempt to establish the anion densities in the discharge, and to explain the observed dependence of anion signals on afterglow time, we have modelled afterglow ambipolar diffusion with recombination. This is initially dominated by electron-cation, and later by anion-cation ambipolar diffusion with a large mixture of anion masses. The observed mass-dependent delay to anion arrival in the mass spectrometer can be reproduced by the calculation, but the mass dependence of the anion signal decay is somewhat problematic. These and other comparisons to the measurements will be presented.

**JWP 45 Ionization coefficients and electron drift velocities in  $SF_6/CO_2$  mixtures\*** J. DE URQUIJO, E. BASURTO, C. CISNEROS, I. ALVAREZ, Centro de Ciencias Fisicas, UNAM, Mexico We have measured the effective ionization coefficient and the electron drift velocity in 10:90 and 30:70  $SF_6/CO_2$  mixtures, using a Pulsed Townsend Technique. The reduced electric field strength, E/N, was varied between 160 and 480 Td ( $1Td=10^{-17} V cm^2$ ). For fixed E/N, the above two parameters increase as the  $SF_6$  share in the mixture decreases, since the mixture becomes less electronegative. The critical values of E/N for which ionization equals attachment are 188 and 242 Td for the 10:90 and 30:70  $SF_6/CO_2$  mixtures, respectively, which are in good agreement with those of Aschwanden<sup>1</sup> and Lee<sup>2</sup>.

\*Work supported partially by DGAPA, IN113898.

<sup>1</sup>Th. Aschwanden, Ph. D Thesis, ETH, Zürich, 1985.

<sup>2</sup>Z.Y. Lee, IEEE Trans. El. Insul. 6 637 (1983).

**JWP 46 Ion Mobilities in Xe/Ne Mixtures** J. DE URQUIJO, E. BASURTO, Centro de Ciencias Fisicas, UNAM, Mexico A.V. PHELPS, JILA, Boulder, CO D. PISCITELLI, L.C. PITCHFORD, CPAT, Toulouse, France The modeling of glow discharges in the xenon/neon mixtures used for plasma display panels requires accurate ion mobilities. Neither experimental ion mobility data nor ion-neutral cross sections needed to calculate the ion mobilities are published. We are collaborating to measure and calculate these data. Ion mobilities are reported for 20% Xe/80% Ne at E/N up to 650 Td for  $Xe^+$  and up to 1200 Td for  $Ne^+$ . These are compared with results from Monte Carlo calculations using cross sections from the literature for  $Xe^+-Xe$  and  $Ne^+-Ne$  collisions and our theory for  $Ne^+-Xe$  and  $Xe^+-Ne$  collisions. The calculated  $Ne^+$  mobilities agree fairly well with measurements, but the  $Xe^+$  mobilities agree less well. At low ion energies, the main collision process determining the  $Xe^+$  mobility is elastic scattering in  $Xe^+-Ne$  collisions. We evaluate the effect of anisotropy in the differential cross sections on the calculated mobilities. The cross section sets used for these calculations will be presented. Calculations will be shown that allow one to evaluate the use of Blanc's law for deriving ion mobilities in other Xe/Ne mixtures.

**JWP 47 Relaxation of electrons ejected from high voltage tip to gas phase** A. KAWAI, J. MATSUI, N. NAKANO, Z.LJ. PETROVIC, T. MAKABE, Department of Electronics and Electrical Engineering, Keio University at Yokohama, Japan A transport of electrons ejected from a high voltage tip by tunneling effect is interesting as a source of micro-meter scale local heating of functional material. In particular, the relaxation of the energy of cold electrons is of practical importance under a non-uniform field region in the vicinity of the tip, set in a gas. In our previous work, we developed a direct numerical procedure (DNP) of the Boltzmann equation of electrons in velocity space and in phase space.<sup>1</sup> In the present study, we numerically investigate the transport of electrons ejected from the high field tip into gas phase by considering the velocity distribution by using DNP of the Boltzmann equation in one-D position and two-D velocity space. The spatial development of the velocity distribution of electrons with an arbitrary initial energy is first calculated in a uniform field, i.e., E/N, in order to investigate the relaxation distance of energy and momentum as a function of initial energy and external E/N. Typical example of the transport of tunneling electrons ejected from the tip into the atmospheric pressure condition in  $O_2$  and  $N_2$  is shown and discussed as a function of position from the tip.

<sup>1</sup>J.Matsui, M.Shibata, N.Nakano, and T.Makabe, J.Vac.Sci.Tech-nol. A16(1), 294 (1998).

**JWP 48 Spatio-Temporal Relaxation of Electrons in Non-Isothermal Plasmas** DETLEF LOFFHAGEN, ROLF WINKLER, Institut für Niedertemperatur Plasmaphysik, 17489 Greifswald, Germany The spatio-temporal evolution of electrons under the action of an electric field in the inhomogeneous krypton column plasma of a glow discharge between plane electrodes is studied. To analyze the behavior of the electrons, we have developed a powerful method for solving the electron Boltzmann equation including both the space and time dependence. The treatment of this kinetic equation is based on the conventional two-term approximation of the velocity distribution function expansion. The resultant three-dimensional partial differential equation for the isotropic distribution is solved as an initial-boundary value problem over the space of spatial coordinate and energy. Starting from an appropriate initial distribution and assuming a continuous flux of electrons into the plasma region at the cathode side and their partial reflection at the anode side, pronounced spatial structures in the distribution function and related macroscopic quantities develop during the transient process. These structures propagate from the cathode side towards the anode. In particular, the period of the spatio-temporal relaxation into a spatially structured, time-independent state is found to be considerably larger than that to reach steady state in spatially uniform plasmas and is mainly controlled by the macroscopic electron transport velocity.

**JWP 49 SWARM PARAMETERS IN NON-UNIFORM CROSSED ELECTRIC AND MAGNETIC FIELDS** IKUYA HORIE, Hokkaido Institute of Technology S. NAKAMURA, Hokkaido Polytechnic College P.L.G. VENTZEK, Motorola Inc. K. KITAMORI, Hokkaido Institute of Technology Evaluating swarm parameters in crossed electric and magnetic fields is crucial to being able to model both magnetron plasmas and magnetically enhanced plasma sources. Typically one would relate a swarm parameter or transport parameter to a local value of reduced electric and magnetic field. Putting aside questions of locality that come with lower pressure long mean free path systems, there still is the question of whether or not in the numerical experiment used

to determine a swarm parameter, the experiment is initial condition dependent. When an electron enters a high magnetic field region, are its swarm parameters frozen in? This question has been investigated using a Monte Carlo simulation and except for transient effects, we find that the swarm parameters are not "frozen in." For example, the mean energy in argon in a crossed reduced electric field of 283 Td and reduced magnetic field of 2000 Gauss/Torr comes to the same equilibrium value in approximately the same time for initial electron energies from 1 to 100 eV. The same is true for methane. The results will be discussed in the context of the modeling of magnetrons and MERIE's.

**JWP 50 Measurement of Electron Transport Parameters in NO-Ar Mixture and Pure NO** T. TAKEUCHI, *Faculty of Science and Technology, Keio University* M. HAYASHI, *Gaseous Electronics Institute* Y. NAKAMURA, *Faculty of Science and Technology, Keio University* The drift velocity and the product of the gas number density and the longitudinal diffusion coefficient ( $ND_L$ ) in the 4.99% nitric oxide (NO)-argon (Ar) mixture and in pure NO have been measured by using the double shutter drift tube, over the range of  $E/N$  from 0.1 to 50 Td at gas pressure between 1 and 300 Torr in 4.99% NO-Ar mixture and over the range of  $E/N$  from 0.4 to 500 Td at gas pressure between 0.15 and 25 Torr in pure NO. All measurements were carried out at room temperature. The goal of these measurements is to derive a set of electron collision cross sections for NO molecule by using a Boltzmann equation analysis so that the set can reproduce all electron transport coefficients studied in pure NO and in NO-Ar mixture simultaneously. In NO-Ar mixture, the drift velocity showed a broad peak at 2.5 Td and the  $ND_L$  a narrow peak at 3.5 Td. The present measurement in pure NO covers broader  $E/N$  range than any of previous measurements. We also observed asymmetrical TOF signals at higher pressures ( $> 10$  Torr) and lower  $E/N$  ( $< 10$  Td) in pure NO, possibly suggesting electron autodetachment following after three-body attachment.

**JWP 51 An Application of Simplex Algorithm to Electron Swarm Method** HIROKI HASEGAWA, YOSHIHARU NAKAMURA, *Faculty of Science and Technology, Keio University* Electron collision cross sections for atoms and molecules can be derived from electron swarm parameters measured in the relevant gases. The method, however, needs a number of trial and error procedures and is usually time consuming. In order to overcome this drawback Morgan[Phys.Rev.A, 44, 1677 (1991)] applied a numerical optimization (downhill simplex) algorithm in the process of deriving the elastic momentum transfer cross section of argon atom from electron swarm data. We also applied a similar algorithm and derived the elastic momentum transfer cross section of the xenon atom from our measurement of the drift velocity and the longitudinal diffusion coefficient of electrons in pure xenon over the  $E/N$  range 0.03 - 60 (Td). We succeeded to determine the cross section over the electron energy range 0.1 - 8 (eV), including the Ramsauer-Townsend minimum. The lower limit of the energy range was set by the gas temperature. The estimated cross section is capable of reproducing all electron swarm parameters fairly well: within our experimental error limits of the drift velocity (2%) and of  $ND_L$  (5%), simultaneously. These results prove the effectiveness of applying downhill simplex method to electron swarm method.

**JWP 52 Measurements of electron transport coefficients in the 0.468% and 4.91% c-C<sub>4</sub>F<sub>8</sub>/Ar mixtures and pure c-C<sub>4</sub>F<sub>8</sub>** MASAHIRO YAMAJI, YOSHIHARU NAKAMURA, *Faculty of Science and Technology, Keio University* This report presents the results of the electron drift velocity ( $W$ ), the product of the gas number density and the longitudinal diffusion coefficient ( $ND_L$ ), and the attachment coefficient ( $\eta/N$ ) over the range  $0.7 < E/N < 100$ (Td) in the 0.468% c-C<sub>4</sub>F<sub>8</sub>/Ar mixture, the range  $10 < E/N < 100$ (Td) in the 4.91% c-C<sub>4</sub>F<sub>8</sub>/Ar mixture, and the range  $200 < E/N < 1000$ (Td) in the pure c-C<sub>4</sub>F<sub>8</sub>. Measurements were carried out by using the double shutter drift tube with variable drift distance [J.Phys.D30, 1610 (1991)]. These values of mixture are compared with the calculated values which is derived from the cross section set of Itoh [J.Phys.D:Appl.Phys.24, 277 (1991)]. The calculated values are higher than the measured values at low  $E/N$  range. This fact shows that the cross section set must be improved. The method of calculation is the Boltzmann's multi-term approximation, but we found that this method is not applied well to c-C<sub>4</sub>F<sub>8</sub>, because the  $ND_L$  values at low  $E/N$  range are unstable. The measured pure c-C<sub>4</sub>F<sub>8</sub> results of  $W$  are compared with the measured values of Naidu [J.Phys.D5, 741 (1972)], and the difference between these data is apparent at high  $E/N$  range.

**JWP 53 On the Nature of Sonoluminescence** ANDREW ANGUS, *Absolute Foundation* The purpose of this article is to explain the nature of sonoluminescence. The author explains sonoluminescence using mathematical equations. An important application of sonoluminescence is the inducing of nuclear fusion at low energy.

#### JWP 54 LIGHT SOURCES/UV SOURCES

**JWP 55 A new variable color fluorescent lamp** LEON BAKKER, GERRIT KROESEN, *Eindhoven University of Technology* Recently, there is a growing interest in variable colour fluorescent lamps. In the past, several options for changing the color of a fluorescent lamp were proposed. Most of these options use radio frequency or pulsed excitation of the gas discharge. By changing the electrical excitation, the electron energy distribution function changes. This causes the output spectrum of the lamp to change. A disadvantage of such a lamp is the expensive power sources that are required. We propose a new lamp with a variable color. The working principle of this lamp is based on mercury depletion in the positive column of a neon-mercury discharge. Under certain experimental conditions, this mercury depletion results in the addition of neon radiation to the emission spectrum of the lamp. We used several diagnostics to understand the mercury depletion process. We will present the results of Thomson scattering, UV absorption, spatially resolved absolute emission, and electrical measurements.

**JWP 56 Simulating the energy balance of a high-pressure sulphur discharge** COLIN JOHNSTON, HARM VAN DER HEIJDEN, GER JANSSEN, BART HARTGERS, JAN VAN DIJK, *Dept. of Applied Physics, Eindhoven University of Technology* There are several interesting properties of high-pressure sulphur discharges. Firstly, the emitted spectrum lies almost entirely in the visible range of wavelengths: there is very little infrared and almost no UV produced. Secondly, since the spectrum is molecular in origin and the vapour pressure is several atmospheres, the spectrum appears continuous. Finally, the radiation efficiency is high; up to 70% of input power is emitted as visible light. Hence sulphur ought to be ideal for use lighting applications. In order to

understand the energy balance of the discharge the plasma simulation program, Plasimo, has been used. In order to manage the substantial number of radiative transitions and their contribution to heat transport, the so-called Classical Franck Condon approach has been used. We present the results of these simulations for sulphur discharges at different pressures and input powers. Numerical results are compared to experimental results.

**JWP 57 Determination of the partial pressure of Tl in metal halide lamps from optically thick self-reversed Tl-lines** B. SCHALK, G. HARTEL, L. HITZSCHKE, G.H. LIEDER, *OSRAM GmbH, Germany* In metal halide lamps, Tl usually is not only the main electron supplier but its spectrum also gives an important contribution to the radiation output. Therefore, the knowledge of the partial pressure of Tl in the arc plasma,  $p_{Tl}$ , is of high importance. In this poster the optically thick Tl-lines at 377.572 nm and at 535.046 nm have been used to determine  $p_{Tl}$  by comparing the measured with calculated wavelength separations  $\Delta\lambda$ . The  $\Delta\lambda$  show only a weak dependence on the assumed total pressure or the temperature profile of the arc plasma, but a very strong dependence on  $p_{Tl}$ . Tl is filled in the lamps in form of TII. Several lamps have been examined for which the amount of TII varies in a wide range to assure either that the filled in TII completely vaporizes or that most of it remains condensed. If the amount of TII is low enough, so that it completely vaporizes,  $p_{Tl}$  can be calculated from the total pressure and the ratios of the filled in substances. Thus, lamps containing little TII have been used to adjust the broadening constants of the Tl-lines. On the other hand, if the amount of TII is large enough, so that a part of it remains condensed,  $p_{Tl}$  can be related to the vapor pressure of TII at the coldest temperature in the discharge vessel. The resulting  $p_{Tl}$  will be compared with that from the  $\Delta\lambda$ .

**JWP 58 A Large Area, CW, High Power, Efficient 172nm Xenon Excimer Light Source** M. SALVERMOSER, D.E. MURNICK, *Department of Physics, Rutgers University, Newark NJ 07102* The possibility of building a large area ( $\sim$  ft<sup>2</sup>) CW 172nm Xe<sub>2</sub> excimer light source with VUV output power on the order of 1W/cm<sup>2</sup> and a wallplug efficiency on the order of several 10% has been investigated. Using a corona needle as an electron source in a dense Xe gas ( $\sim$  bars) with a point to plane geometry, a conversion efficiency from electrical power into VUV light of 40% has been measured. Total VUV output power for a single needle-plane system is on the order of 10mW. Due to the resistive nature of the corona discharge, many needles can be switched in parallel. We are developing a corona needle array with up to 100 needles/cm<sup>2</sup> and project power output of order 1 W/cm<sup>2</sup> in the 172nm Xe<sub>2</sub>\* excimer band.

**JWP 59 RF excited CW atomic Xe laser. Experimental performance and theoretical study.** S.A. STAROSTIN, *Quantum Electronics Group, Department of Applied Physics, University of Twente, P.O.Box 217, 7500 AE Enschede, The Netherlands* P.J.M. PETERS, K.J. BOLLER, *Quantum Electronics Group, Department of Applied Physics, University of Twente, P.O.Box 217, 7500 AE Enschede, The Netherlands* Y.B. UDALOV, *Nederlands Centrum voor Laser Research, P.O.Box 2262, 7500 CR Enschede, The Netherlands* I.V. KOCHETOV, A.P. NAPARTOVICH, *Troitsk Institute of Innovative and Thermonuclear Research, 142092, Troitsk, Moscow region, Russia* The performance of a RF excited cw atomic xenon laser at wavelengths of 2.03  $\mu$ m and 2.65  $\mu$ m was studied theoretically and experimentally as a function of elec-

trode distance. Results for inter-electrode distances from 2 to 0.25 mm are presented. A high pumping rate resulted in strong 40 mW cw amplified spontaneous emission at 2.65  $\mu$ m wavelength from the configuration with smallest distance between the electrodes. The maximum laser output of 2.7 W (0.24 W/cm<sup>3</sup>) was obtained with an active medium of 2x15x370 mm<sup>3</sup> while the maximum specific output of 1.9 W/cm<sup>3</sup> was received for an active medium volume of 0.25x2.25x370 mm<sup>3</sup>. A fluid model of the RF discharge was developed to analyze the laser behavior for different distances between the electrodes.

**JWP 60 Comparison of D-X and B-X Molecular Band Emission from a Microwave Produced XeCl Discharge** S. A. ANDERSON, *University of Michigan* SARA BERNAL, *University of Michigan* CARRI GLIDE, *University of Michigan* R. B. ANDERSON, *University of Michigan* MARY BRAKE, *University of Michigan* Ultraviolet (UV) lamps are becoming increasingly important in the curing and material processing sectors of manufacturing. With the use of these lamps on the rise, the efficiency of these lamps, i.e. the amount of emission in the useful wavelength band, is becoming an important economical factor. A XeCl excimer plasma produces UV emission from several molecular transitions including D-X at 236 nm and B-X at 308 nm. This paper examines the relative light output from these two transitions from a microwave generated XeCl plasma. The effect of concentration, power, and pressure will be examined and the optimal conditions for light output in the various molecular bands will be discussed.

**JWP 61 Dual Chamber Discharge at Atmospheric Pressure** HYUN PARK, MUTHUSWAMY NAVIN, SHIRSHAK DHALI, *Southern Illinois University at Carbondale* The UV irradiation in a dielectric-barrier discharge is known to increase the number of microdischarges in atmospheric air.<sup>1</sup> We have used a duel chamber device to generate plasma in air at atmospheric pressure. A single supply (3 kHz or 13.45 MHz) is used to excite discharges in both chambers. The low pressure chamber generates UV, which is coupled to the high pressure chamber through a quartz dielectric. Through the Jhoshi effect, the UV enhances the high pressure discharge characteristics. Results of CCD camera pictures will be presented and compared with a dielectric-barrier discharge. Power and current measurements will also be presented for low frequency and high frequency operation. The results show that a duel pressure discharge is capable of generating uniform plasma at atmospheric pressure and performs better than a dielectric-barrier discharge.

<sup>1</sup>B. Pashaie, S. K. Dhali and F. Honea, *J. Phys. D: vol. 27, 2107(1994)*.

**JWP 62 A Radiation Transport Coupled Particle-In-Cell Model for Hg-Ar Discharges** HAE JUNE LEE, J.P. VERBONCOEUR, H.B. SMITH, G.J. PARKER, C.K. BIRDSALL, *University of California at Berkeley* PLASMA THEORY AND SIMULATION GROUP TEAM, We simulate a radial slice of the fluorescent lamp discharge in the positive column with a radiation transport coupled particle-in-cell (RT-PIC) code. In this model, the radiative and meta stable excited states of Hg-Ar mixture and their collisions as well as radiation transport are simulated by the fluid equations. The motions of electrons and ions and collisions with neutral or excited states are simulated by the conventional particle-in-cell method. We consider radiation transport of excited states using the Holstein equation[1] including the time varying

nonuniform background gas density. The background gas density is calculated from the temperature profile by solving the heat transfer equation. The motion of charged particles are simulated by using the 1-D cylindrical particle-in-cell code, XPDC1[2]. Separate time scales are used for the charged particles, the excited states, and the neutral gas, respectively, and parallel processing can be used for the expensive calculation including radiation transport. This work was supported in part by General Electric Company contract GE-20000181. [1] T. Holstein, *Phys. Rev.* 72, 1213 (1947). [2] J. P. Verboncoeur, M. V. Alves, V. Vahedi, and C. K. Birdsall, *Journal of Computational Physics* 104(2), 321, (1993).

**JWP 63 Radiative lifetimes, branching fractions, and transition probabilities for Lu I, Lu II, and Lu III\*** J. E. LAWLER, J. A. FEDCHAK, E. A. DEN HARTOG, *Dept. of Physics, University of Wisconsin, Madison, WI, 53706* P. PALMERI, P. QUINET, E. BIMONT, *Astrophysique et Spectroscopie, Universit  de Mons-Hainaut, B-7000 Mons, Belgium* Rare-earth salts are used in many commercial metal-halide high intensity discharge lamps. Lutetium is known to enhance the red region of the spectra from metal-halide lamps. Accurate transition probabilities are needed in the models used for lamp design and for diagnostics. Lutetium is also of interest in astrophysical studies of heavy element nucleosynthesis. We have determined accurate radiative lifetimes for the first three spectra of Lu using time-resolved laser-induced fluorescence on a slow beam of Lu ions and atoms. Lu I branching fractions have been determined from emission spectra taken with a 1.0 m Fourier transform spectrometer at the National Solar Observatory (NSO). These are combined with the radiative lifetimes to produce 38 accurate transition probabilities for Lu I. Lutetium is also an interesting case for comparison to theory because it has only a few valence electrons, depending on the ionization stage, outside of a closed shell of 14 f electrons. The Lu I measurements are compared to new relativistic Hartree-Fock calculations.

\*Supported by NSF grant AST-9819400. J. E. L. is a guest observer at the NSO on Kitt Peak, AZ.

#### JWP 64 MATERIALS PROCESSING/DUSTY PLASMAS

**JWP 65 Effects of H irradiation on properties of Cu films deposited by plasma CVD** Y. WATANABE, K. KOGA, H.J. JIN, K. TAKENAKA, T. KINOSHITA, M. SHIRATANI, *Graduate School of Information Science and Electrical Engineering, Kyushu University, Japan* Future generation of ULSI technology will rely heavily on sub-micron Cu interconnections. In order to fabricate such fine interconnections, we have developed a plasma CVD reactor equipped with an H atom source, which realizes control of Cu filling property in sub-micron trench by changing surface reaction probability of Cu containing radicals even at a constant substrate temperature under the deposition conditions of 100% Cu films.<sup>1</sup> In this work, effects of H irradiation on purifying Cu films and improving their surface roughness as well as size and orientation of Cu grains in films have been examined using the plasma CVD reactor. The H irradiation is found to be effective in purifying the Cu films, increasing the grain size up to the film thickness of ~ 500 nm, and reducing significantly the surface roughness down to several nm, while it has no effect on the grain orientation.

<sup>1</sup>H. J. Jin, M. Shiratani, Y. Nakatake, T. Fukuzawa, T. Kinoshita, Y. Watanabe and M. Toyofuku, *Jpn. J. Appl. Phys.*, **38** (1999), 4492-4495 <http://www.jjap.or.jp/cgi-bin/getarticle?magazine=JJAPvolume=38number=7Spage=4492-4495>

**JWP 66 Plasma radical sources for low pressure MOCVD of InAsN** H. NAOI, S. SAKAI, *Department of Electrical and Electronic Engineering, The University of Tokushima, Minami-Josanjima 2-1, Tokushima, 770, Japan* D. M. SHAW, G. J. COLLINS, *Dept. of Electrical Engineering, Colorado State University, Fort Collins, CO 80523* Due to its low and perhaps even negative bandgap, InAsN is an interesting new material Ohmic contacts and infrared device applications. To date there have been only a few reports demonstrating InAsN growth. Traditional MOCVD techniques using NH<sub>3</sub> as the nitrogen source, AsH<sub>3</sub> as the arsenic source, and trimethylindium (TMI) as the In source resulted only in InAs formation, even when the NH<sub>3</sub>/AsH<sub>3</sub> ratio is as high as 100. The failure to form InAsN was explained by the low pyrolysis efficiency of NH<sub>3</sub> in the low temperature range required for InAsN growth (T<sub>g</sub> 500 C). Herein we use two microwave plasma sources placed upstream of the growth region to allow low temperature, low pressure (750 mTorr) InAsN epitaxy. First, we replace the NH<sub>3</sub> with a nitrogen discharge which provides a large flux of atomic and molecular nitrogen radicals to the substrate. Additionally, the AsH<sub>3</sub> is replaced with a separate plasma that forms unsaturated arsine radical species AsH<sub>x</sub> (where x = 1 - 3) from atomic hydrogen and solid arsenic. By delivering the AsH<sub>x</sub> and N radicals directly to the growth zone of the reactor along with TMI, high quality epitaxial InAsN film growth is possible, with nitrogen content as high as 13 verified by x-ray diffraction measurements. In this work, the two plasma radical sources as well as the resulting InAsN films are characterized and interrelations are elucidated.

**JWP 67 Surface-Wave Plasma Deposition of a-C:H Films for Field Emission** TORU SANO, MASAOKI NAGATSU, NORIHARU TAKADA, HIROTAKA TOYODA, HIDEO SUGAI, *Department of Electrical Engineering, Nagoya University* W. X. GUANG, TAKASHI HIRAO, *Department of Electrical Engineering, Osaka University* NAOKI TOYODA, *Nissin Inc.* Recently crystalline diamond or diamondlike carbon (DLC) thin films prepared by the plasma enhanced CVD techniques have been widely studied as a new material of electron emitter for the next generation large-area field emission display. Among them, DLC films grown at low temperature are more attractive from an aspect of industrial manufacturing. In this study, we have carried out the deposition of hydrogenated amorphous carbon(a-C:H) films using a high density, low pressure surface-wave plasma (SWP). The SWP was produced in a 40cm-diameter vacuum chamber by introducing 2.45 GHz microwave through a quartz window via slot antennas. The a-C:H films were deposited on a silicon substrate immersed in He/CH<sub>4</sub> plasma, under discharge conditions of 700 W microwave power and 200 mTorr total pressure. Excellent field emission characteristics were obtained: the threshold electric field defined at an emission current density of 1 μA/cm<sup>2</sup> was obtained to be 4 V/μm. Other film characteristics measured with the XPS and FT-IR are also presented. This work was supported by a Grant-in-Aid for Science Research from the Ministry of Education, Science, Sports and Culture in Japan.

**JWP 68 Atomic-Scale Simulation of Plasma-Assisted Deposition of Diamond-Like Carbon Films** VLADIMIR SERIKOV, *Nippon Sheet Glass Co., Ltd., Japan* CAMERON ABRAMS, *Dept. Chem. Eng., University of California at Berkeley, USA* DAVID GRAVES, *Dept. Chem. Eng., University of California at Berkeley, USA* A molecular dynamics model has been developed and applied to simulations of diamond-like carbon film deposition by energetic C-atom beams. The results obtained for different

bombardment energies show a substantial increase in the film density and amount of 4-coordinated carbon atoms at 40 eV, as compared to the film grown at 1 eV that has much lower density and larger content of graphitic 3-coordinated atoms. Besides, it is clearly shown that concurrent bombardment of the film growing at a low energy of 1 eV by energetic argon ions of 40 to 150 eV can essentially improve the diamond-like properties of the film. The simulation results for hydrogenated diamond-like carbon film deposition either by C plus H atoms or C<sub>2</sub>H radicals are also to be presented and discussed.

**JWP 69 Influence of oxygen plasma on the structure of the carbon thin films deposited by pulsed laser deposition\***

YOSHIYUKI SUDA, TOMOYUKI ONO, MASAMICHI AKAZAWA, YOSUKE SAKAI, *Hokkaido University, Sapporo, 060-8628, Japan* Pulsed laser deposition (PLD) is an effective method for depositing diamond-like carbon (DLC) because it can eject high energy ions and neutrals from the target. In PLD of carbon films atomic oxygen or hydrogen introduced as ambient gas plays an important role in etching sp<sup>2</sup> component for improving the film properties (e.g. increase of sp<sup>3</sup> content and crystallinity).<sup>1</sup> In this report we will present the influence of oxygen plasma generated in a helical coil installed between the target and substrate on carbon film properties. The oxygen RF plasma is expected to produce atomic oxygen effectively. The detailed experiment configuration is described in the previous report.<sup>2</sup> The result of the XPS spectra of the films indicates that the C(1s) peak energy shifts to higher values as an oxygen gas pressure and RF power increase. The film property influenced by the plasma and the possibility for decreasing the substrate temperature are discussed.

\*Work in part supported by Grant-in-Aid 11750245 by the Ministry of Education, Science, Sports and Culture, Japan.

<sup>1</sup>M. Yoshimoto, *Nature*, **399**, 340 (1999).

<sup>2</sup>Y. Suda, *Thin Solid Films*, in press.

**JWP 70 C<sub>7</sub>F<sub>16</sub>/He rf plasma CVD of a-C:F films\*** KOHJI HOKOI, MASAMICHI AKAZAWA, HIROTAKE SUGAWARA, YOSUKE SAKAI, *Hokkaido University, Sapporo 060-8628 Japan* Fluorinated carbon is one of the most promising materials with low dielectric constant  $\epsilon_r$  and high dielectric strength  $V_b$ . We have deposited a-C:F films by rf (13.56 MHz) plasma enhanced CVD method using the following liquid materials; C<sub>7</sub>F<sub>16</sub>, (C<sub>3</sub>F<sub>7</sub>)<sub>3</sub>N/(C<sub>4</sub>F<sub>9</sub>)<sub>3</sub>N and C<sub>8</sub>F<sub>18</sub>/C<sub>8</sub>F<sub>16</sub>O.<sup>1</sup> The films showed  $\epsilon_r$  values in a range of 1.9–3.0 and  $V_b > 2$  MV/cm. In this work, we added He (3 Pa) to C<sub>7</sub>F<sub>16</sub> (60 Pa) plasmas, expecting that He atoms in the metastable excited state (He\*, 19.8 eV) would promote C<sub>7</sub>F<sub>16</sub> decomposition in gas phase or activation of the film surface during deposition. The films with the thickness up to 2300 nm were deposited on unheated Si substrate with an rf power of 100 W@. The deposition rate derived from the film thickness measurement by SEM and ellipsometry was about 230 nm/min. This value is roughly two times as large as that of the films deposited by C<sub>7</sub>F<sub>16</sub> (60 Pa) plasmas without He. We discuss the mechanism that leads to such a significant increase in the deposition rate.

\*Work in part supported by Grant-in-Aid for Scientific Research of The Ministry of Education, Science, Sports and Culture, Japan.

<sup>1</sup>C. P. Lungu *et al.*, *Jpn. J. Appl. Phys.* **38**, L1544–6 (1999).

**JWP 71 Ablation Plasma Ion Implantation (APII)** R. M. GILGENBACH, *University of Michigan* BO QI, *University of Michigan* Y. Y. LAU, *University of Michigan* M. D. JOHNSTON, *University of Michigan* G. L. DOLL, *Timken Research* Ablation plasmas are generated by an excimer laser incident on pure metal targets. Initial APII film depositions have implanted Fe into Si wafer substrates at negative voltages up to 10 kV. Thin film properties (e.g., adhesion, morphology) of thin films deposited by laser ablative deposition (zero voltage) will be compared to films deposited with APII. A simple one dimensional theory is developed [1] to calculate the implanted ion current, extracted from the ion matrix sheath, as a function of time for various substrate-plume separations. This model accurately recovers Lieberman's classic results when the plume front is initially in contact with the substrate. [1] B. Qi, Y. Y. Lau, and R. M. Gilgenbach, *Appl. Phys. Lett.* (to be published). This work was supported by NSF. \*Timken Research, Canton, OH 44706-0939.

**JWP 72 Reduction of oxide microtrenching by electron beam assisted etching** M. WATANABE, D. M. SHAW, G. J. COLLINS, *Dept. of Electrical Engineering, Colorado State University, Fort Collins, CO 80523* High density plasma etching of submicron wide oxide trenches often results in non-ideal etched features. For example, microtrenching is the result of higher etch rate near the side wall as compared to the center of the trench. Herein, we apply a previously reported [1] high energy (100 - 900 eV) electron beam directed at the etching wafer surface to reduce microtrenching during the etching of 0.5 micron wide silicon dioxide (SiO<sub>2</sub>) trench patterns in an inductively coupled fluorocarbon plasma. The directed electron beam neutralizes the positive charge buildup at the bottom of the trench and reduces the microtrench formation. Scanning Electron Microscopy (SEM) images of features etched with and without the electron beam show that the electron beam is effective in reducing microtrenching. [1] D. M. Shaw, M. Watanabe, G. J. Collins, and H. Sugai, *Jpn. J. Appl. Phys.* **38**, 87 (1999).

**JWP 73 Electron shading on a macroscopic scale** TSITSI G. MADZIWA, *UCLA* FRANCIS F. CHEN, *UCLA* Damage to thin gate insulators during plasma processing is thought to be caused by the electron shading effect, in which a negative charge on the photoresist prevents electrons from reaching the bottoms of trenches and vias. The resulting positive charge impinging on the oxide layer creates megavolt potentials across it. Though this hypothetical effect has been modeled extensively in computer simulations, it has not been seen in detail in experiment. To test the theory on a macroscopic scale, we have devised an RF discharge at low pressure and low density, such that both the mean free path and the Debye length are larger than the feature sizes, as in actual microcircuits. Circular vias of order 1 mm in diam are drilled in an insulating plate exposed to the plasma, and the current and potential at various depths are measured with charge collectors. The potential distribution in each hole is calculated with a Poisson solver, and the ion trajectories are found numerically, giving the expected I - V characteristics of the collector to be compared with measurements. Of particular interest is the variation of the charging currents during the RF cycle.

**JWP 74 Initial growth of clusters in silane rf discharges** K. KOGA, K. TANAKA, T. TOKUYASU, M. SHIRATANI, Y. WATANABE, *Graduate School of Information Science and Electrical Engineering, Kyushu University, Japan* Since clusters below a few nm in size formed in silane rf discharges have been pointed out to be a possible cause of quality degradation of a-Si:H films, initial growth processes of clusters are studied using two *in-situ* cluster detection methods. One is the double pulse discharge method and the other is the photon-counting laser-light-scattering method.<sup>1</sup> 1) Even under the so-called device quality (low pressure and low power) conditions, there exist clusters, very high compared to a plasma ion density, at  $t =$  several 10's ms after the discharge initiation. 2) The clusters begin to be composed of two size-groups at  $t = 10$  ms: small constant size clusters of  $\sim 0.5$  nm and large size clusters growing in mono-disperse way. 3) For  $H_2/SiH_4 \geq 20$ , growth of large size clusters is significantly suppressed. 4) Grounded electrode heating is useful for driving clusters above a few nm to the RF electrode side due to thermophoretic force. 5) Pulse discharge modulation combined by the heating electrode is very effective in suppressing growth of clusters. 6) The cluster growth rate with a glass or Si substrate is found to be considerably higher than that without the substrate.

<sup>1</sup>M. Shiratani *et al.*, *Jpn. J. Appl. Phys.* **39** (2000), 287–293 <http://www.jjap.or.jp/cgi-bin/getarticle?magazine=JJAPvolume=39number=1Rpage=287-293>

**JWP 75 The Location of Small Particles in a Silane RF Discharge** KAROLY ROZSA, JILA, NIST and Univ. of Colorado, Boulder, CO 80309 GREGORY BANO, same ALAN GALLAGHER, same Silane rf discharges are generally used in the deposition of hydrogenated amorphous silicon (a-Si:H) photovoltaics and thin film transistors. Particles grow rapidly in these discharges, due to the trapping and growth of negative ions, and a copious flux of small (1–20 nm) particles can incorporate into devices. Particle locations within RF discharges influence particle densities and where they incorporate into the films growing on the electrodes. These particle locations within the plasma depend on gas-drag, thermophoretic and ion-wind forces, sheath location and small variations in plasma potential. We have used light scattering to measure, in pure silane discharges, the dependence of particle location and density on a variety of factors, including particle size, discharge power, gas pressure and temperature, temperature gradients and electrode shape. (Particle size is determined from their afterglow diffusion, as described in M.A.Childs and A.Gallagher, *J.Appl.Phys.* 87,1076(2000).) With a thermal gradient between the electrodes, the thermophoretic force pushes the particles to the colder edge of the plasma sheath and increases particle loss to the electrodes, so that fewer survive to observable size. As expected, this force is more effective for larger size (typically 30 nm) particles, which occur after the discharge is on for several seconds. Particle densities and spatial distributions, versus discharge parameters, will be presented.

**JWP 76 Laser-excited shear and compressional waves in a crystallized dusty plasma\*** S NUNOMURA,<sup>†</sup>V NOSENKO, D SAMSONOV,<sup>‡</sup>J GOREE, *Department of Physics and Astronomy, The University of Iowa* A dusty plasma is an ionized gas containing small particles of solid matter. These particles acquire a large negative electric charge. Because of their Coulomb repulsion, they arrange in a Wigner lattice. Like any crystal, this so-called "plasma crystal" sustains two kinds of acoustic modes: compres-

sional and shear. The former is longitudinal, while the latter is transverse.  $\langle p \rangle$  By applying optical pressure from an argon laser beam, we can push particles. Modulating the laser allows us to excite sinusoidal waves, with either the compressional or shear polarization.  $\langle p \rangle$  Experiments have been carried out using a parallel-plate radio-frequency discharge. Polymer microspheres were shaken into the plasma, where they were levitated by the electric field in the sheath above the lower electrode. The particles arranged in a single horizontal layer, with a hexagonal lattice. They were imaged using a video camera, which recorded the particle motion. The motion of the particles in response to the modulated laser beam was analyzed to measure the propagation speed and dispersion of the waves.

\*Work was supported by NASA and NSF.

<sup>†</sup>Supported by the Japan Society for the Promotion of Science.

<sup>‡</sup>present address: MPE, Garching, Germany.

### JWP 77 Post-Deadline Posters

**JWP 78 Particle Number Density Measurement of Sputtered Aluminium Atoms in an Argon Hollow Cathode Glow Discharge** HELMAR SCHEIBNER, JÜRGEN F. BEHNKE, ANDREAS DINKLAGE, STEFFEN FRANKE, CHRISTIAN WILKE, *Institut für Physik, E.-M.-Arndt-Universität, 17487 Greifswald, Germany* Direct current hollow cathode glow discharges are qualified for spectroscopic application and for the study of sputtering processes. By means of diode laser spectroscopy the particle number density of sputtered aluminium atoms in the negative glow of a cylindrical dc hollow cathode glow discharge in argon was investigated (pressure  $p = 1.5$  Torr, current  $i = 10$  mA ... 30 mA, aluminium hollow cathode: diameter  $d = 7$  mm, length  $l = 30$  mm). The absorption measurements followed on the both aluminium resonance lines (396.153 nm, 394.403 nm) combining with the two ground state sublevels  $^2P_{3/2}$  and  $^2P_{1/2}$ . In contrast to earlier absorption measurements with a usual line radiator as light source here absorption line profiles were sampled by the narrowband radiation of a tunable blue-emitting GaN diode laser. The wavelength of the laser radiation was scanned with help of a piezoelectric element and the mode hop-free function of the diode laser was checked by a Fabry-Perot resonator with a free spectral range of 2 GHz. The investigations demonstrate the qualification of the blue-emitting laser diode for spectroscopic measurements and yield better absorption spectroscopic results on the basis of exact line profiles.

**JWP 79 Efficiency improvement of PDP and nonlinear dynamics by two-tiered pulse** MIN SUP HUR, *Pohang Univ. Sci. Tech.* S. DASTGEER, *Pohang Univ. Sci. Tech.* JAE KOO LEE, *Pohang Univ. Sci. Tech.* One of the most important issue in PDP research is the improvement of light efficiency. Generally the discharge efficiency in PDP is believed to increase when the discharge current is low or driving electric field is small. However PDP requires a large number of plasma particles to be accumulated as wall charges for sustaining the stable operation. This restricts the reduction of discharge current or driving electric field. By using a two-tiered pulse shape, the current can be reduced significantly without losing the stable operation of PDP cell. The first tier of low voltage ignites the discharge with small current, while the second tier of high voltage separates the plasma strongly and accumulate enough wall charge to sustain the cell. Overall

discharge efficiency also increases. When the two-tiered pulse is used in general dielectric-barrier-discharges (DBD), interesting nonlinear dynamics is observed. The discharge peaks starts to exhibit irregular patterns as the voltage difference between the first and the second tiers increases. Since a discharge peak during a pulse is related to the previous one by the wall charges, it is possible to find an analytic mapping between them. A sudden transition from period one to chaos was observed from the analysis of that mapping. We also found that the periodic and chaotic states are densely mixed with each other.

**JWP 80 Triggerless vacuum shunting plasma by metallic and solid materials** KEN YUKIMURA, YUUJI TANI, *Department of Electrical Engineering, Doshisha University, Kyotanabe 610-0321, Japan* SADA O MASAMUNE, *Department of electronics and information sciences, Kyoto Institute of Technology, Kyoto, 606-8585, Japan* Shunting discharge is an alternating capacitor discharge through a rod of solid-state or metallic materials. Optimization of the discharge condition has realized self-ignition of the arc discharge with low input power to the rod, leading to a much longer rod life time than in conventional shunting arc or peripheral arc. The shunting-arc-produced plasma contains mainly the ions of the solid-state material, and ion extraction from the plasma has also been demonstrated. Thus, the shunting arc works as a pulsed ion source for solid-state materials for plasma-based ion implantation (PBII) and ion processing. This article describes the characteristics of pulsed shunting arc, using the materials of carbon, niobium and silicon. The capacitor of 10 nF of which charging voltage is 10 to 25 kV using a thyatron as a closing switch. Glow discharge is firstly produced after the heat of the materials and then the plasma changes the style to the arc discharge. A negative high voltage pulse of  $-5$  to  $-10$  kV was applied to a target which was located at 30 cm away from the electrodes. We will discuss the ion species of the shunting plasma and ion extraction from the plasma using the time evolution of target current.

**JWP 81 Observation of a Silent Discharge using a Piezoelectric Transformer in Oxygen** HARUO ITOH, *Chiba Institute of Technology* TORU SUZUKI, *Chiba Institute of Technology* SUSUMU SUZUKI, *Chiba Institute of Technology* Using a piezoelectric transformer PT made from PZT ( $\text{Pb}(\text{Ti}, \text{Zr})\text{O}_3$ ) shaped in thin plate, we found a fact that the PT brightens with a light emission originated from its surfaces. In this case, the secondary circuit of the PT is opened, except for only connection to the oscilloscope for the purpose of the measuring output voltage. The discharge is maintained between the PT and the surface of discharge chamber made of stainless steel and keeping the earth potential. The spatial distribution of the light emission, that is the luminous pattern, is changed significantly with the driven frequency of the PT. If the driven frequency of the PT is adjusted to it might coincide with the natural frequency of the elastic vibration of the PZT, it is called " $\lambda$  mode vibration" and  $\lambda$  means the wavelength of the vibration and also equal to the length of the PZT, a bright of quadruple like luminous pattern was observed surround the both sides of the PT. In contrast, dipole like luminous patterns are also observed by the driven frequency which is adjusted to the frequency corresponding to  $\lambda/2$  and  $3\lambda/2$  modes. When oxygen is filled in the chamber, we observe a sharp peak at 777 nm (O atom) in the emission spectrum. From this result, the existence of ozone is presumed.

**JWP 82 Loss Processes of Metastable Molecules in Cylindrical Cavity** SUSUMU SUZUKI, *Chiba Institute of Technology* HARUO ITOH, *Chiba Institute of Technology* Assuming a closed cylindrical volume, the spatiotemporal variation of the density distribution of the metastable molecules  $\text{N}_2(\text{A}^3\Sigma_u^+)$  in the cylindrical volume are calculated from the diffusion equation analysis under the different reflection coefficients at the flat electrode surfaces and at the cylindrical wall.<sup>12</sup> We solve the diffusion equation by separation of variables using the boundary condition of the third kind that is taken account of the reflection at the electrode surfaces.<sup>3</sup> The obtained solution of the diffusion equation are possible to describe the density profiles along the longitudinal and the radial directions. The influence of the density distribution by the different reflection coefficient at each of electrodes and at the cylindrical wall is investigated. Furthermore, the effective lifetime of the diffusing metastable molecules is also discussed under different reflection coefficients.

<sup>1</sup>S. Suzuki, H. Itoh, N. Ikuta and H. Sekizawa: Jpn. J. Appl. Phys., 39, 1333, 2000.

<sup>2</sup>S. Suzuki, H. Itoh, H. Sekizawa and N. Ikuta: Papers of Technical Meeting on Electrical Discharges, ED-98-128, 17, 1998 (in Japanese).

<sup>3</sup>S. Suzuki, H. Itoh, N. Ikuta and H. Sekizawa: J. Phys. D: Appl. Phys., 25, 1568, 1992.

**JWP 83 Double Peak Structure of Electron Energy Distribution in Low  $E/N$  and Ar, Kr and Xe** HARUO ITOH, *Chiba Institute of Technology* TERUHIRO SUZUKI, *Chiba Institute of Technology* TATSUYA FUKUYAMA, *Chiba Institute of Technology* SUSUMU SUZUKI, *Chiba Institute of Technology* NOBUAKI IKUTA, *Chiba Institute of Technology* Monte Carlo simulation of the electron swarm in low  $E/N$  in Ar, Kr and Xe is performed to make clear the cause of the double peak structure of the electron energy distribution (EED) and to investigate for the observing condition of that. The spatial variation of the EED and the colliding energy distribution of the electron which collides with Ar, Kr and Xe, are obtained together with the electron mean energy, the drift velocity and other transport coefficients using the SST (steady state Townsend) sampling technique. Certainly, the double peak structure of the EED is found only in the  $E/N$  region which correspond to the electron energy near the Ramsauer minimum of the momentum transfer collision cross sections. In this region, the electron mean energy is not constant against the position, that is, the high energy tail of the EED shifts to the high energy value with the increase of the distance from the cathode. It is concluded that the double peak structure of EED is found only in the non-equilibrium region of electron energy and that is not formed as the stationary EED.

**JWP 84 Reference Cell for Growth of Carbon Based Materials** COREY COLLARD, *University of Michigan* MARY BRAKE, *University of Michigan*, SUSAN SONG, *Michigan State University*, VIRGINIA AYRES, *Michigan State University* The Gaseous Electronics Conference (GEC) Reference Cell, in the inductively coupled plasma mode, is used to grow carbon-based materials such as nanotubes. Spatially resolved optical emission is used to examine the plasmas during growth. Mixtures of methane and hydrogen are used to grow the carbon films at pressures of 100 mTorr to 250 mTorr. Experiments examine the composition of the plasma as well as the uniformity of the plasma emission above the

substrate. The carbon structures produced are characterized using scanning electron microscopy, scanning probe microscopies, high-resolution transmission microscopy, and micro-Raman spectroscopy.

**JWP 85 Coincidence Studies of Low Energy Electron Impact Ionization of Rare Gases** BIRGIT LOHMANN, MATTHEW A. HAYNES, *School of Science, Griffith University, Nathan, Queensland, Australia* Measurements of the triple differential cross section using the (e,2e) technique provide a sensitive probe of the dynamics of electron impact ionization. In recent years there has been particular interest both experimentally and theoretically in the low incident energy regime (2-5 times the ionization energy), and in symmetric geometries, where the outgoing electrons have equal energies. A limited number of experiments have been performed on heavier targets at low incident energies, with none of these using the coplanar asymmetric geometry. We present here experimental results for the TDCS for low energy electron impact ionization of helium and argon in symmetric and asymmetric geometries. In particular, we have investigated ionization of the 3s inner-valence orbital in argon in the coplanar asymmetric geometry, at an incident energy of 113.5 eV (5 times the binding energy of 29.3 eV), scattering angle of 15 degrees and ejected electron energies of 2, 5, 7.5 and 10 eV. The choice of target orbital and kinematics was prompted by the existence of published results of distorted-wave Born approximation calculations by Madison and Lang (1981 *J. Phys. B* **14** 4137), which predicted interesting structure in the TDCS. The experimental measurements have been performed in a new low energy coincidence spectrometer. We compare our experimental data with available theoretical results.

**JWP 86 Experimental observation of desorbed products by irradiation of plasma beam during SiO<sub>2</sub> etching** KAZUAKI KURIHARA, YOSHIKAZU YAMAOKA, MAKOTO SEKINE, *Plasma Technology Laboratory, Association of Super-Advanced Electronics Technologies (ASET)* Understanding of fundamental reactions such as adsorption and desorption during etching has been required to develop quantitative models of etching mechanisms leading to reliable process simulators. Although fluorocarbon gases are widely used for SiO<sub>2</sub> etching process, the fundamental reactions are still under investigation. Ions and radicals (plasma beam) effusing from an ECR plasma source were irradiated on a SiO<sub>2</sub> substrate placed in a differentially pumped chamber and desorbed products from the substrate were detected by a quadrupole mass spectrometer (QMS). The plasma beam was mainly composed of CF<sub>3</sub><sup>+</sup>, CF<sup>+</sup>, CF<sub>3</sub> and CF<sub>2</sub> when CF<sub>4</sub>(50%)/Ar gas mixture was used in the plasma source. In order to identify the desorbed products which can not be discriminated by QMS due to the same atomic mass (for example, SiF and COF) heteronuclear C<sup>13</sup>F<sub>4</sub> gas was used. The ion energy was about 500 eV. The main desorbed products were found to be SiF and COF. And an ionic species of SiF<sup>+</sup> was also observed as the desorbed product. This work was supported by NEDO.

**JWP 87 Instabilities in Low-Pressure Inductively Coupled Plasmas** C. S. CORR, *Dept. of Physics, The Queen's University of Belfast, BT7 INN, N. Ireland*, C. M. O. MAHONY, *NIBEC, University of Ulster, BT37 0QB, N. Ireland*, W. G. GRAHAM, *Dept. of Physics, Queen's University Belfast, BT7 INN, N. Ireland* Until recently there have been very few studies of instabilities in rf-driven plasmas (1,2). In the present work instabilities have been

observed in a low-pressure, 13.56 MHz inductively coupled GEC rf reference cell operating in oxygen. A photodiode was used to observe the total visible light output of the plasma. The light intensity was observed to fluctuate. The frequency and magnitude of the intensity fluctuations varied with gas pressure. The fluctuations were observed at gas pressures between 10 and 35 mTorr, with their frequency changing from 5 to 16 kHz respectively. The largest excursion in amplitude was observed at 25 mTorr. No fluctuations were observed under similar conditions in argon. These results are very similar to those reported previously in O<sub>2</sub> (1) and SF<sub>6</sub> (1,2). Negative ion density measurements are now underway to try to determine the cause of these instabilities. 1. M. Tszewski, *J. Appl. Phys.* **79**, 8967 (1996). 2. M. A. Lieberman, A. J. Lichtenberg & A. M. Marakhtanov, *Appl. Phys. Lett.* **75**, 3617 (1999).

**JWP 88 Measuring O atom concentrations using optical emission spectroscopy and two-photon laser-induced fluorescence in O<sub>2</sub>/Ar neutral loop discharge (NLD) plasmas** KENJI KAWASHIMA, ASET SHIGENORI HAYASHI, NOBUO OZAWA, SHUICHI NODA, TETSUYA TATSUMI, MAKOTO SEKING, *ASET* Optical emission spectroscopy was used to measure O atom concentrations in O<sub>2</sub>/Ar neutral loop discharge (NLD) plasmas. Emissions from O at 777.4 and 844.6 nm were measured, and the emission from rare gases (Ar and He) was used to correct for changes in the electron energy distribution. The O atom concentrations were compared to the absolute ground-state O atom density obtained using the two-photon laser-induced fluorescence (LIF) method. Upon varying the oxygen percentage, the actinometry signal (corrected for changes in the electron energy distribution) was proportional to the density measured by the LIF, whereas the conventional actinometry signal was not. This work was supported by NEDO.

**JWP 89 Silver Thin Film Modification with Ar/Cl<sub>2</sub> Inductively Coupled Plasmas for Biomedical Applications** C. N. ESCOFFIER, *NIBEC, University of Ulster, BT37 0QB, N. Ireland*, C. M. O. MAHONY, *NIBEC, University of Ulster, BT37 0QB, N. Ireland*, E. T. MCADAMS, J. A. D. MCLAUGHLIN, W. G. GRAHAM, *Dept. of Physics, The Queen's University of Belfast, BT7 INN, N. Ireland*, P. D. MAGUIRE, *NIBEC, University of Ulster, BT37 0QB, N. Ireland* Here we investigate novel Cl<sub>2</sub> and Ar/Cl<sub>2</sub> plasma based processes to produce inbuilt Ag/AgCl thin films (TFs) for biomedical microsensors. Early work showed that the required Ag TF surface modification was achievable using pure Cl<sub>2</sub> in a 13.56 MHz capacitively coupled plasma (CCP). In conjunction with another project (1), linking plasma parameters during processing to subsequent TF properties, we used Ar/Cl<sub>2</sub> mixtures in a 14 MHz inductively coupled plasma (ICP) to investigate Ag TF modification. Parameters varied were input power, pressure, Cl<sub>2</sub> fraction and processing time. We have identified a promising pressure operating regime around 5 Pa. Here electrochemical impedance spectra are close to device requirements, agreeing with our CCP work. Input power or Cl<sub>2</sub> fraction has less effect. Correlation between the film properties and plasma parameters, particularly atomic chlorine density(1), are being investigated. (1) C. M. O. Mahony *et al.* (this conference).



## SESSION KR1: ELECTRON-ATOM/MOLECULE COLLISIONS II

Thursday morning, 26 October 2000; Grand Ballroom D, Red Lion Hotel at 8:00; Steve Buckman, Australian National University, presiding

## Invited Papers

8:00

**KR1 1 Practical Methods for Studying Collisional Breakup.\***T.N. RESCIGNO, *LLNL/LBNL*

The quantum theory of three-body breakup in Coulomb systems, formulated in the early sixties, has formed the basis of a considerable body of theoretical analysis of low energy electron impact ionization. Although aspects of this theory have been incorporated into various perturbative and distorted-wave treatments, the formal theory has not provided a viable computational approach to a first-principles treatment of ionization, due to the complicated nature of the boundary conditions for three-body breakup in Coulomb systems and the fact that they are only known in the far asymptotic region. Exterior complex scaling allows one to solve the Schrödinger equation without explicit imposition of asymptotic boundary conditions. This approach has produced the first triple differential cross sections for e-H ionization that are in complete agreement with absolute measurements [1]. In this talk, I will review the essential aspects of this approach and present new results on double differential cross sections for e-H ionization. I will also discuss some new methods for extracting dynamical information from numerically obtained wave functions that are more efficient than the flux operator approach we previously employed. These methods allow us to explore ionization in the threshold region and open the way to calculations on systems with more than two electrons, where new physical effects can be studied. [1] T. N. Rescigno, M. Baertschy, W. A. Isaacs and C. W. McCurdy, *Science* 286, 2474 (1999)

\*Work performed under the auspices of the USDOE by the University of California LLNL and LBNL under contract numbers W-7404-Eng-48 and DE-AC03-76F00098.

8:30

**KR1 2 Angular Momentum Partitioning in Electron Collisions with Heavy Noble Gases.\***T.J. GAY,† *University of Nebraska*

Our understanding of collisions with H, He, and the light alkali atoms is good, but calculations of scattering from the heavy noble gases is not yet satisfactory. This is due primarily to the outer p-shell configuration of such atoms and the fact that relativistic effects can be important in some collision channels. While heavy noble gas targets present serious challenges to theory, they also provide a richer variety of physics to study, and are important in plasmas and discharges. In this talk, I discuss a topic that has received little attention to date: how collision-induced angular momentum is partitioned between the subshells of excited targets. To study this, we have investigated the simultaneous ionization and excitation of Ar with polarized electrons by observing the integrated Stokes parameters of the light emitted by the excited residual ions. I will discuss the role of the Rubin-Bederson hypothesis in the analysis of these collisions, and present the first measurement of an ionic hexacontatetrapole (64-pole) moment.

\*Supported by NSF Grant PHY-9732258

†Work done in collaboration with H.M. Al-Khateeb and B.G. Birdsey

## Contributed Papers

9:00

**KR1 3 An Improved Binary-Encounter-Dipole Model for Electron Impact Ionization and the Dissociative Ionization of CF<sub>4</sub>\*** WINIFRED HUO, *NASA Ames Research Center* CHRISTOPHER DATEO, *Eloret* GRAHAM FLETCHER, *Iowa State University* In the Binary-Encounter-Bethe (BED) model<sup>1</sup> for electron-impact ionization, the Bethe cross section has been used to represent long-range dipole interaction. However, the Bethe cross section is applicable only at high kinetic energies, whereas the BED model is frequently used at threshold energies. We have derived a suitable representation of the Born cross section for ionization by studying a convergent series representation of the generalized oscillator strength (GOS) in the complex plane of momentum transfer,  $K$ . An approximate, one-term representation of

the GOS is derived that satisfies both Lassette's limit theorem at  $K = 0$  and the asymptotic behavior at large  $K$  derived by Rau and Fano. The approximate Born cross section so obtained is applicable at all incident energies and provides a more suitable representation of the dipole contribution to the BED model than the Bethe cross section. We apply this model in the study of the dissociative ionization (DI) of CF<sub>4</sub> using a combined electron collision and nuclear dynamics calculation. The dissociation pathways for the three lowest ion states have been calculated using CASSCF. For all channels the minimum energy pathway for dissociation is purely repulsive and no transition state is found. The DI cross section will be compared with experiment.

\*This work is supported by NASA Ames IPT on Devices and Nanote

<sup>1</sup>Y.-K. Kim and M. E. Rudd, *Phys. Rev. A* 50, 3954 (1994)

9:15

**KR1 4 Electron impact ionization of nitrogen trifluoride**  
 CHARLES JIAO, *Mobium Inc.* PETER HAALAND, *Mobium Inc.*  
 ALAN GARSCADDEN, *Air Force Research Laboratory* The absolute cross sections for partial ionization of  $NF_3$  by electron impact have been measured using Fourier transform mass spectrometry from threshold to 200 eV. The most abundant ion at all energies is  $NF_2^+$ . Below 40 eV, the next most abundant ion is the undissociated parent ion  $NF_3^+$ , followed by  $NF^+$ . Above 40 eV, the yield of  $NF^+$  exceeds that of  $NF_3^+$ . The ions  $F^+$  and  $N^+$  are also observed in small yields above 45 eV. The total ionization cross section peaks near 180 eV at  $2.5 \pm 0.4 \times 10^{-20} m^2$ . Charge transfer in mixtures of  $NF_3$  and argon ions appears straightforward with the main reaction channel producing the fragment ion that dominates the electron impact dissociative ionization process,  $NF_2^+$ . The correlation of the measured cross sections with estimates based on *ab initio* electronic structure methods and the role of dissociative ionization in  $NF_3$  etching plasmas are discussed.

9:30

**KR1 5 Calculation of ionization cross sections for electron impact of H<sub>2</sub>, O<sub>2</sub> and CO molecules** YIMING MI, *RACE, The University of Tokyo* SHUICHI IWATA, *RACE, The University of Tokyo* Cross sections of electron impact ionization from H<sub>2</sub>, O<sub>2</sub> and CO molecules have been calculated for different incident energies based on *ab initio* approach and model potential assumption. The acquired results are compared with available experimental and other theoretical data. Other scattering parameters are also discussed in this paper.

9:45

**KR1 6 Ionization of CF<sub>3</sub>I** C.Q. JIAO, *Mobium Enterprises, Inc.* A. GARSCADDEN, *Air Force Research Laboratory* B. GAN-GULY, *Air Force Research Laboratory* C.A. DeJOSEPH JR., *Air Force Research Laboratory* Using Fourier-transform mass spectrometry we have studied the ionization of trifluoroiodomethane (CF<sub>3</sub>I) by electron impact and by ion-molecule reactions. Electron impact ionization on CF<sub>3</sub>I produces molecular ion CF<sub>3</sub>I<sup>+</sup> and fragment ions including I<sup>+</sup>, CF<sub>3</sub><sup>+</sup>, CF<sub>2</sub>I<sup>+</sup>, CF<sub>2</sub><sup>+</sup>, CF<sub>2</sub><sup>+</sup> and CI<sup>+</sup>, with a total cross-section of  $9.0 \pm 0.9 \times 10^{-16} cm^2$  at 70 eV. The parent molecular ion dominates the ion population within the energy range studied (from the threshold to 70 eV). At low electron energies (less than 20 eV) the most important dissociative ionization channel is the production of CF<sub>3</sub><sup>+</sup> and I. In contrast ionization of CF<sub>3</sub>I by charge-transfer reaction with Ar<sup>+</sup> produces CF<sub>2</sub>I<sup>+</sup> as the major product ion, with a rate coefficient of  $14 \times 10^{-10} cm^3 s^{-1}$ . The CF<sub>3</sub>I reaction with CF<sup>+</sup> or CF<sub>3</sub><sup>+</sup> produces CF<sub>2</sub>I<sup>+</sup> mainly also, with the rate coefficients  $5.8$  or  $1.9 \times 10^{-10} cm^3 s^{-1}$ , respectively, while the reaction with CF<sub>2</sub><sup>+</sup> or I<sup>+</sup> produces primarily CF<sub>3</sub>I<sup>+</sup>, with the rate coefficients of  $13$  or  $8.2 \times 10^{-10} cm^3 s^{-1}$ , respectively.

**SESSION KR2: INDUCTIVELY COUPLED PLASMAS II**  
 Thursday morning, 26 October 2000  
 Grand Ballroom C, Red Lion Hotel at 8:00  
 T. Makabe, Keio University, presiding

### Contributed Papers

8:00

**KR2 1 Spatial Distribution of Charged Particles in a Magnetic Neutral Loop Discharge Plasma** YAW OKRAKU-YIRENKYI, *Miyazaki University* YOUL-MOON SUNG, *Miyazaki University* MASAHISA OTSUBO, CHIKAHISA HONDA, KIICHIRO UCHINO, *Kyushu University* KATSUNORI MURAOKA, In order to analyze the spatial distribution of a magnetic neutral loop discharge (NLD) plasma, the electron density (ne), electron temperature (Te) and ion flux were studied experimentally and numerically. The experimental results showed that the Te and ion flux have a peak on the neutral loop (NL) and migrated along magnetic field lines. In contrast, the electron density had a peak at a position inward from the NL [1] along its radius. Analyses of the electron behavior using a 3-dimensional model showed that there exists an electron trapping region at a position radially inward from the NL due to magnetic mirror effect. [1] T. Sakoda et al. *Jpn.J. Appl. Phys. Vol.36 (1997) pp.6981-6985 Part1 No.11, November 1997*

8:15

**KR2 2 Harmonic Content of Electron Impact Source Functions in Inductively Coupled Plasmas Using an "On-the-Fly" Monte-Carlo Technique\*** ARVIND SANKARAN, MARK J. KUSHNER, *University of Illinois/Urbana-Champaign* The electron temperature in low pressure ( $< 10s$  mTorr) inductively coupled plasmas (ICPs) excited at 10s MHz typically is not significantly modulated during the rf cycle. The tail of the electron energy distribution (EED) may, however, be modulated thereby producing time dependent electron impact source functions for high threshold processes. Computer models based on hybrid techniques typically do not resolve this time dependence since only cycle average electron properties are used due to the computational burden of calculating and storing time and spatially dependent EEDs. In this paper, a new Monte Carlo technique, called "on-the-fly" (OTF), is described in which moments of the EED are computed, as opposed to the actual EED. In doing so, spatially dependent electron impact source functions are directly obtained. By computing Fourier components of the source functions "on-the-fly," the time harmonics can also be obtained. The OTF technique was implemented in the Hybrid Plasma Equipment Model, a simulator for low pressure plasmas. The spatially dependent time harmonics of electron impact source functions will be discussed for ICPs in Ar/molecular gas mixtures.

\*Work supported by NSF (CTS99-74962), SRC and AFOSR/DARPA.

8:30

**KR2 3 Formation of Electron Energy Distribution in ICP** VALERY GODYAK, *Osram Sylvania* VLADIMIR KOLOBOV, *CFDRC* We compare measured and calculated EEDF in ICP in a wide range of discharge conditions. The ICP was driven by a planar coil in a frequency range 3.4-13.56 MHz, argon pressures

0.3-300 mTorr, and power absorbed in plasma 12-200 W. We found that 1) EEDF in the center of plasma is nearly Maxwellian at highest plasma densities and substantially non-Maxwellian at lowest plasma densities; 2) The frequency dependence of the EEDF is different at low and high pressures; 3) EEDF is a function of total electron energy in the entire range of studied discharge conditions. For collisional plasma, Boltzmann equation was reduced to a Fokker-Planck equation in three dimensional space (two spatial coordinates and energy) and solved by finite volume method. In the near-collisionless regime, kinetic equation depends only on total electron energy. Peculiarities of the EEDF behavior are explained in part by specifics of collisional and stochastic electron heating.

8:45

**KR2 4 Ion Energy Distributions vs. Frequency at the RF-biased Electrode in an inductively-Driven Discharge** JOSEPH WOODWORTH, *Sandia National Labs* ION ABRAHAM, *Sandia National Labs* MERLE RILEY, *Sandia National Labs* PAUL MILLER, *Sandia National Labs* We demonstrate the effect of varying the bias frequency on the energy distributions of ions striking an rf-biased electrode in discharges in an inductively-driven Gaseous Electronics Conference Reference cell. The discharge in this cell was formed by an inductive drive operating at 13.56 MHz. Using a mass-and-energy sensitive ion analyzer we examined the ion energy spectra for ions of several masses in discharges containing mixtures of the noble gases Ar, Ne, and Xe. The ions were sampled thru a pinhole in the rf-biased lower electrode. Oscillations of the plasma potential and the rf-bias waveforms on the driven electrode were directly measured to compare to the ion energy spectra. The ion energy distributions (IED), which had a single peak and a width of 3.5 eV (FWHM) when the electrode was not biased, split into double peaked distributions as rf-bias was applied to the electrode. The width of the IED for xenon was reduced by a factor of 2.5 by varying the lower electrode driving frequency from 5 MHz to 22 MHz. The widths of the IEDs for neon and argon were less affected, in rough proportion to the square root of their mass. Sandia is a multiprogram laboratory operated by Sandia Corporation, a Lockheed Martin Company, for the United States Department of Energy under Contract DE-ACO4-94AL85000.

9:00

**KR2 5 Diagnostics and Modeling of an Inductively Coupled Plasma** HARMEET SINGH, JOHN COBURN, MARK KIEHLBAUCH, ALEX GORETSKY, DAVID GRAVES, *University of California at Berkeley* We report an analysis of a shielded, inductively coupled plasma system, with a combination of ion and neutral mass spectrometry, Langmuir probe measurements and a model of the plasma. The system is designed as a testbed for models of plasma chemistry, to allow comparison between model predictions and measurements. The Langmuir probe provides plasma density, plasma potential, and eedf. A molecular beam sampled, appearance potential mass spectrometer is used to measure absolute densities of neutral radical and stable species, gas temperature at the wall, and a separate mass spectrometer is used to measure ion composition. The talk will focus on eedf measure-

ments in molecular gases, fluorocarbon radical measurements in CF<sub>4</sub> plasmas, and the role of plasma-induced neutral gas heating. Eedfs in molecular gases are remarkably similar in shape at gas pressures below about 30 mTorr, and the average electron energy and plasma floating potential rise sharply as pressure is reduced below 3 mTorr. Eedfs are quasi-Maxwellian under these conditions. Measured gas temperature at the wall is over 800K at 3 mTorr in CF<sub>4</sub>. Both a global model and a 2-D, axisymmetric model of the plasma are employed to interpret results.

9:15

**KR2 6 Electron Energy Distributions and Non-Collisional Heating in Magnetically Enhanced Inductively Coupled Plasmas\*** RONALD L. KINDER, MARK J. KUSHNER, *University of Illinois/Urbana-Champaign* Magnetically Enhanced Inductively-Coupled Plasmas (MEICPs) can deposit power in the volume of reactors at locations deeper than the conventional skin depth. Mechanisms for power deposition and electron energy transport in MEICPs have been computationally investigated using a 2-dimensional plasma equipment model. Using a tensor conductivity in solution of Maxwell's equations, 3-d components of the inductively coupled electric field are produced from an  $m = 0$  antenna and 2-d static applied magnetic fields. These fields are used in an electron Monte Carlo Simulation to generate electron energy distributions (EEDs), transport coefficients and electron impact source functions. For MEICPs operating at  $< 10$  s mTorr in Ar and Ar/molecular gas mixtures, significant power deposition occurs downstream when the radial and axial components of the electric field are commensurate to the azimuthal component. For  $B > 100$  G and  $p < 10$  mTorr, the tail of the EED ( $> 20$ -30 eV) is heated in the downstream region. This results from non-collisional heating by the axial electric field for electrons in the tail of the EED having long mean-free-paths while low energy electrons are still somewhat collisional.

\*Work supported by NSF (CTS99-74962), SRC and AFOSR/DARPA.

9:30

**KR2 7 Simulation and experimental measurements of inductively coupled CF<sub>4</sub> and CF<sub>4</sub>/Ar plasmas** D. B. HASH, D. BOSE, M. V. V. S. RAO, B. A. CRUDEN, *Eloret Corporation* M. MEYYAPPAN, S. P. SHARMA, *NASA Ames Research Center* The recently developed code SEMS (semiconductor equipment modeling software) [J. Electrochem. Soc. **146**, 2705 (1999)] is applied to the simulation of CF<sub>4</sub> and CF<sub>4</sub>/Ar inductively coupled plasmas (ICP). This work builds upon the earlier nitrogen, transformer coupled plasma (TCP) SEMS research by demonstrating its accuracy for more complex reactive mixtures, moving closer to the realization of a virtual plasma reactor. Attention is given to the etching of and/or formation of carbonaceous films on the quartz dielectric window and diagnostic apertures. The simulations are validated through comparisons with experimental measurements using FTIR (Fourier Transform Infrared) and UV absorption spectroscopy for CF<sub>x</sub> and SiF<sub>x</sub> neutral radicals, QMS (quadrupole mass spectrometry) for the ions, and Langmuir probe measurements of electron number density and temperature in an ICP GEC reference cell.

## SESSION LR1: ATMOSPHERIC DISCHARGES/ENVIRONMENTAL APPLICATIONS

Thursday morning, 26 October 2000; Grand Ballroom D, Red Lion Hotel at 10:30; Sylvain Coulombe, GE Research and Development, presiding

## Invited Paper

10:30

**LR1 1 Upper Atmospheric Heating, Ionization and Optical Emissions Induced by Lightning Discharges.**UMRAN INAN, *Stanford University*

A number of fascinating luminous optical phenomena occurring at high altitudes above active thunderstorms have recently (past decade) been discovered, including gigantic luminous glows known as sprites, thin-laterally-extended-disk-shaped optical flashes referred to as elves, and gamma-ray flashes. All of these "discharge" phenomena are believed to be driven by intense quasi-static and electromagnetic fields released by lightning discharges. The total available potential between the cloud-tops and the lower ionosphere can sometimes exceed 100 MeV during the few hundred millisecond duration of these intense fields. Understanding these phenomena often requires the complete solution of Boltzmann's equation (in some cases for a relativistic beam) in the presence of a highly collisional weakly ionized plasma. An extensive set of optical and radio measurements have been conducted to quantify the associations between driving electric fields and optically evidenced discharges. A description of recent experimental and theoretical results will be reviewed, identifying outstanding questions and remaining challenges.

## Contributed Papers

11:00

**LR1 2 Lightning Initiation by Laser Radiation in an Atmosphere.\***

OLEG SINKEVICH, DENIS GERAASIMOV, VASILY GLAZKOV, *Moscow Power Eng. Inst. (Technical University)* The development of systems of protection from a discharge of a linear lightning represents important scientific and technical problem. Most promising appears a method of laser lightning protection. Influence of laser radiation on electron avalanche formation is investigated and expression for the dynamics of electron avalanches is presented. The laser beam of sub-critical intensity can nevertheless initiate development of electron avalanche in the channel of a laser beam. In this case laser spark is initiated by development of electron avalanche generated by the laser beam and sustained by an external electrical field. For a case, when the CO<sub>2</sub> laser beam is in parallel to vector of intensity of an external electrical field and intensity of laser radiation and form of a laser beam during development of an avalanche does not depend on time, expression for change of electron concentration in an avalanche is found. >From the expression obtained follows, that the sub-critical laser radiation renders influence on development of an electron avalanche by two ways. First, it changes the ionization rate of atoms by electronic impact. Second, it results in photoionization of the exited atoms, which are formed by electron impact and by absorption of the discharge radiation. The obtained expression describes development of an electron avalanche down to achievement by it of the critical size. If the laser pulse is shorter than time of an avalanche - streamer transition, it further development occurs only under action of an external constant electrical field. The further development of streamers, generated by avalanches results in formation of a spark, named as a long laser spark.

\*This research is supported by the International Science Technical Center (Grant No 880).

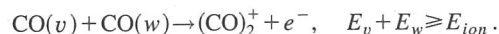
11:15

**LR1 3 High-Pressure Unconditionally Stable Nonequilibrium Molecular Plasmas**

PETER PALM, ELKE PLOENJES, IGOR ADAMOVICH, J. WILLIAM RICH, *Department of Mechanical Engineering, The Ohio State University, 206 West 18th Avenue, Columbus, OH 43210* A novel method of sustaining unconditionally stable, large-volume, high-pressure nonequilibrium plasmas is suggested. The plasma is initiated by resonance absorption of CO laser radiation by carbon monoxide gas mixed with nitrogen and oxygen or nitric oxide in an absorption cell followed by overpopulation of high vibrational levels of CO in vibration-vibration (V-V) energy exchange collisions,



and subsequent ionization by an associative ionization mechanism,



Free electrons produced by associative ionization are heated by a sub-breakdown RF field applied to the optically pumped plasma. The heated electrons lose their energy primarily in collisions with the molecules, thereby vibrationally exciting all molecules. This is followed by overpopulation of high vibrational levels of the molecules by the V-V exchange process and further associative ionization. Unconditional stability is enabled by a negative feedback between gas heating and ionization due to an increase of vibration-translation relaxation rates with temperature leading to rapid depopulation of high vibrational levels needed for associative ionization.

11:30

**LR1 4 Simultaneous Remediation of NO<sub>x</sub> and Oxidation of Soot Using Dielectric Barrier Discharges\***

RAJESH DORAI, MARK J. KUSHNER, *University of Illinois/Urbana-Champaign* KHALED HASSOUNI, *LIMHP, CNRS-UPN, Villetaneuse, France* Plasma remediation of atmospheric pressure gases is being investigated as a means to remove nitrogen oxides (NO<sub>x</sub>) from automobile exhaust. In actual exhausts, unburned hydrocarbons (UHCs) and soot are unavoidably present which impacts the plasma chemistry of NO<sub>x</sub> removal. In this regard, the feasibility of

using a dielectric barrier discharge to simultaneously oxidize soot particles and remove  $\text{NO}_x$  from simulated exhausts has been computationally investigated. The model system is a mixture of  $\text{N}_2/\text{O}_2/\text{CO}_2/\text{H}_2\text{O}$  with ppm levels of  $\text{CO}$ ,  $\text{H}_2$ ,  $\text{NO}$ ,  $\text{C}_3\text{H}_6$ ,  $\text{C}_3\text{H}_8$  and soot particles. The model is a global kinetics simulation modified to account for diffusive transport to and from the soot and reactions on the soot surface. Charging of soot due to electrons and ions is also included. Significant changes in gas-phase  $\text{NO}_x$  chemistry occur when including surface reactions due to reduction of  $\text{NO}_2$  and deactivation of oxidizing radicals generated from the UHCs. Oxidation of the soot particles produces significant increases in  $\text{CO}$ .

\*Work supported by Ford Motor Company and NSF (CTS99-74962).

#### 11:45

**LR1 5 Influence of Ethene on NO Removal in a Homogeneous Pulsed Discharge\*** F. FRESNET, G. BARAVIAN, L. MAGNE, S. PASQUIERS, C. POSTEL, V. PUECH, A. ROUSSEAU, *LPGP, Universit Paris-Sud / CNRS, France* The photo-triggering is a useful technique to achieve high pressure homogeneous discharge in air-like mixtures. It allows effective comparison between time resolved measurements of pollutant density,  $[\text{NO}]$ , after a single shot, and predictions of a kinetic model. The LIF diagnostic at 226 nm has been used to measure  $[\text{NO}]$  during the post-discharge in  $\text{N}_2/\text{NO}$  mixtures, after a 75ns-duration current pulse<sup>1</sup>. Our recent analysis of these results, using a fully self-consistent 0D-discharge model, emphasizes that  $\text{NO}$  is in great part dissociated through collisions with the excited singlet state of molecular nitrogen. At given values of the initial pollutant density and of the deposited electrical energy in the plasma, addition of ethene to the mixture leads to a decrease of the  $\text{NO}$ -destruction efficiency. We conclude on the influence of quenching collisions between  $\text{N}_2$

singlet state and  $\text{C}_2\text{H}_4$ , which gives rise to a decrease of the  $\text{NO}$  dissociation frequency. Good agreement, on  $\text{NO}$  density during the post-discharge, between LIF-measurements and predictions is obtained for a quenching rate equal to  $4.10^{-10}\text{cm}^3\text{s}^{-1}$ , on a wide range of  $\text{C}_2\text{H}_4$ -concentration and deposited energy values.

\*Work in part supported by GIE : PSA Peugeot-Citron / RENAULT, ECODEV-CNRS, and ADEME.

<sup>1</sup>F. Fresnet, G. Baravian, S. Pasquiers, C. Postel, V. Puech, A. Rousseau, M. Rozoy, *J. Phys. D*, 33 (2000) 1315

#### 12:00

**LR1 6 Removal of aqueous organic pollutants via pulsed-corona discharges** D. HAYASHI, G. DOOMS, W.F.L.M. HOEBEN, E.M. VAN VELDHUIZEN, W.R. RUTGERS, G.M.W. KROESEN, *Eindhoven University of Technology* The removal of hazardous organic pollutants from waste water is currently a growing issue in environmental researches. Recently, corona discharges have been intensively studied for the degradation of phenol ( $\text{C}_6\text{H}_5\text{-OH}$ ) in aqueous solutions.<sup>1</sup> We have applied point-to-plate electrode geometry to the production of pulsed-corona discharges for the phenol degradation and verified that pulsed-corona discharges have great advantages in the reduction of aqueous organic pollutants from waste water.<sup>2,3</sup> We here introduce laser induced fluorescence spectroscopy as an *in-situ* diagnostic for phenol and intermediate products in an aqueous solution.<sup>4,5</sup> Temporal variations of the concentrations of phenol and intermediate products are measured during the degradation process. The reaction chemistry of phenol degradation is elucidated. <sup>1</sup> W.F.L.M. Hoeben, PhD thesis, Technische Universiteit Eindhoven, ISBN 90-386-1549-3 (2000), and references therein. <sup>2</sup> W.F.L.M. Hoeben *et al.* *J. Phys. D* 32 L133 (1999). <sup>3</sup> W.F.L.M. Hoeben *et al.* accepted for publication in *Plasma Sources Sci. Technol.* (2000). <sup>4</sup> D. Hayashi *et al.*, *J. Phys. D* 33 (2000). <sup>5</sup> D. Hayashi *et al.*, submitted to *Appl. Opt.*

### SESSION LR2: DIAGNOSTICS I

Thursday morning, 26 October 2000; Grand Ballroom C, Red Lion Hotel at 10:30; G. Hebner, Sandia National Laboratories, presiding

#### Invited Paper

#### 10:30

**LR2 1 Investigations on High-Frequency Gas Discharges by Laser Spectroscopic Electric Field Measurements.** U. CZARNETZKI, *Institut für Laser- und Plasmaphysik, Universität GH Essen, D-45117, Germany*

Electric field distributions play a key role in gas discharge physics. Strong fields are found in the boundary layers in front of electrodes with an applied DC- or RF-potential and grounded structures where the sheath is related to the plasma potential. These sheaths determine the plasma surface interaction, particularly the ion energy distribution at the surface. The field strength is much lower within the plasma bulk. Here the fields drive currents or cause high frequency electron oscillations as in microwave discharges. In addition, local microfields are present even without external fields. These microfields are a measure of the plasma density. The measurement of the electric field distribution can, therefore, enable a very direct access to number of other important parameters like currents, densities, potentials and their temporal development. A number of different laser spectroscopic techniques have been developed for the noninvasive measurement of electric fields in plasmas over the last 15 years. Recently, we have introduced a novel technique in atomic hydrogen which allows the measurement of very low electric fields down to 5 V/cm with high temporal (4 ns) and good spatial resolution (0.1 mm). The laser spectroscopic method probes the Stark-splitting of highly excited Rydberg states (typically  $n=14-20$ , maximum  $n=55$ ) with a three-photon fluorescence-dip technique. This technique has been applied to the investigation of RF- and pulsed DC-discharges in the GEC-cell and microwave discharges in an industrial slit-antenna-reactor (SLAN). All discharges are operated in pure hydrogen. An overview on recent results on the dynamics of collisional RF-sheaths and the field reversal effect, ion dynamics in DC-sheaths, microfields and microwave fields will be presented.

## Contributed Papers

11:00

**LR2 2 Diagnostics of  $C_3$  Radicals in High-Density  $C_4F_8$  Plasmas by Laser-Induced Fluorescence Spectroscopy** K. SASAKI, K. TAKIZAWA, K. KADOTA, *Department of Electronics, Nagoya University, Japan* Spatial and temporal variations of  $C_3$  density in high-density octafluorocyclobutane ( $c-C_4F_8$ ) plasmas were investigated using laser-induced fluorescence (LIF) spectroscopy. Excitation and fluorescence spectra were examined carefully in order to confirm that  $C_3$  radicals were detected by LIF spectroscopy. The  $C_3$  density varied slowly for a long time after the initiation of discharge, suggesting the importance of surface chemistry for the formation of  $C_3$ . Hollow-shaped spatial distributions (the  $C_3$  density adjacent to the chamber wall was higher than that in the plasma column) were observed in the  $C_3$  density. This result indicates that  $C_3$  radicals are produced from fluorocarbon film on the chamber wall and are lost in the plasma column due to electron impact processes. The surface production of  $C_3$  was also observed in the afterglow during 1 ms after the termination of rf power. The decay time constant of the  $C_3$  density in the late ( $> 1$  ms) afterglow, where the surface production of  $C_3$  stopped, was almost independent of discharge parameters, suggesting that the loss of  $C_3$  due to gas-phase reactions is negligible.

11:15

**LR2 3 PLIF Investigation of  $CF_2$  in Fluorocarbon Etching Plasmas with and without Si Wafers** KRISTEN L. STEFFENS, MARK A. SOBOLEWSKI, *National Institute of Standards and Technology* In semiconductor processing of silicon wafers, fluorocarbon plasmas are widely used for etching, which involves a competition between substrate removal and deposition of a fluorocarbon polymer layer on the wafer surface. Although the mechanisms are not fully understood, the  $CF_2$  radical is recognized as a major participant in the formation of this polymer layer. Thus, measurements of the  $CF_2$  radical are crucial to the understanding of etching plasmas. In this work, planar laser-induced fluorescence (PLIF) was used to measure 2-D images of  $CF_2$  density in  $CF_4$  and  $C_2F_6$  plasmas in the capacitively-coupled Gaseous Electronics Conference rf Reference Cell at powers from 30 to 150 W, without a substrate and with a Si wafer present, in pure fluorocarbon and in oxygen/fluorocarbon mixtures. We also obtained broadband emission images and measurements of the rf current and voltage at the electrodes. The spatial distribution of  $CF_2$  density depended on substrate material and on plasma power. In addition,  $CF_2$  density increased with the Si wafer present, and decreased with the addition of  $O_2$ . The results of this study will help to elucidate the role of  $CF_2$  in fluorocarbon plasmas and to provide data for validation of plasma simulations.

11:30

**LR2 4 Transport of particles in plasma expansion: a laser spectroscopic study** STÉPHANE MAZOUFFRE, *Eindhoven University of Technology, Dpt of Physics, PO Box 513, 5600 MB Eindhoven, The Netherlands* MAARTEN BOOGAARTS, RICHARD ENGELN, DANIEL SCHRAM, *Eindhoven University of Technology, Dpt of Physics, PO Box 513, 5600 MB Eindhoven, The Netherlands* Plasma expansion from a high pressure source into a low pressure domain is a very general physical problem that covers a broad range of phenomena. On large scale, it concerns astrophysical objects; on intermediate scale, plasma outflow into the divertor region of Tokamak and remote plasma system; on small scale, laser induced plasmas and vacuum arc spots. Apart

from the large differences in size those phenomena exhibit numerous similarities. As it is advantageous to study the physics of expanding plasmas on the intermediate scale as then the system is well suited for diagnostics, in this contribution the expansion of a cascaded arc generated thermal plasma into a low pressure background serves as an example. A combination of various laser-based diagnostic techniques (Thomson-Rayleigh scattering, LIF, TALIF, CARS) has been used to study in details the physics of plasma expansion, i.e. the transport mechanisms of mass and energy.

11:45

**LR2 5 Optical Tomography of the ICP-GEC RF Reference Cell** ERIC BENCK, *National Institute of Standards and Technology* KASRA ETEMADI, *State University of New York at Buffalo* Determining a plasma distributions from optical emission measurements is complicated by the fact that each measurement is actually equal to the plasma emissivity integrated along the line-of-sight through the plasma. In order to determine the actual 2D plasma distribution, measurements need to be obtained from many different positions and angles and then inverted with a tomographic inversion program. In order to efficiently obtain the necessary optical emission measurements, a fiber optic based optical tomography sensor has been developed for measuring plasma uniformity in plasma chambers with limited optical access. This sensor has been used to characterize the plasma distributions within the inductively coupled version of the GEC RF Reference Cell. The distributions for a variety of different feed gases and plasma conditions have been investigated. In addition, the influence of the electrostatic shield, quartz confinement ring, and different coil powering arrangements have also been studied. Initial time-resolved measurements from a pulsed ICP plasma will also be presented. The calculated distributions from two different types of tomographic inversion programs will be compared.

12:00

**LR2 6 Thomson scattering in fluorescent lamps** LEON BAKER, GERRIT KROESEN, *Eindhoven University of Technology* Performing Thomson scattering in low-density plasmas is experimentally extremely difficult. This is due to the very low cross section in combination with the low density of scattering particles. The use of state of the art lasers and detectors solve the low intensity problem. However, the problem of stray light remains. In order to solve this problem, we use a sodium absorption cell that absorbs the stray light in the detection branch. The main challenge is to find a laser with a sufficient spectral purity that can produce photons with a wavelength corresponding to one of the resonant transitions of the sodium atom. We use a dye laser with a specially developed Amplified Spontaneous Emission filter. This filter consists of twenty dispersion prisms and two spatial filters. We will present the results we obtained with this Thomson scattering set up. One of the results is the electron density and the electron temperature in an argon mercury positive column. Because of the efficient stray light reduction, this is the first time that performing Thomson scattering is possible in such a discharge.

**SESSION MR1: LOW PRESSURE LAMPS AND DISCHARGES**

Thursday afternoon, 26 October 2000

Grand Ballroom D, Red Lion Hotel at 13:30

Bob Piejak, Osram Sylvania Research and Development, presiding

*Contributed Papers*

13:30

**MR1 1 Determination of Radiated Power and Excited-State Populations in a Highly-Loaded Hg-Ar Discharge\*** J. J. CURRY, J. E. LAWLER, *Department of Physics, University of Wisconsin* G. G. LISTER, *OSRAM SYLVANIA, INC., Beverly, Massachusetts* The absolute population densities of the Hg  $6^1P_1$  and  $6^3P_1$  resonance levels and the  $6^3P_0$  and  $6^3P_2$  metastable levels have been determined in a low-pressure Hg-Ar discharge operated at high current densities. Power radiated on the 254nm and 185nm Hg resonance lines as a fraction of input power to the positive column has been determined by combining measured resonance level populations with realistic Monte Carlo simulations of radiation transport. Measurements were obtained over a range of current densities from approximately  $0.05A\text{ cm}^{-2}$  to approximately  $0.6A\text{ cm}^{-2}$ . The discharge is inductively-coupled with a radius of 2.5 cm and an Ar buffer gas pressure of 300 mTorr. Resonance level populations have been measured using high sensitivity absorption spectroscopy. The Monte Carlo simulations of radiation transport<sup>1</sup> employed fully realistic lineshapes including the complete hyperfine and isotopic structure and the effects of partial frequency redistribution.

\*Supported by the Electric Power Research Institute and OSRAM SYLVANIA, INC.

<sup>1</sup>Lawler, Curry, and Lister, *J. Phys. D: Appl. Phys.* **33**, 252 (2000); Meningen and Lawler, *J. Appl. Phys.*, (2000).

13:45

**MR1 2 Modeling the Power Balance of Electrodeless Fluorescent Lamps\*** GRAEME G. LISTER, *OSRAM SYLVANIA INC., Beverly, Massachusetts* J. J. CURRY, *Department of Physics, University of Wisconsin* J. E. LAWLER, *Department of Physics, University of Wisconsin* Electrodeless fluorescent lamps often operate under conditions of higher current density than conventional fluorescent lamps. Calculations using numerical models for highly loaded lamps have tended to overestimate radiation output, and consequently the maintenance electric field in these discharges [1]. It is therefore important to understand the power balance in these discharges in terms of the important collisional and radiative processes. Results of a numerical model are presented and compared to those obtained from absorption spectroscopy [2] and Langmuir probe measurements [3]. The experiments were performed in an inductively coupled Hg-Ar discharge with cylindrical section of radius of 2.5 cm and Ar buffer gas pressure of 300 mTorr. The model includes a revised description of the radiation transport of resonance lines, including the effects of foreign gas broadening and mercury depletion on axis, together with updated cross sections for relevant atomic processes. The sensitivity of these results to the accuracy of the available fundamental data will also be discussed. [1] G.G. Lister, in H. Schlter and A. Shivarova, Editors,

Advanced Technologies Based on Wave and Beam Generated Plasmas, NATO ASI Series; Plenum (1999), p65 [2] J J Curry, J E Lawler and G G Lister, this conference [3] R Piejak, B Alexandrovich and V Godyak, in preparation

\*Reserach performed as participants in the EPRI/ALITE Program

14:00

**MR1 3 Axial mercury vapor pressure distributions in DC operated low pressure mercuryargon discharges** JOHN GIELEN, SIMON DE GROOT, *Philips Lighting, Central Development Lamps, PO Box 80020, 5600 JM Eindhoven, The Netherlands* JAN VAN DIJK, JOOST VAN DER MULLEN, *Eindhoven University of Technology, Physics Dept., PO Box 513, 5600 MB Eindhoven* In a steady state DC operated (cylindrical) low pressure mercuryargon discharge, an electric field exists in axial direction which results in a non-uniform axial mercury vapor pressure distribution; this phenomenon is termed cataphoresis. In a discharge tube covered with a fluorescent powder this gives in a non-uniform axial light distribution. Towards lighting applications this is a potential disadvantage, which is not present in AC operated fluorescent lamps. The dependence of the axial mercury vapor pressure distribution under DC operation on discharge tube and discharge parameters has been investigated. A model has been developed to predict the axial mercury vapor pressure distribution, in which the balance equations for particle and momentum conservation are solved in combination with a plasma physical model, and experiments have been performed to validate the model. In the present contribution the model and experimental results will be discussed and it will be demonstrated that the applied theoretical approach provides a better description of the axial mercury vapor pressure distribution compared to previous models known from literature.

14:15

**MR1 4 Numerical Predictions of Radiation Production by Low-Pressure Ba Discharges\*** J. J. CURRY, *Department of Physics, University of Wisconsin* G. G. LISTER, *OSRAM SYLVANIA, INC., Beverly, Massachusetts* J. E. LAWLER, *Department of Physics, University of Wisconsin* A one-dimensional fluid model of the positive column is used to explore characteristics of low-pressure Ba discharges<sup>1</sup>. Of particular interest are attributes that would make low-pressure Ba discharges useful for lighting applications. The model consists of a global power balance and particle balances for a large number of excited states of both neutral and singly-ionized Ba. (Ba ions have been shown to contribute a significant fraction of the visible radiation under some operating conditions<sup>2</sup>.) Not all of the potentially important cross-sections are known, and not all of the measured or calculated cross-sections are known with a high degree of confidence. However, the results of the model are useful for indicating the major trends in low-pressure Ba discharges, including radiation production, and for providing strong incentive for continued experimental work.

\*Work at the University of Wisconsin funded by the National Science Foundation.

<sup>1</sup>G. G. Lister, J. J. Curry, and J. E. Lawler, to be published in *Phys. Rev. E* (2000)

<sup>2</sup>J. J. Curry, H. M. Anderson, J. MacDonagh-Dumler, and J. E. Lawler, *J. Appl. Phys.* **87**, 2058 (2000)

14:30

**MR1 5 Electron Kinetics and Self-Consistent Modeling of High Current Positive Column Plasmas** UWE KORTSHAGEN, *University of Minnesota, Minneapolis, MN* J. DARRYL MICHAEL, *General Electric Corp. R&D, Niskayuna, NY* JOHN H. INGOLD, *Bratenahl Physics, Cleveland, OH* We present results of a recently developed self-consistent plasma model for high-current positive column plasmas. The model solves the Boltzmann equation in the two-term approximation accounting for the radial plasma nonuniformity. Coulomb collisions are included by using a well-known Fokker-Planck operator. Our Boltzmann solver is based on a control volume approach. The resulting system of equations is solved using a relaxation method. The ambipolar space charge potential is determined from the Poisson equation. For a given electron density as input parameter, we self-consistently determine the axial electric field strength such that the ionization-wall loss balance for the column is fulfilled. This work was supported in part by NSF (grant ECS-9713137), DOE (grant ER54554), the University of Minnesota Supercomputing Institute, and General Electric.

14:45

**MR1 6 A Nonlocal Moment Model for the Low Pressure Positive Column** VIKAS MIDHA, *General Electric Corp. R&D, Niskayuna, NY 12309* J. DARRYL MICHAEL, *General Electric Corp. R&D, Niskayuna, NY 12309* JOHN H. INGOLD, *Bratenahl Physics, Cleveland, OH 44108* A time-dependent, 1D radial model based on the nonlocal moment equations for a low pressure positive column discharge is described. This model allows investigation of transient effects in the discharge and also eliminates the need for matching boundary conditions at the wall of the positive column by the shooting technique [1]. Positive column discharges of neon- and argon-like gases are chosen for illustration. The model is used to capture the transition from the local to the non-local regime as a function of PR (positive column pressure times radius). Similarly, the effect of electron-electron collisions on the departure from field equilibrium is investigated for various degrees of fractional ionization [2]. Results of the nonlocal moment method are benchmarked by comparison with experiments and corresponding solutions of the 1D Boltzmann equation including electron-electron collisions [3]. [1]J. H. Ingold, *Phys. Rev. E* **56**, 5932 (1997). [2]J. D. Michael and J. H. Ingold, *Bull. Am. Phys. Soc.* **44**, 17 (1999). [3]C. Busch and U. Kortshagen, *Phys. Rev. E* **51**, 280 (1995).

15:00

**MR1 7 Comparison of Experiments and Self-Consistent Monte Carlo Simulations of Helium Positive Column Discharges\*** J. E. LAWLER, *Univ. of Wisconsin-Madison* U. KORTSHAGEN, *Univ. of Minnesota-Minneapolis* Techniques have been recently developed to produce fully Self-Consistent Monte Carlo Simulations of positive column discharges using modest computers [*J. Phys. D: Appl. Phys.* **32**, 3188 (1999)]. Although the primary motivation for the work was to generate benchmark simulations for comparison to other more efficient types of simulations, it is also interesting to compare some of these very detailed Monte Carlo simulations with experimental results. For such comparisons helium is preferred because it has better known cross sections than any other gas. Our initial comparisons emphasize small radius-gas

density products for which single step ionization is dominant. We explore low currents where the discharge has a non-negligible Debye length and a substantial negative dynamic resistance. The simulations reproduce the experimental voltage and negative dynamic resistance within a few percent.

\*Supported by NSF ECS-9710234

15:15

**MR1 8 A Radiation Transport Coupled Particle-In-Cell Model for Hg-Ar Discharges** HAE JUNE LEE, J.P. VERBONCOEUR, H.B. SMITH, G.J. PARKER, C.K. BIRDSALL, *University of California at Berkeley* PLASMA THEORY AND SIMULATION GROUP TEAM We simulate a radial slice of the fluorescent lamp discharge in the positive column with a radiation transport coupled particle-in-cell (RT-PIC) code. In this model, the radiative and meta stable excited states of Hg-Ar mixture and their collisions as well as radiation transport are simulated by the fluid equations. The motions of electrons and ions and collisions with neutral or excited states are simulated by the conventional particle-in-cell method. We consider radiation transport of excited states using the Holstein equation[1] including the time varying nonuniform background gas density. The background gas density is calculated from the temperature profile by solving the heat transfer equation. The motion of charged particles are simulated by using the 1-D cylindrical particle-in-cell code, XPDC1[2]. Separate time scales are used for the charged particles, the excited states, and the neutral gas, respectively, and parallel processing can be used for the expensive calculation including radiation transport. This work was supported in part by General Electric Company contract GE-20000181. [1] T. Holstein, *Phys. Rev.* **72**, 1213 (1947). [2] J. P. Verboncoeur, M. V. Alves, V. Vahedi, and C. K. Birdsall, *Journal of Computational Physics* **104**(2), 321, (1993).

15:30

**MR1 9 Ionization Waves and Virtual Anode Propagation in a Fast Capillary Discharge** IGOR RUTKEVICH, *Department of Mechanical Engineering, Ben-Gurion University, Beer-Sheva, Israel* MICHAEL MOND, *Department of Mechanical Engineering, Ben-Gurion University, Beer-Sheva, Israel* YITZHAK KAUFMAN, *Department of Mechanical Engineering, Ben-Gurion University, Beer-Sheva, Israel* PETER CHOI, *Ecole Polytechnique, Palaiseau 91128, France* MARIO FAVRE, *Facultad de Fisica, Pontificia Universidad Catolica de Chile* The propagation of ionization waves (IW) in a hollow-cathode assisted, shielded, fast capillary discharge intended for a soft x-ray emission is investigated in the range of high values of the electric field to gas pressure ratio. In this range, a beam-like electron distribution function is employed for calculating the ionization source and for deriving the electron momentum equation. A system of quasi-one-dimensional macroscopic equations for the on-axis distributions of the plasma parameters and the electric field is obtained, that takes into account the radial electric field. Steady-state numerical calculations for argon filled capillary, demonstrate a new type of cathode-directed IW propagating in an opposite direction to the ionizing electron beam and transferring the virtual anode potential to the cathode hole. The wave velocity has been found to be an increasing function of the gas pressure. This result is in reasonable agreement with the experimentally observed behavior of the time delay for the electric breakdown.



## SESSION MR2: ETCHING/DEPOSITION

Thursday afternoon, 26 October 2000; Grand Ballroom C, Red Lion Hotel at 13:30; K. Nanbu, Tohoku University, presiding

## Invited Paper

13:30

**MR2 1 Electron Collisions with Fluorocarbons and Hydrofluorocarbons.\***CARL WINSTEAD, *California Institute of Technology*<sup>†</sup>

Plasma processing of semiconductors, in particular plasma etching, relies on a variety of fluorocarbon and hydrofluorocarbon feed gases. Inelastic collisions between electrons and gas molecules are a principal mechanism of fragmentation and ionization giving rise to reactive species, while elastic electron-molecule collisions determine electron transport properties. A thorough understanding of plasma behavior thus depends on knowledge of the relevant electron-molecule collision cross sections. However, such cross sections are difficult to measure and are often unknown for the molecules of interest. Over the past several years, we have been using the Schwinger Multichannel method, a first-principles variational formulation, to calculate cross sections for numerous  $C_xF_y$  and  $C_xH_yF_z$  species, including not only feed gases such as  $C_2HF_5$  and  $c-C_4F_8$  but also radicals that may be formed within the plasma such as CHF and  $CF_2$ . In this talk, I will give an overview of these calculations and examples of the results we have obtained. Similarities and differences among the cross sections of related molecules will be discussed, and comparison will be made with experimental data and other calculations where possible.

\*Work supported by Sematech, Inc., the Department of Energy, and Intel Corp.

<sup>†</sup>Work done in collaboration with Vincent McKoy, Márcio H. F. Bettega, and Chuo-Han Lee

## Contributed Papers

14:00

**MR2 2 Elastic electron scattering from  $C_6H_6$  and  $C_6F_6$**  R J GULLEY, H CHO, L J UHLMANN, S J BUCKMAN, *Australian National University* K SUNOHARA, M KITAJIMA, H TANAKA, *Sofia University, Japan* We report absolute differential cross section measurements for vibrationally elastic electron scattering from benzene ( $C_6H_6$ ) and hexafluorobenzene ( $C_6F_6$ ). The measurements have been performed in our two laboratories on different crossed-beam apparatuses for scattering angles between  $10^\circ$  and  $130^\circ$  -  $C_6H_6$  at the Australian National University in the energy range from 1.1 to 40 eV, and  $C_6F_6$  at Sofia University in the energy range from 1.5 to 100 eV. The cross sections are characterised by strong forward-angle scattering due to the large dipole polarizabilities of the molecules and large-angle oscillations due to the effect of shape resonances. The cross sections for  $C_6H_6$  are favourably compared with recent calculations, including one incorporating an exact static exchange plus correlation-polarization potential and one employing the Schwinger variational technique. To our knowledge, there are no other experimental or theoretical results available in the literature for comparison with our  $C_6F_6$  cross sections.

14:15

**MR2 3 Plasma Chemistry Study in an Inductively Coupled Dielectric Etcher** CHUNSHI CUI, KEN COLLINS, JOHN TROW, STEVE SHANNON, *Applied Materials, Inc., 974 E. Arques Ave., Sunnyvale, CA 94086, USA* Precise control of the plasma chemistry in dielectric etch is necessary. We present a study of a  $C_4F_8$  based plasma in an inductively coupled plasma (ICP)  $SiO_2$  etcher. Molecular species are measured using energy selective ion mass spectrometry (IMS) and optical emission spec-

troscopy (OES); plasma characteristics are measured by Langmuir probe. OES spectra are characterized by strong C2 emission (as was previously reported<sup>1</sup>), indicating that C rich polymers are formed on the walls. For all cases investigated the IMS data show mostly  $CF^+$  with lesser amounts of heavier  $CyFx$  ions, indicating a high degree of dissociation. Although the species mix can be varied somewhat by changing the process parameters, the high degree of dissociation still remains. This is believed to cause the poor selectivity and the small process window in commercially available ICP tools. Ongoing studies are comparing various plasma sources including MERIE and new concepts.

<sup>1</sup>K. Guinn et al., *J. Vac. Sci. Tech. A* 14(3), June 1996, 1137-1141.

14:30

**MR2 4 IMPACT OF DIFFERENT LEVELS OF DETAIL IN ATOMIC METAL PLASMA CHEMISTRY ON MULTIDIMENSIONAL PLASMA EQUIPMENT MODELS** P.L.G. VENTZEK, *Motorola Inc.* S. RAUF, *Motorola Inc.* V. ARUNACHALAM, *Motorola Inc.* A. ELETSKII, *Soft-Tec* A. AS-TAPENKO, *Soft-Tec* M. GOLUBKOV, *Soft-Tec* V. GOLUBKOV, *Soft-Tec* V. KUDRYA, *Soft-Tec* The metric of goodness for a plasma chemistry model for a high-density metal plasma that one would use for metal deposition is how accurately it permits the flux of different charged and neutral species incident into a structure to be estimated for given process conditions. While electron impact cross-sections are not the only variables that impact this metric, they are often the weaker part of a model, especially for low-pressure high density systems. Further, the number of states one must consider for heavier metals atoms is large and the impact processes for those states a matter that compounds the difficulty of constructing an adequate plasma chemistry model. We have developed plasma chemistry models for a number of metals and also

have developed a formalism for the compression of the cross-section sets into pieces that are manageable for multi-dimensional plasma source models. We will describe it in the presentation using Mg and a heavy metal as examples in an IPVD simulation. How one groups or chooses to not consider certain cross-sections is shown to lead to factors of two or more differences in plasma parameters crucial to estimating fill parameters in features.

14:45

**MR2 5 Loss Kinetics of Carbon Atoms in Diamond Deposition Employing Low-Pressure Inductively Coupled Plasma** HARUHIKO ITO, *Nagoya Municipal Industrial Research Institute, JAPAN* KUNGEN TEII, HIKARU FUNAKOSHI, MASARU HORI, TOSHIO GOTO, *Nagoya University, JAPAN* MASAFUMI ITO, *Wakayama University, JAPAN* TAKASHI TEKEO, *Nagoya Municipal Industrial Research Institute, JAPAN* Nanocrystalline diamond has been successfully synthesized in low-pressure CO/H<sub>2</sub>/CH<sub>4</sub> inductively coupled plasmas (ICPs) in our previous study. For a better understanding of the mechanism of diamond film deposition, vacuum ultraviolet absorption spectroscopy with a carbon hollow cathode lamp was applied to the measurement of decay rate of C-atom and was employed to determine the diffusion constant in the afterglow of low-pressure CO and CO/H<sub>2</sub> ICPs. The transition line used for the measurement was  $2p3s\ ^3P_2-2p^2\ ^3P_2$  at 165.7 nm for measurement. The dependence of the decay rate of C-atoms density on pressure revealed that C-atoms were dominantly lost at the surface rather than in gas phase in both CO and CO/H<sub>2</sub> plasmas. However, in the case of CO/H<sub>2</sub> plasma at higher pressures over 6 Pa, C-atoms were lost in the gas phase reaction as well as at the surface. The diffusion constants of C-atom in both CO and CO/H<sub>2</sub> plasmas were estimated to be  $3.1 \times 10^4\ \text{cm}^2\text{Pas}^{-1}$  and  $3.7 \times 10^4\ \text{cm}^2\text{Pas}^{-1}$ , respectively. These values are higher than that of the reported diffusion constant ( $8.7 \times 10^3\ \text{cm}^2\text{Pas}^{-1}$ ) of CF<sub>2</sub> in DC pulsed CF<sub>4</sub> discharge plasma. The loss kinetics of C-atoms in plasmas are also discussed.

15:00

**MR2 6 Numerical Model of Plasma Enhanced CVD for SiC in a Novel Two Stage RF Reactor** GEORGE PETROV, *Berkeley Research Associates, Inc., Springfield, VA, 22150* JOHN GIULIANI, *Plasma Physics Division, Naval Research Laboratory, Washington, DC, 20375* Chemical Vapor Deposition (CVD) is one method of growing Silicon Carbide (SiC) films. In the simplest system, the precursor gases, silane and propane diluted in H<sub>2</sub>, flow at atmospheric pressure over a graphite susceptor which is heated by a low frequency RF powered coil. However, the high temperature and pressure near the growth surface in this configuration has been found to cause defects. An alternative approach is plasma enhanced CVD. This work presents a two stage RF reactor wherein an second high frequency (MHz) powered coil is used to form a plasma upstream of the susceptor. Plasma heating dissociates the silane and propane under non-equilibrium conditions away from the growth surface while the gas flow carries the plasma products over the growth substrate. We have developed a 1-D flow code to investigate the proposed design. The model treats the inductive coupling as a volumetric power deposition and follows the plasma chemistry for silane, propane, and H<sub>2</sub> into 40

species with 200 reactions. Also an isothermal deposition model is developed to estimate growth rates. It is found that while silane readily dissociates, the breakup of propane occurs at gas temperatures of 1600K in the plasma region. Pressures between 1-10 Torr can provide a typical growth flux of  $10^{15}\ \text{cm}^2/\text{sec}$ . The required power for these conditions is 300 W/cm. The ion density over the susceptor rapidly decreases away from the plasma, while the flux of potential growth species remain nearly constant. For the 5 cm radius design, the optimum conditions predict a growth rate of 2 microns/hr at 500 sccm flow rate and 3 Torr pressure.

15:15

**MR2 7 Inside Sputter Coating of Narrow Tubes by Mirror Type Electron Cyclotron Resonance Plasmas** HIROSHI FUJIYAMA, *Faculty of Engineering, Nagasaki University* In order to coat thin films onto the inner surface of long and narrow tubes with high aspect ratios in length to inner diameter, we have developed a coaxial electron cyclotron resonance (CECR) plasma reactor with 20 solenoid coils. Mirror-type magnetic field was formed by switching on two coils. By using such a mirror-type magnetic field, we have succeeded in low pressure discharge, high deposition rate and good uniformity of axial distribution of deposition rate in metallic tubes. CECR plasmas, it was found that the electric field of microwave in insulated tube was increased, and the discharge for low pressure and low microwave incident power was realized by inserting insulated tube into metallic tube. The titanium films have been successfully coated on the inner wall of glass tube of 27mm in inner diameter and 2m length by scanning mirror-type ECR magnetic field. The present inner coating system was applied to reactive sputter deposition of TiN films, and the trial deposition was successfully performed by TiN inner coating of metallic tube of 30mm in inner diameter and 2m in length. The CECR plasmas could be also generated in ferromagnetic metallic tubes.

15:30

**MR2 8 Particle Nucleation in Silane Plasmas** UPENDRA BHANDARKAR, UWE KORTSHAGEN, STEVEN L GIRSHICK, *University of Minnesota, Mechanical Engineering* MARK T SWIHART, *University at Buffalo (SUNY)* As a first step in modeling particle generation in PECVD plasmas, we have developed a plasma chemistry model for particle nucleation in silane. Thermochemical properties of various silicon hydrides with upto ten silicon atoms were calculated using group additivity rules. Electron Affinity data were calculated using extensive density functional theory calculations. Reactions and corresponding rate coefficients were defined based on known reactions between smaller silicon hydride clusters. Calculations were performed using a code which accounted for plasma quasineutrality and the self-consistent determination of the electron temperature. Clustering was found to proceed mainly via anion-neutral reactions. Two reaction chains which involve silyl and silylene anions reacting with silane (SiH<sub>4</sub>) were found to be the predominant cluster formation pathways. This work was supported by NSF (grant ECS 9731568) and the Minnesota Supercomputer Institute.

**SESSION NR1: LAB TOURS**

Thursday afternoon, 26 October 2000; University of Houston at 16:00

**SESSION NR2: NEW MATERIALS/DUSTY PLASMAS**

Thursday afternoon, 26 October 2000; Grand Ballroom C, Red Lion Hotel at 16:00; Uwe Kortshagen, University of Minnesota, presiding

*Invited Papers***16:00****NR2 1 Carbon Nanotube based Nanotechnology.**M. MEYYAPPAN, *NASA Ames Research Center, Moffett Field, CA*

Carbon nanotube(CNT) was discovered in the early 1990s and is an off-spring of C60(the fullerene or buckyball). CNT, depending on chirality and diameter, can be metallic or semiconductor and thus allows formation of metal-semiconductor and semiconductor-semiconductor junctions. CNT exhibits extraordinary electrical and mechanical properties and offers remarkable potential for revolutionary applications in electronics devices, computing and data storage technology, sensors, composites, storage of hydrogen or lithium for battery development, nanoelectromechanical systems(NEMS), and as tip in scanning probe microscopy(SPM) for imaging and nanolithography. Thus the CNT synthesis, characterization and applications touch upon all disciplines of science and engineering. A common growth method now is based on CVD though surface catalysis is key to synthesis, in contrast to many CVD applications common in microelectronics. A plasma based variation is gaining some attention. This talk will provide an overview of CNT properties, growth methods, applications, and research challenges and opportunities ahead.

**16:30****NR2 2 Effective Arc-Production of Fullerenes by Controlling Gravity and Magnetic Field.**TETSU MIENO, *Dept. Physics, Shizuoka Univ.*

By using an arc discharge in helium gas atmosphere, fullerenes and nano-tubes are produced, where sublimated carbon atoms from an anode collide each other and they self-organize new carbon molecules. This process occurs only in high temperature gas (2000-4000 K). In usual discharge on the ground, there is a strong heat convection (more than 1 m/s), which cools the reaction gas. If the heat convection is suppressed, motion of carbon molecules is governed by thermal diffusion in collisional system and large carbon molecules can remain in hot plasma region for longer time. This would enable the efficient production of giant fullerenes and endohedral metallo-fullerenes. In order to confirm this gravity effect, a vertical-swing-tower 12 m high was constructed, by which an arc reactor was swung vertically. The discharge current is synchronous modulated with gravity modulation and integrated long gravity-free time (13 min) is obtained. By using this tower, fullerenes are produced. By analyzing produced soot, it is found that production rate of metallo-fullerenes La@C82, in gravitation-free condition is about 14 times larger than that in the steady state condition. [1] A new JxB arc method has also been developed. [1] T. Mieno, *Jpn. J. Appl. Phys.* 37 (1998) L761.

**17:00****NR2 3 Liquid and Crystalline Plasmas.**G. E. MORFILL, *Max-Planck-Institute for extraterrestrial physic, 85741 Garching, Germany*

It has been shown that under certain conditions "complex plasmas" (plasma containing ions, electrons and charged microspheres) may undergo spontaneous phase changes to become liquid and crystalline, without recombination of the charge components. Hence these systems may be regarded as new plasma states - "condensed plasmas." The ordering forces are mainly electrostatic, but dipolar effects, anisotropic pressure due shielding, ion flow focussing etc. may all play a role, too. Complex plasmas are of great interest from a fundamental research point of view because the individual particles of one plasma component (the charged microspheres) can be visualised and hence the plasma can be studied at the kinetic level. Also, the relevant time scales (e.g.  $1/\text{plasma frequency}$ ) are of order 0.1 sec, the plasma processes occur practically in "slow motion." Technologically, it is expected that colloidal plasmas will also become very important, because both plasma technology and colloid technology are widely developed already. In this overview first the basic forces between the particles are discussed, then the phase transitions, the lattice structures and finally results from active experiments will be presented, including wave propagation and the observation of Mach cones in plasma crystals.

*Contributed Papers*

17:30

**NR2 4 Laser-excited pulses in a crystallized dusty plasma\*** V NOSENKO, S NUNOMURA,<sup>†</sup>J GOREE, *Dept. of Physics and Astronomy, The Univ. of Iowa* A dusty plasma is an ionized gas containing small particles of solid matter. These particles acquire a large negative electric charge. Polymer microspheres were shaken into a capacitively-coupled parallel-plate rf plasma. The particles were levitated by the electric field in the sheath above the lower electrode. The particles settled in a single horizontal layer, arranged in a hexagonal lattice. They were imaged using a video camera, to record the particle motion. Like any crystal, this so-called "plasma crystal" sustains compressional sound waves, which can be launched as a pulse. There are several ways these waves can be excited, including applying a force from the radiation pressure of a laser beam. By chopping an argon laser beam that is directed at the lattice, it is possible to launch a pulsed wave in the lattice. We evaluate the pulse's shape and propagation speed, and test whether it has the properties of a shock.

\*Work was supported by NASA and NSF

<sup>†</sup>Supported by the Japan Society for the Promotion of Science

17:45

**NR2 5 Spatial profile of dust particles near RF powered electrode** YASUNORI OHTSU, HARUMICHI ODA, HIROHARU FUJITA, *Department of Electrical and Electronic Engineering, Saga University, 1 Honjo-machi, Saga 840-8502, Japan* FUJITA LAB. TEAM Few experimental studies of relation between dust particle and plasma parameters have been done in dust plasma. In this work, we present spatial profile of particle near the powered RF electrode in capacitively coupled RF plasma, which is used widely as plasma source and have investigated suspending mechanism of particles in plasma. Spatial profile of particles near a RF electrode was observed in capacitively coupled RF plasma by means of a laser light scattering method. Here, the diameter of the various particles emitted by speaker was in the range of 0.01- 1  $\mu\text{m}$  and the plasma was produced at  $p=1\text{Torr}$  of the He gas. It was found that profile of particles near the RF electrode became void structure, localizing at an edge region of electrode. The suspending mechanism of particles was explained from radial concave profile of plasma potential, which was measured by Langmuir probe technique.

**SESSION OR1: BANQUET**

Thursday afternoon, 26 October 2000; Grand Ballroom, Red Lion Hotel at 19:30

**SESSION PF1: DISCHARGE KINETICS**

Friday morning, 27 October 2000

Grand Ballroom D, Red Lion Hotel at 8:00

William Lowell Morgan, Kinema Research and Software, presiding

**Contributed Papers****8:00**

**PF1 1 Reactions of sulfur fluorides and benzenes in a low temperature plasma** PETER KLAMPFER, *Institute Jožef Stefan, Ljubljana, Slovenia* TOMAZ SKAPIN, *Institute Jožef Stefan, Ljubljana, Slovenia* BOGDAN KRALJ, *Institute Jožef Stefan, Ljubljana, Slovenia* DUŠAN ŽIGON, *Institute Jožef Stefan, Ljubljana, Slovenia* ADOLF JESIH, *Institute Jožef Stefan, Ljubljana, Slovenia* The introduction of pentafluorosulfanyl, SF<sub>5</sub>, group into molecules can substantially change their physical, chemical and biological properties, making them potentially useful for a number of applications: high temperature and oxidation resistant materials, blood substitutes, energetic materials and surface-active agents. With the aim to determine possible formation of pentafluorosulfanylbenzenes, C<sub>6</sub>H<sub>5</sub>SF<sub>5</sub>, in plasma, the gases SF<sub>6</sub>, CF<sub>3</sub>SF<sub>5</sub> and ClSF<sub>5</sub> were allowed to react with benzene, chlorobenzene and bromobenzene in an inductively coupled radio-frequency discharge. Reaction products were collected in a cold trap held at 77 K and subsequently analysed by combined GC-MS and GC-FTIR spectroscopy. The main reaction products were different halogenated benzenes along with sulfides, disulfides and biphenyl. The pentafluorosulfanylbenzene was produced in all reactions in very small quantities, which amounted to less than 1 % of all reaction products in favorable cases.

**8:15**

**PF1 2 Investigation of Hydrogen Atom on Hydrogen Atom Excitation and Ionization by Numerical Solution of the Time-Dependent Schrodinger Equation** MERLE RILEY, *Sandia National Laboratories, Albuquerque, NM 87185* BURKE RITCHIE, *Lawrence Livermore National Laboratory, Livermore, CA 94550* Hydrogen atom - hydrogen atom scattering is a prototype for many of the fundamental principles of atomic collisions. In this work we present a self-consistent-field description of the H+H system for scattering in the intermediate energy regime of 1 to 100 keV. We allow for the evolution of the electrons by numerically solving a 3D self-consistent Schroedinger equation for each electron orbital by the Implicit Split Operator Procedure (ISOP)<sup>1</sup>. The results capture many features of the problem and are in harmony with recent theoretical studies. Excitation and ionization cross sections are computed and compared to other theory and experiment. New insight into the importance of exchange for excitation and ionization is inferred from the solutions. Difficulties in computing accurate results for certain inelastic processes during slow collisions will be discussed.

<sup>1</sup>M. E. Riley and A. B. Ritchie, *J. Phys. B*, 32,5279 (1999)

**8:30**

**PF1 3 Kinetics of Electrons in the Anode Region of Cylindrical Glow Discharge Plasmas** DIRK UHRLANDT, STEFAN ARNDT, ROLF WINKLER, *Institut für Niedertemperatur Plasmaphysik, 17489 Greifswald, Germany* The anode region of a cylindrical glow discharge represents a typical interaction region of a plasma and a conducting surface which absorbs electrons.

There, the transition from the axially uniform and radially non-uniform positive column to the equipotential anode surface takes place. The electron kinetic behavior in this region is studied considering a planar anode which covers the whole inner tube cross section. In particular, the relevant Boltzmann equation of electrons is solved in two space dimensions to reveal the formation of the electron kinetic properties in radial and axial direction. The solution method is based on the two-term expansion of the velocity distribution and the introduction of a total energy coordinate. Finally, a three-dimensional initial boundary value problem has to be treated. Beside appropriate boundary conditions describing e.g. the electron absorption at the anode, an axial electric field, which starts with the constant axial field in the positive column and increases in front of the anode, and the action of a radially increasing radial space charge field are taken into account. The rigorous kinetic description allows among others the determination of axial and radial particle and energy fluxes of electrons in the anode region. Results are presented for neon discharges at pressures around one Torr.

**8:45**

**PF1 4 Spacial Relaxation of Electrons in Axially and Radially Inhomogeneous Plasmas** STEFAN ARNDT, DIRK UHRLANDT, ROLF WINKLER, *Institut für Niedertemperatur Plasmaphysik, 17489 Greifswald, Germany* The properties of spatially structured, anisothermal steady-state plasmas at low pressures are mainly determined by the nonlocal properties of the electrons. The solution of the relevant space-dependent Boltzmann equation is required for the strict kinetic description of the electrons in such plasmas. Up to now, this equation has been accurately treated only for one-dimensional spatial structures or rough approximations have been applied. A new method for the study of the electron kinetics in radially and axially inhomogeneous cylindrical plasmas is presented. It is based on the solution of the two-dimensional space-dependent kinetic equation in two-term expansion without further approximations. As a first application of this method, axially directed relaxation phenomena in cylindrical dc column plasmas have been investigated. In particular, the response of the electron gas to a local disturbance of its axial homogeneity under the influence of a radial space-charge confinement has been analyzed. A considerable modification of the results with respect to those obtained by earlier relaxation studies in one spatial dimension has been found. For example, axially periodic modulations of macroscopic electron properties have been found, the maxima of which are shifted towards the anode with increasing radial positions. A similar shift has already been observed in some experiments.

**9:00**

**PF1 5 Electron Swarm Parameters in Divergent Electric Fields** H. DATE, *Hokkaido University* P.L.G. VENTZEK, *Motorola Inc.* M. SHIMOZUMA, *Hokkaido University* H. TAGASHIRA, *Muroran Institute of Technology* The behavior of electron swarms in divergent electric is presented focusing on the effects of the curvilinear motion of electrons orbiting an anode with angular momentum. The "spiral motion" of electrons lengthens the transit time passing through shells of like potential drop. As a result, the swarm parameters may have different values than one would expect in curvilinear system using swarm parameters constructed with non-divergent field geometries with the same local field magnitude. We demonstrate the motion of electron swarms using a Monte Carlo simulation technique in cylindrical and spherical

field models, and compare the swarm parameters with those given in the one-dimensional (i.e., non-divergent) field condition. In addition, we develop a Boltzmann equation description accounting for the electron motion associated with the conservation of angular momentum.

9:15

**PF1 6 The onset voltage and radiation efficiency of Xe/Ar/He and Xe/Ar/Ne mixtures\*** SATOSHI UCHIDA, TSUNEO WATANABE, *Tokyo Metropolitan University* HIROTAKE SUGAWARA, YOSUKE SAKAI, *Hokkaido University* BYOUNGHEE HONG, *Samsung Display Devices* For improvement of PDPs, we evaluated the effect of Ar addition to Xe/He and Xe/Ne mixtures on the onset voltage  $V_s$  and radiation efficiency  $\eta$  by calculating the electron swarm parameters and concentrations of excited species in Xe/Ar/He and Xe/Ar/Ne with a Boltzmann equation method. With increasing mixture ratio of Ar,  $K_{Ar}$ , the effective secondary electron emission coefficient  $\gamma_{eff}$  of both mixtures decreases at  $pd < 2$  cmTorr and the ionization coefficient  $\alpha$  largely decreases at  $pd > 2$  cmTorr. Since  $V_s$  strongly depends on both  $\gamma_{eff}$  and  $\alpha$ ,  $V_s$  becomes higher than that in the Ar-free mixtures at any  $pd$ . Under a constant input power ( $50 \text{ Wcm}^{-3}$ ) to electrons,  $\eta$  of Xe/Ar/Ne increases with  $K_{Ar}$  in a region of  $E/p_0$  from 5 to  $100 \text{ Vcm}^{-1}\text{Torr}^{-1}$ . Since Ar addition induces less excitation of Xe to the resonance level, more electron accumulation and more  $\text{Xe}_2^*$  production,  $\eta$  sensitively changes under the balance between these reaction processes. In Xe/Ar/He,  $\eta$  becomes large in a wide range of  $E/p_0$  from 1 to  $400 \text{ Vcm}^{-1}\text{Torr}^{-1}$  with increase in  $K_{Ar}$  because of remarkable reduction of the electron energy loss due to elastic collision and increase in the electron concentration.

\*Work in part supported by Grant-in-Aid for Scientific Research of The Ministry of Education, Science, Sports and Culture, Japan.

9:30

**PF1 7 The multi-component Tonks-Langmuir problem** K.-U. RIEMANN, TH. WELLIE, *Theoretische Physik I, Ruhr-University Bochum, D-44780 Bochum, Germany* The quasineutral description of a plasma breaks down at the "sheath edge." This breakdown is closely related to the marginal validity of the Bohm criterion and may be used to formulate boundary conditions both for the separate description of the sheath and of the plasma body (presheath). In a multi-component system we are confronted with the problem to find the boundary conditions for various ion components from one Bohm criterion [1]. We discuss this principal problem with the general analysis of Tonks-Langmuir type problems. In a hydrodynamic analysis it proves to be rather inconvenient and difficult to account for more than one ion component. The kinetic analysis of multi-component Tonks-Langmuir problems, in contrast, can be reduced under very general conditions to the corresponding one-component problem. [1] K.-U. Riemann, *IEEE Trans. Plasma Sci.* **23**, 709 (1995)

## SESSION PF2: DIAGNOSTICS II

Friday morning, 27 October 2000

Grand Ballroom C, Red Lion Hotel at 8:00

L. Overzet, University of Texas at Dallas, presiding

## Contributed Papers

8:00

**PF2 1 Detection of Halide in Nitrogen Gas by Means of Microwave Breakdown Spectroscopy** HIROSHI SUTO, MUTSUMI MATSUURA, KOICHI IINUMA, SHUNSUKE UCHIDA, *Department of Quantum Science and Energy Engineering, Graduate School of Engineering, Tohoku University, Aramaki, Aoba-ku, Sendai 980-8579 Japan* KEN TAKAYAMA, *High Energy Accelerator Research Organization, 1-10ho, Tsukuba, Ibaraki 305-0801 Japan* SUNAO MAEBARA, MAKOTO SHIHO, *Japan Atomic Energy Research Institute, 801-1Mukoyama, Naka-machi, Ibaraki 311-0193 Japan* A pulsed microwave breakdown apparatus combined with time-resolved spectrometer has been developed for a basic study of monitoring the trace gas components in the atmosphere. An X-band (9.4GHz) pulse generator producing over  $30\text{kW/cm}^2$  of peak power density has been used as a breakdown power source. The gas pressures in the range of 1Torr to 100Torr have been used for some halides and nitrogen gas mixtures. The time-resolved emission spectra in the region of 300nm-900nm have been obtained by a streak camera in the duration time of 0  $\mu\text{s}$ -20 $\mu\text{s}$ . The typical spectra assigned at present are those of  $\text{N}_2(1^{st}$  and  $2^{nd}$  positive bands),  $\text{N}_2^+(1^{st}$  negative bands), and Cl atom (837.5nm). The time correlation of their intensity has been examined for the analysis of their mutual exchange reactions.

8:15

**PF2 2 A Planar Probe for Ion Flux and Electron Temperature in the Electrode of a GEC Cell** A. GOODYEAR, W. LUBEIGT, P.B. VERDONCK, P.R.J. BARROY, N.ST.J. BRAITHWAITE, *The Open University*\* A radio frequency (rf) self-biased planar probe technique<sup>1</sup> for the measurement of positive ion flux and electron energy distribution functions has been implemented into the Gaseous Electronics Conference (GEC) standard reference cell. Results are presented across a wide range of power-pressure parameter space. Insertion of electrostatic probes into plasmas can lead to perturbation of the plasma and this is particularly problematic in the GEC cell where the inter-electrode distance is small. Planar probes are inherently large, requiring a guard ring (at least as large as typical sheath thicknesses) to ensure that the sheath in front of the probe is truly planar. Once this criterion is satisfied, analysis of current-voltage (IV) characteristics obtained in this planar geometry is relatively straightforward. A planar probe has been engineered into the surface of the showerhead electrode of the GEC cell, aimed at minimal perturbation to the GEC standard, in terms of both physical presence and electrical influence. The probe is self-biased by a burst of rf voltage. It is then allowed to return to its original floating condition under the arrival of charged particles from the plasma. An IV characteristic is recorded during this time, giving positive ion flux and the high energy tail (a few eV and above) of the electron energy distribution function.

\*Work supported by the EPSRC, Grant No. GR/L82380.

<sup>1</sup>J P Booth, N St J Braithwaite, A Goodyear, and P Barroy, *Rev. Sci. Instrum.*, in press (July 2000)

8:30

**PF2 3 Langmuir Probe Measurements of Inductively Coupled Plasmas in  $CF_4/Ar/O_2$  mixtures\*** M.V.V.S. RAO\*, M MEYYAPPAN, S.P. SHARMA, *NASA-Ames Research Center* Fluorocarbon gases, such as  $CF_4$ , and their mixtures are widely used in contemporary low-pressure and high-density plasma processing techniques. In such plasmas Langmuir probe is one of the most commonly employed diagnostic techniques to obtain electron number density ( $n_e$ ), electron temperature ( $T_e$ ), electron energy distribution function (EEDF), mean electron energy ( $E_e$ ), ion number density ( $n_i$ ), and plasma potential ( $V_p$ ). In this paper we report probe data for planar inductively coupled plasmas in  $CF_4/O_2/Ar$  mixtures. By varying the relative concentrations in the mixture, radial profiles of  $n_e$ ,  $n_i$ ,  $T_e$ ,  $E_e$ ,  $V_p$ , EEDF were measured in the mid-plane of the plasma at 10 mTorr and 20 mTorr of gas pressures, and 200 W and 300 W of RF powers. Data show that  $n_e$  and  $n_i$  decrease with increase of  $CF_4$  content and decrease of gas-pressure but they increase with increase of RF-power, whereas  $V_p$  increases with decrease of gas-pressure and remains independent of RF-power. However, they all peak at the center of the plasma and decrease towards the edge while  $T_e$  follows the other way and increases a little with increase of power. The measured EEDFs exhibit Druyvesteyn-like distribution at all pressures and powers. Data are analyzed and will be presented.

\*ELORET

8:45

**PF2 4 Large Area Plasma Processing System Based on Electron-Beam Ionization** DARRIN LEONHARDT, DAVID BLACKWELL,\*SCOTT WALTON,†WILLIAM AMATUCCI, DONALD MURPHY, RICHARD FERNSLER, ROBERT MEGER, *US Naval Research Laboratory, Plasma Physics Division Code 6750* EDBERTHO LEAL-QUIROS,‡ *Polytechnic University of Puerto Rico* Electron beam ionization is both efficient at producing plasma and scalable to large area (square meters). The beam ionization process is also fairly independent gas composition, capable of producing low temperature plasma electrons in high densities. A 'Large Area Plasma Processing System' has been developed based on the beam ionization process, with the goal of modifying the surface properties of materials over large areas. The system consists of a planar plasma distribution generated by a magnetically collimated sheet of 2-5kV, 10 mA/cm<sup>2</sup> electrons injected into a neutral gas background (oxygen, nitrogen, argon, neon). Typical operating pressures range from 20-200 mtorr with beam-collimating magnetic fields strengths of 100-300 Gauss. Thus far, electron beams have been produced using pulsed (10-4000 ms pulse length, >50dc hollow cathode discharges in dielectric as well as conducting chambers. Temporally resolved plasma characteristics deduced from Langmuir probes, electrostatic energy analyzers, optical emission spectroscopy and microwave transmission measurements will be presented. Over large areas (100s cm<sup>2</sup>), results show low electron temperature ( $T_e$  0.3 and 1.5 eV in molecular and noble gases, respectively) in a bulk diffusion-dominated plasma with densities ranging from  $10^9$  to  $10^{12}$  cm<sup>-3</sup>. Temporally resolved plasma-to-surface fluxes (via mass spectrometry) and their energy distributions will be presented to give further insight into LAPPS for material processing applications. Additional details of in situ diagnostics in LAPPS will also be presented by co-authors<sup>3</sup>. <sup>3</sup>See presentations by coauthors at this conference.

\*NRL/NRC Postdoctoral Research Associate

†NRL/NRC Postdoctoral Research Associate

‡NRL/NRC Faculty Research Associate

9:00

**PF2 5 Particle Flux and Energy Measurements at Electrode Surfaces in LAPPS\*** S.G. WALTON,†D. LEONHARDT, D.D. BLACKWELL,‡D.P. MURPHY, R.F. FERNSLER, R.A. MEGER, *Plasma Physics Division, Naval Research Laboratory* In situ mass and energy resolved measurements of ion and neutral fluxes to a conducting electrode surface in NRL's Large Area Plasma Processing System (LAPPS) are presented. LAPPS uses a magnetically confined sheet of high-energy electrons to ionize a background gas, producing a high-density ( $10^9$ - $10^{12}$  cm<sup>-3</sup>) planar plasma that is scalable to large areas (meters<sup>2</sup>). The electron beam, produced by a hollow cathode, is embedded in a 100-300 Gauss magnetic field and injected into 20-200 mTorr of background gas. Hence, plasma production is independent of both the reactor geometry and electrode surfaces. The relative fluxes and energy distributions are reported for a grounded and rf-biased electrode and as a function of plasma-electrode separation. Ion and neutral species are sampled through a small orifice (sub-Debye length diameter) located in the center of the electrode and analyzed via an energy selector in series with a mass spectrometer. Measurements are presented for discharges in Ar, O<sub>2</sub>, Ne, and their mixtures over a range of conditions (pressure, mixture ratios). Additional details concerning LAPPS are presented by co-authors at this conference.

\*Work supported by the Office of Naval Research

†NRC/NRL Postdoctoral Research Associate

‡NRC/NRL Postdoctoral Research Associate

9:15

**PF2 6 In Situ 2D Surface Charging Potential Monitoring for a High Current Ribbon Beam** SVETLANA RADOVANOV, REUEL LIEBERT, PHIL COREY, JAMES CUMMINGS, GORDON ANGEL, JIM BUFF, *Varian Semiconductor Equipment Associates, Gloucester MA 01930, U.S.A.* Monitoring of the wafer surface charging potential distributions during ion beam implantation on the VISta 80 serial high current ion implanter is key to an improved understanding of the beam space charge compensation for broad beam technology. In steady state, when a plasma flood gun is in use, charge neutralization occurs and reduces local imbalance between ion and electron currents. Where the beam potential and current density is high a potential barrier in the sheath region is formed and inhibits the flow of electrons, thus preventing reduction of the wafer surface charge. Where there is no direct ion-surface interaction, primary electrons coming from the plasma neutralization system and secondary electrons can cause negative charging. The major goal is to obtain sufficient electron flux of low electron energies coming from the plasma flood gun to reduce the plasma potential and the potential fall at the wafer surface. An in-situ floating potential monitor has been developed for the VISta 80 high current serial ion implanter. A monitor wafer with a two dimensional array of flux probes is used. These probes measure the potential difference between the different sites and system ground. The probes are connected through a vacuum feed-through to a data acquisition board that provides real time measurement of the surface charging potential with and without the beam. In order to clarify the behavior of the plasma flood, electron energy and flux measurements done by a multi-pixel scanning Faraday were compared with the floating potential measurements. Data were taken at various beam and plasma flood conditions. Experimental results were compared to the beam potential distribution obtained by the 2D particle in-cell code XOOPIE [1]. Good agreement was obtained between experimental and calculated beam potential distributions. References [1] J.P.

Verboncoeur, A.B. Langdon and N.T. Gladd, *Comp.Phys.Comm* 87, May, 1995.

**SESSION QF1: MICRODISCHARGES FOR DISPLAYS AND LAMPS**

Friday morning, 27 October 2000

Grand Ballroom D, Red Lion Hotel at 10:15

Graeme Lister, Osram Sylvania Research and Development, presiding

*Contributed Papers*

10:15

**QF1 1 Three Dimensional Analyses of Microdischarges in Unit Cell of an AC-type Plasma Display Panel** K. TACHIBANA, K. MIZOKAMI, J. SHINOZAKI, *Dept. of Electronic Science and Engineering, Kyoto University* T. SAKAI, *Display Research Laboratories Co., Ltd.* For improving the luminous efficiency of plasma display panels (PDPs), characteristics of microdischarges depending on the cell structure and the operating conditions must be understood. We have developed special panels suitable for the front-view and side-view observations, and measured spatio-temporal behaviors of excited Xe atom densities in the  $1s_5$  and  $1s_4$  levels by a microscopic laser absorption technique. In the front observation, there appeared a sharp density peak on the temporal anode side and a broad peak on the temporal cathode side. From the side observation, it was seen that the distance of both peaks from the dielectric (MgO) electrode surface tended to increase as the gas pressure or the pulsed discharge period decreases. Similar measurements were also done on the optical emissions from several excited levels of Xe and Ne atoms by using a gated CCD camera. From these measurements, a three dimensional image of microdischarge phenomena in a PDP cell has been obtained on the characteristic behaviors of plasma parameters and the production rates of excited atoms leading to the VUV radiations.

10:30

**QF1 2 Predicted characteristics of a micro-cell plasma in Ne/Xe mixture by using RCT model** M. KURIHARA, T. MAKABE, *Keio university, JAPAN* One of the disadvantages of the conventional PDP is a low efficiency of UV radiation inherent in the low frequency discharge. In our precious work, frequency characteristics of a micro-cell plasma are discussed in pure Xe. In this work, we numerically investigate the characteristics of a micro-cell plasma with ring shaped driving electrode in Ne/Xe mixture at 100 Torr and 50 MHz as a function of percentage of Xe under constant power. At 13 mW, the peak of the plasma density in Ne/Xe(10%) amounts to  $10^{13} \text{cm}^{-3}$  which is the same as that in pure Xe. However, the effective volume of the plasma in mixture is wider than that in pure Xe, because of the arrangement of a ring shaped electrode and of higher ionization rates in Ne/Xe mixture. Penning ionization is less effective ( $< 1\%$  of total electron production). In mixture of a few percentage of Xe, stepwise ionization processes are dominant in low electric field. The efficiency of UV radiation from  $\text{Xe}(^3\text{P}_1)$ ,  $\text{Xe}_2^*$  becomes higher with increasing the percentage of Xe. Otherwise, the plasma can be sustained by lower applied voltage in low percentage of Xe. Furthermore we will investigate the minimum sustaining voltage at 13.56 MHz as a

function of percentage of Xe, and explain the margin for writing and erasing.

10:45

**QF1 3 Comparison between simulation models and experimental results for a planar He-Xe microdischarge** GEORGIOS VERONIS, *Stanford University* UMRAN INAN, *Stanford University* VICTOR PASKO, *Stanford University* A one-dimensional self-consistent simulation of a dc planar He-Xe microdischarge is used to investigate the effect of gas mixture composition and pressure on the breakdown and current-voltage characteristics, and on the vacuum ultraviolet efficiency of the discharge. The time dependent continuity equations for electrons and ions and Poisson's equation are solved successively until steady state is reached. The electric model is coupled to a model of the excited species kinetics and VUV emission. The efficiency of resonant emission of xenon atoms at 147 nm and of xenon dimers at 150 nm, defined as the ratio of the volume density of VUV emission intensity versus dissipated electrical power, is maximized at a specific pressure for mixtures with specific xenon concentration. The results of the 1D model are compared with other experimental and theoretical studies of He-Xe microdischarges. A similar 1D model of an ac plasma display panel cell is used to investigate similar pressure dependent maxima for ac PDPs.

11:00

**QF1 4 Microhollow Cathode Discharge Excimer Sources\*** M. MOSELHY, A. EL-HABACHI, W. SHI, R.H. STARK, K.H. SCHOENBACH, E Microhollow cathode discharges (MHCDs) are direct current, high-pressure, non-equilibrium gas discharges. When operated in Ar, Xe, ArF and XeCl, these discharges were found to be intense sources of excimer radiation at 130, 172, 193, 308 nm, respectively. Internal conversion efficiencies (from input electrical power to output optical power) of 1% (Ar), 8% (Xe), 2% (ArF) and 3% (XeCl) were achieved [1,2,3]. The spatial distribution of the xenon excimer source was studied by means of an ICCD-MAX intensified CCD camera. The measurements showed that the source expands with current and becomes reduced in size with pressure. The maximum radiant emittance (radiant power per source area) was measured as  $2 \text{ W/cm}^2$  at atmospheric pressure and a discharge current of 3 mA. The peak irradiance (radiant power per target area) for a single discharge was calculated to be  $3 \text{ mW/cm}^2$  at a distance of 1 cm from the source. Operating multiple discharges in parallel allows us to generate flat panel excimer lamps with an irradiance approaching the value of the radiant emittance ( $2 \text{ W/cm}^2$ ). In order to increase the irradiance further MHCDs could be operated in series. First experiments with two discharges in series have shown that the radiant emittance increases linearly with the number of discharges [3]. Besides using systems of MHCDs as lamps, efforts to utilize stacked discharges as excimer laser medium are underway. This work is supported by NSF and DARPA. 1. Ahmed El-Habachi and Karl H. Schoenbach, *Appl. Phys. Lett.* 73, 885 (1998). 2. Wenhui Shi, Ahmed El-Habachi, and Karl H. Schoenbach, *Bull. Am. Phys. Soc.* 44, 25 (1999). 3. Ahmed El-Habachi et. al., *Series Operation of Direct Current Xenon Chloride Excimer Sources*, to appear in *J. Appl. Phys.*

\*Old Dominion University, Norfolk, VA 23529



11:15

**QF1 5 Excitation of a Microdischarge with a Reverse Biased PN Junction\*** CLARK WAGNER, SUNG-JIN PARK, GARY EDEN, *University of Illinois, Department of Electrical and Computer Engineering, Urbana, Illinois 61801* Excitation of cylindrical microdischarges 300-360 microns in diameter by a reverse biased pn junction has been demonstrated. Devices fabricated from commercial diodes have been constructed and operated in neon at pressures ranging from 200 to 700 Torr, and voltages as low as 120 volts. Spectra acquired on Ne discharges show strong emission from Ne ion states for gas pressures above 300 Torr. For a Ne pressure of 700 torr, the wavelength integrated output power for a 360 micron diameter device operating at 5.72 mA is 47.7 micro watts (emitted into a solid angle of  $5 \cdot 10^{-2}$  steradians). Details of the operating characteristics will be presented.

\*Work supported by AFOSR

11:30

**QF1 6 PERFORMANCE OF MICRODISCHARGE DEVICES AND ARRAYS FABRICATED IN METAL/POLYIMIDE/METAL STRUCTURES** SUNG-JIN PARK, *University of Illinois, Laboratory for Optical Physics and Engineering, Department of Electrical and Computer Engineering* CLARK J. WAGNER, *University of Illinois, Laboratory for Optical Physics and Engineering, Department of Electrical and Computer Engineering* J. GARY EDEN, *University of Illinois, Laboratory for Optical Physics and Engineering, Department of Electrical and Computer Engineering* Cylindrical microdischarge devices and arrays, having discharge channel diameters between 50 and 150 microns, have been fabricated in metal/polymer/metal structures. The polymer film (typically polyimide) serves as the dielectric and has a thickness of 7-130 microns. Having specific power loadings of tens of  $kW - cm^{-3}$ , these devices produce stable glow discharges at rare gas pressures above 800 Torr. When operated with Ni or Cu screens serving as the anode and/or cathode, the microdischarges operate at voltages below 100V and exhibit hollow cathode behavior for pressures beyond 300 Torr Ne. Details of the spectral and electrical properties of these devices in DC and AC operation will be discussed.

11:45

**QF1 7 Dependence of Micro Discharge Characteristics on Rectangular Voltage Waveforms** HARUAKI AKASHI, *Dept. of Appl. Phys., National Defense Academy, Japan* AKINORI ODA, *Div. of Electron. and Info. Eng., Graduate School of Hokkaido University, Japan* YOSUKE SAKAI, *Div. of Electron. and Info. Eng., Graduate School of Hokkaido University, Japan* Excimer lamps have been developed using DBD as an important VUV light source, however the physics of DBD is not understood well. For further development of efficient DBD excimer lamps, understanding of the characteristics of DBD is necessary. In this paper, dependence of discharge properties in a micro discharge on the waveform of applied voltage is studied. DBDs are calculated using a 1D fluid model with Poisson's equation considering microdischarge radius. The rectangular voltages with various rising ratio (rise-time) are applied to a dielectric barrier Xe excimer lamp. The driving frequency is 200kHz, and the amplitude is 5kV. The spatio-temporal distribution of electron density, electric field, excimer density is examined. The discharge evolution depends significantly on the rising ratio of the applied voltage. As the voltage rising ratio becomes higher, the discharge in the lamp becomes glow-like discharge. Because the applied voltage rises up to its maximum before the electrons are accelerated to the electrode.

12:00

**QF1 8 Stable High Brightness CW Discharge Lamps at 193nm (ArF\*) and 157nm (F<sub>2</sub>\*)** M. SALVERMOSER, D.E. MURNICK, *Department of Physics, Rutgers University, Newark NJ 07102* Using a discharge between 2 needle electrodes separated by several 100  $\mu m$  in a high pressure ( $\sim 900$ mbar) rare gas fluorine system, CW 193nm ArF\* and 157nm F<sub>2</sub>\* lamps have been demonstrated. Total CW output power in  $4\pi$  was measured to be 30mW for ArF\* and 20mW for F<sub>2</sub>\*. The brightness of the light sources is estimated to be on the order of several  $W/cm^2 sr$ . With DC excitation, electrode lifetimes were limited to several minutes due to fluorine salt deposits. However, using an AC field at a well defined frequency to drive the discharge, the lifetime of the lamps increased to more than 24 hrs. The technology can be adapted to many other wavelengths and promises even higher powers in future.

## SESSION QF2: DIAGNOSTICS III

Friday morning, 27 October 2000; Grand Ballroom C, Red Lion Hotel at 10:15; Yosuke Sakai, Hokkaido University, presiding

## Invited Paper

10:15

**QF2 1 High Sensitivity UV Reflection-Absorption Spectroscopy for Benzene on Metal Surfaces.\***

L. W. ANDERSON,<sup>†</sup> *Physics Department, University of Wisconsin, Madison, WI 53706*

The use of high sensitivity ultraviolet reflection-absorption spectroscopy (UVRAS) is reported for the study of benzene molecules physisorbed on gold, silver and copper surfaces. The electronic transition  $^1A_{1g} \rightarrow ^1B_{2u}$  (near 250 nm) is observed<sup>1</sup>. We have previously developed and used high sensitivity white light absorption spectroscopy for the study of molecules and radicals in the gas phase. This work extends the technique to the study of molecules physisorbed on metal surfaces. A continuum light source is reflected from a metal surface and the reflected light is observed with a spectrometer and detector array both with and without benzene adsorbed on the surface. The change in the reflectivity due to the adsorbed benzene molecules is analyzed in terms of a thin benzene film with a complex index of refraction. We are able

to detect very small surface coverage and to determine the center frequencies, the line widths, and the oscillator strengths for the vibronic transitions resulting from the benzene. We are able to detect a surface coverage due to a 3.5 Langmuir exposure with a S/N ratio of 100. Another interesting feature of this experiment is that the linewidths are as narrow as  $100 \text{ cm}^{-1}$ . We anticipate that this technique will be useful for the high sensitivity detection of various adsorbates on surfaces under a variety of processing conditions.

\*Research supported by Army Research Office Grant DAAH-04-96-1-0413.

†This work was carried together with X. L. Peng, J. R. Peck, C. J. Goebel, and J. E. Lawler.

‡J. R. Peck, X. L. Peng, L. W. Anderson, and J. E. Lawler, *Chem. Phys. Lett.* **318**, 476 (2000).

### Contributed Papers

10:45

**QF2 2 Studies on Absolute H Atom Density in Material Plasma Processes Using Vacuum Ultraviolet Absorption Spectroscopy Employing Microplasma** TAKASHIMA SEIGOU, MASARU HORI, TOSHIO GOTO, *Nagoya University* KATSUMI YONEDA, *Nippon Laser & Electronics LAB.* H atoms play important roles in reactive plasmas. In the previous study, we have developed a measurement technique for absolute H atom densities in plasmas using a vacuum ultraviolet absorption spectroscopy (VUVAS) employing a high-pressure microdischarge hollow cathode lamp (MHCL) as a Lyman  $\alpha$  emission light source.<sup>1</sup> However, the light of high energy (10eV) has been used as a light source in the VUVAS, where the background absorption due to parent gases and species produced in reactive plasma might be occurred. In this study, we have developed the measurement technique of the background absorption. The background absorption was estimated by measuring the absorption intensity of the resonance line of N atom at 120nm with VUVAS employing a N<sub>2</sub> MHCL. Using these methods, we have carried out the absolute H atom density measurement in the reactive plasmas, such as inductively coupled CH<sub>4</sub>/H<sub>2</sub> plasmas and ultrahigh frequency (UHF) SiH<sub>4</sub>/H<sub>2</sub> plasmas. H atom density was found to be on the order of  $10^{13} \text{ cm}^{-3}$  at a SiH<sub>4</sub>/H<sub>2</sub> ratio of 2/200 sccm, a pressure of 20 Pa, and an UHF power of 1000W in the UHF plasma.

<sup>1</sup>S. Takashima et al, *Appl. Phys. Lett.* **75** 3929 (1999).

11:00

**QF2 3 Measurement of Negative-Ion Density in High-Density Plasmas Using Laser Photodetachment Technique Combined with Millimeter-Wave Resonance Technique** A. KONO, K. KATO, M. KONISHI, *Nagoya University, Nagoya 464-8603, Japan* A new technique has been developed for measuring negative ion density non-intrusively in high-density processing plasmas. The plasma is produced between two aluminum mirrors ( $\sim 10$ -cm diameter, separated by  $\sim 60$  cm) constituting a Fabry-Perot-type open millimeter-wave (35 GHz) resonator. A small electron density variation in the plasma is detected as the change in the millimeter-wave intensity in the resonator when the mirror separation is set at a slightly off-resonant position. Negative ions were detected as the electron density perturbation when the plasma was irradiated by frequency-quadrupled Nd:YAG laser (266 nm), which causes photodetachment of electrons from negative ions. The technique was applied to the study of the negative-ion density in a low-pressure ( $\sim 25$  mTorr), high-density ( $n_e \sim 10^{11} \text{ cm}^{-3}$ ), inductively-coupled C<sub>4</sub>F<sub>8</sub>/Ar plasma. In the C<sub>4</sub>F<sub>8</sub> mixing-ratio

range of 5~ 20%, the negative ion density was comparable to or higher than the electron density. SF<sub>6</sub>, CF<sub>4</sub> and other electronegative plasmas are under investigation.

11:15

**QF2 4 Spatial plasma structure of narrow-gap RIE measured by a plasma absorption probe** KEIZO KINOSHITA, ASET NAOKI TOYODA, *Nissin Inc.* SHOUHEI NANKOU, *Nissin Inc.* TETSUYA TATSUMI, ASET MIYAKO MATSUI, ASET NOBUO OZAWA, ASET SHUICHI NODA, ASET HIDEO SUGAI, *Nagoya Univ.* MAKOTO SEKINE, ASET The narrow-gap (2-cm-gap parallel plates) RIE system is now widely used as an oxide etcher. However, the spatial structure of the plasma has not been well known until now. This is because, the plasma is confined in a very narrow region between the top electrode and wafer stage. In this study, we describe the first measurement results of the spatial distribution of the plasma in the narrow-gap system by using the Plasma Absorption Probe (PAP) technique [1]. One of the characteristics of the PAP is that it can work in the process plasma which deposit polymer on the probe chip. Two types of dual-frequency, narrow-gap systems were measured. They had 27 MHz/800 kHz and 60 MHz/2 MHz power sources for the top/bottom electrodes. The 27-MHz source showed hollow distribution when there was no bias on the wafer stage. The wafer bias lift the density, and it showed very flat distribution when the Vpp of the bias is near the process condition (1400 V). On the other hand, the 60-MHz source had a higher density region at both the center and the edge region. It also showed flat distribution when the bias was applied to the stage. Both plasma sources showed very low density at the outside of the stage. This work was supported by NEDO. [1] H. Kokura, et al., *Jpn. J. Appl. Phys.*, **38** (1999) 5262.

### SESSION RF1: PLASMA MODELING: NEEDS AND OPPORTUNITIES

Friday afternoon, 27 October 2000

Grand Ballroom C, Red Lion Hotel at 12:15

P. Ventzek, Motorola, Inc., presiding

**RF1 1** This session will be an informal discussion pertaining to the present status and future of plasma modeling. Issues to be addressed include integration of equipment and feature scale models, fundamental data needs, technology transfer (from model developers to users), and modeling roadmap.

## Author Index

- A**  
 Abada, Hana JWP 21, JWP 39  
 Abraham, Ion AT2 1, KR2 4  
 Abrams, Cameron JWP 68  
 Abramzon, Nina ETP 37  
 Adamovich, Igor JWP 33, LR1 3  
 Aflatooni, K. CT1 4  
 Akashi, Haruaki QF1 7  
 Akazawa, Masamichi AT2 7, JWP 69, JWP 70  
 Ali, M.A. ETP 39  
 Alves, L.L. CT2 2, ETP 4  
 Amatucci, William E. ETP 49, PF2 4  
 Anderson, L.W. QF2 1  
 Anderson, R.B. ETP 19, JWP 60  
 Anderson, S.A. ETP 19, JWP 60  
 Andrew, Yasmin AT2 6  
 Angel, Gordon PF2 6  
 Angus, Andrew JWP 53  
 Arndt, Stefan PF1 3, PF1 4  
 Arnush, Donald JWP 13  
 Arunachalam, V. MR2 4  
 Asatani, Syu-ichiro ETP 33  
 Astapenko, A. MR2 4  
 Auntin, F. JWP 42
- B**  
 Bai, K.H. JWP 8  
 Bakker, Leon JWP 55, LR2 6  
 Bano, Gregory JWP 75  
 Baravian, G. LR1 5  
 Barrault, J. JWP 42  
 Barroy, P.R.J. ETP 51, PF2 2  
 Bartschat, Klaus ETP 35  
 Basner, R. ETP 38  
 Basurto, E. JWP 46  
 Becker, Kurt ETP 37, ETP 38  
 Behnke, J. F. ETP 22, JWP 30  
 Behnke, J.F. ETP 22, JWP 29, JWP 30  
 Behnke, Jorgen F. CT2 9, CT2 9  
 Behnke, Juergen F. JWP 34  
 Behnke, Jürgen F. JWP 78  
 Benck, Eric LR2 5  
 Benilov, M.S. BT2 4, DT1 2  
 Bernal, Sara JWP 60
- Bhandarkar, Upendra MR2 8**  
 Bhuiyan, Mohammad K.H. JWP 36  
 Bimont, E. JWP 63  
 Birdsall, C.K. JWP 62, MR1 8  
 Bixler, David ETP 45  
 Blackwell, David D. ETP 49, PF2 4  
 Blackwell, D.D. PF2 5  
 Bogaers, Annemie ETP 69  
 Bogdanov, E.A. JWP 4  
 Boisse-Laporte, C. CT2 2  
 Boller, K.J. JWP 59  
 Boniche, I. CT1 2  
 Boogaarts, Maarten LR2 4  
 Booth, Jean-Paul JWP 21, JWP 39  
 Bose, D. KR2 7  
 Bose, Deepak BT2 3, DT2 1  
 Boswell, R.W. DT2 2  
 Bowden, M.D. ETP 56, ETP 64, JWP 18  
 Braithwaite, N.St.J. ETP 51, PF2 2  
 Brake, Mary JWP 60  
 Brake, M.L. ETP 19  
 Brandenburg, Ronny ETP 25, ETP 73  
 Bratescu, M.A. ETP 62, ETP 63  
 Brooks, Philip R. ETP 43  
 Brown, Michael ETP 59  
 Buckman, S J IW1 6, MR2 2  
 Buff, Jim PF2 6  
 Burrow, Paul CT1 4
- C**  
 Čadž, Iztok GW1 2  
 Cartry, Gilles JWP 39  
 Chabert, P. DT2 2, DT2 3  
 Chang, Hong-Young JWP 9  
 Chang, H.Y. JWP 8  
 Chayka, M.O. JWP 5  
 Chen, Francis F. JWP 13, JWP 73  
 Chilton, J. Ethan IW1 4  
 Cho, H IW1 6, MR2 2  
 Choi, Peter MR1 9  
 Christophorou, Loucas CT1 6, GW1 1  
 Chung, ChinWook JWP 9  
 Coburn, John KR2 5  
 Collaboration, Low Temperature Plasma Physics and Chemistry ETP 73  
 Collaboration, Modeling of low temperature plasma ETP 69  
 Collaboration, Plasma chemistry in dielectric barrier discharges JWP 34  
 Collins, Alan DT2 6  
 Collins, G.J. JWP 11, JWP 12, JWP 66, JWP 72  
 Collins, Ken MR2 3  
 Coman, L. CT1 2  
 Cooper, Gregory D. ETP 31  
 Corey, Phil PF2 6  
 Corr, C.S. IW2 3, JWP 15  
 Costa i Bricha, E. IW2 3, IW2 4  
 Coulombe, Sylvain DT1 1  
 Cox, Michael DT2 6  
 Crothers, D.S.F. ETP 46  
 Crowe, Albert IW1 1  
 Crowley, B DT2 4  
 Cruden, B.A. KR2 7  
 Csambal, C. JWP 29  
 Cui, Chunshi MR2 3  
 Cummings, James PF2 6  
 Cunge, Gilles DT2 4, JWP 39  
 Cunha, M.D. DT1 2  
 Curry, J.J. MR1 1, MR1 2, MR1 4  
 Czarnetzki, U. ETP 70, ETP 71, LR2 1
- D**  
 Dandapani, E. ETP 60  
 Dastgeer, S. JWP 79  
 Date, H. PF1 5  
 Dateo, Christopher KR1 3  
 Daube, Th. JWP 6  
 de Urquijo, J. JWP 45, JWP 46  
 DeJoseph Jr., C.A. KR1 6  
 Den Hartog, E.A. JWP 63  
 Deutsch, H ETP 38  
 Dhali, Shirshak JWP 61  
 Dias, F.M. CT2 5  
 Dijk, Jan van MR1 3  
 Dinh, T. ETP 7  
 Dinklage, Andreas ETP 17, JWP 78  
 Döbele, H.F. ETP 58, ETP 70, ETP 71  
 Doll, G.L. JWP 71  
 Donnelly, Vincent M. BT1 2
- Dooms, G. LR1 6**  
 Dorai, Rajesh LR1 4  
 Dubey, Naren DT2 6  
 Dunning, F. Barry AT1 3
- E**  
 Economou, Demetre AT2 2, ETP 8, ETP 32, JWP 2  
 Eden, Gary QF1 5  
 Eden, J. Gary QF1 6  
 Eletsii, A. MR2 4  
 El-habachi, A. QF1 4  
 Engeln, Richard LR2 4  
 Etemadi, Kasra LR2 5  
 Evans, John D. JWP 13
- F**  
 Favre, Mario MR1 9  
 Faxas, M. CT1 2  
 Fedchak, J.A. JWP 63  
 Fendel, P. ETP 71  
 Fernsler, R.F. PF2 5  
 Fernsler, Richard F. ETP 49, PF2 4  
 Ferreira, C.M. CT2 5  
 Fletcher, Graham KR1 3  
 Francis, A. ETP 71  
 Franke, Steffen ETP 17, JWP 78  
 Fraser, Hamish JWP 33  
 Fresnet, F. LR1 5  
 Fujita, Hiroharu DT2 5, ETP 9, JWP 19, NR2 5  
 Fujita, T. ETP 28  
 Fujiyama, Hiroshi MR2 7  
 Fukuyama, Tatsuya JWP 83  
 FUNAKOSHI, HIKARU MR2 5  
 Furuhashi, H. ETP 21
- G**  
 Gallagher, Alan JWP 44, JWP 75  
 Ganguly, B. N. KR1 6  
 Ganguly, Biswa ETP 59  
 Ganguly, B.N. ETP 67  
 Gans, T. ETP 58  
 Garscadden, A. KR1 6  
 Garscadden, Alan KR1 4  
 Gavrilenko, V.P. ETP 56  
 Gay, T.J. KR1 2  
 Geraasimov, Denis LR1 2  
 Getty, W. ETP 19  
 Ghanashev, I. CT2 1  
 Gielen, John MR1 3  
 Gijbels, Renaat ETP 69  
 Gilbert, S.J. ETP 40

- Gilgenbach, R.M. ETP 19,  
**JWP 71**
- Girshick, Steven L MR2 8
- Giuliani, John MR2 6
- Glazkov, Vasily LR1 2
- Gleizes, Alain **DT1 4**
- Glide, Carri JWP 60
- Godyak, Valery **KR2 3**
- Goeckner, M.J. **ETP 29**,  
ETP 30, JWP 22
- Goedheer, Wim ETP 69
- Golubkov, M. MR2 4
- Golubkov, V. MR2 4
- Golubovskii, Y.B. **ETP 22**
- Golubovski, Juri B. CT2 9
- Golubovskii, Y.B. JWP 30
- Gomez, S. **ETP 23**, IW2 3,  
JWP 15
- Gomez, Sergi **AT2 4**
- Gonzalez, JJ DT2 6
- Gonzalez, J.J. **JWP 11**,  
**JWP 12**
- Goodyear, A. ETP 51,  
**PF2 2**
- Goree, J JWP 76, NR2 4
- Goretsky, Alex KR2 5
- Gortchakov, S. ETP 14
- Goto, M. ETP 68
- Goto, N. **ETP 6**
- Goto, T. ETP 21
- GOTO, TOSHIO ETP 57,  
MR2 5, QF2 2
- Gousset, G. CT2 2, ETP 4
- Govindan, T.R. BT2 3,  
DT2 1
- Goyette, A.N. **ETP 5**
- Graham, W.G. ETP 23,  
ETP 65, **IW2 3**, IW2 4,  
JWP 15, JWP 17
- Graham, William G. AT2 4
- Graves, David JWP 68,  
KR2 5
- Greenwood, C.L. JWP 10
- Groot, Simon de MR1 3
- Guang, W.X. JWP 67
- Guerra, V. **CT2 4**, **CT2 5**
- Gulley, R J **IW1 6**, **MR2 2**
- Guo, X IW1 3
- H**
- Haaland, Peter KR1 4
- Hala, Ahmed **BT2 5**
- Harb, T. **IW1 5**
- Hardy, Kenneth **CT1 2**
- Hartel, G. JWP 57
- Hartgers, Bart JWP 56
- Hartig, Michael DT2 7
- Hasegawa, Hiroki **JWP 51**
- Hash, D.B. **KR2 7**
- Hassouni, Khaled LR1 4
- Hatton, P.J. JWP 27
- Hayashi, D. **CT1 5**,  
JWP 26, **JWP 38**, **LR1 6**
- Hayashi, M. JWP 50
- Hebner, Greg **ETP 55**,  
**IW2 2**
- Hemerik, M.M. JWP 38
- Herbert, P.A.F. ETP 23
- Hirao, Takashi JWP 67
- Hitzschke, L. JWP 57
- Hoeben, W.F.L.M. LR1 6
- Hokoi, Kohji **JWP 70**
- Honda, Chikahisa JWP 31,  
KR2 1
- Hong, Byoung-Hee PF1 6
- Hong, J.I. JWP 8
- HORI, MASARU ETP 57,  
MR2 5, QF2 2
- Horie, Ikuya **JWP 49**
- Hsueh, H. **ETP 60**
- Huo, Winifred **KR1 3**
- Hur, Min Sup **JWP 79**
- I**
- IINUMA, Koichi PF2 1
- Ikuta, nobuaki JWP 83
- Imamura, Nariaki **ETP 33**
- Inan, Umran **LR1 1**, QF1 3
- Ingold, John H. MR1 5,  
MR1 6
- Inoue, Yousuke ETP 9
- Irikura, K.K. ETP 39
- ISHII, NOBUO ETP 57
- Itazu, N. **ETP 61**
- Ito, Akira CT2 3
- ITO, HARUHIKO **MR2 5**
- ITO, MASAFUMI MR2 5
- Itoh, H. JWP 40
- Itoh, Haruo **JWP 81**,  
JWP 82, **JWP 83**
- Iwase, Hirohiko JWP 28
- Iwata, Shuichi KR1 5
- J**
- Janssen, Ger JWP 56
- Jesih, Adolf PF1 1
- Ji, B. ETP 60
- Jia, Beike ETP 43
- Jiang, Chunqi CT2 6
- Jiao, Charles **KR1 4**
- Jiao, C.Q. **KR1 6**
- Jin, H.J. JWP 65
- Jindal, A.K. ETP 29,  
**ETP 30**
- Johnston, Colin **JWP 56**
- Johnston, M.D. JWP 71
- Joran, A. JWP 42
- K**
- Kadota, K. ETP 68,  
JWP 26, LR2 2
- Kamada, T. ETP 62
- Kanakasabapathy,  
Sivananda **AT2 3**
- Karwacki, E. ETP 60
- Kato, K. QF2 3
- Kaufman, Yitzhak MR1 9
- Kawahata, K. ETP 68
- Kawai, A. **JWP 47**
- Kawamoto, Shinji JWP 28
- Kedzierski, W. IW1 5
- Kessaratikoon, P. JWP 3
- Khakoo, M.A. IW1 3
- Khater, Marwan AT2 3
- Khater, M.H. JWP 22
- Kiehlbauch, Mark KR2 5
- Killian, T. **GW1 4**
- Kim, Chang-Koo AT2 2,  
**ETP 32**
- Kim, Doosik **AT2 2**
- Kim, H.J. ETP 56
- Kim, J.B. ETP 56
- Kim, Y.-K. ETP 39
- Kimura, Mineo **CT1 3**
- Kimura, T. **JWP 14**
- Kinder, Ronald L. **KR2 6**
- Kinoshita, Keizo **QF2 4**
- Kinoshita, T. JWP 65
- Kitajima, M MR2 2
- Kitamori, K. JWP 49
- Klampfer, Peter **PF1 1**
- Kleiban, G IW1 3
- Ko, Eunsuk AT2 6
- Kochetov, I.V. JWP 59
- Koga, K. JWP 65, **JWP 74**
- Kogure, Masamichi  
**JWP 41**
- Kokubu, H. **JWP 26**
- Kolobov, Vladimir KR2 3
- Konishi, M. QF2 3
- Kono, A. **ETP 21**, **QF2 3**
- Kortshagen, U. MR1 7
- Kortshagen, Uwe ETP 24,  
JWP 16, **MR1 5**, MR2 8
- Kozlov, Kirill V. ETP 25,  
ETP 73, JWP 34
- Kralj, Bogdan PF1 1
- Krishnaraj, Paddy DT2 6
- Kroesen, Gerrit JWP 20,  
JWP 55, LR2 6
- Kroesen, G.M.W. CT1 5,  
JWP 38, LR1 6
- Kroutilina, Valja ETP 72
- Kudoh, N. JWP 40
- Kudrna, P. JWP 29
- Kudrya, V. MR2 4
- Kudryavtsev, A.A. JWP 4,  
**JWP 5**
- Kulin, S. GW1 4
- KURIHARA, M. **QF1 2**
- Kushner, Mark J. CT2 7,  
KR2 2, KR2 6, LR1 4
- L**
- Lai, Ken DT2 6
- Lane, Chris DT2 6
- Lang, N. ETP 52
- Larsen, M. **IW1 3**
- Larsson, Mats **CT1 1**
- Lau, Y.Y. ETP 19, JWP 71
- Lavery, S. JWP 17
- Lawler, J.E. **JWP 63**,  
MR1 1, MR1 2, MR1 4,  
**MR1 7**
- Leal-Quiros, Edbertho  
ETP 49, PF2 4
- Lee, Hae June **JWP 62**,  
**MR1 8**
- Lee, Jae Koo JWP 79
- Leipold, Frank CT2 6,  
**ETP 53**
- Leonhardt, D. PF2 5
- Leonhardt, Darrin ETP 49,  
**PF2 4**
- Lerch, Rene ETP 72
- Li, Yan-Ming **DT1 3**
- Lichtenberg, A.J. DT2 2,  
DT2 3
- Lieberman, M.A. DT2 2,  
DT2 3
- Liebert, Reuel PF2 6
- Lieder, G.H. JWP 57
- Lim, M. GW1 4
- Lin, Chun C. IW1 4
- Lister, G.G. MR1 1, MR1 4
- Lister, Graeme G. **MR1 2**
- Loewenhardt, Peter DT2 6
- Loffhagen, Detlef **JWP 48**
- Loureiro, J. CT2 4
- Lubeigt, W. PF2 2
- Luggenhölscher, D. **ETP 70**
- M**
- MacAdam, Keith B. **AT1 1**
- Machima, Jasmine AT2 6
- Madziwa, Tsitsi G. **JWP 73**
- MAEBARA, Sunao PF2 1
- Maeshige, K. ETP 3
- Magne, L. LR1 5
- Maguire, P.D. JWP 15,  
JWP 17
- Mahoney, Len DT2 6

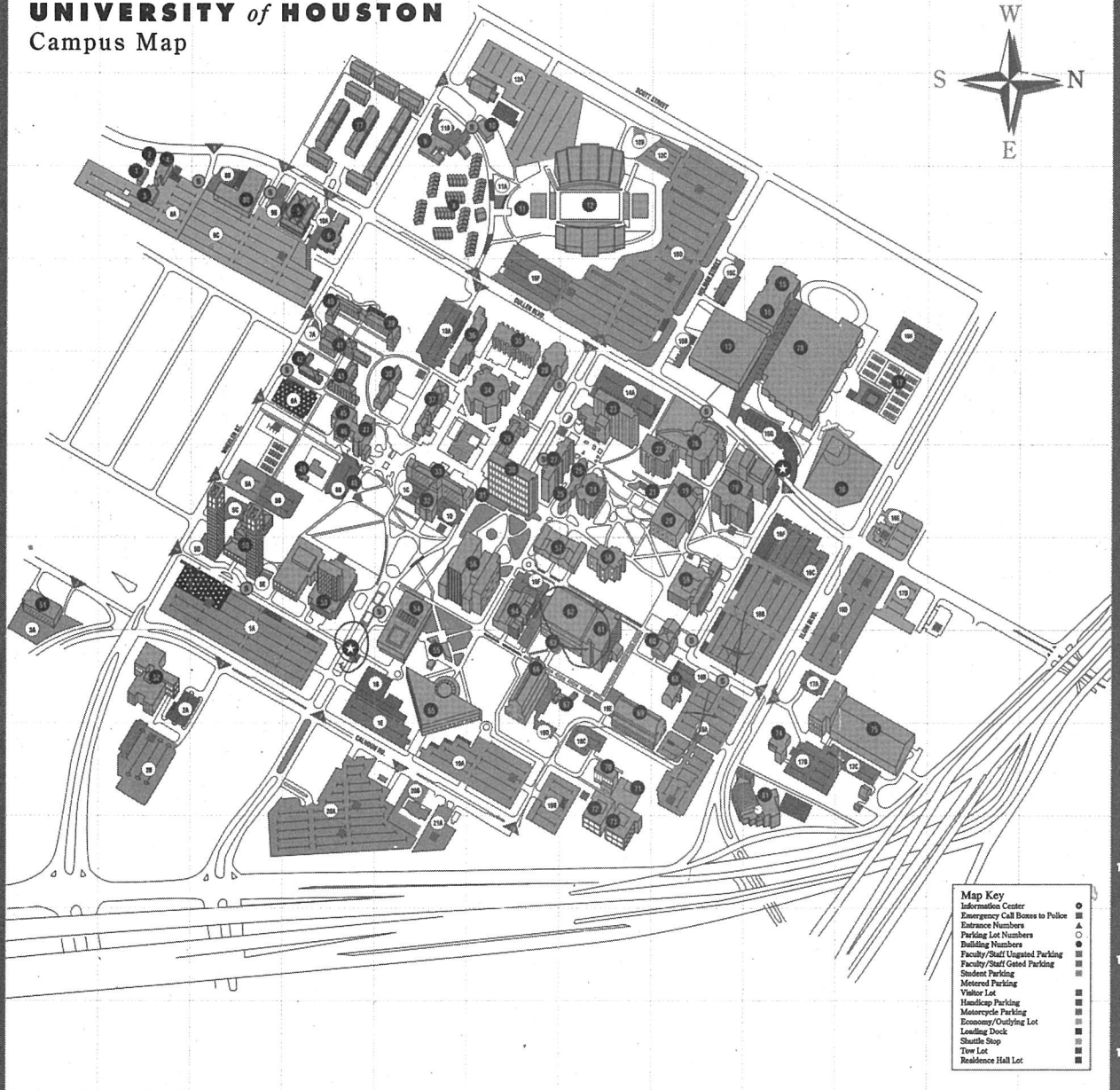
- Mahony, C.M.O. IW2 3,  
IW2 4, **JWP 15**, JWP 17  
Maiorov, V. ETP 22  
Maiorov, Vsevolod A.  
CT2 9  
Makabe, T. ETP 3, ETP 6,  
ETP 61, JWP 47, QF1 2  
Makabe, Toshiaki ETP 10  
Mano, T. ETP 28  
Marakhtanov, A.M. **DT2 2**,  
DT2 3  
Markham, B.J. ETP 29,  
ETP 30  
Marquis, J.M. ETP 29,  
ETP 30, **JWP 22**  
Martinez, Arturo DT2 7  
Martus, Kevin ETP 37  
Masamune, Sadao JWP 80  
Massines, Françoise ETP 25  
Matsui, J. JWP 47  
Matsui, Miyako QF2 4  
Matsuoka, A. ETP 64  
MATSUURA, Mutsumi  
PF2 1  
Maurice, Carole **JWP 20**  
MAZOUFFRE, Stéphane  
**LR2 4**  
McConkey, J.W. IW1 5  
McFarland, J. IW2 3  
McGrath, R. ETP 60  
McSherry, D.M. **ETP 46**  
Meger, R.A. PF2 5  
Meger, Robert A. ETP 49,  
PF2 4  
Meichsner, Juergen ETP 72  
Merhi, Hisham CT2 6  
Messier, R. ETP 60  
Meyyappan, M BT2 3,  
DT2 1, ETP 48, KR2 7,  
**NR2 1**, PF2 3  
Mi, Yiming **KR1 5**  
Michael, J. Darryl MR1 5,  
MR1 6  
Michel, Peter ETP 25,  
ETP 73  
Midha, Vikas **ETP 8**,  
**MR1 6**  
Mieno, Tetsu **JWP 36**,  
**JWP 37**, **NR2 2**  
Miller, Paul AT2 1, KR2 4  
Mills, D.J. JWP 27  
Minea, T. **JWP 42**  
Mishakov, V.G. JWP 5  
Miyoshi, Y. ETP 61  
MIZOKAMI, K. QF1 1  
Mizuno, M. ETP 63  
Mond, Michael MR1 9  
Moore, John H. ETP 31  
Morfill, G.E. **NR2 3**  
Morita, S. ETP 68  
Morrison, Michael A.  
AT1 2  
Morrow, T. ETP 23,  
ETP 65  
Moselhy, M. **QF1 4**  
Mullen, Joost van der  
MR1 3  
Muraoka, K. ETP 56,  
ETP 64, ETP 66, JWP 18  
Muraoka, Katsunori  
JWP 31, KR2 1  
Murnick, D.E. JWP 58,  
QF1 8  
Murphy, A.B. **DT1 5**  
Murphy, Donald P. ETP 49,  
PF2 4  
Murphy, D.P. PF2 5
- N**  
Nagatsu, Masaaki **CT2 3**;  
JWP 67  
NAKAMURA,  
MASAYUKI **ETP 57**  
Nakamura, S. JWP 49  
Nakamura, Y. JWP 50  
Nakamura, Yoshiharu  
JWP 51, JWP 52  
Nakano, N. ETP 3, JWP 47  
Nakano, Nobuhiko **ETP 10**  
Nanbu, K. **BT1 3**  
Nankou, Shouhei QF2 4  
Naoi, H. **JWP 66**  
Napartovich, A.P. JWP 59  
Narishige, S. **ETP 66**  
Nasser, Mahmood **DT2 5**,  
**JWP 19**  
Navin, Muthuswamy  
JWP 61  
Neale, I.D. JWP 10,  
JWP 27  
Noda, Shuichi QF2 4  
Noguchi, M. JWP 18  
Noguchi, Y. **ETP 64**  
Nosenko, V JWP 76,  
**NR2 4**  
Nunomura, S **JWP 76**,  
**NR2 4**
- O**  
Obara, Kozo ETP 33  
Oda, Akinori QF1 7  
Oda, Harumichi NR2 5  
Ohe, K. JWP 14  
Ohtsu, Yasunori **ETP 9**,  
**NR2 5**  
Okpalugo, O.A. JWP 15,  
**JWP 17**  
Okraqu-Yirenyi, Yaw  
**JWP 31**, **KR2 1**  
Olthoff, James CT1 6,  
**IW2 1**  
Ono, Tomoyuki AT2 7,  
JWP 69  
Orloff, Jon ETP 31  
O'Rourke, S.F.C. ETP 46  
Otsubo, Masahisa JWP 31,  
KR2 1  
Otte, Matthias ETP 17  
Overzet, Lawrence J.  
AT2 3, **BT1 1**  
Overzet, L.J. JWP 22  
Ozawa, Nobuo QF2 4
- P**  
Palm, Peter JWP 33, **LR1 3**  
Palmeri, P. JWP 63  
Park, Hyun **JWP 61**  
Park, Sung-Jin QF1 5,  
**QF1 6**  
Parker, G.J. JWP 62,  
MR1 8  
Pasko, Victor QF1 3  
Pasquiers, S. JWP 42,  
LR1 5  
Peters, P.J.M. JWP 59  
Petrov, George ETP 15,  
**MR2 6**  
Petrova, Tsvetelina **ETP 15**  
Petrovic, Z.Lj. JWP 47  
Pfau, S. ETP 14  
Phelps, A.V. **ETP 44**,  
JWP 46  
Phillips, S.J. JWP 10  
Pinheiro, Mario J. **CT2 8**  
Pinnaduwege, Lal **GW1 3**  
Piscitelli, D. JWP 46  
Pitchford, L.C. JWP 46  
Ploenjes, Elke **JWP 33**,  
LR1 3  
Popović, S. ETP 7,  
**ETP 16**, **JWP 3**  
Porokhova, I.A. **JWP 30**  
Porokhova, Irina A. CT2 9  
Postel, C. LR1 5  
Puech, V. LR1 5
- Q**  
Qi, Bo JWP 71  
Quinet, P. JWP 63
- R**  
Radovanov, Svetlana **PF2 6**  
Ramamurthi, Badri ETP 8,  
**JWP 2**  
Rao\*, M.V.V.S. ETP 48  
Rao, M.V.V.S. KR2 7  
Rao\*, M.V.V.S. **PF2 3**  
Rauf, S. MR2 4  
Rauf, Shahid **BT2 1**  
Raynor, Thomas ETP 37  
Read, P.A. **JWP 27**  
Rees, J.A. **JWP 10**,  
JWP 27  
Rescigno, T.N. **KR1 1**  
Rich, J. William LR1 3  
Rich, William JWP 33  
Riemann, K.-U. **JWP 6**,  
**PF1 7**  
Riley, Merle AT2 1,  
KR2 4, **PF1 2**  
Ritchie, Burke PF1 2  
Roberto, Marisa **ETP 11**,  
**ETP 12**  
Roepcke, J. ETP 52  
Rolston, S. GW1 4  
Rousseau, A. **ETP 52**,  
JWP 42, LR1 5  
Rozsa, Karoly **JWP 75**  
Rusz, J. JWP 29  
Rutgers, W.R. LR1 6  
Rutkevich, Igor **MR1 9**
- S**  
Sá, P.A. CT2 4  
Saha, Bidhan **ETP 42**  
Sakaguchi, Jyun ETP 33  
Sakai, S. JWP 66  
SAKAI, T. QF1 1  
Sakai, Y. ETP 62, ETP 63  
Sakai, Yosuke AT2 7,  
JWP 69, JWP 70, PF1 6,  
QF1 7  
Sakoda, T. ETP 66  
Salabas, A. **ETP 4**  
Salvermoser, M. **JWP 58**,  
**QF1 8**  
Samsonov, D JWP 76  
Sanabia, Jason E. **ETP 31**  
Sankaran, Arvind **KR2 2**  
Sano, Toru **JWP 67**  
Sasaki, H. BT1 3  
Sasaki, K. ETP 68, JWP 26,  
**LR2 2**  
Satoh, K. **JWP 40**  
Schalk, B. **JWP 57**  
Scheibner, Helmar **JWP 78**  
Schmidt, Martin ETP 17,  
ETP 38  
Schoenbach, Karl H.  
CT2 6, ETP 53  
Schoenbach, K.H. QF1 4  
Schram, Daniel LR2 4

- Schulz-von der Gathen, V.  
ETP 58
- Schweigert, Vitaly A.  
**ETP 24, JWP 16**
- Scofield, James ETP 59
- SEIGOU, TAKASHIMA  
**QF2 2**
- Sekine, Makoto QF2 4
- Serikov, Vladimir **JWP 28, JWP 68**
- Seymour, D.L. JWP 10
- Shannon, Steve MR2 3
- Sharma, S.P. **ETP 48, KR2 7, PF2 3**
- Shaw, D. M. JWP 66
- Shaw, D.M. JWP 11,  
JWP 12, JWP 72
- Shi, W. QF1 4
- SHIHO, Makoto PF2 1
- Shimozuma, M. JWP 40,  
PF1 5
- SHINOZAKI, J. QF1 1
- Shiozawa, M. BT1 3
- Shiraki, T. **ETP 2**
- Shiratani, M. JWP 65,  
JWP 74
- Shizgal, Bernie BT2 2
- Sigeneger, F. **ETP 14**
- Silapunt, Rarchawdee  
AT2 6
- Simiand, N. JWP 42
- Simons, L. CT1 2
- Singh, Harmeet **KR2 5**
- Sinkevich, Oleg **LR1 2**
- Skapin, Tomal z PF1 1
- Skoblo, I.N. JWP 5
- Smith, H.B. JWP 62,  
MR1 8
- Smith, Helen ETP 11,  
ETP 12
- Sobolewski, Mark A.  
**IW2 5, LR2 3**
- Solyman, Samir ETP 17
- Sonnenfeld, Axel **JWP 34**
- Stark, R.H. QF1 4
- Stark, Robert H. **CT2 6, ETP 53**
- Starostin, S.A. **JWP 59**
- Steen, P.G. ETP 23,  
ETP 65, IW2 3, IW2 4,  
JWP 15
- Steen, Philip G. AT2 4
- Steffens, Kristen L. **LR2 3**
- Steimle, Robert **DT2 7**
- Stelbovics, Andris T **IW1 2**
- Stewart, M.D. IW1 4
- Straub, Sherry DT2 7
- Suanpoot, P. JWP 18
- Subramaniam, Vish JWP 33
- Subramonium, Pramod  
**CT2 7**
- Suda, Y. ETP 63
- Suda, Yoshiyuki **AT2 7, JWP 69**
- Sugai, H. CT2 1
- Sugai, Hideo CT2 3,  
JWP 67, QF2 4
- Sugawara, Hirotake  
JWP 70, PF1 6
- Sugiyama, T. ETP 21
- Sullivan, J.P. **ETP 40**
- Sung, Youl-Moon JWP 31,  
KR2 1
- Sunohara, K MR2 2
- Surko, C.M. ETP 40
- SUTO, Hiroshi **PF2 1**
- Suzuki, S. ETP 66
- Suzuki, Susumu JWP 81,  
**JWP 82, JWP 83**
- Suzuki, Teruhiro JWP 83
- suzuki, Toru JWP 81
- Swihart, Mark T MR2 8
- T**
- TACHIBANA, K. **QF1 1**
- Tachibana, Kunihide  
**JWP 35**
- Tagashira, H. JWP 40,  
PF1 5
- Tagashira, Hiroaki **FW1 1**
- Takada, Noriharu JWP 67
- Takahashi, Kazuo JWP 35
- Takahashi, N. JWP 11
- TAKASHIMA, SEIGO  
ETP 57
- TAKAYAMA, Ken PF2 1
- Takenaka, K. JWP 65
- Takeuchi, T. **JWP 50**
- Takizawa, K. LR2 2
- Tanaka, H MR2 2
- Tanaka, J. **AT2 5**
- Tanaka, K. JWP 74
- Tani, Yuuji JWP 80
- Tarnovsky, V ETP 38
- Tatarova, E. CT2 5
- Tatibouet, J.M. JWP 42
- Tatsumi, Tetsuya QF2 4
- Tayal, Swaraj **ETP 36**
- Team, Fujita Lab. DT2 5,  
ETP 9, JWP 19, NR2 5
- Team, Low Temperature  
Plasma Physics and  
Chemistry ETP 72
- Team, Physics Department  
California State University  
Fullerton IW1 3
- Team, Plasma Simulation  
ETP 69
- Team, Plasma Theory and  
Simulation Group  
JWP 62, MR1 8
- Team, Reactive Sputtering  
JWP 34
- Teboul, E. ETP 52
- TEII, KUNGEN ETP 57,  
MR2 5
- Teixeira, Ana I. AT2 6
- TEKEO, TAKASHI MR2 5
- Thompson, C.E. **ETP 65, IW2 3**
- Tichy, M. JWP 29
- Tkachenko, T.L. JWP 5
- Tochikubo, Fumiyoshi  
JWP 41
- Tokuyasu, T. JWP 74
- Toyoda, Hirotake JWP 67
- Toyoda, Naoki CT2 3,  
JWP 67, QF2 4
- Tran, David DT2 6
- Trow, John MR2 3
- Tsai, Wilman JWP 24
- Tsendin, L. CT2 1
- Turner, M M **DT2 4, ETP 26**
- Tuszewski, M. DT2 2
- U**
- Uchida, Satoshi **PF1 6**
- UCHIDA, Shunsuke PF2 1
- Uchida, Y. ETP 21
- Uchino, K. ETP 64,  
ETP 66, JWP 18
- Uchino, Kiichiro JWP 31,  
KR2 1
- Uchiyama, H. JWP 12
- Udalov, Y.B. JWP 59
- Uhlmann, L J MR2 2
- Uhrlandt, Dirk **ETP 17, PF1 3, PF1 4**
- V**
- Valfells, A. ETP 19
- van der Heijden, Harm  
JWP 56
- van Dijk, Jan JWP 56
- van Veldhuizen, E.M.  
LR1 6
- Vasenkov, Alex **BT2 2**
- Vender, D DT2 4
- Ventzek, P.L.G. JWP 49,  
**MR2 4, PF1 5**
- Verboncoeur, J.P. JWP 62,  
MR1 8
- Verdonck, P.B. **ETP 51, PF2 2**
- Veronis, Georgios **QF1 3**
- Viswanathan, Babu JWP 33
- Vukovic, Mirko **JWP 23**
- Vušković, L. ETP 7,  
ETP 16, JWP 3
- W**
- Wagner, Clark J. **QF1 5, QF1 6**
- Wagner, Hans-Erich  
**ETP 25, ETP 72, ETP 73**
- Walton, Scott G. ETP 49,  
PF2 4
- Walton, S.G. **PF2 5**
- Wang, Shiang-Bau AT2 6
- Wang, Yicheng ETP 5
- Washio, G. **ETP 3**
- Watanabe, M. JWP 11,  
JWP 12, **JWP 72**
- Watanabe, Tsuneo JWP 41,  
PF1 6
- Watanabe, Y. **JWP 65, JWP 74**
- Wellie, Th. PF1 7
- Wendt, Amy E. AT2 6,  
**ETP 50**
- Wilke, Christian **CT2 9, ETP 17, JWP 78**
- Williamson, J.M. **ETP 67**
- Winkler, R. ETP 14
- Winkler, Rolf JWP 48,  
PF1 3, PF1 4
- Winstead, Carl **MR2 1**
- Wong, Manus DT2 6
- Woodworth, Joseph AT2 1,  
**KR2 4**
- Wrkich, J IW1 3
- Wu, Han-Ming **JWP 24**
- Y**
- Yamaguchi, H. **ETP 68**
- Yamaji, Masahiro **JWP 52**
- Yamashiro, Akira JWP 37
- Yan, Min **ETP 69**
- YONEDA, KATSUMI  
QF2 2
- Yukimura, Ken **JWP 80**
- Z**
- Zhan, Jiping **ETP 43**
- Zigon, Dušan PF1 1

## NOTES

# UNIVERSITY of HOUSTON

## Campus Map



Map Key	
Information Center	○
Emergency Call Boxes to Police	▲
Entrance Numbers	△
Parking Lot Numbers	□
Building Numbers	●
Faculty/Staff Unattended Parking	■
Faculty/Staff Gated Parking	■
Student Parking	■
Metered Parking	■
Visitor Lot	■
Handicap Parking	■
Motorcycle Parking	■
Economy/Outlying Lot	■
Landing Dock	■
Shuttle Stop	■
Tow Lot	■
Residence Hall Lot	■



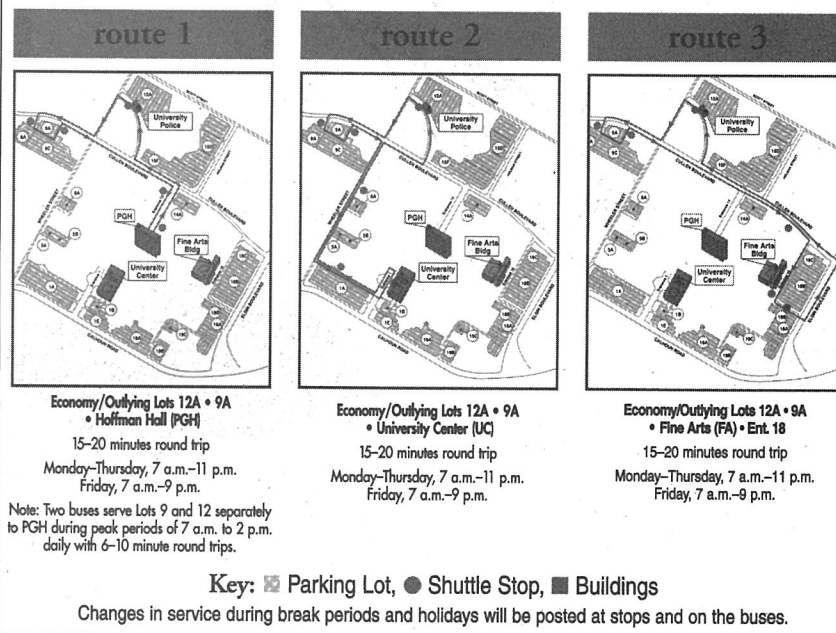
## Map Legend

For your convenience, we've provided the map legend in this format: buildings are listed in numerical order according to the corresponding numbers on the map, followed by the building name, abbreviation of the building name, and (grid position).

### Building number, name, abbreviation, (grid position)

- 1 KUHT-TV Production, P2 (B3)
- 2 KUHT-TV Film Production, P1, (B2)
- 3 Development/Association for Community Television, ACT, (B3)
- 4 KUHT-TV, TV, (B2)
- 5 South Office Annex, SOA, (D3)
- 6 Cameron Building, CAM, (D3)
- 8 Cougar Place (Residence Halls), CP, (E3)
- 9 Child Care Center, CCC, (E2)
- 10 Police Department, UPD, (F2)
- 11 Field House, FLD, (F3)
- 12 Robertson Stadium, RS, (G3)
- 13 Hofheinz Pavilion, HP, (H4)
- 15 Melcher Gymnasium, MEL, (I4)
- 16 Garrison Gymnasium, GAR, (I4)
- 17 Tennis Courts, TEN, (J5)
- 18 Baseball Diamond, HIL, (J6)
- 19 Wortham Theatre Complex, WT, (H6)
- 20 Communications Building, COM, (H6)
- 20 KUHF-FM, COM, (H6)
- 21 University Center Satellite (underground facility), UCS, (G6)
- 22 Science and Research 2 Building, SR2, (H6)
- 23 Science and Research Building, SR, (G5)
- 24 Social Work Building, SW, (G6)
- 25 Agnes Arnold Auditorium 1, AUD1, (G6)
- 26 Agnes Arnold Auditorium 2, AUD2, (G6)
- 27 Agnes Arnold Hall, AH, (F6)
- 28 Fleming Building, F, (F5)
- 29 Science Building, S, (F5)
- 30 Hoffman Hall, PGH, (F6)
- 31 Cullen Underground Annex, CUA, (F6)
- 32 Cullen Performance Hall, A, (E6)
- 33 Ezekiel Cullen Building, E, (E6)
- 34 Farish Hall, FH, (F5)
- 35 McElhinney Hall, M, (F4)
- 36 Heyne Building, H, (F4)
- 37 Roy G. Cullen Building, C, (E5)
- 38 A.D. Bruce Religion Center, ADB, (E5)
- 39 Bates (Residence) Hall, BH, (E4)
- 40 Law (Residence) Hall, LH, (D4)
- 41 Oberholzer (Residence) Hall, OB, (D4)
- 42 Settegast (Residence) Hall, SH, (D5)
- 43 Taub (Residence) Hall, TH, (D5)
- 45 Student Services II, SS2, (D5)
- 46 Health Center, HC, (D5)
- 47 Student Service Center, SS, (D5)
- 48 Cougar Cage, COU, (D6)
- 49 Swimming Pool, PL, (D6)
- 50 Moody Towers Residence Halls, MR, (C7)
- 51 South Park Annex, SPA, (A7)
- 52 J. Davis Armistead Building, JDA, (B8)
- 53 Hilton College of Hotel and Restaurant Management, CHC, (D7)
- 54 University Center, UC, (E7)
- 55 University Center Underground, UCU, (E8)
- 56 M.D. Anderson Memorial Library, L, (F7)
- 57 Technology Annex, T, (G7)
- 58 Technology College Building, T2, (G7)
- 59 Fine Arts Building, FA, (H7)
- 60 Architecture College Building, ARC, (H8)
- 61 Cullen College of Engineering Building, North Wing, D3, (G7)
- 62 Cullen College of Engineering Building, D, (G7)
- 63 Engineering Lecture Hall (Lecture 2), D2, (F8)
- 64 Power Plant, PP, (F7)
- 65 Melcher Hall, MH, (E8)
- 66 Engineering Laboratory, Y, (F8)
- 67 Allied Geophysical Laboratories, AGL, (G8)
- 68 Band Annex, BAND, (H8)
- 69 Art and Engineering Annex, ARA, (G8)
- 70 Krost Hall, KH, (G9)
- 71 Law library (underground facility), LL, (G9)
- 72 Bates Law Building, BL, (G9)
- 73 Teaching Unit 2, TU2, (G10)
- 74 Computing Center, CC, (I9)
- 75 General Services Building, GEN, (J9)
- 76 University of Houston Science Center, HSC, (H5)
- 77 Cambridge Oaks Apartments, CO, (D2)
- 78 Athletic Alumni Facility, AAF, (I4)
- 79 Rebecca and John J. Moores School of Music, MSM, (H6)
- 80 Clinical Research Services, CRS, (C3)
- 81 The Leroy and Lucile Melcher Center for Public Broadcasting, CPB, (I9)

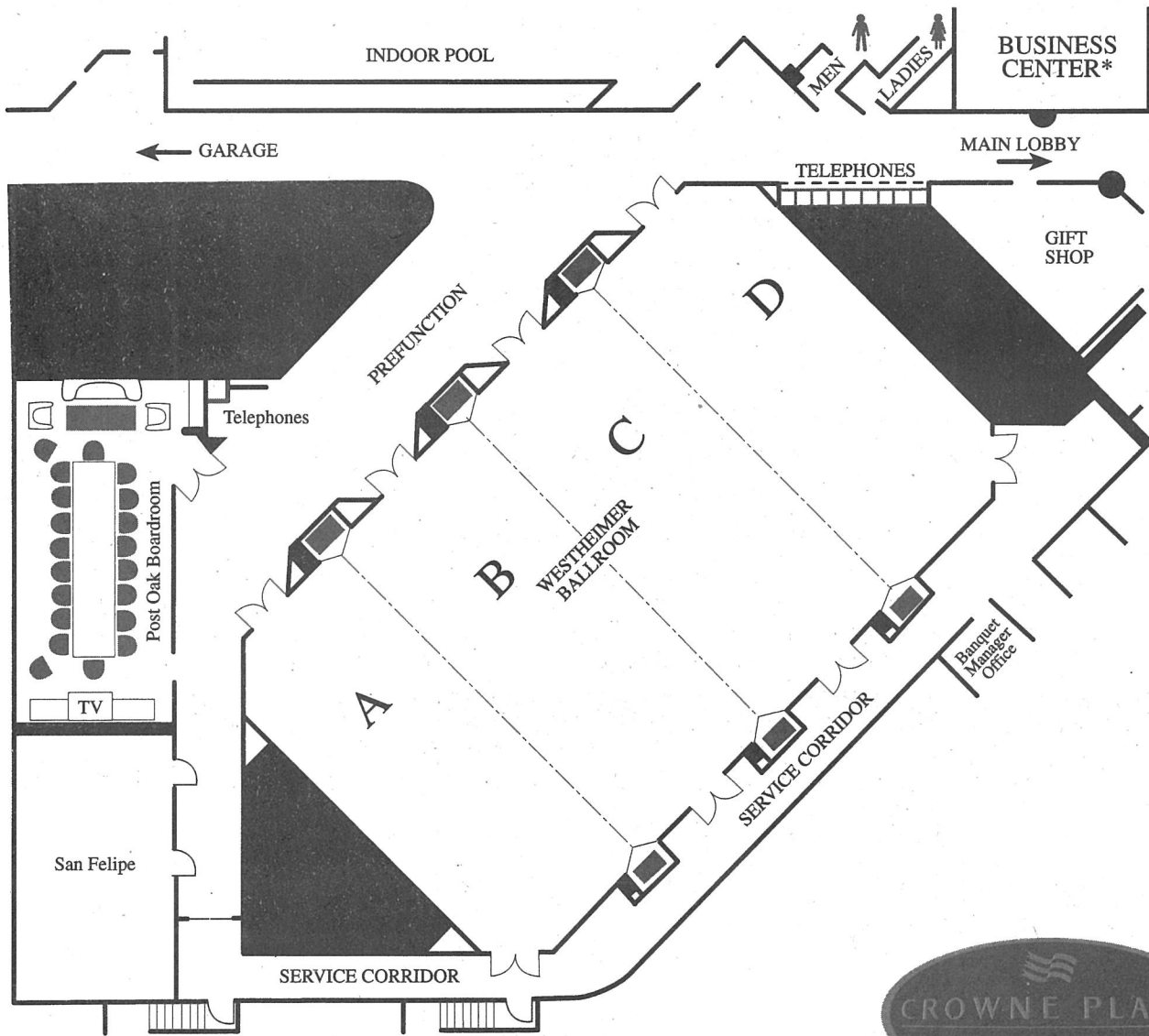
## University of Houston—Shuttle Service



Revised 9/98

The University of Houston reserves the right to make changes without notice in any Parking and Traffic Regulation as necessitated by university or legislative action. Exceptions to these regulations must be approved by the officials of the University of Houston and Parking and Transportation Services.

# CROWNE PLAZA / FIRST FLOOR



HOUSTON • NEAR THE GALLERIA

# Epitome of the 2000 GEC Meeting

8:15 TUESDAY MORNING  
24 OCTOBER 2000

- AT1 **Rydberg Atom Phenomena**  
*MacAdam, Morrison, Dunning*  
Grand Ballroom D, Red Lion Hotel
- AT2 **Plasma-Surface Interactions**  
Grand Ballroom C, Red Lion Hotel

10:30 TUESDAY MORNING  
24 OCTOBER 2000

- BT1 **Chlorine Plasmas**  
*Overzet, Donnelly, Nanbu*  
Grand Ballroom D, Red Lion Hotel
- BT2 **Sheaths and Boundary Layers**  
*Rauf*  
Grand Ballroom C, Red Lion Hotel

13:30 TUESDAY AFTERNOON  
24 OCTOBER 2000

- CT1 **Electron-Molecule/Molecular Ion Interactions**  
*Larsson, Kimura*  
Grand Ballroom D, Red Lion Hotel
- CT2 **Glow Discharges**  
Grand Ballroom C, Red Lion Hotel

16:15 TUESDAY AFTERNOON  
24 OCTOBER 2000

- DT1 **High Pressure Arcs**  
*Coulombe, Gleizes, Murphy*  
Grand Ballroom D, Red Lion Hotel
- DT2 **Inductively Coupled Plasmas I**  
Grand Ballroom C, Red Lion Hotel

20:00 TUESDAY EVENING  
24 OCTOBER 2000

- ETP **Poster Session I**  
Westheimer Ballroom, Crowne  
Plaza Galleria

8:00 WEDNESDAY MORNING  
25 OCTOBER 2000

- FW1 **Foundations of Gaseous Electronics**  
*Tagashira*  
Grand Ballroom, Red Lion Hotel

9:45 WEDNESDAY MORNING  
25 OCTOBER 2000

- GW1 **Interactions with Excited Species**  
*Christophorou, Čadež, Pinnaduwage*  
Grand Ballroom, Red Lion Hotel

11:30 WEDNESDAY MORNING  
25 OCTOBER 2000

- HW1 **General Business Meeting**  
Grand Ballroom, Red Lion Hotel

14:00 WEDNESDAY AFTERNOON  
25 OCTOBER 2000

- IW1 **Electron-Atom/Molecule Collisions I**  
*Crowe, Stelbovics*  
Grand Ballroom D, Red Lion Hotel
- IW2 **GEC Cell—10 Year Perspective**  
*Olthoff, Hebner, Sobolewski*  
Grand Ballroom C, Red Lion Hotel

16:30 WEDNESDAY AFTERNOON  
25 OCTOBER 2000

- JWP **Poster Session II**  
Westheimer Ballroom, Crowne  
Plaza Galleria

8:00 THURSDAY MORNING  
26 OCTOBER 2000

- KR1 **Electron-Atom/Molecule Collisions II**  
*Rescigno, Gay*  
Grand Ballroom D, Red Lion Hotel
- KR2 **Inductively Coupled Plasmas II**  
Grand Ballroom C, Red Lion Hotel

10:30 THURSDAY MORNING  
26 OCTOBER 2000

- LR1 **Atmospheric Discharges/Environmental Applications**  
*Inan*  
Grand Ballroom D, Red Lion Hotel
- LR2 **Diagnostics I**  
*Czarnetki*  
Grand Ballroom C, Red Lion Hotel

13:30 THURSDAY AFTERNOON  
26 OCTOBER 2000

- MR1 **Low Pressure Lamps and Discharges**  
Grand Ballroom D, Red Lion Hotel
- MR2 **Etching/Deposition**  
*Winstead*  
Grand Ballroom C, Red Lion Hotel

16:00 THURSDAY AFTERNOON  
26 OCTOBER 2000

- NR1 **Lab Tours**  
University of Houston
- NR2 **New Materials/Dusty Plasmas**  
*Meyyappan, Mieno, Morfill*  
Grand Ballroom C, Red Lion Hotel

19:30 THURSDAY EVENING  
26 OCTOBER 2000

- OR1 **Banquet**  
Grand Ballroom, Red Lion Hotel

8:00 FRIDAY MORNING  
27 OCTOBER 2000

- PF1 **Discharge Kinetics**  
Grand Ballroom D, Red Lion Hotel
- PF2 **Diagnostics II**  
Grand Ballroom C, Red Lion Hotel

10:15 FRIDAY MORNING  
27 OCTOBER 2000

- QF1 **Microdischarges for Displays and Lamps**  
Grand Ballroom D, Red Lion Hotel
- QF2 **Diagnostics III**  
*Anderson*  
Grand Ballroom C, Red Lion Hotel

12:15 FRIDAY AFTERNOON  
27 OCTOBER 2000

- RF1 **Plasma Modeling: Needs and Opportunities**



0003-0503(200010)45:6;1-7